Load Optimization for Connected Smart Green Buildings Using Machine Learning

by

Seyed Morteza Moghimi
B.Sc., Islamic Azad University, 2013
M.Sc., Islamic Azad University, 2016

A Dissertation Submitted in Partial Fulfillment of the Requirements
for the Degree of Doctor of Philosophy
in the Department of Electrical and Computer Engineering

We acknowledge and respect the Lək̓ʷəŋən (Songhees and Xʷsepsəm/Esquimalt) Peoples on whose territory the university stands, and the Lək̓ʷəŋən and W̱SÁNEĆ Peoples who continue to this day.

Supervisory Committee

Dr. T. Aaron Gulliver
Supervisor
Department of Electrical and Computer Engineering, University of Victoria

Dr. Ilamparithi Thirumarai Chelvan
Co-Supervisor
Department of Electrical and Computer Engineering, University of Victoria

Dr. Hossen Teimoorinia
Outside Member
Department of Physics and Astronomy, University of Victoria

Supervisory Committee

Dr. T. Aaron Gulliver
Supervisor
(Department of Electrical and Computer Engineering, University of Victoria)

Dr. Ilamparithi Thirumarai Chelvan
Co-Supervisor
(Department of Electrical and Computer Engineering, University of Victoria)

Dr. Hossen Teimoorinia
Outside Member
(Department of Physics and Astronomy, University of Victoria)

ABSTRACT

Energy efficiency plays a crucial role in mitigating Greenhouse Gas (GHG) emissions, particularly in the building sector, where residential buildings are among the largest energy consumers. Despite the potential of buildings to generate Renewable Energy (RE), increasing energy demands pose both environmental and economic challenges. This dissertation presents a Machine Learning (ML)-based framework for optimizing energy consumption in Connected Smart Green Townhouses (CSGTs), focusing on efficiency, cost-effectiveness, emission reduction, and occupant comfort. A comprehensive study of adaptive, occupant-aware, and ML-based energy optimization is presented for Smart Green Townhouses (SGTs) and CSGTs. The goals are prediction, optimization, and real-time management of energy consumption, with a focus on sustainability, occupant comfort, and system intelligence.

A model for CSGTs operating in grid-connected mode is presented. This model incorporates sustainable building materials, smart sensors, Photovoltaic (PV) systems, and energy-efficient components. A hybrid Long Short-Term Memory–Convolutional Neural Network (LSTM-CNN) model is considered with real utility datasets. The results show that this approach outperforms traditional ML models such as Linear Regression (LR), CNN, LSTM, Random Forest (RF), and Gradient Boosting (GB). The Mean Absolute Percentage Error (MAPE) is below 5%, and the coefficient of determination (R^2) is above 0.85, which validates the accuracy for different bedroom configurations.

A robust ML-based optimization framework is proposed for CSGT energy and load management in island mode. The integration of Electric Vehicles (EVs) with Vehicle-to-Grid (V2G) functionality is shown to improve system resilience. The LSTM-CNN model provides a MAPE of 4.43% and a Root Mean Square Error (RMSE) of 3.49 kWh for the four-bedroom unit. The results confirm that occupant-aware optimization significantly

improves performance under isolated conditions.

An adaptive control framework to enable automatic transitions between grid-connected and island modes is developed. By incorporating occupancy, weather, and electricity price data, the system dynamically optimizes load consumption using LSTM-CNN and Multi-Objective Particle Swarm Optimization (MOPSO). Efficiency gains of 3–5% in grid-connected mode and 10–12% in island mode are observed with a 4–6% reduction in carbon emissions, demonstrating the value of real-time adaptive management.

An occupant-centric load optimization system leveraging real-time Internet of Things (IoT) data is proposed. This human-centric approach significantly improves comfort and operational efficiency. Energy loads are reduced by 7–13%, peak loads by 11%, and carbon emissions by 15–24%. Cost savings of 13–21% are achieved, and occupant satisfaction increases with a 19% improvement in thermal comfort and 14% better lighting adequacy.

The results presented highlight the effectiveness of advanced, applicable, and scalable ML-driven energy optimization in SGTs. The proposed approaches offer scalable, adaptable, and occupant-centric solutions for energy-efficient, cost-effective, and environmentally sustainable residential buildings. Future research directions include integrating advanced renewable energy storage management, real-time grid interaction, federated learning, and edge Artificial Intelligence (AI) deployment to improve the adaptability and efficiency of smart energy and load management in CSGTs. Integrating advanced ML models, real-time sensor data, and adaptive control techniques will provide solutions to address the economic, environmental, and social challenges in sustainable urban housing.

Contents

List of Tables

List of Figures

List of Acronyms

ACH	Air Changes per Hour
ADWIN	Adaptive Windowing
AHP	Analytic Hierarchy Process
AI	Artificial Intelligence
ALPLA	Adaptive and Lightweight Physical Layer Authentication
ANN	Artificial Neural Network
APG	Appliance Group
ARIMA	Auto-Regressive Integrated Moving Average
ARMA	Auto-Regressive Moving Average
BC	British Columbia
BMA	Bayesian Model Averaging
BMS	Building Management System
BP	Back Propagation
BREEAM	Building Research Establishment Environmental Assessment Method
CAD	Canadian Dollar
CART	Classification and Regression Tree
CEI	Control Efficiency Index
CGBC	Canada Green Building Council
CNN	Convolutional Neural Network
COA	Coati Optimization Algorithm
COP	Coefficient of Performance
CSGTs	Connected Smart Green Townhouses
CV	Cross-Validation
DDM	Drift Detection Method
DER	Distributed Energy Resource
DP	Demand Prediction
DQN	Deep Q-Network
DR	Demand Response
DRL	Deep Reinforcement Learning
DSM	Demand Side Management
DT	Decision Tree
DTR	Decision Tree Regression
ECE	Electrical Consumption Efficiency
EDA	Exploratory Data Analysis
EER	Energy Efficiency Ratio
EL	Ensemble Learning
EMS	Energy Management System
ESN	Echo State Network
ESS	Energy Storage System
EV	Electric Vehicle
FL	Flexible Load
FRG	Furnace Room Gas
FSA	Fish Swarm Algorithm

GA	Genetic Algorithm
GB	Green Building
GCE	Gas Consumption Efficiency
GDP	Gross Domestic Product
GEB	Grid-Interactive Efficient Building
GHG	Greenhouse Gas
GHGI	Greenhouse Gas Index
GNNs	Graph Neural Networks
GRU	Gated Recurrent Unit
HEC	Home Energy Calculator
HEMS	Home Energy Management System
HP	Horsepower
HSPF	Heating Seasonal Performance Factor
HTW	Hot Water
HVAC	Heating, Ventilation, and Air Conditioning
IAQ	Indoor Air Quality
IDC	International Data Corporation
IoT	Internet of Things
KNN	K Nearest Neighbors
LASSO	Least Absolute Shrinkage and Selection Operator
LED	Light Emitting Diode
LEED	Leadership in Energy and Environmental Design
LM	Levenberg-Marquardt
LR	Linear Regression
LSTM	Long Short-Term Memory
MAE	Mean Absolute Error
MAPE	Mean Absolute Percentage Error
MG	Micro-Grid
ML	Machine Learning
MOEA/D	Multi-Objective Evolutionary Algorithm based on Decomposition
MOPSO	Multi-Objective Particle Swarm Optimization
MRP	Material Recycling Percentage
MSE	Mean Squared Error
NB	Naive Bayes
NLP	Natural Language Processing
NN	Neural Network
NSGA-II	Non-dominated Sorting Genetic Algorithm II
NZEB	Nearly Zero-Energy Building
P2P	Peer-to-Peer
PCA	Principal Component Analysis
PI	Permutation Importance
PP	Peak Power
PPO	Proximal Policy Optimization
PSO	Particle Swarm Optimization
PV	Photovoltaic

R^2	Coefficient of determination
RB	Residential Building
RE	Renewable Energy
REI	Renewable Energy Integration
RES	Renewable Energy Source
RF	Random Forest
RNN	Recurrent Neural Network
ROI	Return on Investment
RR	Ridge Regression
SB	Smart Building
SGB	Smart Green Building
SG	Smart Grid
SGI	Smart Grid Integration
SGT	Smart Green Townhouse
SL	Supervised Learning
SOC	State of Charge
SS	Storage System
SST	Solid-State Transformer
STLF	Short-Term Load Forecasting
STUI	Smart Technology Utilization Index
SVM	Support Vector Machine
SVR	Support Vector Regression
TCL	Thermostatically Controlled Load
TEDI	Total Energy Demand Intensity
TEUI	Total Energy Use Intensity
Tanh	Hyperbolic Tangent
TOU	Time-Of-Use
TWMU	Total Weight of Materials Used
UHI	Urban Heat Island
USD	United States Dollar
V2G	Vehicle-to-Grid
V2H	Vehicle to Home
VAE	Variational Autoencoder
VOC	Volatile Organic Compound
Volt-VAR	Voltage and Volt-Ampere Reactive Control
VPP	Virtual Power Plant
WRM	Weight of Recycled Materials
WRR	Waste Recycling Rate
WRW	Weight of Recycled Waste
YOLO	You Only Look Once

Acknowledgments

I would like to express my sincere gratitude to the following individuals and institutions, and above all to God, the source of all wisdom and strength, for their support and contributions throughout my PhD journey.

- **Dr. T. Aaron Gulliver** for his exceptional mentorship, guidance, encouragement, and patience, as well as for his invaluable insights and continuous support.
- **Dr. Ilamparithi Chelvan** for his thoughtful feedback and valuable comments, which have greatly contributed to my research.
- **Dr. Hossen Teimoorinia** for his guidance, support, and constructive discussions.
- **The University of Victoria (UVic)**, for providing financial support through a fellowship and bursary and fostering an enriching academic environment.
- **Janice Closson**, **Ashleigh Carlsen**, and **Dan Mai**, for their continuous assistance and support throughout my time at UVic.
- **Hani**, for her unwavering support, patience, and encouragement during the challenging times of my academic journey.
- My lovely mother, father, and brothers, for their unwavering love, support, and encouragement, which have been fundamental to my success.

I am deeply grateful for all the guidance, encouragement, and support I have received, without which this dissertation would not have been possible.

Dedication

This work is dedicated to my wonderful wife, Hani, for her endless patience and love.

Plant the tree of friendship, for it will bear the fruit of your heart's desire.
Uproot the sapling of enmity, for it will bring endless sorrow.

- Hafez

Chapter 1

Introduction

1.1 Background

The increasing global emphasis on sustainability and energy efficiency has led to a growing interest in the development of Smart Green Buildings (SGBs). These buildings aim to optimize energy use, reduce greenhouse gas (GHG) emissions, and enhance the environmental performance of urban infrastructure. Central to achieving these objectives is the efficient management of energy demand [1, 2].

Efficient energy management is critical for multiple reasons. It enables building operators and utilities to reduce peak loads, improve energy distribution, and minimize waste. Additionally, it supports the integration of Renewable Energy Sources (RESs), such as Photovoltaic (PV) solar systems, which are inherently variable and depend on environmental conditions.

Recent advances in Machine Learning (ML) have introduced powerful tools for energy demand optimization in SGBs. ML techniques can extract insights from large, complex datasets and automate predictions to support energy-efficient decision-making. However, the performance of ML models depends on several factors including data quality, algorithm selection, model complexity, feature engineering, and the amount of training data.

Various ML algorithms have been employed for building energy optimization. These include Artificial Neural Networks (ANNs), Long Short-Term Memory (LSTM), Convolutional Neural Networks (CNN), Linear Regression (LR), Support Vector Machine (SVM), Decision Trees (DTs), and ensemble methods such as Random Forest (RF) and Gradient Boosting (GB). Each algorithm presents tradeoffs between interpretability, computational requirements, and prediction accuracy. For example, while ANNs can model complex nonlinear relationships, they often require substantial data and training time. Simpler models like LR are more interpretable but may lack prediction precision in dynamic environments.

In the context of building design, especially for residential settings, incorporating energy-efficient strategies and renewable technologies is essential to reducing the carbon foot-

print and improving occupant comfort. Key considerations include passive design, high-efficiency systems, insulation, and intelligent control mechanisms.

1.2 Significance of This Study

The significance of this dissertation is its potential to advance energy optimization in SGBs through deep hybrid ML models. By overcoming the limitations of current methods and introducing new approaches, the aim is to improve accuracy, efficiency, and performance. The results also contribute to sustainable urban development, supporting global climate change mitigation and environmental sustainability.

Connected Smart Green Townhouses (CSGTs) in Burnaby, British Columbia (BC), are considered as a case study to evaluate the proposed ML models. The focus of Burnaby on sustainability makes it an ideal setting. A framework for integrating ML models in optimizing energy use is developed. The insights gained can be applied to similar urban areas, promoting the adoption of energy-efficient practices in residential buildings. The results are expected to influence policy decisions, guide future research, and aid in developing smart, sustainable urban environments.

1.3 Research Objectives and Scope

The primary objective is to develop and evaluate a hybrid ML model for energy optimization in SGBs. To support this objective, the following research goals guide the scope and direction of the work.

- **Development of a CSGT Simulation Model** Design a residential-scale CSGT model that integrates smart and green technologies such as PV systems, energy-efficient HVAC, and IoT-enabled controls.
- **Implementation of a Deep Hybrid ML Framework** Develop a hybrid LSTM-CNN model for forecasting energy demand and apply multi-objective optimization techniques (e.g. MOPSO), to improve cost-efficiency, performance, and emission reduction.
- **Performance Evaluation and Validation** Evaluate the proposed model using real-world datasets. Compare its performance with traditional models using metrics such as MAE, RMSE, MAPE, and R^2.
- **Occupant-Centric and Grid-Aware Optimization** Incorporate occupancy behavior and grid conditions into the model to enable adaptive load management under both grid-connected and island modes of operation.

By addressing these research objectives, this dissertation aims to bridge the gap between ML-driven energy optimization and practical implementation in smart residential townhouses, ultimately contributing to sustainable, low-carbon, and intelligent energy management systems.

This dissertation also considers the design and modeling of residential Smart Green Townhouses (SGTs) including CSGTs. The focus is not only on physical design but also on incorporating smart and green technologies to improve sustainability, efficiency, cost, and emission reduction.

1.4 Organization

The seven chapters of this dissertation are organized as follows.

- **Chapter 1: Introduction** provides the background, significance, objectives, and scope of the work. It outlines the design and modeling of CSGTs and introduces the structure of the dissertation.
- **Chapter 2: Literature Review** presents a comprehensive review of existing Machine Learning (ML) techniques used in Smart Green Buildings (SGBs). The chapter categorizes these methods into engineering-based, data-driven, AI-based, and hybrid approaches, while identifying research gaps targeted for future investigation.
- **Chapter 3: Resource Optimization for Grid-Connected Smart Green Townhouses Using Deep Hybrid Machine Learning** examines the formulation, modeling, and design of CSGTs in grid-connected mode. It evaluates the performance of hybrid ML models, particularly LSTM-CNN, in optimizing electricity, water, and gas consumption, with metrics such as MAPE and R^2.
- **Chapter 4: Load Optimization in Connected Modern Buildings Using Deeper Hybrid Machine Learning in Island Mode** provides a detailed analysis of CSGTs operating in island mode. It focuses on accuracy, resilience, and emission reduction under isolated conditions. The integration of renewable energy sources (RESs) and Electric Vehicle (EV)-based Vehicle-to-Grid (V2G) strategies are also addressed.
- **Chapter 5: Adaptive Machine Learning for Automatic Load Optimization in Connected Smart Green Townhouses** proposes an adaptive framework that enables automatic transitions between grid-connected and island modes. Real-time occupancy, weather, and pricing data are integrated using LSTM-CNN and optimized via Multi-Objective Particle Swarm Optimization (MOPSO).
- **Chapter 6: Occupant-Centric Load Optimization in Smart Green Townhouses Using Machine Learning** provides a human-centric optimization framework leveraging real-time IoT data and LSTM-CNN models. It focuses on improving occupant comfort while reducing peak load, cost, and emissions.
- **Chapter 7: Conclusion and Future Work** summarizes the results and contributions of the research and outlines future directions including federated learning, advanced inverter functions, and stochastic optimization for smart, scalable building energy systems.

1.5 Publications

- Energy Management in Modern Buildings Based on Demand Prediction and Machine Learning—A Review, Energies 2024, 17(3), 555.
- Energy Optimization for Grid-Connected Smart Green Townhouses Using a Deep Hybrid Machine Learning, Energies, 2024, 17(23), 6201.
- Load Optimizing in Connected Modern Building Using a Deeper Hybrid Machine Learning in Island Mode, Energies, 2024, 17(24), 6475.
- Adaptive Machine Learning for Automatic Load Optimization in Connected Smart Green Townhouses, Algorithms, 2025, 18(3), 132.
- Occupant-Centric Load Optimization in Smart Green Townhouses Using a Machine Learning, Energies, 2025, 18(13), 3320.

Chapter 2

Energy Management in Modern Buildings Based on Demand Prediction and Machine Learning—A Review

This chapter examines energy DP and optimization for the SGBs aims to reduce energy use. In addition, ML methods have been used to improve building energy consumption, but not all have performed well in terms of accuracy and efficiency. In this chapter, these methods are examined and evaluated for SGBs as MB energy DP and optimization. This section sets the stage by introducing the importance of designing residential SGBs and highlights the key considerations that will be addressed in subsequent sections. It serves as a precursor to the in-depth discussions and analyses that follow, guiding the reader through the various facets of the design, formulation, and modeling process. Furthermore, the dissertation includes a comprehensive review of the literature of the ML methods applied to SGBs, providing a foundation for the methodologies used in the proposed research.

The design and construction of residential and commercial buildings are among the most energy intensive activities worldwide. Buildings contribute 20% to 40% of total energy usage [1] According to the European Union (EU) [2], urban buildings are responsible for 40% of global energy consumption and 33% of GHG emissions. Consequently, governments are motivated to address increasing energy consumption by reducing emissions and improving energy efficiency while ensuring the comfort of building residents [3]. To reduce energy consumption, the European Commission (EC) has proposed nearly zero energy buildings (NZEBs) for 2030 [3].

Fig. 2.1 illustrates the significance of energy reduction in terms of CO_2 emissions and cost based on data from home energy calculators (HECs) [4]. Fig. 2.1 gives the results of comprehensive questionnaires administered by a United Kingdom (UK) university. Study participants were randomly assigned one of three versions of the HEC which presented energy consumption in kilowatt hours. Responses were thematically coded by two inde-

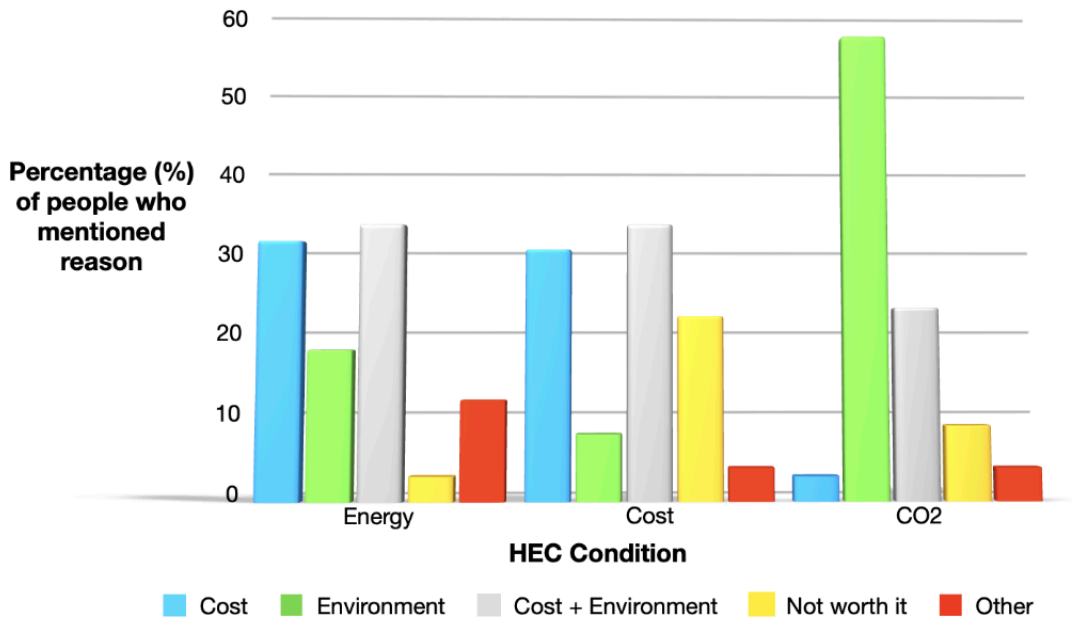

Figure 2.1: Reasons why reducing energy consumption is important [4].

pendent reviewers, leading to five distinct classes on the following.

Energy-related, cost, environmental, a combination of cost and environmental, and 'not worth it', indicating a lack of incentive to reduce energy use, among others.

Strategies for Demand Prediction (DP) [5] are among the solutions recommended by the European Commission (EC) to reduce energy consumption [6, 7]. These strategies include price-based demand response (DR), incentive-based DR, time-based DR, automated DR, and capacity-based DR.

However, the implementation of DP strategies faces several challenges, such as operational and technological constraints, as well as limitations in data availability and accuracy [8]. To address these issues, various Machine Learning (ML) methods have been proposed [8, 9].

In modern energy management, optimization techniques are increasingly utilized to reduce energy consumption and associated costs. This chapter evaluates ML techniques based on their deployment potential, prediction accuracy, cost-effectiveness, and overall efficiency in modern buildings (MBs), particularly Smart Green Buildings (SGBs).

To provide a comprehensive understanding of the domains influencing energy consumption prediction and optimization in SGBs, this dissertation adopts the conceptual framework illustrated in Fig. 2.2. The figure outlines the critical components of energy management, including demand response, cost reduction, and emission mitigation, all interconnected through advanced ML approaches such as Deep Learning (DL) and Neural Networks (NNs). By examining these interconnected areas, this work aims to develop a holistic methodology for forecasting and optimizing energy performance in SGBs, thereby

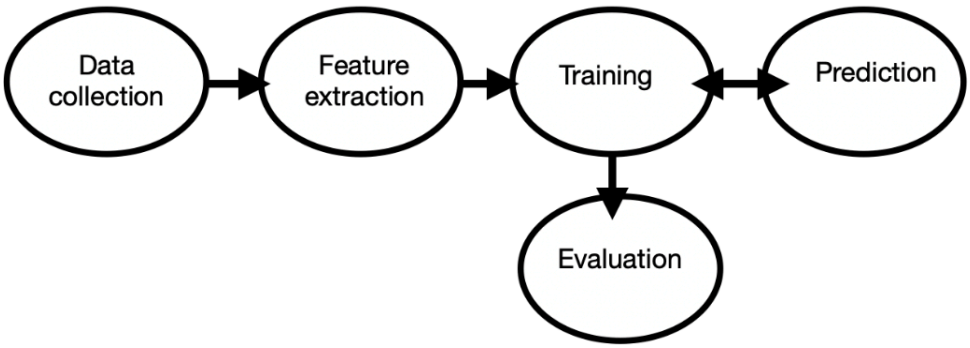

Figure 2.2: The Machine Learning (ML) process.

promoting sustainability, operational efficiency, and energy-conscious design.

The remainder of this chapter is structured as follows. Section 2.2 presents an overview of current ML methods and their applications in energy systems. Section 2.3 provides a literature review on ML techniques used for energy prediction in buildings, as well as related datasets. Finally, Section 2.4 concludes the chapter with a summary of insights and research gaps identified.

2.1 ML Methods

Fig. 2.2 illustrates the ML process, which includes data collection, feature extraction, training, evaluation, and prediction [10, 11, 12]. ML methods have been designed for diverse tasks such as data analysis and pattern recognition.

ML methods can be categorized into three primary groups on the following. Supervised Learning (SL), Unsupervised Learning (UL), and Reinforcement Learning (RL) [10, 11]. Semi-supervised learning combines aspects of both SL and UL. ML methods can also be classified as categorical or continuous. Continuous methods include algorithms such as Singular Value Decomposition (SVD), Principal Component Analysis (PCA), K-means, RF, regression (linear and polynomial), and Decision Trees (DTs). Categorical methods are used in RL algorithms for tasks such as robot navigation and gaming. UL methods commonly employ hidden Markov models, clustering, and association analysis. Clustering methods often involve SVD, PCA, and K-means. NN are employed in SL and UL for tasks such as regression, classification, sequence-to-sequence tasks, clustering, and dimensionality reduction. The selection of an NN architecture depends on the specific problem and the available data [10, 11]. Fig. 2.3 illustrates the variety of ML algorithms.

Supervised Learning (SL)

SL employs feedback for prediction by learning the map from input to output [10, 11]. SL algorithms can be categorized as follows.

- **Regression Algorithms** Regression algorithms are used to predict advertising popularity, estimate life expectancy, forecast markets, predict population growth, and forecast weather. Issues with these algorithms include over-fitting, under-fitting, multicollinearity, heteroscedasticity, outliers, missing data, non-linearity, autocorrelation, data scaling, and data transformation. These issues can be addressed through data preprocessing, feature engineering, model selection, and regularization [13, 14, 15].
- **Classification Algorithms** Classification algorithms are used to determine a mapping based on the input to classify or categorize the output. Classification algorithms include LR, Ridge Regression (RR), NN Regression (NNR), Least Absolute Shrinkage and Selection Operator (LASSO), DT Regression (DTR), RF, K-nearest Neighbors (KNNs), and Support Vector Machines (SVMs) [13, 14, 15].

Unsupervised Learning (UL)

UL leverages the inherent structure within a dataset for categorization. The goal is to partition the data based on similar traits [16]. NNs are frequently used in UL as they can uncover patterns or structures within unlabeled data. UL applications include clustering, dimensionality reduction, feature learning and extraction, anomaly detection, generative modeling, and density estimation [15, 16].

Reinforcement Learning (RL)

RL is used to solve problems by maximizing anticipated rewards. It often employs a Markov Decision Process (MDP) which has states, strategies, actions, and functions. RL reinforces important rules while diminishing the effects of others [17]. In summary, clustering concentrates on data point grouping, classification assigns data to classes, regression predicts continuous values, UL uncovers patterns without labels, and SL trains models based on labeled data for prediction. The use of ML methods in applications such as MBs [18] can be categorized as single, hybrid, or ensemble methods [19]. For performance evaluation, metrics such as MSE, MAE, accuracy, and precision are often employed.

Single ML Methods

In this case, a single method such as SVD is employed. Recurrent NN (RNN) and Back Propagation (BP) Artificial NN (ANN) methods were employed in [20]. These single ML methods were used to compare DP results with official data on electricity consumption in Turkey. An Adaptive Neuro-Fuzzy Inference System (ANFIS) was used in [21] for a case study in Ontario, Canada. The thirty years of data available in [20] were used with the proposed model for electricity and energy DP.

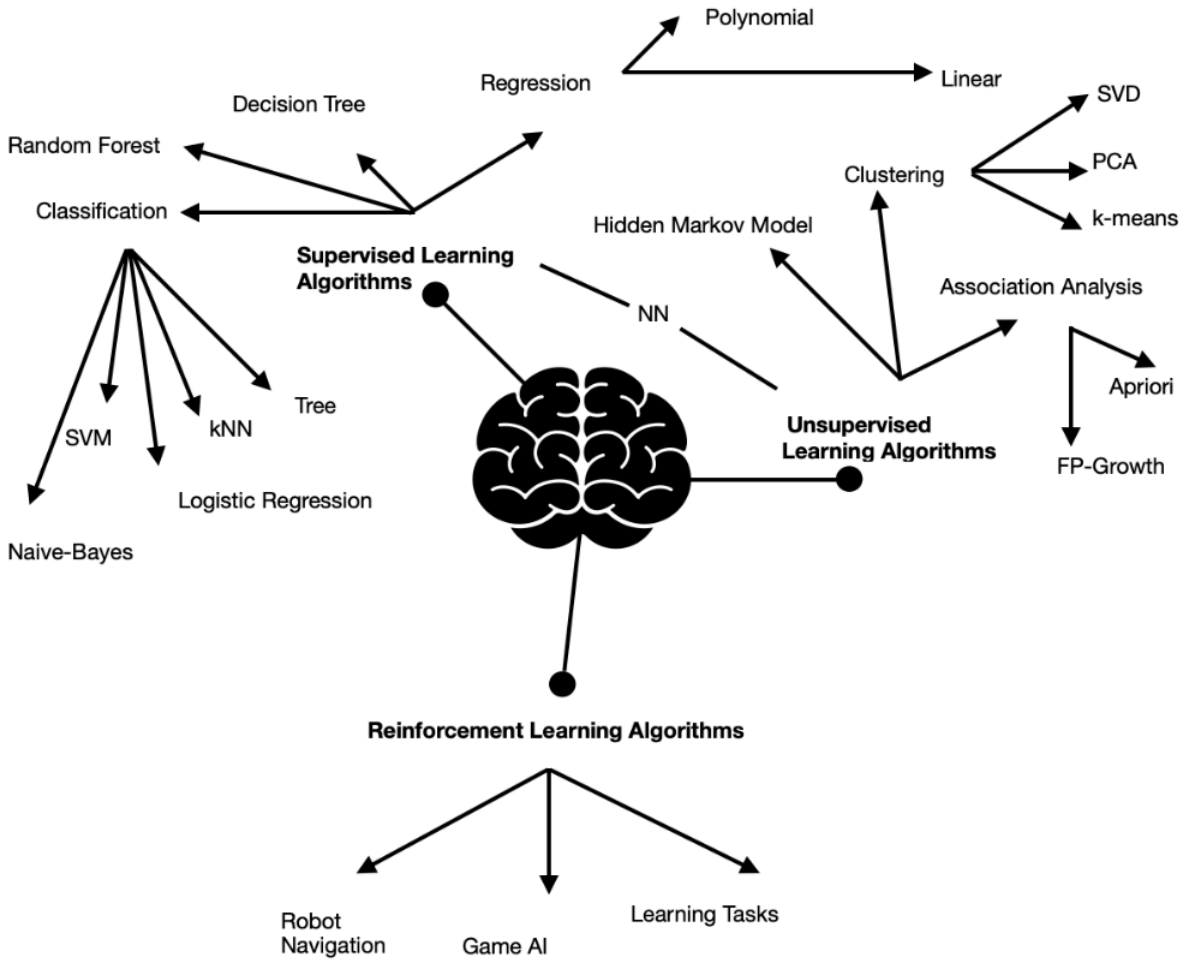

Figure 2.3: ML algorithms [15, 16].

Hybrid ML Methods

Hybrid ML methods combine two or more approaches to enhance performance [22]. This can improve accuracy and provide flexibility in handling complex tasks. Particle Swarm Optimization (PSO) and a Genetic Algorithm (GA) were employed in [23] for electricity DP within India. A hybrid model that incorporates Wavelet Decomposition (WD) and Support Vector Regression (SVR) was used for hourly electricity prediction in [24] using data collected from hotels and malls.

Hybrid ML methods can also adapt to different data types and problem domains by leveraging the strengths of the methods. However, the scalability and feasibility of hybrid methods in real-world applications can be a concern due to factors such as computational complexity, data volume, and data quality. Thus, the decision to employ single or hybrid ML methods should consider the problem, data, resources, and objectives.

Ensemble ML Methods

Ensemble ML methods involve multiple classifiers and can be sequential or parallel. Given the constraints of hybrid and single methods such as data collection and model design, ensemble prediction methods have been developed such as the approach in [25]. An ensemble method which employs regression for electricity DP in the USA was proposed in [26]. Results were obtained using a small number of building datasets. Ensemble Bagging Trees (EBTs) method was introduced in [27] to provide improved building energy prediction performance compared to the Classification And Regression Tree (CART) method. A comparison between ML and regression-based methods is now given.

Comparison of ML and Regression-Based Methods

Regression is extensively employed in ML models. It is frequently used to estimate the relationship between load and other variables by predicting the correlation between a variable or predictor and an object [28]. When considering model selection and regularization techniques for an application, it is important to consider methods that align with the data characteristics and analysis. The choices for several application areas are given below [13, 14, 29].

Economics and Finance

Model: Depending on the complexity of the relationships between economic indicators, LR or more advanced techniques such as polynomial regression (PR), RR, or LASSO regression can be employed.

Regularization: LASSO can be advantageous for better generalization and handling multicollinearity.

Natural Language Processing (NLP)

Model: Techniques such as logistic regression are often used for sentiment analysis and text classification. Language modeling typically employs methods such as RNNs or transformer-based models.

Regularization: Techniques such as dropout are beneficial to prevent overfitting in NNs.

Image and Signal Processing

Model: CNNs are often used for image denoising, deblurring, and super-resolution tasks.

Regularization: Techniques such as weight decay and batch normalization are commonly used to regularize CNNs in image processing.

Energy and Power Systems

Model: Depending on complexity, LR or more advanced methods such as Autoregressive Integrated Moving Average (ARIMA) can be applied for power grid load forecasting.

Regularization: LASSO or RR can be used to overcome multicollinearity and overfitting in energy consumption prediction models.

Transportation and Traffic Engineering

Model: LR, time series analysis, or autoregressive models are suitable for traffic flow prediction and transportation demand modeling.

Regularization: RR has been used to improve robustness and prediction accuracy in traffic-related models.

The suitability of methods and techniques can also depend on dataset size, noise, and other factors unique to the application. Regression methods are also used to model time series data and explore causal links between variables. Thus, they are employed in many engineering applications [13, 14, 29].

Statistical methods, known as regression analysis, have been employed to uncover relationships between variables. The methods used in regression analysis for ML include LR, logistic regression, PR, Softmax Regression (SR), RR, LASSO, and Elastic Net Regression (ENR). Prediction is essential in establishing relationships between dependent and independent variables [13, 14, 29]. In [29], both ANNs and hedonic pricing were used with real residential property data to estimate market prices.

As previously mentioned, the primary regression methods are simple LR, multiple LR, PR, SVM, DTR, and RF. Each method has advantages and disadvantages which should be considered in selecting the most appropriate method for a given application.

Classification and Regression Methods in ML

Classification involves identifying or seeking a model or function to divide data into different categories. Classification and regression methods are commonly employed to solve prediction problems. Regression is often used with continuous data, as indicated in Table 2.1 [29]. Table 2.1 presents a comparison between classification and regression methods based on value, types, mapping, prediction data, evaluation metrics, and sample/example algorithms.

Various methods have been considered for DP including multiple regression, exponential smoothing, iterative re-weighted least-squares, autoregressive moving average (ARMA), ARIMA, adaptive load forecasting, AR stochastic time series, SVM, GA, FL, and NN. A comparison of regression and ML methods for DP was presented in [30]. Gaps in existing research and some research challenges were given in [31]. The performance of supervised ML models including KNN, LR, and RF was considered in [32] for hourly

Table 2.1: Comparison of classification and regression methods [13, 14, 29].

Factor	Classification	Regression
Mapping	Predefined categories	No predefined categories
Values	Discrete	Continuous
Predicted Data Type	Unordered	Ordered
Metric	Accuracy	RMSE
Sample Algorithms	Decision Tree (DT), Linear Programming, Neural Networks (NN), Statistical Methods	Regression Tree (RT), Simple and Multiple Regression, Logistic Regression (LR), Nonlinear Regression

DP using an electricity dataset from Sydney, Australia. It was shown that KNN provides the best performance.

Understanding the merits and drawbacks of regression and classification, and the associated methods and algorithms, is essential to achieving satisfactory DP performance. In [13, 14, 29] it was demonstrated that soft-computing-based DP strategies can yield substantial performance benefits. Furthermore, hybrid methods have gained popularity due to their improved precision and efficiency in solving prediction tasks [13, 14, 29]. These results indicate that ML methods have had a pivotal role in shaping DP strategies.

2.2 Literature Review

2.2.1 ML Methods for DP

In the past three decades, ML methods have received significant research attention across a diverse range of applications [33]. This section examines the use of these methods for DP. Wang et al. [27] used the EBT algorithm for energy DP in buildings on the University of Florida campus with the goal of reducing energy consumption. Chen et al. [24] employed SVR and Multi-resolution Wavelet Decomposition (MWD) for DP of hourly electricity consumption considering data from hotels and malls and the Non-Stationary Operated Building (NSOB) problem for a 24-hour cycle. Li et al. [34] used K-means with a spatiotemporal structure for travel within Shenzhen, China, to investigate transportation demand. Zhou et al. [35] integrated Multi-output SVM (MSVM) and Multi-Task Learning (MTL) for traffic DP in Taipei, Taiwan. Chouikhi et al. [36] leveraged a PSO algorithm based on an effective learning process [37] to tune an Echo State Network (ESN) for time series prediction.

Amasyali et al. [31] employed ML algorithms such as SVM and ANN for energy consumption DP within several types of buildings. Buddhahai et al. [38] introduced a multipurpose classification system with a new learning structure using K-means clustering for high-power load monitoring. DP and load behavior were analyzed to optimize power consumption performance. Ahmadzadeh et al. [39] investigated the application of ML and Deep Learning (DL) algorithms to distributed Smart Grids (SGs) considering security and reliability [40]. The KNN, naïve Bayes, and DT methods were shown to improve

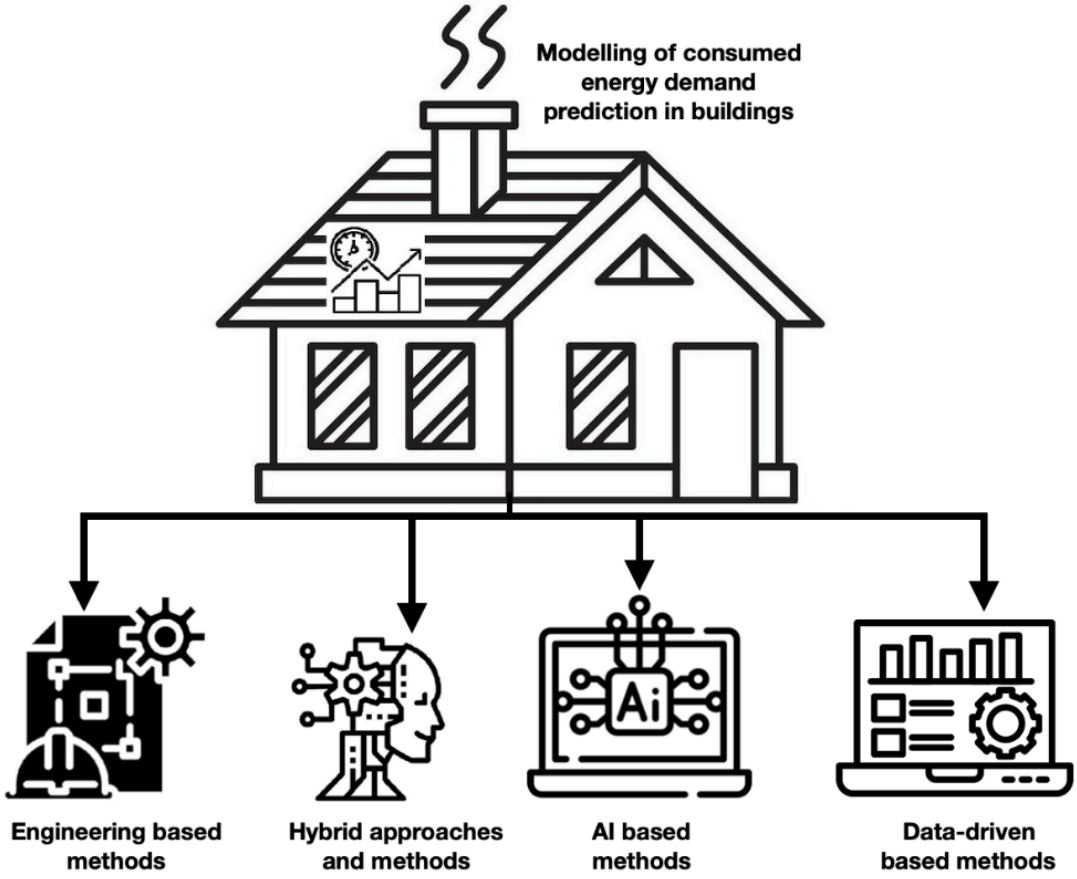

Figure 2.4: Building energy consumption demand prediction (DP) categories [31].

offloading decision accuracy and thus energy efficiency.

ML methods have been employed in various domains, including energy management in malls and hotels [24], energy reduction in buildings [27], heating and cooling demand management [28], property market price analysis [29], and building energy consumption [31]. Other applications include power load analysis [33], urban traffic control [34], time series prediction [36], antenna design [38], adaptive authentication for wireless networks [41], distributed SG performance enhancement [39], energy efficiency [40], and load maintenance and peak shaving in buildings [42].

2.2.2 ML-Based Prediction Methods

Figure 2.3 shows that ML algorithms for DP in buildings can be categorized into engineering-based, AI-based, hybrid, and data-driven methods. Engineering-based methods use thermodynamic principles to model and analyze energy demand, while data-driven methods extract insights from available data [31]. Furthermore, ML-based prediction methods have been developed to improve performance and efficiency.

Johannesen et al. [32] considered ML-based prediction methods including KNN, linear, and RF regression for electricity network load demands. Al Mamun et al. [43] employed DP within power systems for robust load management, including fault prediction. The results obtained illustrate the advantages of hybrid methods. Queen et al. [44] developed an ML model for prediction within IEEE 14 and 30 bus networks. LR and PR models were employed to forecast costs and stabilize voltage in an investigation of the interplay between technology and economics in RESs.

Zhang et al. [45] introduced a self-adaptive and hierarchical methodology for real-time voltage stabilization. A hierarchical power system model was developed that incorporates discrete learning. Luque et al. [46] used historical data and economic factors to anticipate demand in a Spanish electrical network. The power consumption behavior of 27 million users was examined using regression, variance analysis, and categorization based on spatial and cost considerations specific to Spain. The results were used to guide decision making for electricity retailers in the power market. Ahmad et al. [47] examined ML and data mining methods for DP, including ANN, SVM, clustering, and statistical-based methods for energy mapping, profiling, and prediction. The four approaches to energy DP, namely engineering-based, AI-based, hybrid, and data-driven, as shown in Fig. 2.4, were considered [31].

2.2.3 Validation in DP

Management of energy consumption within Micro-Grids (MGs) plays a pivotal role in the evolution of SGs and Smart Buildings (SBs). Real-time prediction and load scheduling are critical to leveraging the tradeoff between energy demand and cost. This requires validation to substantiate results and corroborate assertions. For example, Queen et al. [44] used Cross-Validation (CV) to select a suitable model. Also, Godinho et al. [9] used MAE and RMSE for model evaluation, while while Shahriar et al. [48] employed K-fold CV for Electric Vehicle (EV) charging prediction. Dataset testing and model validation to evaluate ML models' accuracy were conducted in [49]. Sajjad et al. [50] proposed a hybrid ML-based energy DP model that combines CNNs with Gated Recurrent Units (GRUs). Testing and validation within a two-tiered structure were conducted to ensure accurate electricity consumption prediction.

2.2.4 MB Features

Smart and environmentally conscious MBs are being designed to provide a variety of features catering to both building owners and inhabitants. The focus is on sustainable buildings (SUBs) [51, 52] that incorporate elements such as intelligent, automated, and adaptable management systems, indoor climate regulation, and energy-efficient measures. However, the promise of SBs has yet to be realized [53].

Market adoption in the context of SGBs (see its characteristics in Fig. 2.6) was explored in [54]. It was argued that this depends on how users perceive the benefits. For example, enhanced energy management can result in diminished control over building opera-

tions. MBs share many features with SBs including advanced HVAC systems, sophisticated information processing capabilities, and comprehensive Building Management Systems (BMS) [55].

2.2.5 MB Components

MBs employ components from advanced HVAC systems to responsive BMSs. They play a vital role in realizing the vision of a sustainable and intelligent future. These components are discussed below.

Building Heating and Cooling Systems

The solutions proposed in [56] not only contribute to improvements in building electrical systems and their components, but also facilitate user energy savings, particularly when coupled with RESs [57]. Furthermore, the adoption of effective policies and solutions [58] plays a crucial role in stabilizing and reducing GHG emissions. The energy performance assessment of buildings conducted by the EC [59] from 2010 to 2018 illustrates the steps being taken [60] and the tradeoffs between economic growth, urban building energy consumption, and economic outcomes. A significant percentage of building heating and cooling systems have sub-optimal efficiency. It was shown in [61] that over 80% of GHG emissions are from such systems. This necessitates examining the energy demands associated with HVAC systems, as well as the heating and lighting requirements [61], [62]. Thermostatically controlled loads (TCLs) including air conditioners, hot water storage tanks [63], and water heaters have emerged as promising and adaptable resources to meet energy demands. TCLs are Flexible Loads (FLs) that can be used to reduce the effects of power consumption fluctuations on thermal generators [64].

Technologies such as traditional and pulsating heat pipes have been shown to improve the energy efficiency of HVAC systems [65] via efficient heat exchange [66]. Pulsating heat pipes provide high thermal conductivity and can rapidly and efficiently cool building components [67]. Heat pipes are an important component of building heating and cooling systems to improve energy conservation and reduce GHG emissions.

Component Integration with SGB Technologies

Fig. 2.6 illustrates the SGB concept, which includes sustainable site practices, water-efficiency measures, energy and atmospheric considerations, material and resource strategies, indoor environment quality enhancements, and innovative design processes. The SB concept includes the Voice over Internet Protocol (VoIP), data networks, video-distribution mechanisms, wireless systems, robust cabling infrastructure, HVAC control systems, power management solutions, programmable elements, lighting controls, and comprehensive facility management. The shared traits are energy optimization, enhanced performance, supplementary commissioning, precise measurement and verification, carbon dioxide monitoring, adaptable system control, and continuous monitoring. They allow SGBs to attain energy savings, reduce their environmental impact, and provide healthier and more

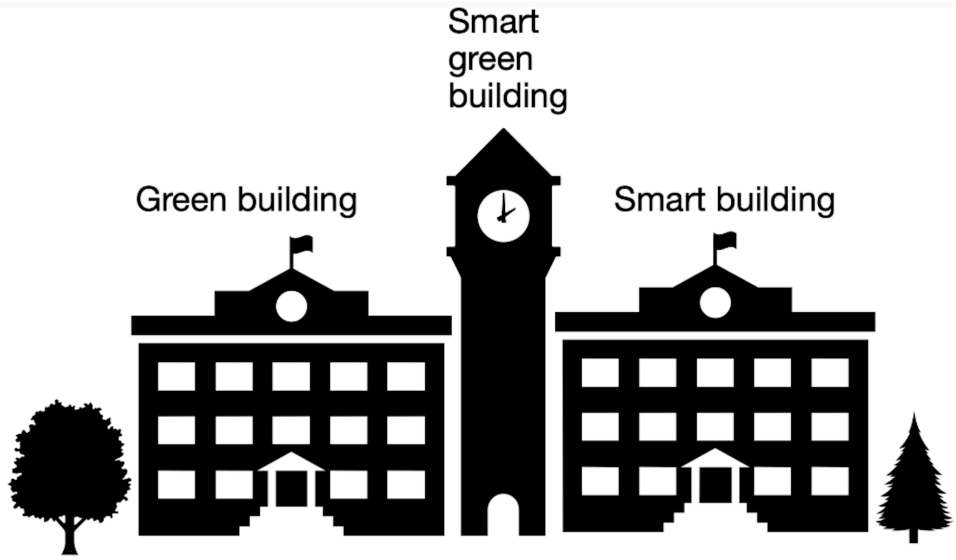

Figure 2.5: The SGB characteristics [17].

comfortable living and working environments for occupants. Figure 2.5 illustrates that Smart Green Buildings (SGBs) combine the key characteristics of both green buildings and smart buildings, integrating their features and characteristics into a unified framework. FLs can be used to mitigate the challenges associated with DR. They allow power consumption management within designated time intervals [63, 64]. Moreover, TCLs can be used to reduce energy consumption during peak periods. This is important as electricity consumption within MBs is projected to outpace the growth in energy generation, thereby increasing the discrepancy between supply and demand [68]. To address this problem, RESs and MGs have emerged as solutions to improve local reliability, energy management [69], and network efficiency [70]. Amir et al. [71] examined the integration of SBs and GBs. SBs were shown to be well suited to improving energy efficiency in [70]. The International Data Corporation (IDC) has reported an increase in the number of SBs from 6.3 billion in 2014 to 17.4 billion in 2019 [71]. System automation and control in SBs can lower life-cycle expenses [72, 73], and distributed energy resources (DERs) and MGs can be used to satisfy user needs via energy-management tools. SB lighting solutions have been shown to reduce energy consumption by 50% [72, 73]. GBs and SBs are complementary components of SGBs [55]. SBs improve the performance of GBs while GBs improve the intelligence of SBs. GBs represent a holistic approach to constructing and operating environmentally conscious and resource-efficient structures, encompassing all stages from siting and design to construction, operation, maintenance, renovation, and eventual deconstruction. This augments the traditional focus on economic viability, utility, durability, and comfort within buildings [70, 74]. The BMS is a key component of SBs and GBs. It was shown to provide up to 30% energy savings by monitoring, measuring, and optimizing building performance [70, 72]. The BMS controls diverse functions including HVAC systems, chillers, and lighting management [72, 73].

2.2.6 DP in MBs

Efforts to address the challenges with MBs center around effective management of power supply and consumption using techniques such as peak shaving, load reduction, DP, and efficiency models [75, 76, 77]. Numerous methods have been proposed for SGBs and MG systems [1, 78]. Mohammed et al. [79] considered Mixed-integer Linear Programming (MILP) for Economic Dispatch (ED) with grid-connected MGs to reduce operational costs and thermal energy usage. Smith et al. [80] used DP to improve the efficiency and performance of multi-carrier MG systems. A multi-carrier MG system provides more flexible, efficient, and intelligent energy management to lower costs and decrease thermal energy consumption. Kamal et al. [81] used MGs to optimize distribution network energy management. These approaches employ mechanisms such as DR, load shifting, energy storage, grid integration, predictive maintenance, and renewable energy integration. Multiple MGs have been used to enhance system operation and reliability via improved energy consumption decision making [82, 83]. In [8, 9, 76], SGBs were shown to improve energy efficiency and performance while reducing energy consumption. Homaei et al. [84] considered robust high-performance building designs in smart cities considering climate and occupant uncertainties. An energy-management system using an aggregator, MILP Model Predictive Control (MPC), and Q-learning for an SB was proposed in [85] considering uncertainties in real-time data. Wang et al. a [27] employed a homogeneous ensemble prediction model for energy demand in an institutional building. Ding et al. [86] used a model to analyze the energy consumption in GBs in China by leveraging payment data. Load prediction for GBs was investigated in [87]. Historical data were used in an energy management system (EMS) to improve performance considering energy storage. Masburah et al. [88] estimated real-time uncertainty in building loads using Gaussian Process (GP) learning. GBs with MGs were examined in an ED context.

Analytic Hierarchy Process (AHP)

The analytic Hierarchy Process (AHP) [89] has emerged as an invaluable tool in understanding the impact of SGB innovations, particularly in the context of decision making. Gluszak et al. [72] studied the impact of SGB innovation on real estate markets using the AHP [90]. This shows the AHP method is relevant for DP in MBs. The prediction accuracy is based on three factors on the following. The prediction method, the data quality, and the amount of data. A suitable prediction method combined with sufficient high-quality data can yield precise and dependable building performance prediction, including energy consumption for heating and cooling. The AHP is important as it aids in the assessment and prioritization of these factors, enabling more informed and effective decision making.

2.2.7 ML Methods Applied in MBs

ML methods such as ANN and RNN, and DL models such as Unidirectional LSTM (ULSTM) and bidirectional LSTM, have been used for energy DP to improve the accuracy, robustness, and efficiency of MB modeling [9, 27, 67, 77, 91, 92, 93, 94]. In [93], Olu-Ajayi

et al. considered ANN, RL, and decision algorithms for energy storage, cost reduction, management, and DP. RNNs, ULSTMs, and bidirectional LSTMs were used in hybrid DL models to forecast energy demand in [68]. It was shown that bidirectional LSTMs can effectively capture energy consumption patterns in SGBs.

Amasyali et al. [31] used ML models such as ANN, GB, Deep NN (DNN), RF, KNN, SVM, DT, and LR for energy consumption prediction in residential buildings using a large residential dataset. DNN was shown to be the best model, especially in forecasting annual building energy consumption. Godinho et al. [9] examined ML methods such as LR, PR, ANN, and SVM for SB cost reduction and performance improvement. They determined that ANNs provide a 10–20% improvement in forecasting heating demand compared to other methods. Zhao et al. [77] used the commercial solver MOSLEK 8.1 in MATLAB to obtain good MG accuracy with computational and operational efficiency while providing a cost reduction. Peng et al. [95] studied Bayesian Regularization (BR), Levenberg–Marquardt (LM), and ANN methods for commercial and residential building load forecasting. They evaluated the accuracy over different time periods and determined that ANNs provide the best day-ahead and hour-ahead forecasting results. Lu et al. [96] adressed DR in home energy management systems (HEMS) using RL and ANN methods [97]. Price and user energy cost prediction, smart home performance, and controllable and non-controllable loads were examined. Dagdugui et al. [8] employed an NN and learning algorithms for load forecasting.

Table 2.2 presents a performance comparison of ML algorithms considering eight metrics. Tables 2.3 and 2.4 present a comparison of research and review papers selected based on their relevance and importance. They provide a comprehensive perspective on the methods employed in the literature and indicate that AI systems play a pivotal role in the MBs, facilitating advanced automation, optimization, and decision making. Figure 2.6 shows that these systems within the MBs contribute to improved energy efficiency and occupant comfort, increased safety and security, and more effective facility management [44, 75].

Based on Table 2.2 Most algorithms perform well in terms of accuracy and energy consumption, but many are lacking in areas such as training speed and cost efficiency. The work in the current study (”This work” in Tables 2.2, and 2.4) shows superior performance across all metrics, indicating a more comprehensive and balanced approach.

Table 2.2: ML algorithm performance comparison.

Reference	Computation Time	Accuracy	Efficiency	Energy Consumption	Cost	Uncertainty	Reliability	Training Speed
[8]	-	✓	✓	✓	-	-	-	-
[17]	✓	✓	-	✓	-	✓	-	-
[19]	-	✓	✓	✓	-	✓	-	-
[27]	✓	✓	-	-	-	-	-	✓
[28]	-	✓	-	-	-	-	-	-
[63]	-	-	-	✓	-	-	-	-
[66]	✓	✓	-	✓	✓	✓	-	-
[77]	✓	✓	✓	✓	✓	-	✓	-
[84]	-	-	✓	✓	✓	✓	-	-
[92]	-	✓	-	✓	✓	✓	-	✓
[93]	-	✓	✓	✓	-	-	-	-
[95]	-	-	-	✓	-	-	-	-
[96]	-	-	-	✓	✓	-	-	-
[98]	-	-	-	✓	-	-	-	-
[99]	✓	✓	-	✓	-	-	-	-
[100]	-	✓	-	✓	✓	-	-	-
[101]	-	✓	-	✓	✓	✓	-	-
This work	✓	✓	✓	✓	✓	✓	✓	✓

Table 2.3: Comparison of ML methods.

ML Methods	Ref.	Year	Model Components	Objectives
BR, LM, ANN	[8]	2019	SCRB	Building energy forecasting using an NN model
RT	[17]	2019	SBRS	Hybrid ML model (ARIMA, logistic regression, ANN) for peak load forecasting
Extreme GB, Bayesian optimization	[19]	2023	RES, PV-driven air conditioner	Real-time energy DP
EBT	[27]	2018	BMS	Stability and prediction
SVM, MLP, CNN, DT, RF	[28]	2018	Autonomous car	Road image recognition
ADWIN, FSA, DDM	[99]	2020	RB	Automated modeling of residential appliances
ANN	[30]	2020	Bicycle sharing station	Hybrid ML for bicycle-sharing DR
Online algorithms	[63]	2017	HVAC system in an SB	Real-time occupancy prediction for building automation
Hybrid DL	[66]	2014	SGB	Grid frequency regulation in a commercial building
Two-stage robust optimization	[77]	2018	DER, NMG	Improving power system resilience
MPC, Q-learning	[85]	2022	ESS, Aggregator, SB	Energy management of residential resources (TCLs, PV systems, EVs)
ANN, RL	[92]	2021	SS, HEMS, RES	Reducing energy cost, customer dissatisfaction, and grid overloading
ANN, GB, DNN, RF, Stacking, KNN, SVM, DT, LR	[93]	2022	RB	Predicting annual building energy consumption
RL	[95]	2020	SH	Adaptive home automation for energy DP
RL, ANN	[96]	2019	HEMS	Hour-ahead DR
CNN, ANN	[98]	2017	RB	Energy load forecasting
Hybrid models	[100]	2019	DER, MG	Energy system analysis using a taxonomy of models and applications

Table 2.3 shows the diversity in ML approaches applied to energy and building-related challenges. For instance, studies using NNs often focus on energy forecasting, while hybrid models are commonly used for optimization in complex energy systems. The use of modern ML techniques has expanded significantly in recent years, indicating growing interest and development in the field.

Table 2.4: ML in MBs.

Reference	Applications	Objectives	Year
[1]	RBs	Net-zero-energy building optimization and design	2021
[19]	SBs, SGs	DP analysis and optimization with a hybrid ML model	2023
[43]	SBs, SGs	Load forecasting with a hybrid ML model	2017
[59]	SBs, smart cities	Energy savings and efficiency	2020
[73]	SBs	ML method and big data analytics evaluation	2019
[88]	SGBs	Analysis of SUB features, e.g., automation	2019
[97]	Buildings	Building energy use forecasting using NNs	2019
[100]	Energy systems	ML models for energy systems and their applications	2019
[101]	SBs	Crowdsourcing for fault detection	2017
[102]	SBs	HEMS for energy reduction	2018
[103]	Mobile multimedia	Soft/hard frameworks	2017
[104]	Non-residential buildings	Energy analysis and optimization	2017
[105]	Commercial buildings	Electricity load forecasting	2017
[106]	GBs	Construction cost prediction	2022
[107]	SBs, smart cities	Intelligent environment evaluation	2018
[108]	SBs	DRL for energy management	2021
[109]	SB control	RL for energy and security control	2020
This work	MBs, energy systems	ML methods evaluation	2023

In Table 2.4, ML is extensively used for optimizing energy consumption and improving building efficiency in both residential and commercial settings. The variety of applications (e.g., net-zero buildings, fault detection) shows that ML techniques are integral in advancing sustainable and intelligent building management systems.

2.2.8 Materials and Technologies for Energy Efficient Buildings

The selection of appropriate materials and technologies is important for sustainable and energy-efficient building design [110]. Innovative solutions are required to reduce energy consumption and the environmental impact. Hybrid Multiple-Criteria Decision Making (MCDM) [111] has been shown to be an effective methodology for assessing and selecting materials that align with energy efficiency objectives. It combines decision-making techniques to evaluate multiple criteria and the tradeoffs in material selection. MCDM provides a systematic framework to prioritize materials based on factors such as thermal performance, durability, cost-effectiveness, and environmental sustainability. In [112], a hybrid MCDM model was proposed to evaluate polymeric materials for flexible pulsating heat pipes. This contributes to the use of energy-efficient building materials and technologies by providing valuable insights for architects, engineers, and stakeholders in

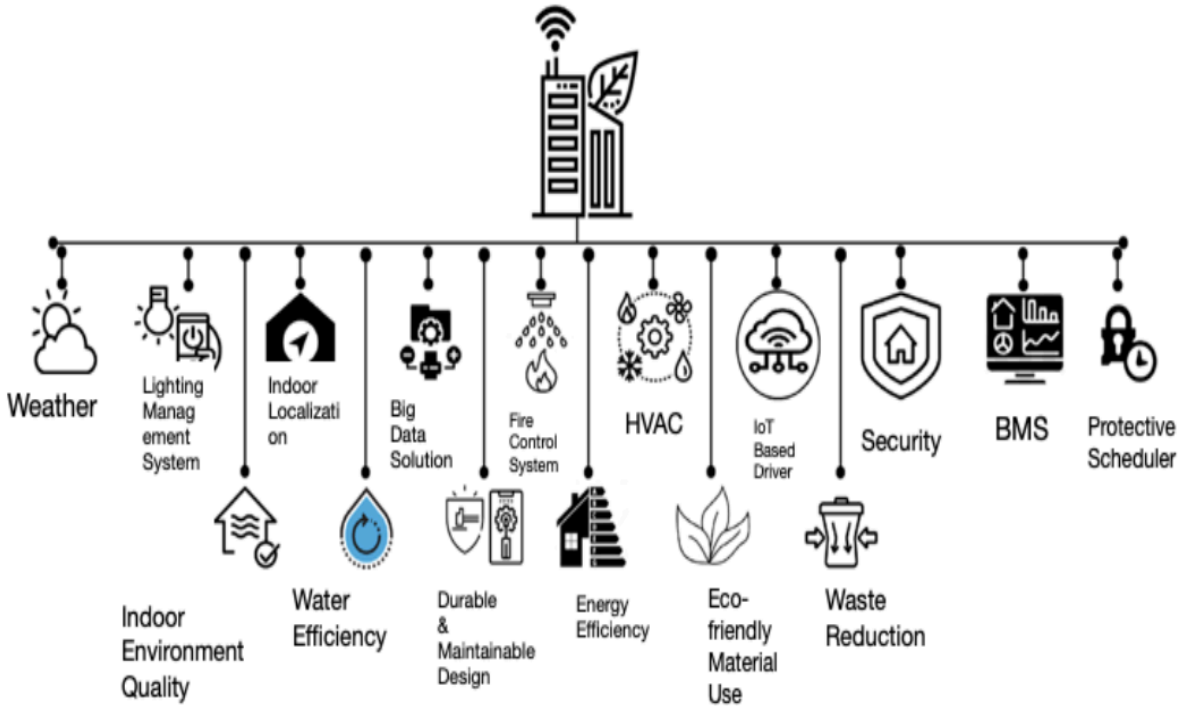

Figure 2.6: Artificial Intelligence (AI) system components in MBs [44, 75].

the construction industry. Hybrid MCDM has also been employed with ML methods for building applications [110, 111, 113].

Model ML offers a variety of models for SB tasks such as DP, energy optimization, and fault detection. Hybrid MCDM can be used to evaluate ML models and select the most appropriate one for a building-related task based on criteria such as accuracy, interpretability, computational cost, and available data.

Feature Selection Feature engineering and selection are crucial in building ML models. Hybrid MCDM can help choose the best set of features (variables) for a prediction or optimization task in a building context. This can lead to more efficient and accurate models.

Algorithm Tuning ML algorithms have hyperparameters that need to be tuned for optimal performance. Hybrid MCDM can aid in selecting the best hyperparameter values considering the performance metrics and constraints specific to building applications.

Data Preprocessing Building datasets can be complex with various types of data, e.g., sensor, weather, and occupancy data. Hybrid MCDM can guide decisions on data preprocessing such as handling missing data, data scaling, and outlier detection to ensure high-quality data for ML models.

Ensemble Methods Ensemble ML models are often employed to improve prediction performance. Hybrid MCDM can be used to determine the best ensembles considering

the strengths and weaknesses of individual models.

Model Evaluation Hybrid MCDM can assist in evaluating the performance of ML models. This includes the selection of appropriate evaluation metrics, e.g., MAE, RMSE, and F1-score, and weighting them based on their importance in the context of building applications.

Risk Assessment In building management, there may be risks associated with ML approaches. Hybrid MCDM can help in assessing these risks and making decisions that balance factors such as accuracy, robustness, and potential negative impacts.

Energy Optimization ML is commonly used for energy optimization in SBs. Hybrid MCDM can assist in choosing the right ML methods to optimize energy consumption considering factors such as building type, occupancy patterns, and available technologies.

In summary, hybrid MCDM can enhance the use of ML methods in building-related tasks by assisting in model and feature selection, algorithm tuning, and evaluation. This will help ensure that ML solutions are tailored to the specific requirements and constraints of SB applications, leading to more effective and efficient building management.

2.2.9 Datasets

It has been demonstrated that model accuracy depends on the method employed as well as data quality and quantity [97]. Thus, the availability of real historical datasets is important for effective building models. In [68], hybrid ML methods were used with two real energy consumption datasets to forecast energy consumption in SBs considering the appliances. ML was employed in a real hospital dataset in [49] for prediction and treatment purposes. In [9], a one-year real historical dataset with hourly measurements of occupancy profiles, solar gains through glazing, outdoor dry-bulb temperatures, and heating and cooling fluid temperatures was considered.

2.3 Conclusions

This chapter examined ML methods for energy management prediction in MBs. It was observed that hybrid and ensemble ML methods such as Support Vector Machines (SVM) combined with RF outperform single prediction models. In particular, hybrid ML models can achieve up to 15% higher accuracy in energy consumption prediction than single ML models. The results presented show that ML methods can be used for accurate and efficient energy management in MBs. Furthermore, incorporating additional attributes in the dataset can improve energy prediction accuracy and efficiency.

Chapter 3

Resource Optimization for Grid-Connected Smart Green Townhouses Using Deep Hybrid Machine Learning

Resource optimization in Smart Buildings (SBs) has advanced significantly with a focus on efficiency, performance, and cost reduction while minimizing emissions [1, 2, 5, 114, 115]. Integrating Renewable Energy Sources (RES) such as Photovoltaic (PV) systems is essential for sustainable energy use in cities. Predictive analytics and supportive energy policies also play vital roles in SB optimization [116, 117, 8]. Studies show that Smart Grid (SG) integration can lower costs, reduce emissions, and improve building performance [9, 11, 118]. Connected Smart Green Buildings (CSGBs) aim to increase resource efficiency and sustainability. They utilize advanced technologies and RES to achieve economic and environmental benefits [12, 13, 14].

Buildings contribute significantly to energy use and emissions. For instance, the U.S. building sector accounted for 32% of primary energy use in 2019, with similar trends in other countries [97, 119, 120]. Improving efficiency is crucial for lowering Greenhouse Gases (GHGs) and costs. In the EU, a 20% increase in building efficiency can save around 60 billion Euros annually [121]. Managing energy use in buildings can help address climate change. There is a need for advanced Heating, Ventilation, and Air Conditioning (HVAC) systems and predictive energy strategies to improve SB efficiency [122, 123, 124]. Data-driven energy management systems can further optimize energy use.

Machine Learning (ML) and predictive analytics enable real-time control and adaptability for SBs [125] to increase efficiency, lower emissions, and provide accurate energy predictions. ML-based models such as Long Short-Term Memory (LSTM) and Convolutional Neural Networks (CNN) can improve energy management in grid-connected buildings [122, 123, 124, 125]. This chapter introduces a deep hybrid LSTM-CNN model for resource optimization in CSGBs. This model improves resource use and aligns with sus-

tainability goals. Cross-sector collaboration is key to advancing sustainable practices for CSGBs. The focus here is on optimizing energy use in grid-connected CSGBs [126, 127].

The remainder of chapter 3 is organized as follows. Section 2 presents the CGST model. Sections 3.3 and 3.4 present the model details, results, and insights on energy optimization for a sustainable future. Finally, Section 5 gives some concluding remarks.

3.1 CSGT Modeling

This section presents the CGST model emphasizing effective technology-driven solutions. SGBs provide a sustainable architecture by merging advanced technology with eco-friendly design [128]. Energy modeling is essential in sustainable construction as it helps predict building performance and balance resource efficiency with environmental goals while prioritizing occupant well-being.

Grid-connectivity is a key aspect of this work as it enables dynamic energy optimization by utilizing real-time data from the grid for better load balancing and demand response. This mode integrates RESs like PV systems with the grid to ensure a stable supply when RESs are insufficient. It enhances operational efficiency by allowing for the sale of excess renewable energy and optimization based on time-of-use pricing. Grid-connected model also supports scalability, providing a foundation for smart communities with microgrids and energy hubs.

3.1.1 Climate

This chapter considers the energy and climate challenges in Canada, focusing on the unique environment of Burnaby, BC. The impact on load consumption and energy optimization in smart and green buildings is examined. Understanding the climate is crucial for designing SGTs [125, 129, 130, 131].

Fig. 3.1 gives the average daylight hours (blue bar) which is the time from sunrise to sunset each month. This shows how long the sun is above the horizon, regardless of the weather. Also given are the sunshine hours (orange bars) which are the actual hours of sunlight without obstruction. These hours are typically less than daylight hours due to clouds or rain. Fig. 3.1 indicates that maximum daylight occurs in June with 16.02 hours and the minimum occurs in December with 8.03 hours.

Heating Degree Days (HDD) are used to estimate the energy needed to heat buildings based on outdoor temperatures. HDD measures how much and for how long the outdoor temperature is below 18°C, indicating when heating is needed. The unit is °C·days. Architects and engineers use HDD to design heating systems and improve resource efficiency. Utilities use HDD to predict heating fuel demand and manage supply. By understanding HDD trends, energy use can be optimized, reducing emissions and enhancing sustainability. Fig. 3.2 shows the climate zones in BC based on HDD which are crucial for climatic analysis. HDD provides vital data for designing efficient heating systems in the proposed SGTs.

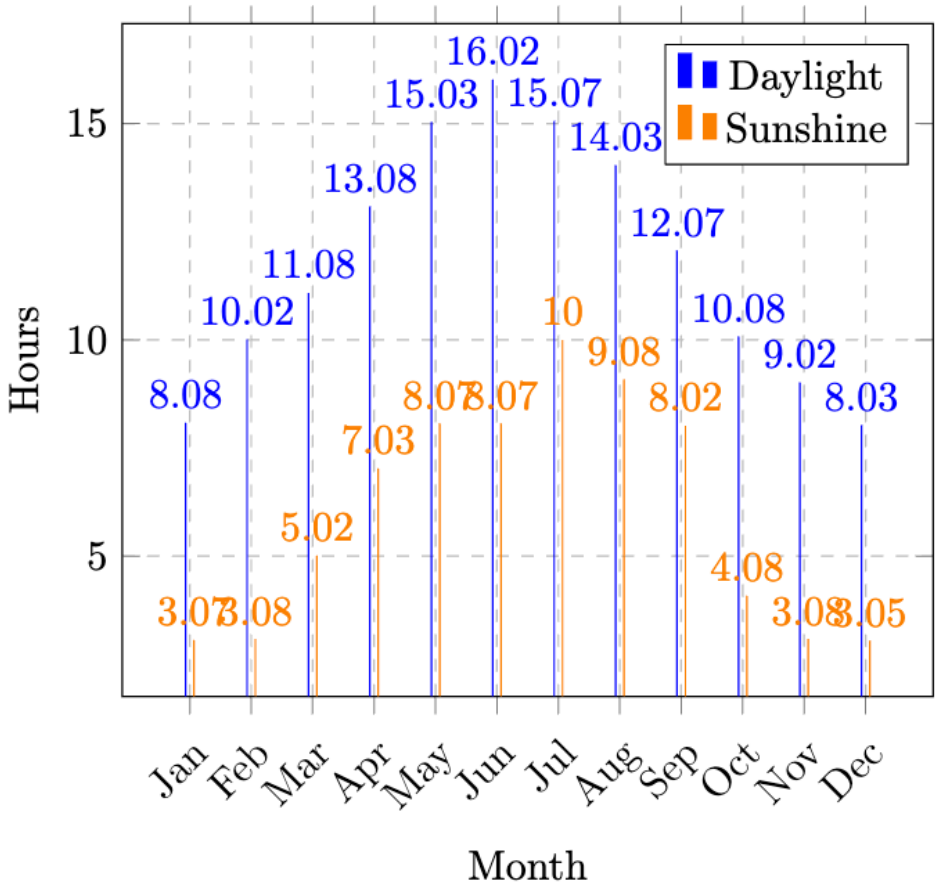

Figure 3.1: Average daylight and sunshine in Burnaby [131] during January to December 2023.

3.1.2 SGT Formulation

This work considers a characteristic home from [128, 132, 133], with slight modifications for a one-story townhouse in Burnaby. The base model is a two-story townhouse (2,140 sq ft) built in 1995 and renovated in 2007-2008 [128]. Major renovations typically occur every 15-20 years. The home is oriented south to enhance resource efficiency. The 1-Bd SGT is for a young couple in their 30s without children. The 2-Bd SGT is for a couple in their late 30s with one child. The 3-Bd SGT is for a couple in their early 40s with two teenage children. The 4-Bd SGT is for a mature couple in their mid-40s with a family of five.

Leadership in Energy and Environmental Design (LEED) certification and Canada Green Building Council (CGBC) standards are crucial for resource efficiency and emission reduction [128]. The approach focuses on limiting emissions by using electricity as the sole energy source and installing PV systems for net-zero energy [134]. This eliminates on-site fossil fuel usage. Surplus electricity can be exported to neighbors during sunnier months. Neighbors with their own PV systems may also generate excess energy, particularly during

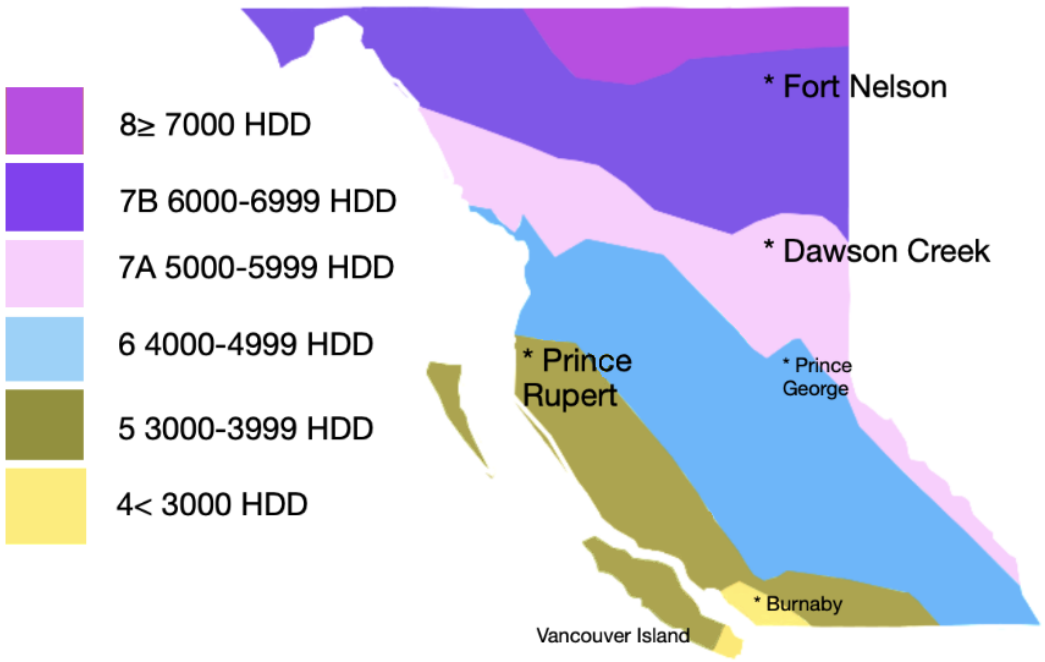

Figure 3.2: BC climate zones based on Heating Degree Day (HDD) [13].

peak sunlight hours.

Table 3.1 lists the sustainable materials and components used for SGTs in Canada [124]. Each is selected for its eco-friendly properties and contribution to sustainable living. Many are already widely used in sustainable buildings globally. Bamboo flooring is renewable, durable, and aesthetically appealing. Recycled and reclaimed wood are commonly used for structural and decorative purposes, promoting waste reduction and resource conservation. PV panels, LED lighting, and heat pumps are essential for energy-efficient buildings. They are employed in residential and commercial buildings and GBs [135, 136, 137]. They meet local and international codes for sustainability, resource efficiency, fire safety, and structural integrity [138, 139, 140] including LEED and Building Research Establishment Environmental Assessment Method (BREEAM) standards.

Having both air conditioners and heat pumps in SGB designs ensures efficient temperature control year-round, saving energy and reducing environmental impact [141, 142]. Heat pumps transfer heat rather than generate it, making them more energy-efficient than traditional heating systems. They can provide both heating and cooling, reducing the need for separate systems. As heat pumps use electricity, they help reduce GHG emissions. High-efficiency air conditioners are better suited for extreme cooling needs. Modern air conditioners, especially those connected to smart systems, allow remote control and optimized cooling cycles for energy reduction [141, 142]. This work considers R6 windows that reduce heat transfer and improve insulation, thus lowering energy consumption for heating and cooling [124]. This conforms with the R2000 program, a Canadian energy

Table 3.1: The sustainable materials and components of SGTs.

Material	**Properties**
Bamboo Flooring	Renewable, durable, and eco-friendly.
Recycled Wood	High strength, recyclable, and long-lasting.
Recycled Glass Countertops	Eco-friendly, durable, and visually appealing.
Cork Wall Insulation	Renewable, lightweight, and excellent insulation.
Reclaimed Wood	Recycled, unique aesthetic, and reduces deforestation.
PV Solar Panels	Renewable energy source (RES), reduces electricity costs.
Low Volatile Organic Compounds (VOC) Paints	Low VOC content reduces indoor air pollution.
Rainwater Harvesting System	Collects rainwater for landscape irrigation.
Light Emitting Diode (LED) Lighting	Energy-efficient, long-lasting, and reduces electricity consumption.
Recycled Insulation Materials	Utilizes recycled materials for thermal insulation.
Hot Water Tank	Efficient water heating with insulated storage.
Heat Pump	Energy-efficient heating and cooling.
Smart Home (SH) Hub	Connects and manages smart devices, facilitates remote monitoring without necessarily implementing automation features.
Air Conditioner	High-efficiency cooling system.
Smart Meters	Monitors and optimizes resource consumption.
Smart Plugs	Enables remote control and energy monitoring.
Smart Thermostat	Programmable and energy-efficient temperature control.
Connected Appliances	Appliances with internet connectivity for remote monitoring and control.
Envelope & Structural Mass	Enhances building insulation and thermal mass for resource efficiency.
R6 Windows	High-performance windows with an insulation value of R6, reducing heat loss and improving resource efficiency.

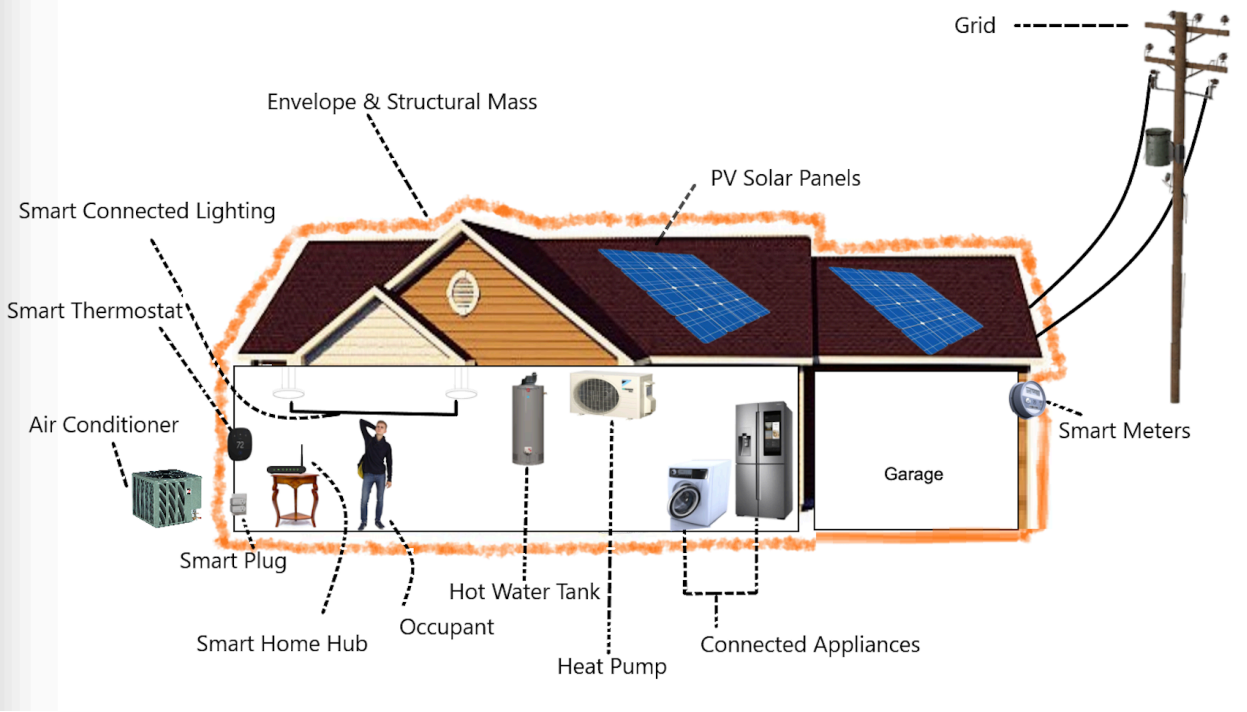

Figure 3.3: SGT components in grid-connected mode.

efficiency standard [143]. Fig. 3.3 shows the SGT components in grid-connected mode. An HVAC system performance model based on [123, 143, 144] is employed here.

Connecting Townhouses for Improved SGTs

Connecting residential buildings reduces resource consumption and costs [145]. This is crucial in SGTs to lower load consumption, lower costs, and improve efficiency. Connected buildings enable more efficient energy management [145] as they form a single unit similar to Micro-Grids (MGs) [37, 146]. CSGTs in grid-connected mode are considered to reduce electricity consumption, improve demand response, and enhance overall performance. The building consists of four connected townhouses (1, 2, 3, and 4 bedroom CSGTs). Grid connection adds to the system complexity. In this work, the challenges, and solutions related to load consumption in SGTs connected to the grid are examined [145]. The advantages of connecting SGTs include reduced resource consumption, lower costs, improved efficiency, and load optimization. These benefits demonstrate how connected systems contribute to sustainable and efficient SGBs.

Real datasets for connected townhouses include two key components on the following. Connected water systems [128, 147] and party walls [148, 149]. Party walls are shared walls between adjacent properties and are commonly found in townhouses. They are jointly owned and maintained by property owners. Agreements for party walls outline the responsibilities for maintenance, repairs, alterations, and dispute resolution. Connected townhouses depend on these walls for structural integrity, noise reduction, fire safety, and boundary responsibilities. Connected water systems are also crucial for building

performance and occupant comfort [147]. This work investigates the operational aspects of district cooling systems in connected buildings [147]. These systems distribute chilled water to multiple buildings which improves resource efficiency. Resource consumption, temperature management, and system efficiency are examined as well as how building operations impact cooling infrastructure performance.

CGST Formulation

CGST formulation is based on the results in [150, 151]. The heat transfer is given by

$$Q = k \cdot A \cdot \frac{\Delta T}{d} \tag{3.1}$$

where Q is the heat transfer rate, k is the thermal conductivity of the wall material, A is the surface area of the wall, ΔT is the temperature difference across the wall, and d is the thickness of the wall. Equation heat transfer describes conductive heat transfer where thermal energy moves through a solid material. The heat transfer rate is proportional to the thermal conductivity of the material and the cross-sectional area through which the heat moves. It also depends on the temperature difference across the material. However, the rate is inversely proportional to the thickness of the material. This is important for designing energy-efficient systems such as insulation in buildings.

The continuity is

$$\frac{d(\rho A)}{dt} = \dot{m}_{\text{in}} - \dot{m}_{\text{out}} \tag{3.2}$$

Equation (3.2) indicates that the rate of change of mass (ρA) within the volume is equal to the difference between the mass flow rate entering $(\dot{m}_{\text{in}})$ and leaving $(\dot{m}_{\text{out}})$ the system. This is used to analyze fluid behavior in pipes, ducts, and other systems.

The resource consumption is given by

$$\text{Minimize C} = \sum_{i=1}^{n} \text{C}_i \tag{3.3}$$

Equation (3.3) is the sum of the consumptions C_i across different components, systems, or time periods. The goal is to optimize the conditions such as temperature settings and flow rates to minimize consumption while maintaining comfortable temperature levels and ensuring adequate flow rates. The building energy balance is

$$\text{Energy In} - \text{Energy Out} = \text{Energy Storage} \tag{3.4}$$

where in Equation (3.4), Energy In is the total resource consumption and PV output. This includes electricity (lighting, HVAC), gas, and water use. PV output is part of Energy In as it reduces the need for external energy. Energy Out consists of heat loss, heat gain, and total resource consumption output. Heat loss occurs through walls, windows, and the building envelope, while heat gain is the reverse. Total resource consumption output includes energy used by internal systems like HVAC, lighting, and appliances.

Energy Storage refers to changes in energy storage within the building, both internally and externally.

Renewable Energy Integration (REI) refers to the incorporation of RES into the building energy system

$$\text{REI} = \frac{\text{Renewable Energy Used}}{\text{Total Energy Consumption}} \times 100\% \tag{3.5}$$

where in this equation, Renewable Energy Used is the energy derived from renewable sources like PV panels, and Total Energy Consumption is the resources consumed by the building. This provides a quantitative measure of how much of the building resource consumption is being met by RESs. A higher REI indicates a greater reliance on RES. This is desirable to reduce the building carbon footprint and achieve sustainability goals.

The Smart Technology Utilization Index (STUI) is a metric used to quantify the effectiveness and efficiency of smart technology implementation in a building and is given by

$$\text{STUI} = \frac{\text{Number of Smart Devices}}{\text{Total Devices}} \times 100\% \tag{3.6}$$

where Number of Smart Devices is the number of smart devices used in the buildings and Total Devices is the number of devices in the buildings.

Table 3.2 gives a detailed breakdown of the specifications for SGTs ranging from a Base townhouse with 1 bedroom (1-Bd) to a large townhouse with 4 bedrooms (4-Bd). It provides parameters such as bedroom sizes, living spaces, and total area. Table 3.2 summarizes the key energy system parameters for SGTs. Water Heating Demand is the energy required for daily hot water use (kWh/day) and varies with the number of bedrooms and expected water consumption. HVAC System Capacity is the required HVAC capacity (kW) to maintain indoor comfort and varies by townhouse size and layout. Solar PV Capacity is the installed capacity (kW) of the PV panels. This data is used in OpenStudio 3.8.0 to evaluate energy performance and optimize the design for energy-efficient GBs.

Accurate resource consumption modeling depends on the floor plan, building size, and height as in Fig. 3.4 and Table 3.2. Floor plans show the building layout, including bedrooms, kitchen, living room, bathrooms, and storage. Building size and height reflect the volume and capacity of the building, which affect energy needs for heating, cooling, and ventilation. Townhouse sizes are measured in square feet (sq ft).

3.1.3 Experimental Setup

This work employs data collection and software tools to create and test models. Data collection involves building, resource consumption, and weather data. These were gathered through sensors placed within the building. The OpenStudio software 3.8.0 was used for energy simulation by creating virtual building models for resource consumption scenarios and efficiency solutions. Python v3.11.5 [152] was used for energy optimization, with pandas v2.1.1 for data manipulation, NumPy [153] for numerical calculations, and

Table 3.2: The SGT specifications.

Parameter	Base	1-Bd	2-Bd	3-Bd	4-Bd
Bedrooms	1	1	2	3	4
Bathrooms	1	1	2	3	3
Kitchen Size (sq ft)	60	80	100	120	150
Dining Room Size (sq ft)	40	60	80	100	120
Living Room Size (sq ft)	160	120	150	200	250
Entrance Space Size (sq ft)	30	40	50	70	90
Deck Size (sq ft)	40	60	80	120	150
Bedroom 1 Size (sq ft)	100	120	120	120	120
Bedroom 2 Size (sq ft)	N/A	N/A	120	120	120
Master Bedroom Size (sq ft)	N/A	N/A	150	200	250
Second Master Bedroom Size (sq ft)	N/A	N/A	N/A	150	200
Garage Size (sq ft)	N/A	None	None	154.1	173.8
Height (ft)	8.0	16.5	16.5	16.5	16.5
Total Size (sq ft)	680.0	764.4	1080.0	1543.0	1735.9

Table 3.3: OpenStudio SGT specifications for hot water system, HVAC, and PV panel capacity.

Townhouse Type	Water Heating Demand (kWh/day)	HVAC Capacity (kW)	PV Panel Capacity (kW)
Base	18.5	4.2	1.8
1-Bd	22.4	5.3	2.6
2-Bd	27.3	7.0	3.2
3-Bd	33.4	8.2	3.8
4-Bd	39.6	9.1	4.5

Matplotlib [154] for visualization. The Ninja [155] website was used to analyze and compare PV systems [156, 157]. The building model was created in OpenStudio 3.8.0, which integrates with EnergyPlus. OpenStudio automatically converts the .osm file into an EnergyPlus input file (.idf) for execution. The CSGT results were generated using Python and EnergyPlus. Python interfaces with EnergyPlus through the pyenergyplus library. This facilitates simulation automation and the extraction of performance data.

Experiments were conducted to validate the models. Four different townhouse sizes were analyzed to evaluate energy performance, efficiency, and sustainability. Energy performance measures the balance between resources consumed and generated for heating, cooling, lighting, and appliances. Different townhouse sizes cater to various family needs. The models were trained on historical data and validated against real-world observations. Cross-validation was employed to ensure robust solutions.

Real datasets from [128, 132, 140, 141, 142] are used for modeling. Scripts for converting database tables into datasets were obtained from these references. The AMPds2 dataset is openly available via Harvard Dataverse in CSV, tab-delimited, and RData for-

Figure 3.4: 1 to 4 bedroom SGT floor plans.

mats [128, 132, 133, 140].

The data collection system shown in Fig. 3.5 monitors resources such as electricity, water, and gas. Data is collected from meters and sent to data acquisition units, which transmit it to a central server. A WiFi access point and cloud connection allow for remote access and integration of external data, enabling real-time monitoring to optimize resource management [125, 129, 130, 140].

A Building Management System (BMS) is not necessary due to the moderate size of the building network, the simplicity of energy optimization, and the ability to refine strategies through monitoring and assessment. Industrial meters are used for their precision, durability, and reliability. They easily integrate with data acquisition systems for real-time analysis and are suitable for monitoring multiple resources in complex networks like connected townhouses.

Assessing the efficiency, performance, and accuracy of PV panels is key to optimizing RE generation in sustainable housing. Table 3.4 provides PV panel parameters for different SGT sizes. A 1 kW system produces about 1200 kWh/year assuming 1200 hours of effective sunlight and 15% cell efficiency. SGT production is calculated by multiplying

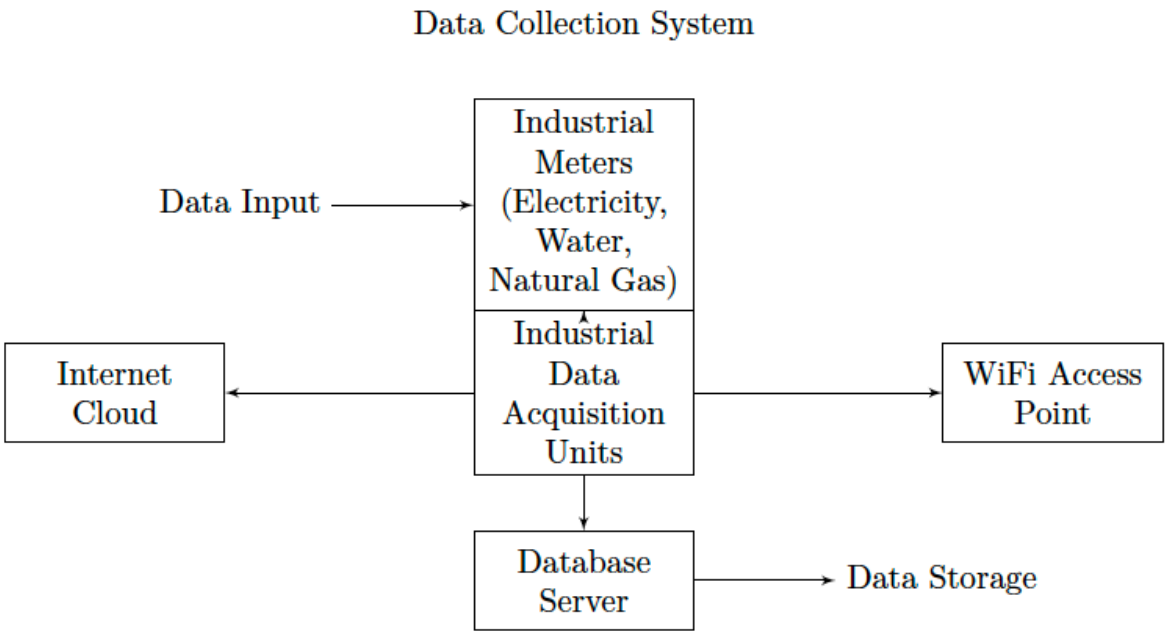

Figure 3.5: Block diagram of the data collection system.

Table 3.4: PV panel parameters for different SGT sizes.

Parameter	1-Bd SGT	2-Bd SGT	3-Bd SGT	4-Bd SGT
Roof Area (m^2)	71.0	100.3	143.2	161.2
Panel Capacity (W)	300	400	500	600
Total PV Capacity (kW)	2.56	3.21	3.84	4.48
Annual Energy Output (kWh/year)	3072	3840	4608	5376
Payback Period (years)	12.4	15.5	18.6	21.6
Energy Saved (kWh/year)	3072	3840	4608	5376
Active Solar Panel Area (m^2)	17.9	23.3	28.7	33.5

capacity (in kW) by 1200 kWh/kW/year. Thus, the 1-Bd SGT (2.56 kW) produces 3072 kWh/year, the 2-Bd (3.21 kW) produces 3840 kWh/year, the 3-Bd (3.84 kW) produces 4608 kWh/year, and the 4-Bd (4.48 kW) produces 5376 kWh/year. The payback period is calculated based on energy savings

$$\text{Payback Period (years)} = \frac{\text{Total Installation Cost}}{\text{Annual Energy Savings}} \tag{3.7}$$

The total installation cost is

$$\text{Total Installation Cost} = \text{Total Capacity (kW)} \times 3500\,\text{CAD} \tag{3.8}$$

and the annual energy savings is

$$\text{Annual Energy Savings} = \text{Average Annual Energy Production (kWh/year)} \times 0.15\,\text{CAD/kWh} \tag{3.9}$$

Then Payback Period for the 1-Bd SGT (2.56 kW) is 12.4 years, 2-Bd SGT (3.21 kW) is 15.5 years, 3-Bd SGT (3.84 kW) is 18.6 years, and 4-Bd SGT (4.48 kW) is 21.6 years. These results provide insights into the financial investment and energy savings for SGTs which help assess their economic viability.

SGT Performance Metrics

This section presents the key metrics for evaluating and improving the resource efficiency, performance, emissions, and cost of SGTs. The Total Energy Use Intensity (TEUI) is

$$\text{TEUI} = \frac{\text{Total Energy Consumption}}{\text{Total Building Area}} \tag{3.10}$$

where Total Energy Consumption is the sum of all energy in kWh and Total Building Area is the floor area in sq ft. This gives an energy efficiency measure per unit area [158]. The Total Energy Demand Intensity (TEDI) is

$$\text{TEDI} = \frac{\text{Total Energy Demand}}{\text{Total Building Area}} \tag{3.11}$$

where Total Energy Demand is the peak demand in kW and Total Building Area is the floor area in sq ft. A lower TEDI indicates better resource efficiency.

The Energy Consumption Based on Size of Home (SOH) is

$$\text{Energy Consumption Based on SOH} = k \times \text{Total Area} \times \text{Energy Consumption Intensity} \tag{3.12}$$

where k is a constant factor to normalize the relationship between the total area of the home and energy consumption intensity. Energy Consumption Intensity is the average rate of resource consumption per unit area. The Control Efficiency Index (CEI) is

$$\text{CEI} = \frac{\text{Actual Energy Usage (AEU)}}{\text{Optimal Energy Usage (OEU)}} \times 100\% \tag{3.13}$$

where AEU is the actual resource consumption and OEU is the optimal energy usage under ideal conditions. The CEI is used to identify inefficiencies in control strategies.

The Waste Recycling Rate (WRR) is

$$\text{WRR} = \frac{\text{Weight of Recycled Waste (WRW)}}{\text{Total Weight of Waste}} \times 100\% \tag{3.14}$$

where Weight of Recycled Waste (WRW) is the total recycled waste weight and Total Weight of Waste is the total weight of the waste generated. A higher WRR indicates better recycling performance. The Material Recycling Percentage (MRP) is

$$\text{MRP} = \frac{\text{Weight of Recycled Materials (WRM)}}{\text{Total Weight of Materials Used (TWMU)}} \times 100\% \tag{3.15}$$

where WRM is the recycled material weight, and TWMU is the total material weight used.

The Indoor Air Quality (IAQ) Index is

$$\text{IAQ Index} = \frac{\text{IAQ Measurement}}{\text{Maximum Acceptable IAQ Level}} \times 100\% \tag{3.16}$$

where IAQ Measurement is the quantitative assessment of indoor air quality parameters such as CO_2, VOCs, CO, and O_3 [159].

The Seasonal Energy Efficiency Ratio (SEER) is

$$\text{SEER} = \frac{1 \times \text{EER}_{100\%} + 42 \times \text{EER}_{75\%} + 45 \times \text{EER}_{50\%} + 12 \times \text{EER}_{25\%}}{100} \tag{3.17}$$

where the EER values are the efficiencies for different cooling capacities. The Energy Efficiency Ratio (EER) is

$$\text{EER} = \frac{\text{BTU}_{\text{cooling}}}{\text{W}} \tag{3.18}$$

where BTU denotes British thermal unit which is a unit of energy used to measure heat, and W is the power consumption of the system in watts. The Heating Seasonal Performance Factor (HSPF) is

$$\text{HSPF} = \frac{\text{BTU}_{\text{heating}}}{\text{W}} \tag{3.19}$$

The Coefficient of Performance (COP) is

$$\text{COP} = \frac{\text{Q}_{\text{useful heat}}}{\text{W}_{\text{input work}}} \tag{3.20}$$

where Q is the useful heat output and W is the work input required.

The Water Efficiency is

$$\text{Water Efficiency} = \frac{\text{Water Saved}}{\text{Total Water Used}} \times 100\% \tag{3.21}$$

where Water Saved is the amount of water saved by efficiency measures and Total Water Used is the total amount of water consumed.

The Electrical Consumption Efficiency (ECE) is

$$\text{ECE} = \frac{\text{Total Useful Electrical Output}}{\text{Total Electrical Input}} \times 100\% \tag{3.22}$$

where Useful Electrical Output is the total electrical energy used by the system and Electrical Input includes energy losses. The Gas Consumption Efficiency (GCE) is

$$\text{GCE} = \frac{\text{Total Useful Heat Output From Gas}}{\text{Total Gas Input}} \times 100\% \tag{3.23}$$

where Heat Output is the useful heat energy from gas and Gas Input is the total gas consumed.

The R-value is a measure of the thermal resistance of a material, indicating how well it resists the flow of heat. It is used to indicate the insulation properties of a material, with higher values indicating better insulation [160]. The R-value of insulation material (in $ft^2 \cdot °F \cdot hr/BTU$) is

$$R = \frac{d}{k} \tag{3.24}$$

where d is the thickness of the insulation material (in inches), and k is the thermal conductivity of the material (in $BTU \cdot in/(ft^2 \cdot °F \cdot hr)$). This value is used to represent the thermal resistance of building components such as walls, windows, roofs, and floors which contribute to the overall thermal efficiency of the building envelope and thus impact energy performance. OpenStudio allows R-values to be input for components to analyze thermal performance. Key R-values include exterior walls (R-30), windows (R-5, triple-pane with low-emissivity coatings), roof/Ceiling (R-50), and floor/slab (R-20, to reduce heat loss through the foundation). OpenStudio provides detailed thermal metrics based on the specified materials and their properties.

The carbon footprint of building operations as Greenhouse Gas Intensity Index (GHGI), expressed in $kgCO_2$, is

$$\text{GHGI} = \frac{\text{Total Greenhouse Gas Emissions (GHGI)}}{\text{Building Floor Area}} \tag{3.25}$$

It includes CO_2, CH_4, and N_2O emissions converted into CO_2 equivalents. The floor area of the building is in sq ft. Regulatory compliance with code standards including TEUI, TEDI, and GHGI thresholds is critical. Meeting or exceeding these benchmarks shows environmental leadership. Buildings with favorable TEUI, TEDI, and GHGI ratings attract more investment, improving long-term viability and economic value. Incorporating these into building design and management improves resource use and reduces environmental impact. It also enhances building resilience [161].

A cost analysis helps evaluate resource consumption savings, ROI, and overall cost-benefit. This is vital for assessing the economic feasibility of efficiency measures and sustainability goals [162]. The cost of energy is

$$\text{Cost of Energy} = \text{Total Energy Consumption} \times \text{Unit Cost} \tag{3.26}$$

where Total Energy Consumption is the total resources consumed by the buildings and Unit Cost is the cost of energy in kWh. Cost savings is the financial savings achieved by comparing costs before and after efficiency measures are implemented

$$\text{Cost Savings} = \text{Cost Before} - \text{Cost After} \tag{3.27}$$

where Cost Before is the cost incurred before implementing resource efficiency initiatives and Cost After is the cost after their implementation. The Return on Investment (ROI) assesses the financial return on the investment made and is given by

$$\text{Return on Investment (ROI)} = \frac{\text{Net Savings}}{\text{Initial Investment}} \times 100\% \tag{3.28}$$

Table 3.5: Outcomes Related to Water Systems and Party Wall Construction in Connected SGTs.

Parameter	**1-Bd SGT**	**2-Bd SGT**	**3-Bd SGT**	**4-Bd SGT**
Daily Hot Water Usage (Gal/Day)	58.9	84.3	108.7	128.6
Energy Savings from Shared Walls (%)	8.2	11.9	14.7	18.1
PV Panel Output (KWh/Day)	6.8	8.5	10.2	11.9
HVAC System Usage (Tons/Day)	1.32	1.85	2.39	2.74

where Net Savings is the total savings achieved from resource efficiency measures and Initial Investment is the cost of implementing these measures. The Net Benefit is the overall financial benefit and is given by

$$\text{Net Benefit} = \text{Total Savings} - \text{Total Costs} \tag{3.29}$$

where Total Savings is the cumulative savings achieved from resource efficiency initiatives and Total Costs is the total cost of implementing and maintaining these measures.

Table 3.5 presents the outcomes for water systems and party wall connections in SGTs. These results are for grid-connected mode and include daily hot water usage, energy savings, PV panel output, and HVAC system usage. This shows that the daily hot water usage increases with the number of bedrooms, from 58.9 gallons for the 1-Bd SGT to 128.6 gallons for the 4-Bd SGT. The energy savings from shared walls improves with townhouse size, from 8.2% in the 1-Bd unit to 18.1% in the 4-Bd unit. The PV panel output increases with unit size from 6.8 kWh for the 1-Bd unit to 11.9 kWh for the 4-Bd unit. HVAC system usage slightly decreases with shared walls, from 1.32 tons for the 1-Bd unit to 2.74 tons for the 4-Bd unit. One ton is 12000 BTU/hour of cooling capacity. As the number of bedrooms increases, resource usage and energy output also increase. Shared walls, however, yield significant energy savings. Comparing Tables 3.5 and 3.3 indicates the improvements in efficiency and resource use with shared infrastructure in CSGTs. These units benefit from better energy management, reduced costs, and greater sustainability. The results in Tables 3.3 and 3.5 show that CSGTs perform better in several key areas. Shared walls reduce total resource consumption. PV panel output indicates effective solar resource use and HVAC usage is lower than the capacity in Table 3.3, reflecting better energy management. Daily hot water use is also optimized in connected SGTs. Thus, CSGTs provide clear improvements in resource efficiency, solar utilization, and HVAC usage.

3.2 Methodology

A goal of this work is to investigate the relationships among parameters impacting smart and green technologies [17, 19]. A hybrid model combining CNN and LSTM networks

is considered to optimize SGTs. It was shown in [163] that hybrid models can outperform other approaches. CNNs can effectively identify spatial features and detect patterns in environmental and energy data. LSTM networks capture temporal dependencies, enabling accurate prediction of resource consumption. A hybrid CNN-LSTM-AE model was developed in [164] for energy prediction. The CNN extracts features that are input to the LSTM encoder and then the LSTM decoder generates the final prediction. This model has lower Mean Square Error (MSE), Mean Absolute Error (MAE), Root Mean Square Error (RMSE), and Mean Absolute Percentage Error (MAPE) compared to other models for data from UCI residential and Korean commercial buildings. Thus, it is more effective in energy optimization. In [165], a CNN-LSTM model was used for indoor temperature modeling of HVAC systems. Traditional methods lack long-term accuracy due to data noise and nonlinearity. The CNN-LSTM model combines the feature extraction of convolutional layers with the sequential learning of LSTM. This hybrid model is more accurate than MLP or LSTM and thus addresses the limitations of traditional ML approaches.

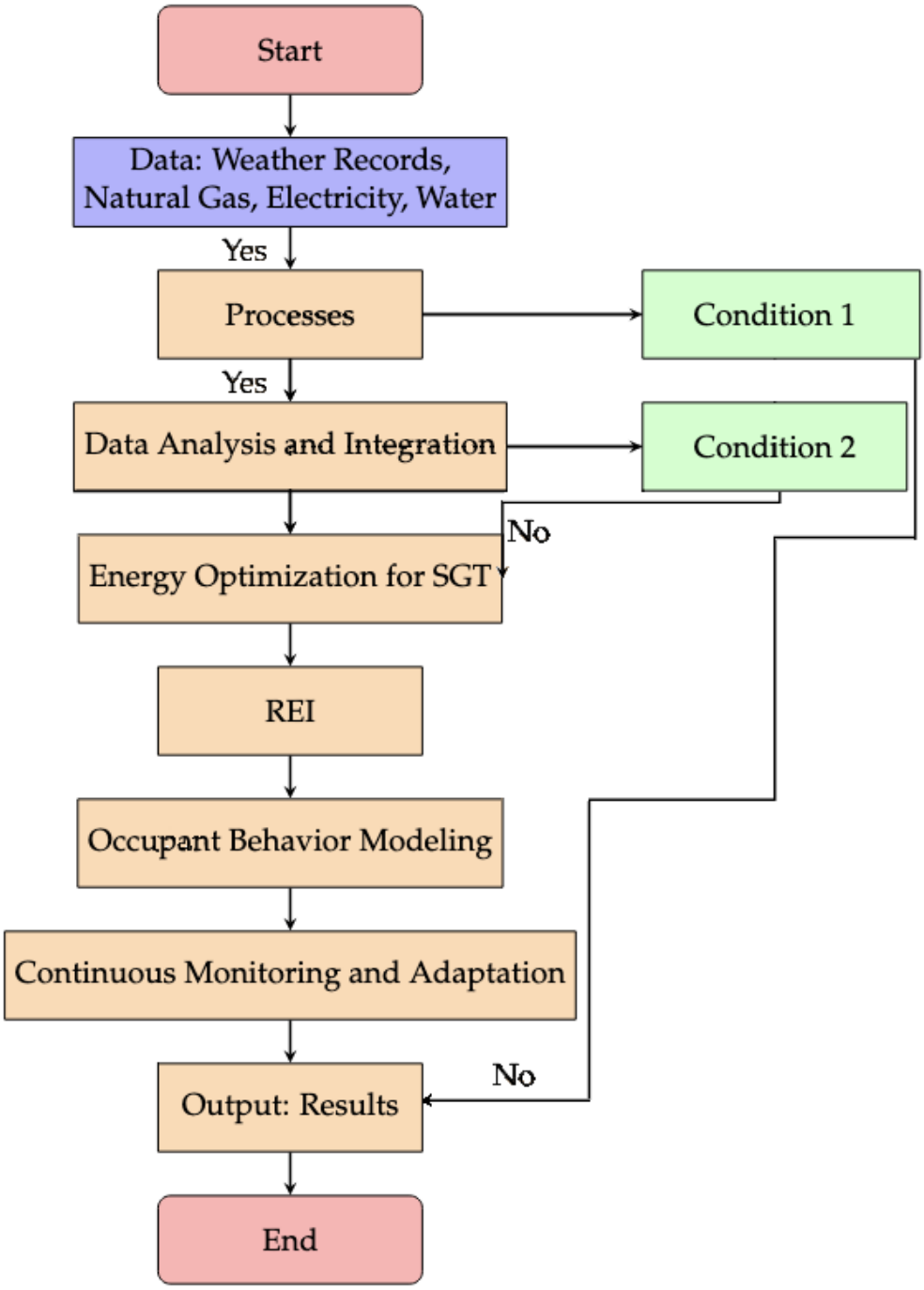

Figure 3.6: Flowchart of the proposed SGT algorithm.

3.2.1 The Proposed SGT Algorithm

This section outlines the proposed ML algorithm. The goal is to optimize resource efficiency, reduce the environmental impact, and improve building performance. A hybrid model combining CNN and LSTM networks is employed [152, 153, 165]. This model can

capture both spatial and temporal dependencies in SGT data. Fig. 3.6 presents a flowchart of the proposed model including data analysis, SB control, RE integration, occupant behavior modeling, and continuous monitoring. The flowchart steps are as follows.

- **Start** Process initiation.
- **Data Input** Weather, gas, electricity, and water data.
- **Preprocessing** Data cleaning, transformation, and normalization.
- **Data Analysis and Integration** Insights and patterns are obtained.
- **Condition 1** This decision point checks analyzed data. If the outcome is yes, proceed to energy optimization, otherwise go to Output: Results.
- **Energy Optimization** Implement the energy optimization.
- **Condition 2** This decision point evaluates the optimization results. If the outcome is yes, proceed to RE Integration, otherwise go to Occupant Behavior Modeling.
- **RE Integration (REI)** Add RES into the energy optimization.
- **Occupant Behavior Modeling** Model occupant influence on energy.
- **Continuous Monitoring and Adaptation** Monitor the parameters and adjust strategies based on occupant behavior and energy use.
- **Occupant Behavior Modeling** Incorporate routines, seasonality, and usage trends. Daily routines are more active in the morning (6-8 AM) and evening (6-10 PM). Seasonal variations include winter heating and summer cooling. Working hours are lower on weekends and more predictable on weekdays. There are more special events during holidays and fewer during vacations. Working from home increases daytime activity and resource use. Temperature, lighting, and smart appliance use vary by occupant. These factors influence energy use patterns and thus SGT efficiency.
- **Output: Results** provides optimized energy usage, cost savings, and recommendations.
- **End** Process conclusion.

3.2.2 Optimization

The proposed deep hybrid LSTM-CNN model addresses two key optimization goals.

1. **Energy Optimization** This minimizes prediction errors (e.g., MAE and RMSE), to reduce energy use and improve system efficiency.
2. **ML Model Optimization** The LSTM-CNN model is refined to provide better prediction accuracy. Iterative training is employed to adjust the weights and biases to improve energy forecasting. This dual focus provides optimized energy management and model performance.

The objectives are as follows.

1. **Cost Reduction**
    - Energy Optimization for efficient scheduling and operation of energy systems to lower costs (e.g., electricity, fuel, maintenance).
    - ML model optimization for accurate predictions to support cost-effective energy decisions.
2. **Emission Reduction**
    - Energy Optimization for forecasts to help decrease reliance on non-RESs, cutting carbon emissions.
    - ML model optimization for predictions for optimal RES integration to reduce emissions.
3. **Performance Improvement**
    - Energy optimization to ensure reliable energy supply to efficiently meet demands.
    - ML model optimization to improve prediction accuracy which aids effective system management.
4. **Efficiency Improvement**
    - Energy optimization to reduce waste and improve energy system resource utilization.
    - ML model optimization to increase computational efficiency for faster more accurate predictions.

The objective function is

$$\alpha C + \beta E - \gamma P - \delta \eta \tag{3.30}$$

where C is cost (minimize), E is emissions (minimize), P is performance (maximize), and η is efficiency (maximize). The factors $\alpha, \beta, \gamma, \delta$ are set based on the importance of each component. Historical data is used to compare and prioritize these objectives. The coefficients used for the objective function are as follows.

- $\alpha = 0.3$ indicates moderate emphasis on minimizing cost as reducing expenses is important but must be balanced with other factors.
- $\beta = 0.2$ indicates lower weight on emission reductions as they are considered to have lower priority than cost.
- $\gamma = 0.4$ indicates the highest weight is on performance improvement which reflects a focus on maximizing system performance.
- $\delta = 0.1$ indicates the lowest weight so efficiency is not a critical factor.

The optimization problem has the following constraints

$$0 \leq \text{TEUI} \leq \text{TEUI}_{\text{max}} \tag{3.31}$$

$$0 \leq \text{TEDI} \leq \text{TEDI}_{\text{max}} \tag{3.32}$$

$$0 \leq \text{REI} \leq 100\% \tag{3.33}$$

$$0 \leq \text{STUI} \leq 100\% \tag{3.34}$$

$$\text{Energy In} + \text{Grid Import} - \text{Energy Out} - \text{Grid Export} = \text{Energy Storage} \tag{3.35}$$

$$\text{Energy Storage}_{\text{min}} \leq \text{Energy Storage} \leq \text{Energy Storage}_{\text{max}} \tag{3.36}$$

Energy In includes local generation and grid imports, while Energy Out includes both consumed energy and exports to the grid. Energy Storage is the energy held within the system. These constraints ensure solutions adhere to practical limits and regulations. According to International Electrotechnical Commission (IEC) 62933 standard for electrical energy storage systems, Energy Storage must be between 10% and 90% of the total capacity [166]. These constraints ensure compliance with building codes and sustainability standards which is crucial for practical deployment. They also support system stability and performance to balance energy use, cost, and environmental impact.

The following limitations must be considered to ensure suitable solutions.

- **Predefined Minimum or Maximum Values** Some variables have strict minimum or maximum limits. For example, thermostat settings may range from 18°C to 25°C, and battery storage capacity is limited to 10%–90% to extend battery life.
- **Computational Limits** Computational resources and time constraints may restrict the complexity and scalability of the optimization approach.
- **Real-world Constraints** Budgetary and regulatory requirements can affect the optimization.

An ML algorithm is employed to predict and optimize resource use to improve sustainability in SGTs and CSGTs. Artificial Neural Networks (ANNs) are powerful tools for SB modeling and energy optimization [92]. They are effective in load forecasting, optimization, occupancy prediction, anomaly detection, and energy optimization [68, 167, 168, 169]. A rule-based approach to predict unusual load conditions, such as on public holidays, was introduced in [167]. These conditions are challenging due to their infrequency and unique patterns. The approach used combines expert insights with statistical models such as Holt-Winters-Taylor exponential smoothing and Auto-Regressive Moving Average (ARMA) to predict both regular and unusual load patterns. Evaluation of this approach using nine years of half-hourly load data for Great Britain showed accurate forecasts up to a day ahead.

The Short-Term Load Forecasting (STLF) model is

$$\hat{Y}_t = f(X_t, X_{t-1}, \ldots, X_{t-n}) \tag{3.37}$$

where $\hat{Y}_t$ is the forecast load at time t, $X_t, X_{t-1}, \ldots, X_{t-n}$ is the historical load data and relevant features up to time t, and f is the prediction function learned by the NN. STLF feature selection using Random Forest (RF) was presented in [168]. This method was used with 243 features from historical data and time information. Then an enhanced sequential backward search based on permutation importance was used to identify an optimal subset of features. This subset is used to train an RF model. This approach achieved higher accuracy than methods such as support vector regression and ANN.

The predicted occupancy at time t is

$$\hat{O}_t = g(T_t, D_t, W_t, O_{t-1}, \ldots, O_{t-n}) \tag{3.38}$$

where T_t, D_t, and W_t are the corresponding time, day, and weather features, $O_{t-1}, \ldots, O_{t-n}$ are the past occupancy data, and g is the prediction function learned by the NN. The hybrid energy prediction method for SG in [68] uses STLF and k-medoid clustering to group transformers by energy profiles to speed up training. The deep NN model has six layers and uses Adam optimization. This approach improves scalability and reduces training time by 44% with no loss in accuracy.

Anomaly detection finds deviations from normal behavior based on historical data. The anomaly score at time t is

$$A_t = h(X_t, X_{t-1}, \ldots, X_{t-n}) \tag{3.39}$$

where $h()$ is the NN function. ANNs have been shown to provide excellent energy optimization results. In [46], an ANN-based predictor was developed to forecast daily HVAC power use. This LSTM-based approach has low error and high correlation with test data which indicates effective real-time prediction. The accuracy is better than with simple one-hour ahead models.

HVAC optimization involves minimizing energy use under comfort constraints

$$\min_u \sum_t C_t(u_t) \tag{3.40}$$

where u is HVAC control input such as temperature and $C_t(u_t)$ is the energy cost at time t. Comfort constraints ensure thermal comfort within buildings. These constraints influence HVAC optimization by penalizing deviations from desired temperature or humidity setpoints.

The system dynamics describe HVAC system behavior over time in response to inputs and disturbances, often modeled using physics-based equations or simulation. ML models like LSTM capture these dynamics through time-series forecasting from historical data. Operational limits define boundaries to ensure efficient and safe system performance. ML models enforce these limits with constraints or penalty terms, ensuring control inputs do not exceed predefined operational ranges. It has been shown that ANNs provide excellent accuracy, efficiency, and performance for building energy optimization, and handle nonlinearities and dynamic environments better than traditional methods.

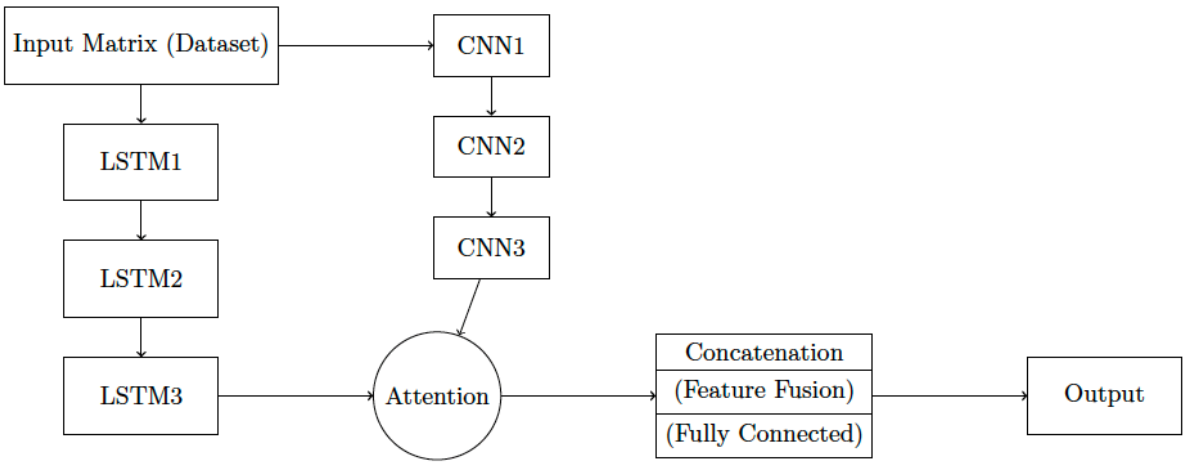

Figure 3.7: The proposed deep ML model architecture.

The Proposed Model

This section describes the architecture of the proposed hybrid ML model which is illustrated in Fig. 3.7. The model captures both temporal dependencies and spatial patterns in data through the integration of LSTM. The architecture is described below.

1. **Input Matrix (Dataset)** The input data is loaded in matrix format.
2. **LSTM Layers with Attention Mechanisms** [170] The LSTM1, LSTM2, and LSTM3 layers use attention mechanisms to focus on relevant parts of the input. This helps capture long-term dependencies and improve predictive accuracy.
3. **CNN Layers with Skip Connections** The CNN1, CNN2, and CNN3 layers have skip connections that allow information to flow directly between the LSTM and CNN layers. This enables simultaneous capture of spatial and temporal features.
4. **Attention Mechanism** The attention mechanism combines the LSTM and CNN outputs by weighting them based on relevance. This improves the ability of the model to capture both sequential and spatial aspects of the data.
5. **Concatenation (Feature Fusion and Fully Connected)** The LSTM, CNN, and attention features are concatenated and processed through a fully connected layer. This generates predictions based on fused features.
6. **Output** The output layer generates predictions based on the processed features to obtain resource consumption patterns in SBs.

The proposed model combines LSTM layers with attention mechanisms and CNN layers with skip connections to capture long-term dependencies (for LSTM) and hierarchical spatial features (for CNN). This hybrid architecture is specifically designed for energy optimization in SGTs to achieve resource efficiency, cost savings, and emission reductions. The attention mechanisms and skip connections create more informative features to learn

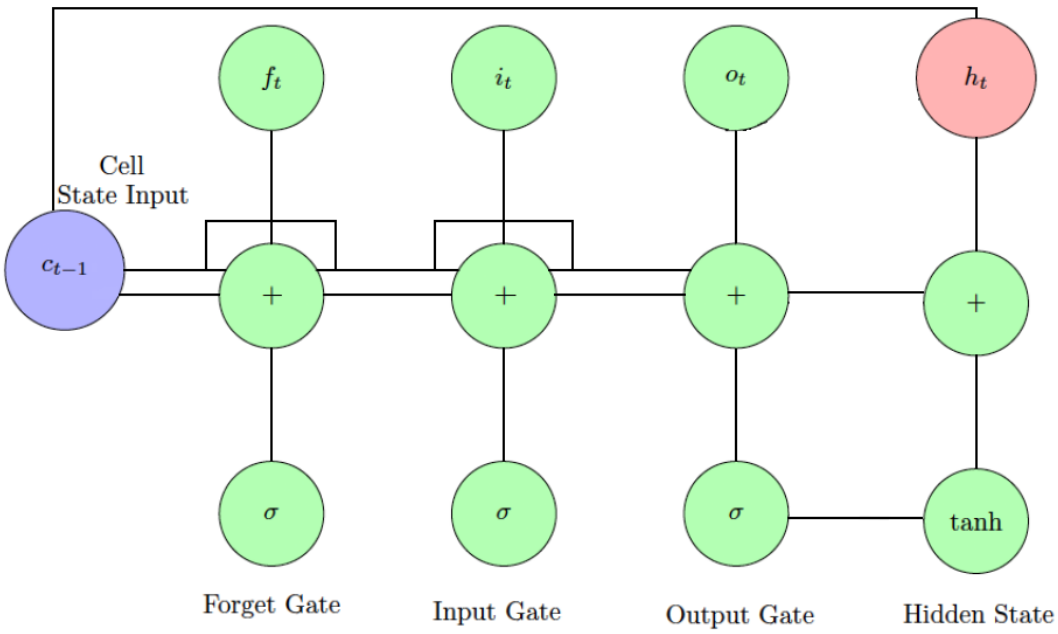

Figure 3.8: The peephole LSTM unit.

rich, hierarchical representations that improve model generalization ability. The attention mechanisms also allow the model to adapt to varying input conditions. It handles different sequence lengths and complexities which makes the model more robust and versatile. Skip connections help prevent the vanishing gradient problem and speed up training.

Fig. 3.8 illustrates the Peephole LSTM unit. It is a type of RNN used in sequence modeling tasks. The input node (blue circle) is the input to the LSTM unit at time step t. The forget, input, and output gates (green circles) control information flow. Each gate uses a sigmoid function to output values between 0 and 1. The forget gate (f_t) decides what to discard, the input gate (i_t) determines what to store, and the output gate (o_t) controls information flow to the output. The hidden state (red circle), denoted h_t, is the output of the LSTM at time step t. The cell state (purple circle), denoted c_t, is the internal memory of the LSTM and is updated based on the gate outputs. The previous cell state c_{t-1} is used to calculate the new cell state.

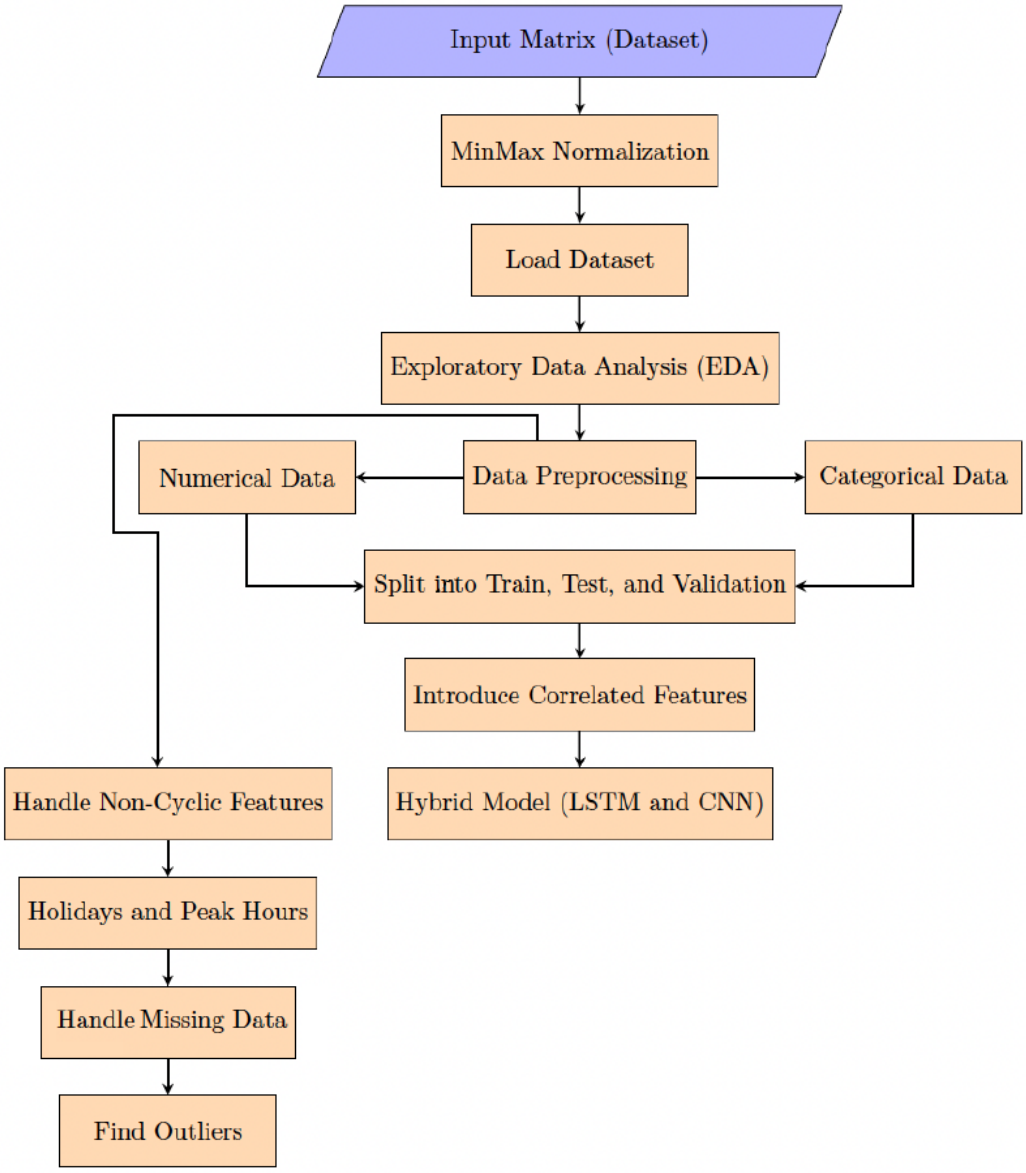

Figure 3.9: The data processing flowchart.

A flowchart of the data processing is given in Fig. 3.9. This ensures data cleanliness and relevance for accurate energy optimization predictions. The steps are described below.

- **Input Matrix (Dataset)** The dataset is loaded. It contains features and target variables for energy optimization. The features include the following.
  - **Timestamp** day, month.
  - **Weather data** Temperature, humidity, wind speed, solar radiation.
  - **Building characteristics** Size, rooms, window size.

- **Energy consumption history** Usage at various intervals.
- **Occupancy** Number of occupants.
- **External factors** Energy prices, grid signals.
- **Categorical data** Appliance types, holidays, peak hours.

The target variables include resource consumption at different time intervals. Data sources include IoT sensors, external weather services, and historical energy usage databases.

- **MinMax Normalization** The input data is scaled to the range [0, 1] to ensure equal contribution from all features.
- **Load Dataset** The dataset is loaded for processing.
- **Exploratory Data Analysis (EDA)** Statistical analysis, pattern identification, and data visualization to understand the structure and issues like missing values or outliers.
- **Data Preprocessing** Cleaning the data, handling missing values, encoding categories, and scaling features for model training.
- **Split into Train, Test, and Validation** The data is divided into subsets for model training, evaluation, and hyperparameter tuning.
- **Cross-Validation** Partition the dataset into K folds (e.g., 5-fold) for cross-validation. In each iteration, one fold is reserved for validation, while the remaining folds are used for training. Then each fold trains and validates the LSTM-CNN model on a unique split, ensuring robust evaluation by exposing the model to varied data subsets. The results are averaged across all K folds to reduce overfitting and improve generalization.
- **Introduce Correlated Features** Add correlated features to improve model performance.
- **Handle Non-Cyclic Features** Separate processing is used for non-cyclic features such as month, day, and hour.
- **Holidays and Peak Hours** Holidays and peak hours (6-9 AM and 4-9 PM), are added as features for better prediction accuracy.
- **Handle Missing Data** Missing data points are imputed or removed to avoid bias in predictions.
- **Find Outliers** Outliers are identified and handled to prevent skewed predictions.

The data is normalized using Min-Max normalization [171]

$$L_{t\text{norm}} = \frac{L_t - L_{\text{min}}}{L_{\text{max}} - L_{\text{min}}} \tag{3.41}$$

where L_t is the tth original value and L_{max} and L_{min} are the maximum and minimum values, respectively.

The feature vector is

$$X = [L, H, D, M, Ho, Wp, Sp, SUp, Apg] \tag{3.42}$$

where L is the past load values, H is the hour of the day (time-based variations), D is the day of the week (daily usage patterns), M is the month (seasonal variations), Ho is the holiday indicator (binary/categorical), Wp is the weather data (e.g., temperature, humidity), Sp is the spatial features (e.g., building size, occupants), SUp is the start-up patterns (e.g., peak times), and Apg is the appliance usage data (aggregated power consumption). These 9 features contain both temporal and spatial patterns in load data and serve as inputs to the ML model.

3.3 Results and Discussion

This section presents the model performance including prediction accuracy, efficiency, cost savings, emission reductions, and overall system effectiveness. Base, SGT, and CSGT results are compared. All townhouses are assumed to be connected to the Burnaby electricity grid managed by BC Hydro, operating at 120/240V single-phase for residential connections.

3.3.1 Resource Optimization

The resource optimization was evaluated for SGTs connected to the Burnaby grid. The availability of RES affects the energy mix and carbon footprint. The weather parameters from 2012-2014 include heating and cooling thresholds at 14°C and 20°C, respectively. The heating power required is 0.3 kW/°C and the cooling power is 0.15 kW/°C. The smoothing rate is 0.5 days^{-1}, solar gain is 0.012°C in W/m^2, and wind chill is -0.2°C in W/m^2. Parameters such as TEUI, TEDI, and GHGI reflect how climate affects resource consumption and emissions. The average annual temperature is 11.5°C, with summer highs of 23.5°C and winter lows of 1.5°C.

Equations (3.1)– (3.42) were implemented using Python v3.11.5 and EnergyPlus with the pyenergyplus library to obtain the parameters given in Table 3.6. The building model was created in OpenStudio 3.8.0, which integrates with EnergyPlus. The cost of energy is in Canadian Dollars (CAD). The base home design was adapted to 1, 2, 3, and 4 bedroom SGTs while maintaining the same location and energy supplies. The key observations from this table are as follows.

1. Improved party wall insulation increased heat transfer efficiency by 5%.
2. Reduced air leakage improved fluid dynamics by 3%.
3. Better temperature regulation reduced resource consumption by 9%.

4. Energy balance improved by 3% with thermal regulation.
5. Control integration provided a 1% improvement.
6. TEUI and TEDI decreased by 5% due to shared systems.
7. HVAC performance improved by 2% with shared systems.
8. Water efficiency increased by 2%, with connected systems improving it by 5% and optimized management adding 3%.

Considering resource efficiency, CSGTs have 6-10% lower resource consumption per square foot, with better HVAC efficiency (3-5%). The environmental impact is improved as CSGTs reduce GHGI by 5-8% and provide a 10-12% improvement in REI, indicating superior use of RESs. CSGTs show a 3-5% improvement in ROI due to better RE integration and resource efficiency, making them more cost-effective. CSGTs outperform SGTs in energy balance and water efficiency, with improvements of 3-6%. This reinforces that connected systems optimize resource use and improve overall performance. The results in Table 3.6 confirm that CSGTs provide superior resource efficiency, environmental impact, and cost-effectiveness, supporting their preference for sustainable urban development.

Fig. 3.10 compares monthly electricity consumption between a two-story townhouse dataset from [128] (blue) and a new one-story Baseline townhouse (red) over 2012-2014. The bars show electricity consumption for each month, illustrating the differences between the two designs. Fig. 3.11 presents the monthly electricity consumption (2012-14) for 1-4 Bd SGTs and CSGTs in grid-connected mode. This shows that CSGTs (light blue), consume less electricity than SGTs (dark blue) in most months. The connected features in CSGTs reduce consumption, especially in December 2012 and January-February 2013. This is because energy-saving features such as improved HVAC and lighting controls are more effective during colder months. The townhouse in [128] consumes 120 GJ of gas annually, while the one-story SGT uses only 80 GJ. This represents a 33% reduction, or 40 GJ, in gas consumption. The reduction is mainly due to the energy-efficient features of the SGT. Shared energy optimization strategies further reduce gas usage for heating and other purposes throughout the year.

Table 3.6: Monthly energy performance for SGTs versus CSGTs without an ML model.

Parameter	Disconnected				Connected				Acceptable Range
	1-Bd	2-Bd	3-Bd	4-Bd	1-Bd	2-Bd	3-Bd	4-Bd	
Efficiency									
Heat Transfer (%)	85.32	86.91	88.75	89.56	86.32	88.12	89.91	91.73	80–90
Fluid Dynamics (%)	80.52	81.93	83.52	84.84	81.21	82.96	84.87	87.12	75–85
Total Energy Consumption (kWh/sq ft)	0.91	0.93	0.98	0.99	0.86	0.89	0.93	0.97	0.65–0.80
Building Energy Balance (%)	89.93	91.21	92.42	93.63	90.89	92.12	93.23	94.13	85–95
TEUI (kWh/sq ft)	0.77	0.73	0.78	0.76	0.69	0.65	0.64	0.61	0.60–0.80
TEDI (kWh/sq ft)	0.52	0.59	0.55	0.53	0.49	0.46	0.41	0.39	0.35–0.50
HVAC Metrics (%)	88.31	90.12	91.26	91.92	91.12	91.75	92.34	93.65	85–95
Water Efficiency (%)	76.83	77.24	77.62	78.13	77.31	77.81	78.14	79.13	75–85
ECE (%)	92.91	93.52	94.12	94.61	93.74	94.45	95.23	95.86	90–98
GCE (%)	88.14	88.91	89.45	89.72	88.74	89.51	90.12	90.25	85–95
Insulation R-Value (%)	24.32	24.71	25.12	25.54	24.73	25.54	26.36	26.73	20–30
Cost Savings (CAD)	400.3	470.6	546.1	609.5	404.7	475.3	551.9	617.2	–
Performance									
RE Integration (%)	21.87	27.31	32.45	35.52	22.82	28.74	33.42	36.13	30–50
STUI (%)	86.32	88.51	90.74	91.86	87.63	89.31	91.53	92.46	90–97
Cooling Energy Consumption (kWh/sq ft)	0.26	0.25	0.23	0.22	0.23	0.22	0.20	0.20	0.20–0.30
CEI (%)	90.83	91.29	91.87	92.21	91.35	91.84	92.65	92.92	85–95
WRR (%)	71.12	74.31	78.13	81.04	72.42	75.24	79.32	82.25	65–75
IAQ (%)	87.58	89.79	91.54	92.24	88.89	90.42	92.14	92.87	85–95
MRP (%)	61.49	64.78	67.57	70.41	62.43	65.85	68.64	71.63	70–80
Emission									
GHGI ($kgCO_2$/kWh)	0.51	0.49	0.46	0.45	0.47	0.47	0.46	0.43	0.40–0.55
Cost									
Cost of Energy (CAD)	615.5	688.0	759.5	832.2	625.5	698.0	769.6	842.2	–
ROI (%)	15.82	16.56	17.38	18.12	16.34	17.14	17.93	18.89	15–25
Net Benefit (CAD)	1272.1	1344.2	1415.6	1481.9	1292.1	1364.2	1435.6	1501.8	–

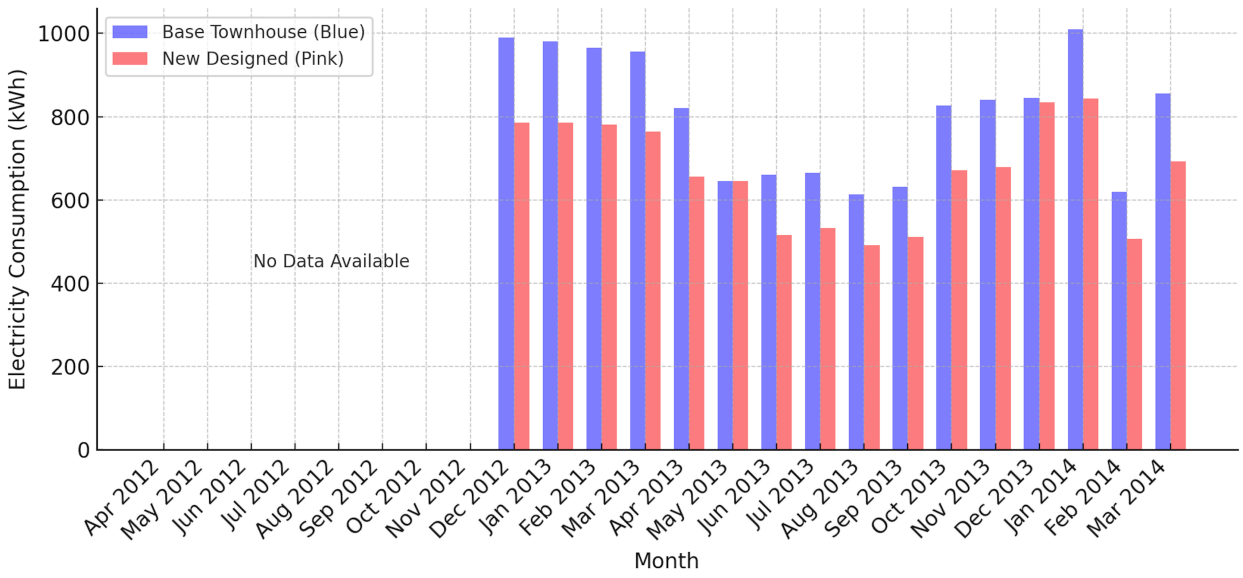

Figure 3.10: Monthly electricity consumption (2012-14) for a new one-story townhouse (pink) and the base townhouse from [128] (blue).

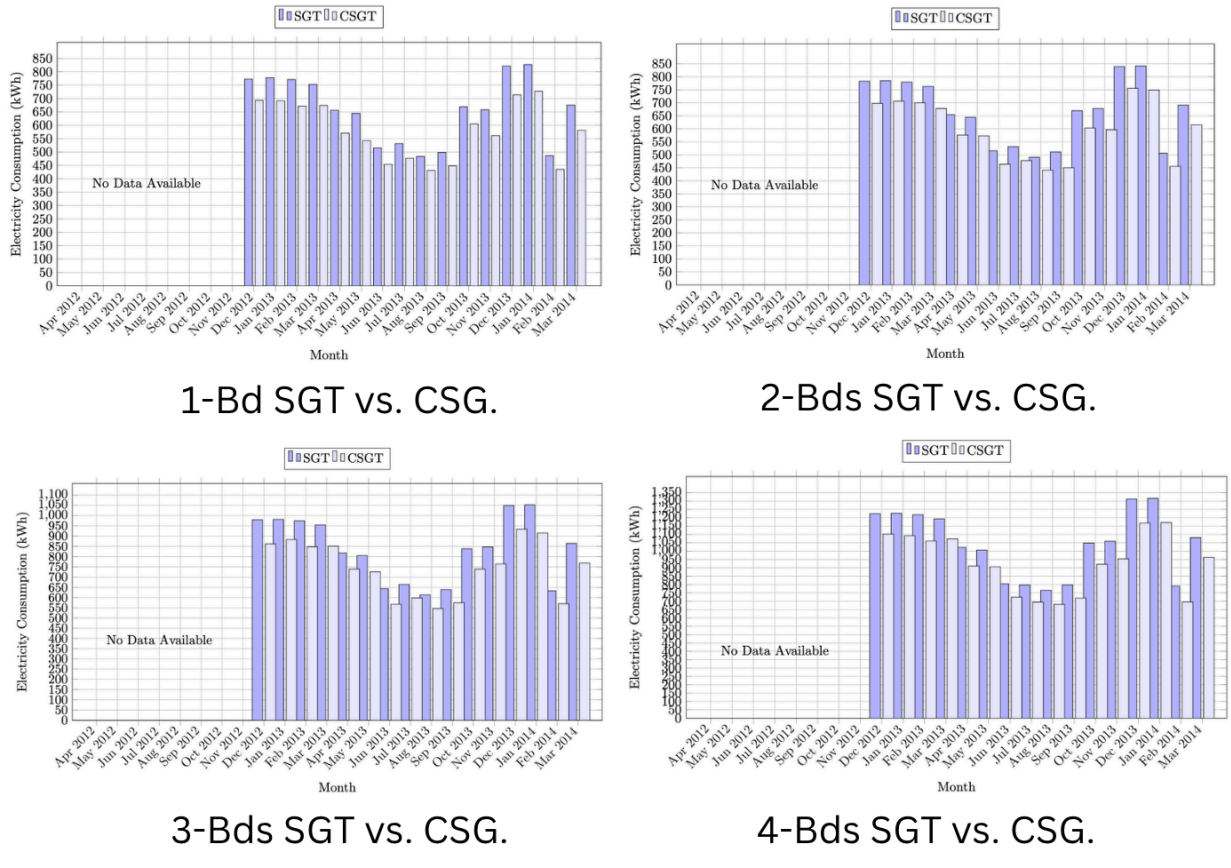

Figure 3.11: Monthly electricity consumption (2012-14) for 1-4 Bd SGTs and CSGTs in grid-connected mode.

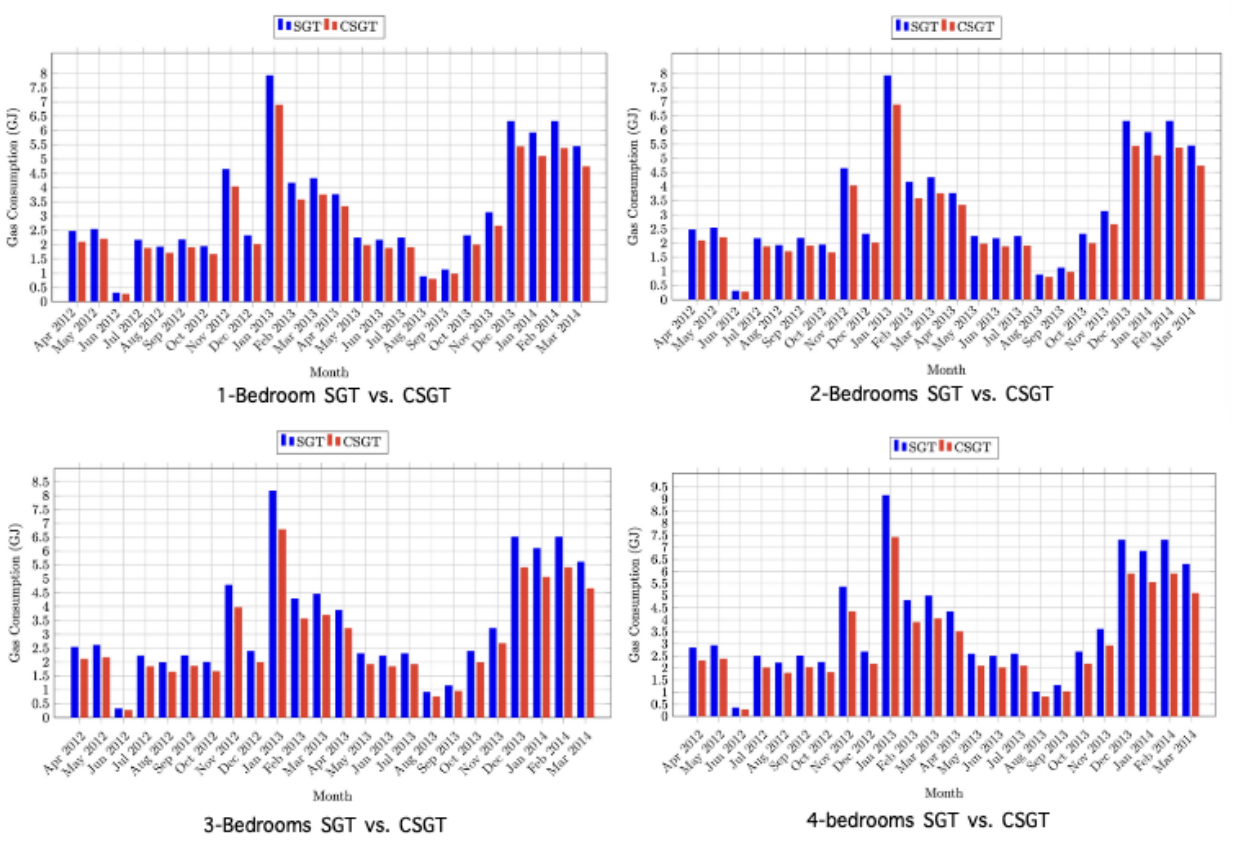

Figure 3.12: Monthly gas consumption (2012-14) for 1 to 4 Bd SGTs and CSGTs in grid-connected mode.

Fig. 3.12 gives the gas consumption of SGTs and CSGTs in grid-connected mode. The 1-Bd CSGT uses 13-15% less gas annually than the 1-Bd SGT. The 2-Bd CSGT consumes 16-17% less gas than the 2-Bd SGT. For the 3-Bd CSGT, gas consumption is 20-21% lower than the 3-Bd SGT. The 4-Bd CSGT shows an 18-19% reduction compared to the 4-Bd SGT. These results highlight the superior energy efficiency of CSGTs and their potential for sustainable residential energy use.

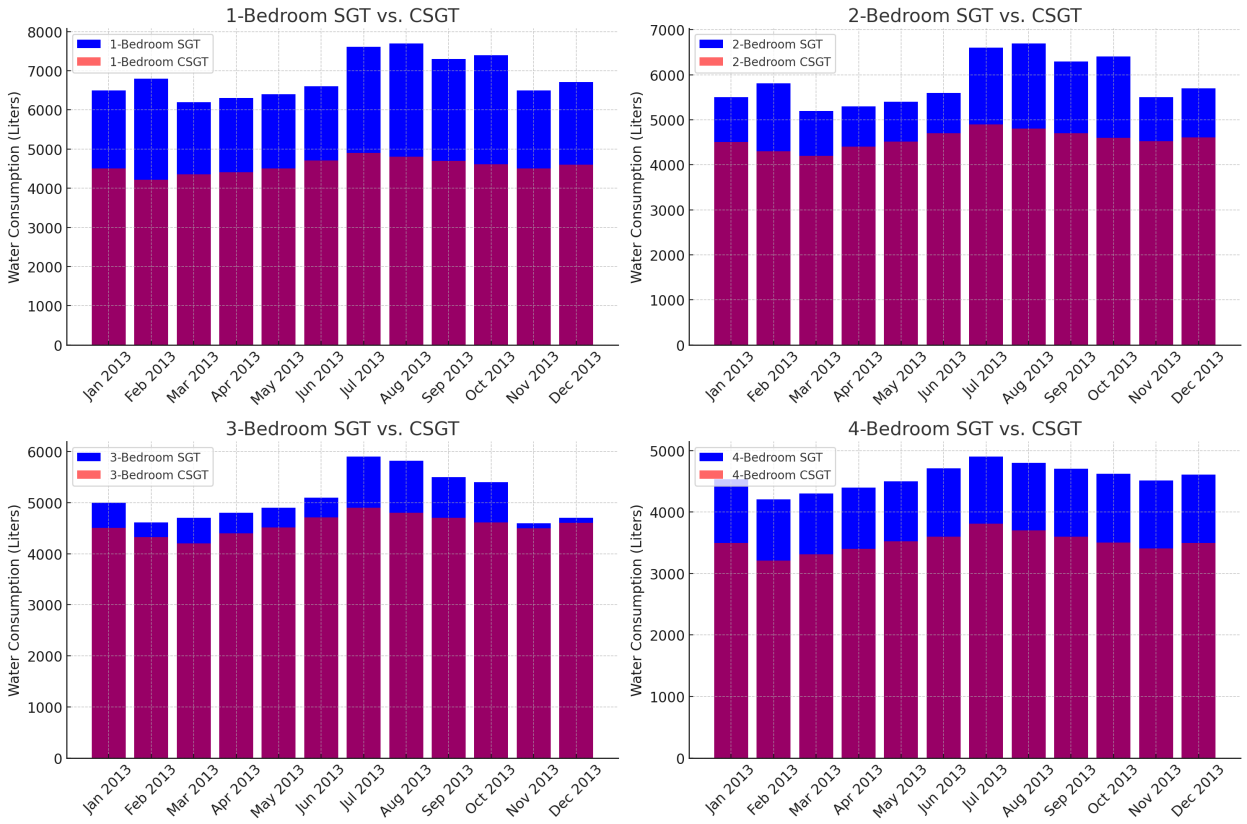

Figure 3.13: Monthly total water consumption for 1 to 4 Bd SGTs and CSGTs in grid-connected mode for January-December 2013.

Fig. 3.13 presents the total water consumption of 1-4 Bd SGTs and CSGTs in grid-connected mode for January-December 2013. This shows that CSGTs outperform SGTs in reducing water consumption for all unit sizes. In January 2013, the 1-Bd CSGT used 4,500 liters which is 30% less than the 6,500 liters for the 1-Bd SGT. The shared infrastructure and smart water management systems contribute to these savings. For 2-Bd units, the CSGT consumed 4,509 liters which is 18% less than the 5,500 liters for SGTs. For 3- and 4-Bd units, CSGTs show reductions ranging from 10% to 23%.

Burnaby has a temperate oceanic climate with mild, wet winters and warm, dry summers. These conditions affect thermal comfort in SGTs. Indoor temperatures are usually kept above 18°C. Winter temperatures between 18°C and 20°C feel cool but comfortable, while the range of 20°C to 23°C is ideal for most of the year. In warmer months, indoor temperatures may reach 23°C to 25°C, which many find comfortable. However, on hot summer days, temperatures above 25°C can occur. Thus, effective cooling is essential to maintain indoor comfort.

3.3.2 The Proposed ML Model Results

The proposed model was evaluated and compared with several well-known models including LR, LSTM, CNN, RF, Gradient Boosting (GB), and hybrid LSTM-CNN. LR serves

as a simple performance baseline, LSTM is good at handling sequential data, CNN is good at recognizing spatial patterns, RF is good at managing non-linear relationships and noisy data, GB improves accuracy through ensemble learning, and hybrid LSTM-CNN is good at capturing both temporal and spatial dependencies. These diverse approaches are considered to evaluate the effectiveness of the proposed model in optimizing energy performance [149].

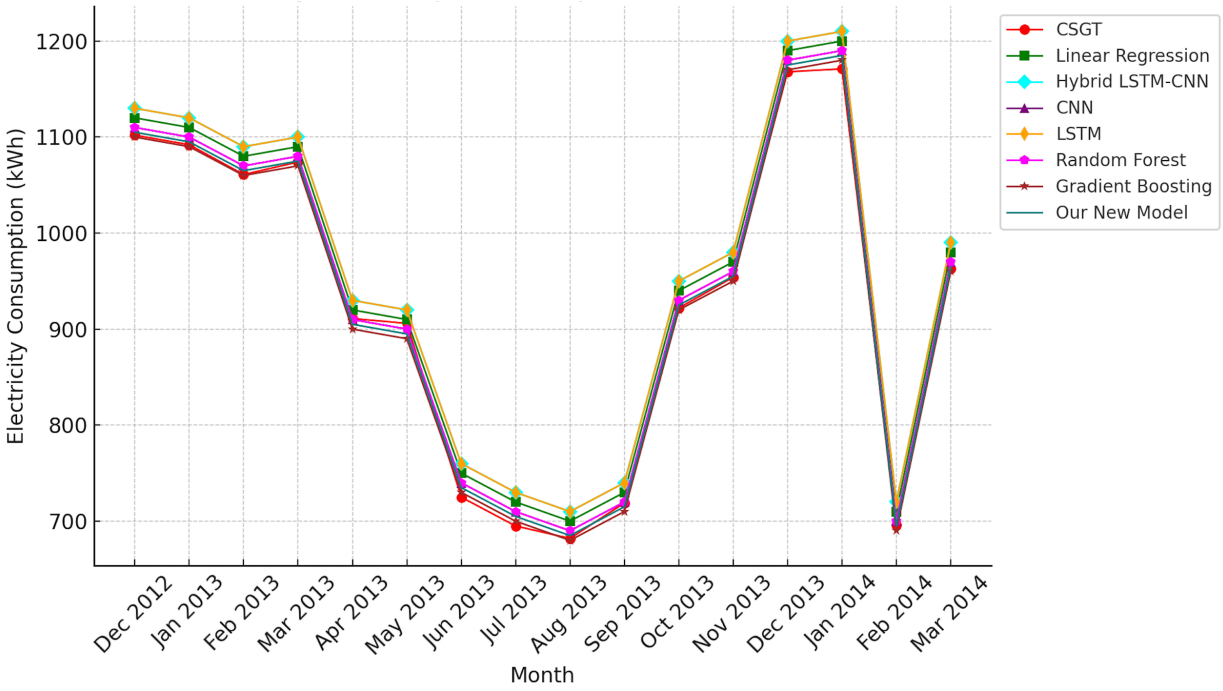

Figure 3.14: Actual versus predicted monthly electricity consumption with seven ML models for a 1-Bd CSGT in grid-connected mode for 2012-14.

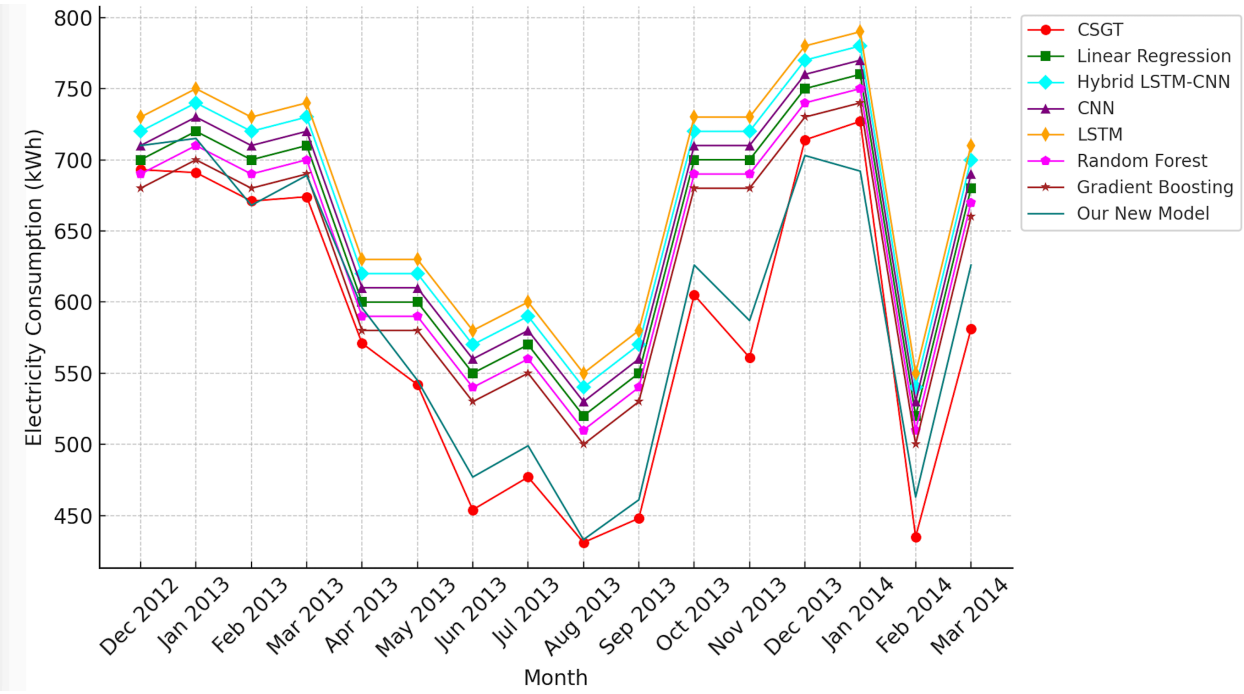

Figure 3.15: Actual versus predicted monthly electricity consumption with seven ML models for a 2-Bd CSGT in grid-connected mode (2012-14).

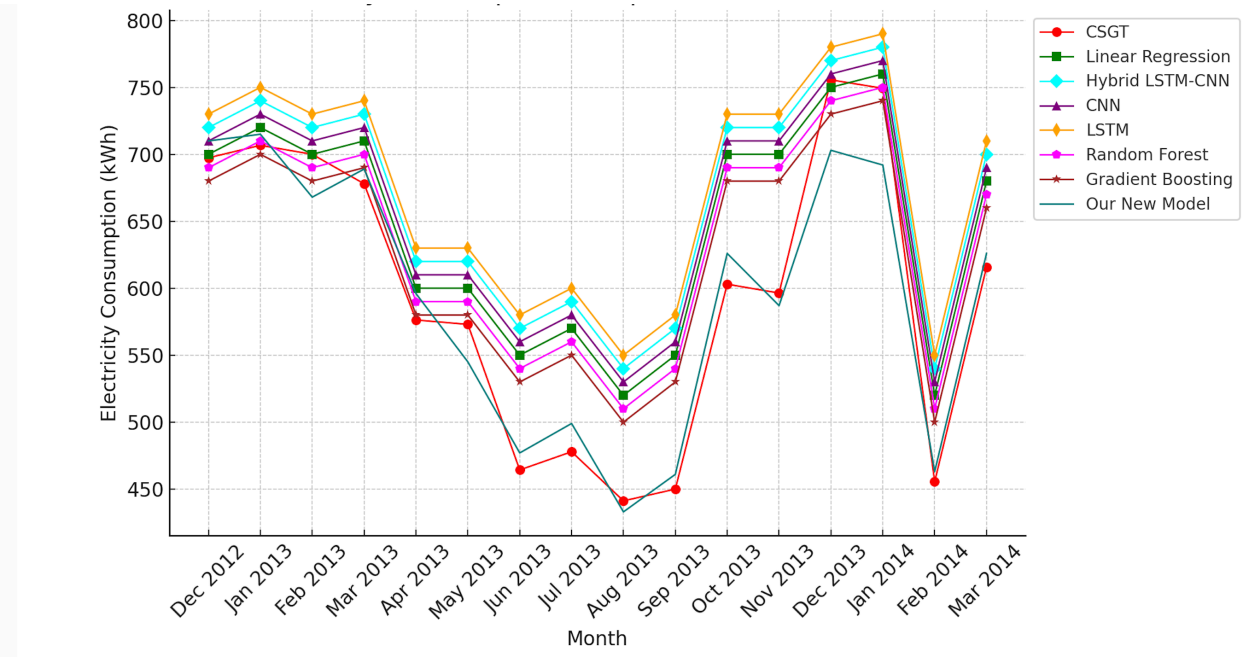

Figure 3.16: Actual versus predicted monthly electricity consumption with seven ML models for a 3-Bd CSGT in grid-connected model (2012-14).

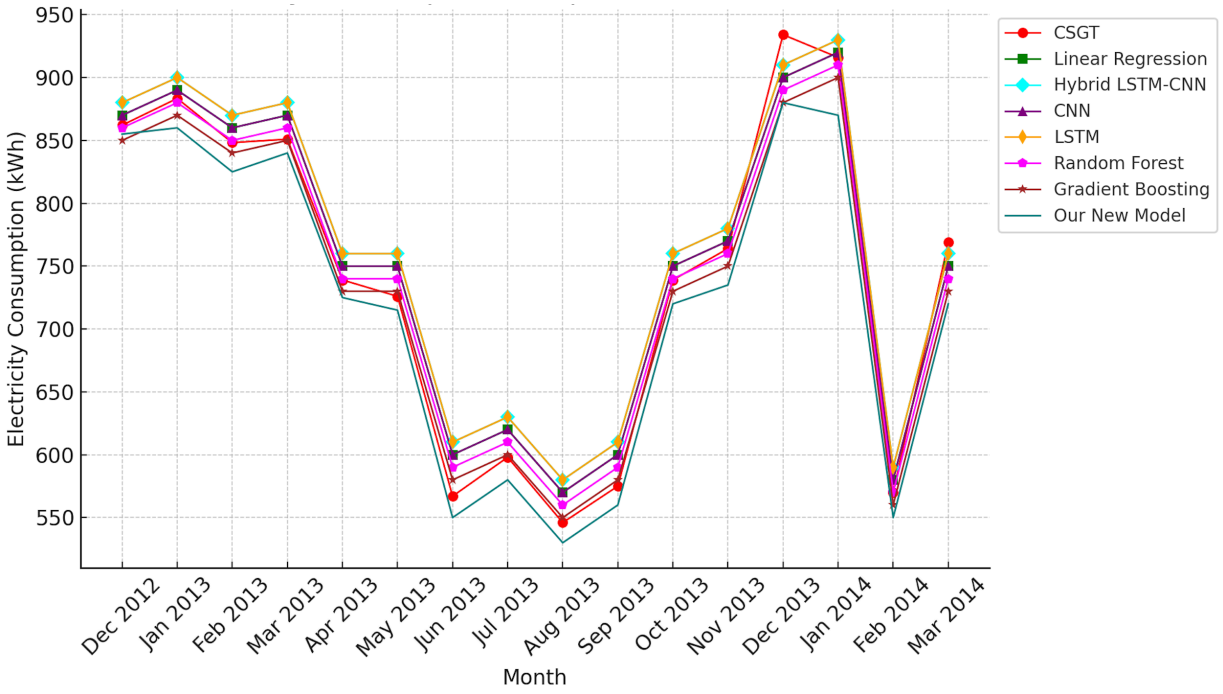

Figure 3.17: Actual versus predicted monthly electricity consumption with seven ML models for a 4-Bd CSGT in grid-connected mode (2012-14).

The monthly electricity consumption for 1-4 Bd CSGTs is shown in Figs. 3.14 to 3.17, respectively. This shows there are peaks in winter due to higher heating demands. As the number of bedrooms increases, so does electricity usage, with 4-Bd units having the highest consumption. These results show that the proposed ML model outperforms the others with minimal deviation from the actual values. Thus, it adapts well to consumption patterns and provides precise estimates, even during low usage. The RMSE and R^2 for the proposed model indicate consistent predictions and superior performance compared to the other models.

Table 3.7 presents the yearly performance for 1-4 Bd SGTs and CSGTs. These results highlight the benefits of CSGTs over SGTs as there are improvements in resource efficiency, sustainability, and cost-effectiveness. CSGTs have better energy efficiency with heat loss of 5-8% compared to 7-10% for SGTs, indicating superior insulation and energy management. CSGTs maintain a tighter temperature range of ± 1.5°C to ± 3°C compared to ± 3.5°C to ± 5°C for SGTs, reflecting better HVAC control and indoor comfort. SGTs have lower carbon emissions, from 0.18 kgCO_2/kWh to 0.22 kgCO_2/kWh, while CSGTs range from 0.22 kgCO_2/kWh to 0.26 kgCO_2/kWh, indicating better use of RESs. SGTs have lower HVAC operating costs, from 30 CAD/unit to 45 CAD/unit, compared to 40 CAD/unit to 55 CAD/unit for CSGTs, showing more efficient systems. Overall, CSGTs outperform SGTs in comfort, sustainability, and cost savings, making them a better choice for long-term savings and lower environmental impact.

Table 3.7: Yearly performance for 1- to 4-bedroom SGTs and CSGTs.

Benefit	**1-Bd**	**2-Bd**	**3-Bd**	**4-Bd**
Heat Loss (%)				
CSGT	8.2	7.1	6.4	5.2
SGT	10.3	9.1	8.6	7.3
Temperature Variance (Comfort, ˚C)				
CSGT	± 3.0	± 2.6	± 2.0	± 1.4
SGT	± 5.0	± 4.7	± 4.0	± 3.3
Carbon Emissions ($kgCO_2$/kWh)				
CSGT	0.22	0.21	0.21	0.18
SGT	0.26	0.24	0.23	0.22
HVAC Costs (CAD/unit)				
CSGT	45	41	36	32
SGT	53	49	46	42

Tables 3.8 and 3.9 present the MAPE, RMSE, MAE, and R^2 for connected and disconnected SGTs with 1 to 4 bedrooms, with and without the proposed ML model. In Table 3.8, the MAPE is 3.51% (1-Bd) to 5.05% (4-Bd), RMSE is 2.79 kWh to 4.16 kWh, and MAE is 2.27 kWh to 3.62 kWh. The R^2 values range from 0.74 to 0.88, indicating good prediction. Table 3.9 shows the performance is improved with the proposed ML model. The MAPE decreases to 2.63% to 4.43%, RMSE drops to 1.93 kWh to 3.47 kWh, MAE decreases to 1.44 kWh to 3.06 kWh, and R^2 improves to 0.80 to 0.92. These results demonstrate that employing an ML model can significantly improve prediction performance and highlight the reliability and robustness of the proposed model in energy prediction for both SGTs and CSGTs. Tables 3.8 and 3.9 also give the corresponding acceptable ranges. The terms ”Very Good” and ”Acceptable” represent performance thresholds for performance metrics. For 1-Bd CSGTs (Fig. 3.14), the range is 200 kWh, with a mean around 600-650 kWh. The 2-Bd (Fig. 3.15) and 3-Bd (Fig. 3.16) units have similar ranges with means of about 700 kWh. The 4-Bd CSGT (Fig. 3.17) has a range of 300 kWh and a mean of 950 kWh. These values are within an acceptable range, confirming the reliability of the model.

Table 3.10 presents the parameters and performance of the 7 ML models, including

Table 3.8: Monthly energy performance of SGTs and CSGTs without an ML model.

Parameter	Connected SGTs				Disconnected SGTs				Acceptable Range
	1-Bd	2-Bd	3-Bd	4-Bd	1-Bd	2-Bd	3-Bd	4-Bd	
MAPE (%)	3.51	4.03	4.46	5.05	3.91	4.25	4.68	5.12	$<$10% (Very Good), 10–20% (Acceptable)
RMSE (kWh)	2.79	3.25	3.64	4.16	2.97	3.42	3.64	4.16	$<$10% of Data Range
MAE (kWh)	2.27	2.69	3.18	3.62	2.38	2.81	3.28	3.75	5–10% of Mean Actual Value
R^2	0.88	0.84	0.81	0.79	0.91	0.87	0.84	0.81	$>$0.8 (Acceptable), $>$0.9 (Very Good)

Table 3.9: Monthly energy performance of SGTs and CSGTs with an ML model.

Parameter	Connected SGTs				Disconnected SGTs				Acceptable Range
	1-Bd	2-Bd	3-Bd	4-Bd	1-Bd	2-Bd	3-Bd	4-Bd	
MAPE (%)	2.63	3.17	3.59	4.22	2.68	3.48	3.61	4.43	$<$10% (Very Good), 10–20% (Acceptable)
RMSE (kWh)	1.93	2.68	3.08	3.44	2.03	2.63	2.93	3.47	$<$10% of Data Range
MAE (kWh)	1.44	2.17	2.93	2.31	1.83	1.98	2.78	3.06	5–10% of Mean Actual Value
R^2	0.89	0.88	0.86	0.85	0.83	0.81	0.81	0.79	$>$0.8 (Acceptable), $>$0.9 (Very Good)

Table 3.10: Number of layers, neurons, average training iterations per epoch, training time, and error for 7 ML models.

Model	Layers	Neurons	Average Training Iterations per Epoch	Average Training Time per Epoch	Error (MAE/MSE)	Accuracy (%)
LR	N/A	N/A	261	55 s	MAE: 0.05	78%
LSTM	3	128	233	4 min	MAE: 0.03	82%
CNN	5	64	324	7 min	MSE: 0.02	83%
RF	Trees: 100	Trees: 100	1120	3 min	MSE: 0.04	85%
GB	Trees: 100	Trees: 100	1051	3 min	MAE: 0.04	86%
Hybrid LSTM-CNN	LSTM: 2, CNN: 3	LSTM: 64, CNN: 64	753	15 min	MAE: 0.02	90%
Proposed Model	LSTM: 3, CNN: 3	LSTM: 128, CNN: 128	827	20 min	MAE: 0.015	95%

number of layers, neurons, training iterations per epoch, training time per epoch, error, and accuracy. These results show that the proposed model provides the best performance with 95% accuracy and a low MAE of 0.015, but it has the highest computational cost due to its complex architecture. The hybrid LSTM-CNN model has a good tradeoff between accuracy (90%) and efficiency, while GB (86%) and RF (85%) perform well with moderate training times and acceptable error rates. The LSTM and CNN models have comparable accuracy (82-83%) and error rates. LR has the lowest accuracy (78%) and highest MAE (0.05), which is expected since it is a simple baseline.

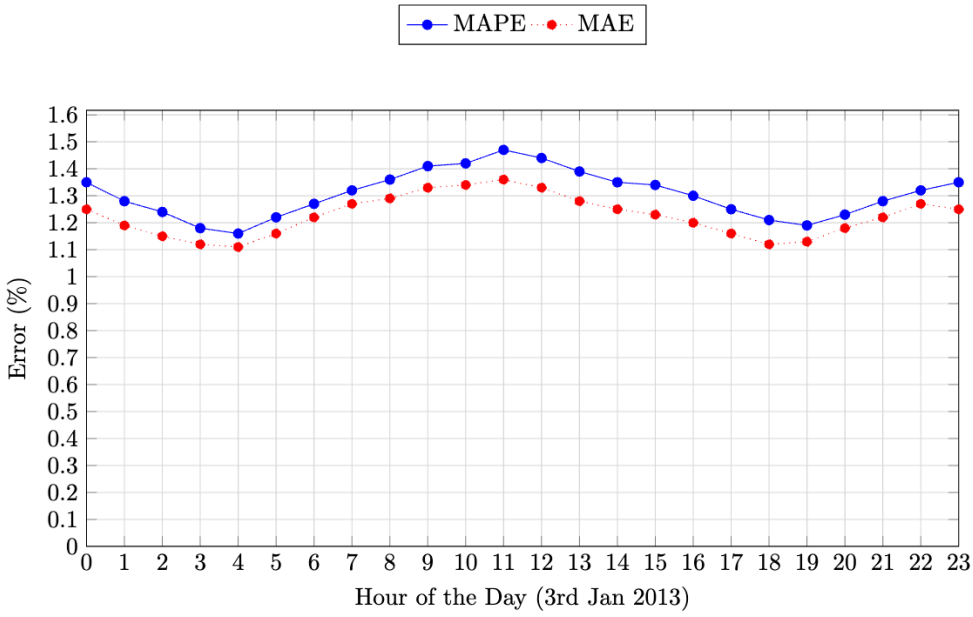

Figure 3.18: Hourly one day ahead prediction MAPE and MAE for January 3, 2013.

The MAPE and MAE for day-ahead predictions for CSGTs vary depending on weather, occupancy, and resource consumption behavior. Fig. 3.18 gives the hourly variations in MAPE and MAE for day ahead predictions for January 3, 2013. This shows that the error fluctuations are between 1.2% and 1.6%, indicating consistent model performance throughout the day. Low MAPE and MAE suggest good accuracy, with minimal fluctuations confirming that the model can handle varying conditions and provide robust energy usage prediction.

The MAPE and MAE for day-ahead predictions for CSGTs vary depending on weather, occupancy, and resource consumption behavior. Fig. 3.18 gives the hourly variations in MAPE and MAE for day ahead predictions for January 3, 2013. This shows that the error fluctuations are between 1.2% and 1.6%, indicating consistent model performance throughout the day. Low MAPE and MAE suggest good accuracy, with minimal fluctuations confirming that the model can handle varying conditions and provide robust energy usage prediction.

The normality and homoscedasticity residuals [172, 173] are used to validate model performance. From January 3 to 10, 2013, the residuals (actual values - predicted values) ranged between 1 and -2 kWh, indicating good prediction accuracy. The normality (Shapiro-Wilk test) residual is $p = 0.081$ and a value is normal if $p > 0.05$. Thus, the normality is verified. The homoscedasticity (Breusch-Pagan test) residual is $p = 0.065$ and $p > 0.05$ indicates consistent variance. The lack of heteroscedasticity suggests that model predictions will be stable across a variety of data, indicating reliability and robustness. The normality and homoscedasticity confirm that the proposed model provides excellent energy prediction for grid-connected CSGTs. Note that practical challenges, including system integration, user acceptance, data privacy, and maintenance, should be considered for successful model deployment in real-world settings.

3.4 Conclusion

This chapter presented a model for Connected Smart Green Townhouses (CSGTs) designed to optimize resource use. The integration of PV solar panels and efficient HVAC systems was shown to reduce resource consumption, promoting sustainable living. The results indicate improvements in cost efficiency, performance, and accuracy for CSGTs in Burnaby, BC. The proposed hybrid deep ML model outperformed the other models, including Gradient Boosting (GB), Random Forest (RF), Long Short Term Memory (LSTM), Convolutional Neural Network (CNN), hybrid LSTM-CNN, and Linear Regression (LR).

The proposed model had lower Mean Absolute Percentage Error (MAPE), Root Mean Square Error (RMSE), and Mean Absolute Error (MAE), and higher R^2, confirming its prediction precision. The accuracy ranged from 1.2% to 1.6%, with predictions closely aligning with actual values. Historical data, combined with model predictions, showed improvements in energy performance, cost savings, and emissions reduction. This indicates that the proposed model is effective for energy optimization in CSGTs. Future work will explore energy management policies and integrate more advanced models for improved system response and optimization.

Chapter 4

Load Optimization for Connected Modern Buildings Using Deep Hybrid Machine Learning in Island Mode

As urban areas grow, the demand for sustainable living solutions increases. Integrating Renewable Energy Sources (RESs) such as Photovoltaic (PV) systems and Electric Vehicles (EVs) into smart green buildings (SGBs) can reduce emissions and improve load efficiency. However, optimizing energy usage in this dynamic environment remains a challenge [1]. In 2019, buildings accounted for 32% of primary energy use in the US, with global consumption projected to rise by 1.3% annually until 2050 [1]. Space heating, cooling, and lighting consume almost half of this energy [174], making load prediction and optimization in SGBs essential for reducing energy waste, costs, and environmental impact [175, 176].

Machine Learning (ML) techniques have been considered to predict and optimize building energy consumption [177]. Hybrid models combining Long Short-Term Memory (LSTM) and Convolutional Neural Networks (CNN) have been shown to improve prediction accuracy by capturing both temporal and spatial dependencies in energy data [178, 179]. These models reduce energy costs and emissions which contribute to building resilience. Hybrid ML models such as Random Forest-Extreme Gradient Boosting-Linear Regression (RF-XGBoost-LR) have been shown to improve real-time prediction accuracy in Smart Buildings (SBs) and Smart Grids (SGs) [180, 181, 182]. The integration of distributed energy resources has been considered to optimize local energy generation and consumption to improve cost-effectiveness and flexibility [183].

To date, there has been limited research on island mode (off-grid) operation in residential buildings [184, 185, 186]. The gap is addressed by evaluating ML models for Connected Smart Green Townhouses (CSGTs) in Burnaby, BC, Canada, with a focus on island mode operation. Performance indicators such as energy efficiency, cost, emissions, and prediction accuracy are employed to support sustainable building operations [187]. A hybrid LSTM-CNN model is introduced to predict load consumption and optimize param-

eters such as Heating, Ventilation, and Air Conditioning (HVAC), lighting, and electricity use. The results demonstrate significant cost savings, emission reductions, and improved load efficiency, and indicate that connected SGBs operating in island mode can contribute to sustainable urban development.

The remainder of chapter 4 is organized as follows. Section 4.2 introduces energy demand prediction for CSGTs in island mode, including performance, cost, and emissions. Section 4.3 outlines the proposed ML model while Section 4.4 presents the performance results. Finally, Section 5 summarizes the chapter and discusses the implications for sustainable urban living.

4.1 SGT Modeling

The design and modeling of SGBs play a critical role in reducing Greenhouse Gas (GHG) emissions and supporting climate goals. These buildings incorporate advanced technologies, such as energy-efficient HVAC systems and photovoltaic (PV) solar panels, to improve load efficiency, resulting in substantial energy savings and cost reductions. As one of the strategies toward a sustainable future, SGBs contribute to environmentally friendly urban development. This section outlines the modeling of Connected SGTs (CSGTs), focusing on the integration of sustainable technologies to optimize performance.

Canada has significant energy and climate challenges but there is a lack of research, particularly regarding the impact on load consumption and energy optimization in SGBs [125, 129, 130]. This is addressed here with a focus on the geographic and climatic conditions of Burnaby, BC. An understanding of these factors is crucial for designing SGTs tailored to environmental conditions. This research offers valuable insights into the challenges and opportunities for CSGTs in Burnaby, advancing sustainable building practices [131].

The daylight hours in a year in Burnaby exceed the sunshine hours. Daylight refers to the total hours of light each day, while sunshine reflects the availability of direct sunlight, which affects solar energy harvesting. The longest daylight hours (16.02) occur in June, while the shortest hours (8.03) occur in December. This variation indicates higher solar energy potential in summer and reduced availability in winter. Heating Degree Days (HDD) are also important for understanding climate and designing efficient heating systems for SGTs. The HDD in Burnaby is approximately 3000 and indicates moderate heating demand. This helps guide the optimal sizing and design of heating systems to meet local needs [13].

4.1.1 SGT Formulation

This chapter considers the characteristic home described in [128, 132, 133] to develop a SGT model. The base model is a two-story townhouse (2140 sq ft) located in Burnaby, BC. It was built in 1995 and underwent significant renovations in 2007-2008 [128]. Major renovations typically occur every 15-20 years, depending on the condition of the building,

regulatory changes, and advances in sustainable technology. The home is oriented south to maximize solar energy utilization.

LEED certification and Canada Green Building Council (CGBC) standards are considered to reduce emissions and improve load efficiency [128]. SGTs are designed to operate solely on electricity to minimize on-site emissions, supported by PV systems with the goal of net zero energy [134]. During sunny months, surplus electricity can be exported to neighboring buildings, offsetting consumption during colder months.

Sustainable materials include bamboo flooring, recycled wood, PV panels, LED lighting, and high-efficiency heat pumps. These materials are widely used in sustainable construction projects [135, 136, 137]. These materials must adhere to applicable local and international building codes, including sustainability and safety requirements [138, 139, 140]. Heat pumps and modern air conditioning systems provide energy-efficient year-round temperature control [141, 142]. Heat pumps supply both heating and cooling and are more energy-efficient than traditional HVAC systems. Smart air conditioners optimize cooling by automatically turning off when not required, reducing energy consumption.

This work employs sustainable materials for SGTs in Canada [124]. Windows with a thermal resistance of R6 are used to reduce heat transfer and improve insulation, helping to maintain indoor comfort and lower heating and cooling loads [124]. This high thermal resistance is especially beneficial for energy efficiency in colder climates. The R2000 standard for energy-efficient housing in Canada is also employed [124]. It incorporates advanced insulation and ventilation systems. Table 4.1 gives the components and materials used in SGTs as well as the technologies and features that contribute to sustainable buildings.

The townhouse sizes and layouts are optimized for different family needs and energy usage. The one-bedroom (one-Bd) SGT is designed for a young couple, focusing on compact living with minimal energy consumption. The two-Bd SGT is suitable for a couple with one young child, providing extra space while being energy efficient. The three-Bd SGT caters to a family with two teenage children, prioritizing efficient zoning and energy distribution. The four-Bd SGT is designed for a family of five, incorporating advanced energy systems to accommodate higher energy demands.

Table 4.1: Materials and smart technologies used in SGTs.

Material/Technology	Description
Air Conditioner	High-efficiency cooling system.
Bamboo Flooring	Renewable, durable, and eco-friendly.
Connected Appliances	Internet connected for remote monitoring and control.
Cork Wall Insulation	Renewable, lightweight, and excellent insulation.
Envelope & Structural Mass	Improved insulation and thermal mass for load efficiency.
EV Charger	Electric vehicle charging station.
Heat Pump	Energy-efficient heating and cooling.
Hot Water Tank	Utilizes recycled materials for thermal insulation.
Light Emitting Diode (LED) Lighting	Energy-efficient and long-lasting.
Low Volatile Organic Compound (VOC) Paint	Reduces indoor air pollution.
PV Panels	RES to reduce electricity costs.
R6 Windows	High-performance windows to reduce heat loss and improve load efficiency.
Rainwater Harvesting System	Collects rainwater for irrigation.
Reclaimed Wood	Recycled, unique aesthetic, and reduces deforestation.
Recycled Glass Countertops	Eco-friendly, durable, and visually appealing.
Recycled Insulation Materials	Eco-friendly materials for thermal insulation.
Recycled Wood	High strength, recyclable, and long-lasting.
Smart Home (SH) Hub	Connect and manage smart devices, facilitating remote monitoring.
Smart Meters	Monitor and optimize load consumption.
Smart Plugs	Enable remote control and energy monitoring.
Smart Thermostat	Programmable and energy-efficient temperature control.
EVs such as a Tesla 3	Environmentally-friendly transportation with zero emissions.

Table 4.2: Specifications for hot water tank, HVAC, and PV capacity in SGTs (island mode).

Townhouse Type	Hot Water Tank Capacity (Gallons)	Daily Hot Water Consumption (Gallons/Day)	HVAC System Capacity (Tons)	PV System Capacity (kW)
Base	20.1	45.3	1.1	2.2
One-Bd	30.3	55.6	1.3	2.8
Two-Bd	39.1	75.2	1.9	3.5
Three-Bd	48.9	95.2	2.5	4.2
Four-Bd	60.3	110.1	2.8	5.4

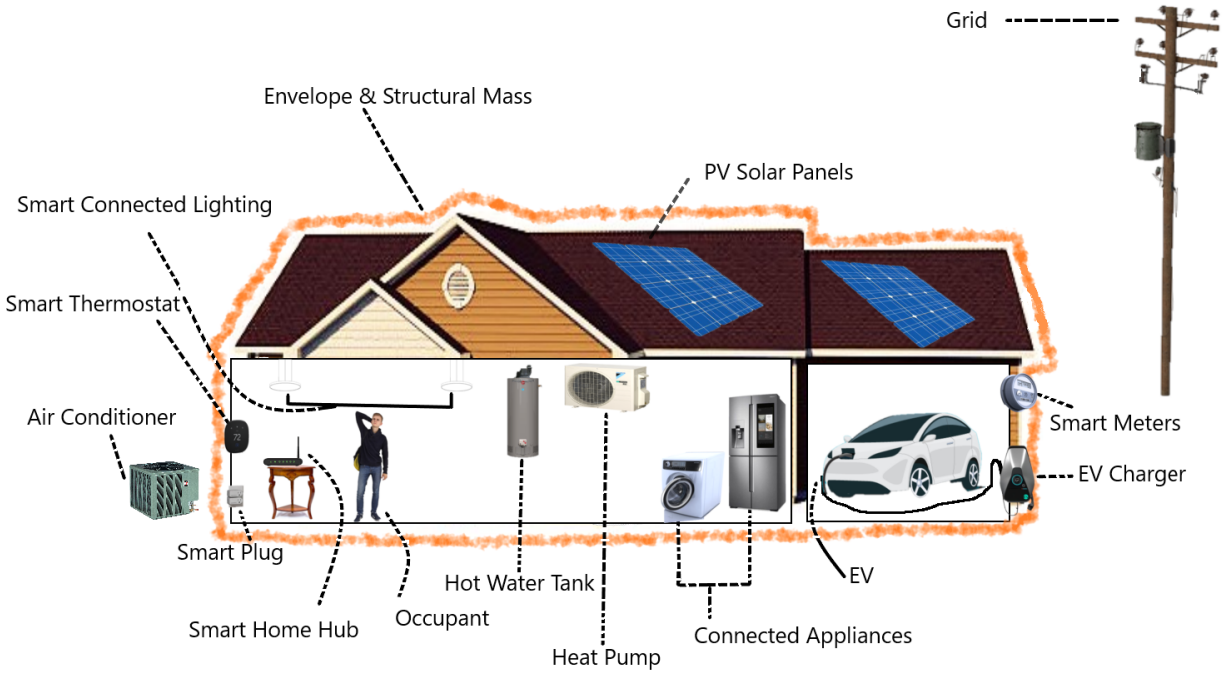

Figure 4.1: The SGT components in island mode.

Table 4.1 gives the specifications for hot water tank, HVAC, and PV capacity in SGTs (island mode). PV system capacity refers to the peak output under ideal sunlight conditions (i.e., under standard test conditions), and does not account for daily or monthly output variations due to location-specific factors such as weather, shading, or panel orientation. Operating in island mode increases resilience and reliability to allow CSGBs to function independently of the grid and ensure an uninterrupted energy supply during outages. This maximizes the use of locally generated renewable energy such as from PV panels, and EV batteries for storage, promoting energy independence and decentralized resource management. Integrating island mode with advanced technologies like Vehicle-to-Grid (V2G) systems and ML models provides an innovative solution to modern energy challenges. These models improve load prediction to optimize energy resources and support sustainability so CSGBs can be an environmentally friendly urban solution.

Fig. 4.1 shows the proposed SGT and its components in island mode. This includes PV panels, energy-efficient HVAC (e.g., heat pump), and a high-performance hot water tank [161]. These systems are modeled in OpenStudio 3.8.0 to evaluate energy performance. Data is collected using meters that measure electricity, water, and gas consumption. This data is processed and stored on a central server. A WiFi access point provides communication between the server and devices, while cloud storage supports remote access and long-term data storage. This setup enables efficient resource management and informed decision-making [125, 129, 130].

Fig. 4.1 shows the proposed SGT and its components in island mode. This includes PV panels, energy-efficient HVAC (e.g., heat pump), and a high-performance hot water

Table 4.3: PV panel and battery storage specifications for SGTs in island mode.

Parameter	1-Bd SGT	2-Bd SGT	3-Bd SGT	4-Bd SGT
Roof Area (sq ft)	764	1080	1543	1736
Panel Capacity per Unit (W)	300	400	500	600
Total System Capacity (kW)	2.6	3.2	3.8	4.5
Estimated Annual Energy Output (kWh)	3070	3840	4610	5380
Energy Saved Annually (kWh)	3070	3840	4610	5380
PV Cell Area (sq ft)	193	251	309	361
Battery Storage (kWh)	9.0	12.0	15.0	18.0
Autonomy Period (days)	1.5	1.5	1.5	1.5

tank [161]. These systems are modeled in OpenStudio 3.8.0 to evaluate energy performance. Data is collected using meters that measure electricity, water, and gas consumption. This data is processed and stored on a central server. A WiFi access point provides communication between the server and devices, while cloud storage supports remote access and long-term data storage. This setup enables efficient resource management and informed decision-making [125, 129, 130].

Table 4.3 presents the PV panel parameters for SGTs including roof area, panel capacity, energy output, payback period, and cell efficiency, as well as the battery system specifications when operating in island mode. These values were obtained using the results in [156, 157]. This shows that the roof area, panel capacity, and estimated annual energy output increase with the number of bedrooms. Larger townhouses have more roof area, supporting higher-capacity panels. The energy saved annually is the same as the PV system output reflecting efficient utilization. Battery storage is specified to provide energy autonomy for 1.5 days. This allows for short-term off-grid operation. The Payback Period here is calculated based on (3.7). SGTs use lithium-ion batteries for energy storage. The capacities range from 9.0 kWh for a 1-Bd unit to 18.0 kWh for a 4-Bd unit, each supporting 1.5 days of off-grid operation. Larger SGTs produce more energy but need more storage and have longer payback periods.

4.1.2 CSGT Formulation

Connecting residential buildings significantly reduces energy consumption and costs [145]. For SGTs, connecting units improves efficiency and enables better energy management. Linking modern residential townhouses is similar to Micro-Grids (MGs) [37, 146]. Here, CSGTs in island mode are examined to assess their performance and determine the benefits for load optimization and sustainability.

Key components of connected townhouses are connected water systems [128, 147] and party walls [148, 149]. Party walls are shared walls between neighboring properties and are common in townhouses and semi-detached homes. They serve as boundaries and are jointly owned and maintained. Party wall agreements specify structural maintenance, repairs, alterations, and dispute resolution [148, 149]. In connected SGTs, party walls provide structural integrity, noise reduction, and fire safety. Connected water systems are important for SGB performance, occupant comfort, and sustainability. District cooling provides chilled water across multiple buildings. This work examines district cooling performance, load patterns, temperature management, and efficiency [147]. It also considers how building operations impact cooling infrastructure effectiveness.

The CGST performance expressions are based on [150, 151]. The heat transfer is given by

$$Q = k \cdot A \cdot \frac{\Delta T}{d} \tag{4.1}$$

where Q is the heat transfer rate, k is the thermal conductivity of the wall material, A is the surface area of the wall, ΔT is the temperature difference across the wall, and d is the thickness of the wall. This describes conductive heat transfer where thermal energy moves through a solid material. It is proportional to the thermal conductivity of the material and the cross-sectional area through which the heat moves. The goal is to minimize heat loss or gain and optimize energy use in CGSTs.

Continuity is very important in fluid dynamics and is given by

$$\frac{d(\rho A)}{dt} = \dot{m}_{\text{in}} - \dot{m}_{\text{out}} \tag{4.2}$$

This indicates that the rate of change of mass (ρA) within a volume is equal to the difference between the mass flow rate entering $(\dot{m}_{\text{in}})$ and leaving $(\dot{m}_{\text{out}})$ the system. This is applied to fluid systems within CSGTs such as HVAC ducts, plumbing systems, and other fluid transport mechanisms such as rainwater harvesting systems.

The load consumption is

$$C = \sum_{i=1}^{n} C_i \tag{4.3}$$

The goal is to minimize C which is the sum of the load consumptions C_i of different components, systems, or time periods, while maintaining comfortable temperature levels and adequate flow rates. The building energy balance is

$$\text{Energy In} - \text{Energy Out} = \text{Energy Storage} \tag{4.4}$$

where Energy In includes total load consumption. Total load consumption includes electrical consumption (lighting, and HVAC), gas consumption, and water consumption. Energy Out includes heat loss, heat gain, total load consumption output, and PV panel output. In island mode, buildings operate independently from the grid, so PV output is considered an output when it is stored in batteries and used to meet building energy

needs. The PV output is a source of energy that contributes to building self-sufficiency. Energy Storage is changes in internal and external energy storage within the building.

Renewable Energy Integration (REI) refers to the incorporation of RESs into a building energy system in island mode and is given by

$$\text{REI} = \frac{\text{Renewable Energy Used}}{\text{Total Energy Consumption}} \times 100\% \tag{4.5}$$

where Renewable Energy Used is the amount of energy derived from RES like PV panels, and Total Energy Consumption is the total energy consumed by the building. It includes electricity consumption (e.g. lighting and HVAC), gas consumption, and water consumption.

The Smart Technology Utilization Index (STUI) is used to quantify the effectiveness and efficiency of smart technology implementation in a building. It is expressed as

$$\text{STUI} = \frac{\text{Number of Smart Devices}}{\text{Total Devices}} \times 100\% \tag{4.6}$$

where Number of Smart Devices is the total number of smart devices used in the building and Total Devices is the total number of devices in the building.

SGTs range from base to 4-Bd units. The base and 1-Bd units have 1 bathroom, the 2-Bd unit has 2 bathrooms, and the 3-Bd and 4-Bd units have 3 bathrooms. Kitchen sizes vary from 60 sq ft (base) to 150 sq ft (4-Bd). Dining rooms range from 40 sq ft (base) to 120 sq ft (4-Bd). Living rooms range from 120 sq ft (1-Bd) to 250 sq ft (4-Bd). Entrance spaces are from 30 sq ft (base) to 90 sq ft (4-Bd). Deck sizes are 40 sq ft to 150 sq ft. The first bedroom is 100 sq ft in the base unit and 120 sq ft in the others. The 2-Bd to 4-Bd units have a second bedroom (120 sq ft) and a master bedroom (150-250 sq ft). There is a second master bedroom (150-200 sq ft) in the 3-Bd and 4-Bd units. Garage space is available only in the 3-Bd (154.1 sq ft) and 4-Bd (173.8 sq ft) units. The base unit is 680 sq ft while the 4-Bd unit is 1735.9 sq ft. Heights are 8.0 ft (base) and 16.5 ft (other units). The base unit has a 20-gallon hot water tank, 1.0 ton HVAC system, and 1.80 kW PV panels. These capacities increase to a 60.3-gallon hot water tank, 3.1 ton HVAC system, and 4.48 kW PV panels in the 4-Bd unit.

4.1.3 Performance Metrics

This section presents the metrics to assess building efficiency, accuracy, performance, emissions, and costs. The Total Energy Use Intensity (TEUI) is

$$\text{TEUI} = \frac{\text{Total Energy Consumption}}{\text{Total Building Area}} \tag{4.7}$$

where Total Energy Consumption is the sum of all forms of energy consumption within the building in kWh and Total Building Area is the total floor area of the building in sq ft. The Total Energy Demand Intensity (TEDI) is

$$\text{TEDI} = \frac{\text{Total Energy Demand}}{\text{Total Building Area}} \tag{4.8}$$

where Total Energy Demand is the sum of the peak energy demand from all sources within the building in kW.

The Control Efficiency Index (CEI) is used to quantify the effectiveness of control systems in achieving desired outcomes within the building and is given by

$$\text{CEI} = \frac{\text{Actual Energy Usage (AEU)}}{\text{Optimal Energy Usage (OEU)}} \times 100\% \tag{4.9}$$

where Actual Energy Usage (AEU) is the actual energy consumed by the building and Optimal Energy Usage (OEU) is the energy usage under ideal conditions. This metric is crucial for building energy management as it helps to identify inefficiencies in control strategies and provides a basis for optimizing performance.

The Indoor Air Quality index (IAQ) is a measure of indoor air quality. It is used to quantify the quality of indoor air within the building and is

$$\text{IAQ} = \frac{\text{IAQ Measurement}}{\text{Maximum Acceptable IAQ}} \times 100\% \tag{4.10}$$

where Maximum Acceptable IAQ is the maximum acceptable level of indoor air quality. It evaluates various indoor air quality parameters such as Carbon Dioxide (CO_2) levels, Volatile Organic Compounds (VOCs), Carbon Monoxide (CO), and Ozone (O_3) [46].

Waste Recycling Rate (WRR) is used to quantify the proportion of waste materials that are recycled or diverted from landfills and is given by

$$\text{WRR} = \frac{\text{Weight of Recycled Waste}}{\text{Total Weight of Waste}} \times 100\% \tag{4.11}$$

where Weight of Recycled Waste is the total weight of the waste materials recycled and Total Weight of Waste is the total weight of the waste materials generated. This reflects the effectiveness of building waste management with higher values indicating better recycling performance. It is used to identify areas within the building where waste recycling practices may need to be improved such as common areas and kitchens. Material Recycling Percentage (MRP) is used to assess the sustainability performance of SGBs and is given by

$$\text{MRP} = \frac{\text{Weight of Recycled Materials (WRM)}}{\text{Total Weight of Materials Used (TWMU)}} \times 100\% \tag{4.12}$$

where WRM is the total weight of the materials recycled and TWMU is the total weight of the materials used. A building with an average MRP of 75% is more likely to achieve green certification, reflecting a commitment to sustainability.

The water efficiency is

$$\text{Water Efficiency} = \frac{\text{Water Saved}}{\text{Total Water Used}} \times 100\% \tag{4.13}$$

It reflects the effectiveness of water-saving measures like low-flow fixtures and rainwater harvesting. The Electrical Consumption Efficiency (ECE) is

$$\text{ECE} = \frac{\text{Total Useful Electrical Output}}{\text{Total Electrical Input}} \times 100\% \tag{4.14}$$

A higher ECE means more input electricity is converted into useful energy. The Gas Consumption Efficiency (GCE) is

$$\text{GCE} = \frac{\text{Total Useful Heat Output From Gas}}{\text{Total Gas Input}} \times 100\% \tag{4.15}$$

It measures the efficiency of gas used for heating.

The insulation R-value measures thermal resistance and is given by

$$R = \frac{d}{k} \tag{4.16}$$

A higher value indicates better insulation which improves building efficiency [35]. Important R-values include exterior walls (R-30, in $\text{ft}^2 \cdot ^\circ\text{F} \cdot \text{h/BTU}$), windows (R-5, triple-pane with low-emissivity coatings), roof/ceiling (R-50, for high insulation), and floor/slab (R-20, to reduce heat loss through the foundation). OpenStudio provides detailed thermal values based on the specified materials and their properties.

TEUI and TEDI quantify load consumption and efficiency to help reduce waste and optimize energy use [162]. GHGI gives the carbon footprint and is expressed as

$$\text{GHGI} = \frac{\text{Total Greenhouse Gas Emissions}}{\text{Building Floor Area}} \tag{4.17}$$

Compliance with TEUI, TEDI, and GHGI standards is crucial, as it ensures sustainability and thus building marketability to investors. High TEUI, TEDI, and GHGI ratings signify superior efficiency, making buildings more competitive. Economic viability [188] considers cost savings, Return on Investment (ROI), and cost-benefit ratios. These support informed decision-making for load efficiency to align with both regulatory and investment goals.

The Total Energy Consumption is

$$\text{Total Energy Consumption} = \text{Energy from Storage} + \text{Energy from Renewables} \tag{4.18}$$

where Energy from Storage is the energy supplied by the battery system and Energy from Renewables is the energy generated by local renewable sources, such as PV systems. This represents the energy used for building operation in island mode. It should be sufficient to ensure continuous function when the building is disconnected from the grid. The cost of energy is

$$\text{Cost of Energy} = \text{Total Energy Consumption} \times \text{Unit Cost} \tag{4.19}$$

where Total Energy Consumption is the total amount of energy consumed by the building and Unit Cost is the unit cost of the energy consumed. The cost savings is

$$\text{Cost Savings} = \text{Cost Before} - \text{Cost After} \tag{4.20}$$

where Cost Before is the total cost before implementing load efficiency initiatives and Cost After is the reduced cost after implementing load efficiency measures. This provides the financial savings by comparing costs before and after load efficiency measures are implemented.

The ROI is

$$\text{ROI} = \frac{\text{Net Savings}}{\text{Initial Investment}} \times 100\% \tag{4.21}$$

where Net Savings is the total savings from load efficiency measures and Initial Investment is the cost of implementing these measures. The net benefit is

$$\text{Net Benefit} = \text{Total Savings} - \text{Total Costs} \tag{4.22}$$

where Total Savings is the savings from load efficiency measures and Total Costs are the expenses for implementing and maintaining them. This provides the overall financial benefit.

The HVAC metric is defined as

$$\text{HVAC Metric} = \frac{1}{n} \sum_{i=1}^{n} \left(\frac{X_i - X_{\text{min},i}}{X_{\text{max},i} - X_{\text{min},i}} \right) \tag{4.23}$$

where X_i is the ith parameter value, $X_{\text{max},i}$ and $X_{\text{min},i}$ are the corresponding maximum and minimum values, and n is the number of parameters. The parameters included in this metric are heat transfer efficiency, fluid dynamics efficiency, building energy balance, TEUI, TEDI, cooling energy consumption, and IAQ index.

In island mode, energy storage, backup power, load management, and resilience must be evaluated to reflect the operational constraints of off-grid systems. The charging and discharging of the battery is modeled by the State of Charge (SOC)

$$\text{SOC}(t) = \text{SOC}(t-1) + \frac{\text{P-charge}(t) \cdot \eta_{\text{charge}} - \text{P-discharge}(t)}{\text{E}_{\text{max}}} \tag{4.24}$$

where $\text{SOC}(t)$ is the battery charge at time t, $\text{P-charge}(t)$ and $\text{P-discharge}(t)$ are the corresponding charging and discharging power, η_{charge} is the charging efficiency, and E_{max} is the maximum energy capacity. The energy balance for the storage system in island mode is

$$\text{E}_{\text{storage}}(t) = \text{E}_{\text{storage}}(t-1) + \text{P}_{\text{PV}}(t) + \text{P}_{\text{backup}}(t) - \text{P}_{\text{load}}(t) - \text{P}_{\text{storage}}(t) \tag{4.25}$$

where $\text{E}_{\text{storage}}(t)$ is the stored energy at time t, $\text{P}_{\text{PV}}(t)$ is the PV system power, $\text{P}_{\text{backup}}(t)$ is the backup power, $\text{P}_{\text{load}}(t)$ is the building load, and $\text{P}_{\text{storage}}(t)$ is the power used for storage operations. The backup efficiency is

$$\text{Backup Efficiency} = \frac{\text{Total Backup Power Output}}{\text{Total Backup Power Input} + \text{Energy from Storage}} \times 100\% \tag{4.26}$$

where Total Backup Power Output is the useful backup power, Total Backup Power Input is the total energy consumed by the backup system, and Energy from Storage is the energy drawn from the storage system. Battery degradation over time is modeled by

$$\text{Capacity}(t) = \text{Capacity}(t-1) \cdot (1 - \text{Degradation Rate}) - \text{Capacity Loss Due to Usage} \tag{4.27}$$

where $\text{Capacity}(t)$ is the remaining battery capacity at time t, Degradation Rate is the loss rate per cycle, and Capacity Loss Due to Usage accounts for additional loss due to use.

Table 4.4: Outcomes related to water systems and party walls in CSGTs in island mode.

Parameter	**1-Bd**	**2-Bd**	**3-Bd**	**4-Bd**
Daily Hot Water Usage (Gal/Day)	55.1	80.7	105.3	125.2
Energy Savings from Shared Walls (%)	8.5	12.1	15.2	18.3
PV Panel Output (kWh/Day)	7.2	8.9	10.5	12.2
HVAC System Usage (Tons/Day)	1.2	1.7	2.3	2.6

Table 4.4 gives the water system and party wall results for CSGTs in island mode. This shows that the PV system output ranges from 7.2 to 12.2 kWh/day, indicating reliable energy generation. HVAC usage is lower, reflecting efficient energy management. Daily hot water usage is consistent across the townhouse sizes, demonstrating good system capability. Energy savings from shared walls range from 8.5% to 18.3% and indicate the impact of connected infrastructure on reducing load. Compared to SGTs in island mode, CSGTs outperform in PV panel output, energy savings, and HVAC efficiency. Thus, connected SGTs are more resilient and sustainable during off-grid operation.

Table 4.5: Monthly energy performance for SGTs and CSGTs in island mode without an ML model.

Parameter	Disconnected				Connected				Acceptance Range
	1-Bd	2-Bd	3-Bd	4-Bd	1-Bd	2-Bd	3-Bd	4-Bd	
Efficiency									
Heat Transfer (%)	84.1	85.2	86.3	87.4	85.0	86.5	87.8	89.1	80-90
Fluid Dynamics (%)	78.2	79.6	80.5	81.6	79.3	80.8	82.0	83.5	75-85
Total Energy Consumption (kWh/sq ft)	0.79	0.73	0.71	0.68	0.76	0.72	0.69	0.67	0.65-0.80
Building Energy Balance (%)	90.2	91.3	92.4	93.5	91.5	92.6	93.7	94.8	85-95
TEUI (kWh/sq ft)	0.81	0.79	0.78	0.76	0.69	0.66	0.64	0.61	0.60-0.80
TEDI (kWh/sq ft)	0.45	0.44	0.41	0.39	0.41	0.38	0.37	0.36	0.35-0.50
HVAC Metric (%)	90.2	91.0	91.8	92.6	91.2	92.1	93.0	93.8	85-95
Water Efficiency (%)	79.5	79.9	80.7	81.3	80.5	80.9	81.6	82.2	75-85
ECE (%)	95.1	95.7	96.3	96.9	96.0	96.5	97.1	97.7	90-98
GCE (%)	87.3	88.1	88.9	89.7	88.5	89.3	90.1	90.9	85-95
Insulation R-Value (%)	24.0	24.3	24.6	24.9	24.7	25.0	25.4	25.7	20-30
Cost Savings (CAD)	380.5	410.6	440.7	470.8	396.0	426.8	457.4	488.2	-
Performance									
RE Integration (%)	30.5	35.1	39.7	44.3	31.2	36.0	40.8	45.6	30-50
STUI (%)	92.5	93.4	94.3	95.2	93.7	94.5	95.4	96.2	90-97
Cooling Energy Consumption (kWh/sq ft)	0.28	0.26	0.25	0.23	0.23	0.22	0.21	0.21	0.20-0.30
CEI (%)	86.2	87.1	88.0	88.9	87.5	88.4	89.3	90.2	85-95
WRR (%)	67.4	69.2	71.0	72.8	68.7	70.6	72.4	74.3	65-75
IAQ (%)	89.0	89.9	90.8	91.7	90.2	91.1	92.0	92.9	85-95
MRP (%)	73.1	73.9	74.7	75.5	74.3	75.1	76.0	76.8	70-80
Energy Storage									
Battery Charging Efficiency (%)	-	-	-	-	89.31	91.25	92.32	92.87	85-95
Battery Discharging Efficiency (%)	-	-	-	-	89.52	90.64	90.89	92.03	85-95
Energy Storage Capacity (kWh)	-	-	-	-	53.15	61.42	72.12	83.21	50-80
Backup Power Duration (hours)	-	-	-	-	4.23	4.95	6.12	7.31	4-8
Emissions									
GHGI ($kgCO_2$/kWh)	0.52	0.49	0.47	0.43	0.50	0.47	0.45	0.41	0.40-0.55
Cost									
Cost of Energy (CAD)	550.5	620.8	690.2	761.7	538.0	607.8	677.2	748.5	-
ROI (%)	16.2	17.3	18.4	19.5	17.0	18.1	19.3	20.4	15-25
Net Benefit (CAD)	307.5	361.2	412.4	459.9	316.8	370.4	421.7	469.5	-

Table 4.5 gives the monthly energy performance for SGTs and CSGTs in island mode without an ML model. These results were generated using Python and EnergyPlus with the pyenergyplus library. The building model was created in OpenStudio 3.8.0 with .osm files converted to EnergyPlus input files (.idf). Table 4.5 shows that CSGTs have 5% to 7% lower energy consumption per square foot due to energy sharing and advanced management. The TEUI is improved by 10% and the TEDI by up to 12%. The HVAC and water efficiency are 2% to 4% better and CO_2 emissions per kWh are 3% to 5% lower. Better insulation and renewable energy use reduce heating and cooling loads, lowering costs by 2% to 4% and increasing ROI by 5% to 7%. These results illustrate

CSGT sustainability, cost-effectiveness, and energy efficiency, making them a superior choice for modern buildings.

4.2 Load Optimization Using the Proposed ML Model

This section integrates empirical data, computational modeling, and ML techniques to analyze critical parameters such as efficiency, accuracy, and cost, which influence smart green technologies. The primary objective is to optimize load consumption in Smart Green Townhouses (SGTs) and enhance sustainability [17, 19, 164, 165].

The proposed hybrid model predicts load consumption and optimizes HVAC and lighting systems, and electricity usage. It combines the spatial feature extraction of CNNs with the temporal learning of LSTM networks. It is trained using historical data [17]. The optimization framework focuses on reducing costs and emissions, improving system performance, and maximizing Renewable Energy Integration (REI) and smart technology for efficient, sustainable operation.

Hybrid models have been shown to outperform traditional ML methods [164, 184]. The CNN-LSTM-AE model developed in [165] achieved lower Mean Square Error (MSE), Mean Absolute Error (MAE), Root Mean Squared Error (RMSE), and Mean Absolute Percentage Error (MAPE) compared to other models using datasets from UC Irvine and Korean commercial buildings. In [165], a CNN-LSTM model was used to improve indoor temperature modeling for HVAC control. The performance was better than MLP and LSTM models over multiple time horizons (1-120 min). The proposed model combines a CNN with LSTM to provide effective load optimization in SGTs as well as insights into energy dynamics and performance.

The proposed algorithm for managing energy in SGTS in island mode employs a deep hybrid model integrating CNN and LSTM networks [189, 167, 170]. Fig. 4.2 presents a flowchart of the proposed algorithm. It involves data analysis, load and energy optimization, SB controls, RE integration, occupant behavior modeling, and continuous monitoring. The algorithm begins with data input, such as load consumption and user behavior, and this is processed using the model.

K-fold cross-validation is employed to train and validate the LSTM-CNN model [190]. LSTM layers with attention focus on important time-series data, while CNN layers with skip connections extract features from spatial and sequential data. The outputs are integrated to improve prediction accuracy. The algorithm includes two decision nodes. If Condition 1 is met, load optimization is conducted, otherwise the results are output. Condition 2 determines if RE integration and/or occupant behavior are modeled. The algorithm produces final predictions to optimize energy performance and load efficiency in CSGTs.

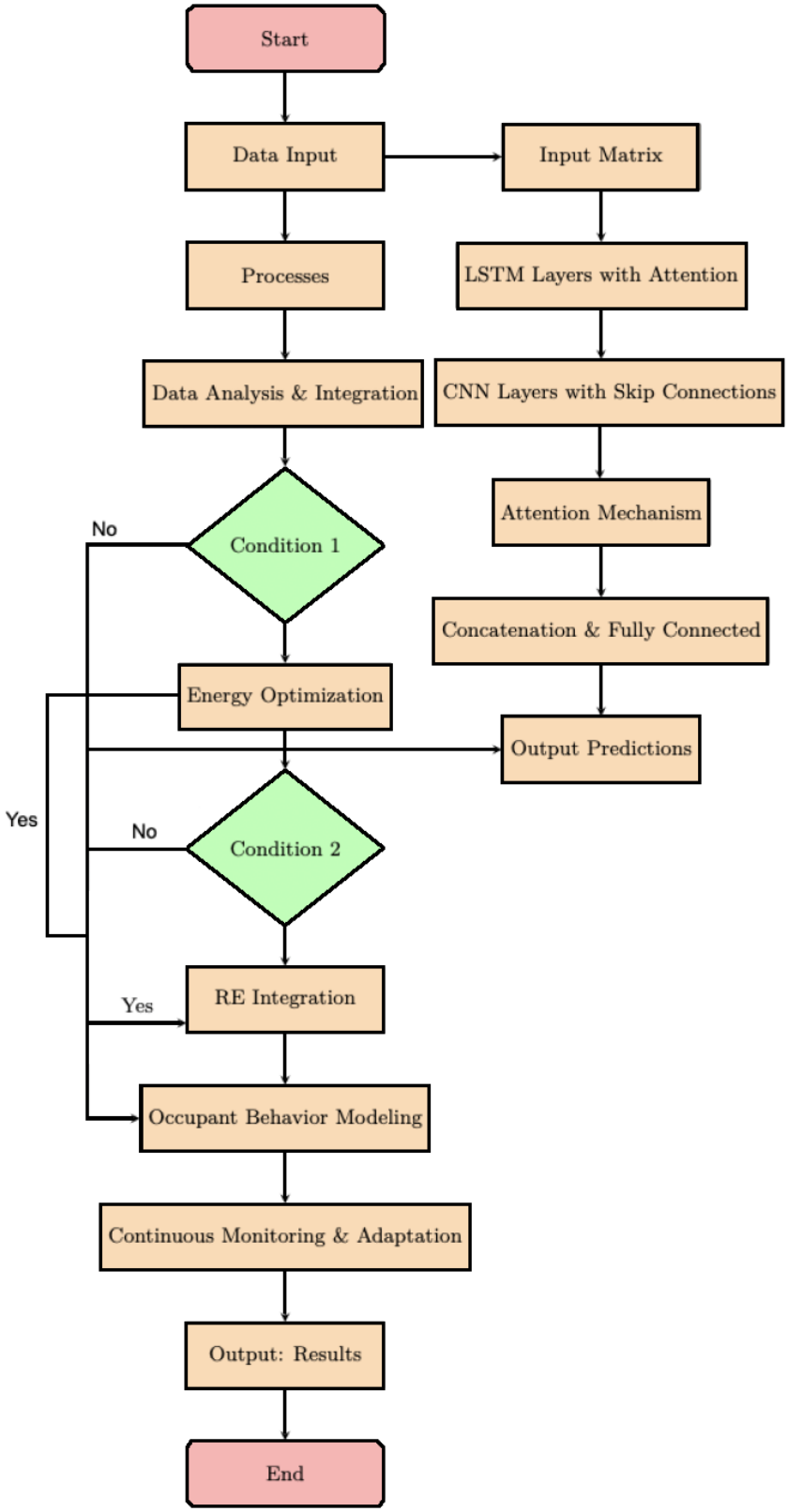

Figure 4.2: The proposed algorithm flowchart.

4.2.1 Optimization Problem

The optimization problem is multi-objective. It aims to reduce costs and emissions while improving performance [191]. The focus is minimizing total energy usage and increasing the integration of RES and smart technologies. The deep ML model predicts load consumption and optimizes system parameters [163, 169]. The objective function is

$$\text{F} = \text{Minimize Total Energy Consumption} - \alpha \times \text{REI} - \beta \times \text{STUI} \tag{4.28}$$

where the coefficients α and β are based on historical data and prioritize the two key objectives. The values chosen are $\alpha = 0.3$ to emphasize cost minimization and $\beta = 0.2$ to focus on emissions reduction with lower priority. This combines load consumption, REI, and STUI into a single function.

The following constraints are used to ensure solutions meet practical and regulatory standards

$$0 \leq \text{TEUI} \leq \text{TEUI}_{\text{max}} \tag{4.29}$$

$$0 \leq \text{TEDI} \leq \text{TEDI}_{\text{max}} \tag{4.30}$$

$$0 \leq \text{REI} \leq 100\% \tag{4.31}$$

$$0 \leq \text{STUI} \leq 100\% \tag{4.32}$$

$$\text{Energy In} - \text{Energy Out} = \text{Energy Storage} \tag{4.33}$$

$$\text{Energy Storage}_{\text{min}} \leq \text{Energy Storage} \leq \text{Energy Storage}_{\text{max}} \tag{4.34}$$

where Energy In includes energy generated from local sources like PV panels, while Energy Out is all energy consumed in the building. Energy Storage is the excess energy stored in batteries. Several variables have minimum or maximum values that restrict possible solutions. For example, thermostat settings are limited to 18–25°C. According to IEC 62933, the minimum energy storage must be 10% and the maximum 90% of total capacity. Constraints, including budget and regulatory requirements, ensure that solutions are realistic and effective.

ML techniques have been used to predict load consumption, optimize resources, and improve sustainability in SGTs and CSGTs. Artificial Neural Networks (ANNs) are effective for load optimization, demand prediction, and anomaly detection. They have also been employed for occupancy forecasting and load anomaly detection using methods such as Holt-Winters-Taylor smoothing and Autoregressive Moving Average (ARMA).

The predicted load, the predicted occupancy, the Anomaly Detection, and the HVAC optimization are calculated based on (3.37) to (3.40) respectively.

Comfort and operational constraints keep the system within acceptable limits. Comfort constraints ensure thermal comfort by penalizing deviations from desired temperature or humidity set-points. HVAC behavior over time is dynamic as it responds to inputs and disturbances. It can be modeled using physics-based equations or simulation and ML models like LSTM can capture these dynamics.

The integration of LSTM and CNN layers enables the model to capture temporal dependencies and spatial patterns. Attention mechanisms focus on the most relevant features while skip connections improve feature representation and generalization. This architecture can adapt to varying input conditions, and handle sequences of different lengths and complexities while mitigating the vanishing gradients problem and ensuring fast convergence. The proposed model has three LSTM layers and three CNN layers. The outputs of these layers are concatenated to fuse temporal and spatial representations. The combined features are passed through a fully connected layer to reduce the dimensionality and refine the data for prediction. The final output layer provides the predictions. The data processing flowchart for island mode is same with Fig. 3.9. The input data is normalized using scaling and preprocessed for cleaning, missing value imputation, and handling outliers. The data is then split into training, testing, and validation sets. Non-cyclic features (e.g., time components) and correlated attributes are used to improve prediction accuracy. The data is normalized between 0 and 1 using (3.41) and (3.42) [171]. The mentioned nine features in section 3.3.2 are the same for the input to the ML model here.

4.3 Performance Results

Building data including system architecture, load consumption, and weather conditions were collected for the SGTs to ensure adaptability to different conditions. OpenStudio 3.8.0 was used to simulate energy use and the Python v3.11.5 libraries (pandas v2.1.1 [152], NumPy [153], and Matplotlib [154]) were employed to analyze and visualize the data. Ninja [155] was employed to compare PV systems. Historical datasets such as AMPds2 [128, 132, 133, 141] were used to train and validate the ML models. Island mode in Burnaby assumes CSGTs disconnected from the BC Hydro grid so energy from PV panels and EVs must be used. This reduces GHG emissions and electricity costs and improves resilience by satisfying household energy needs while selling surplus energy.

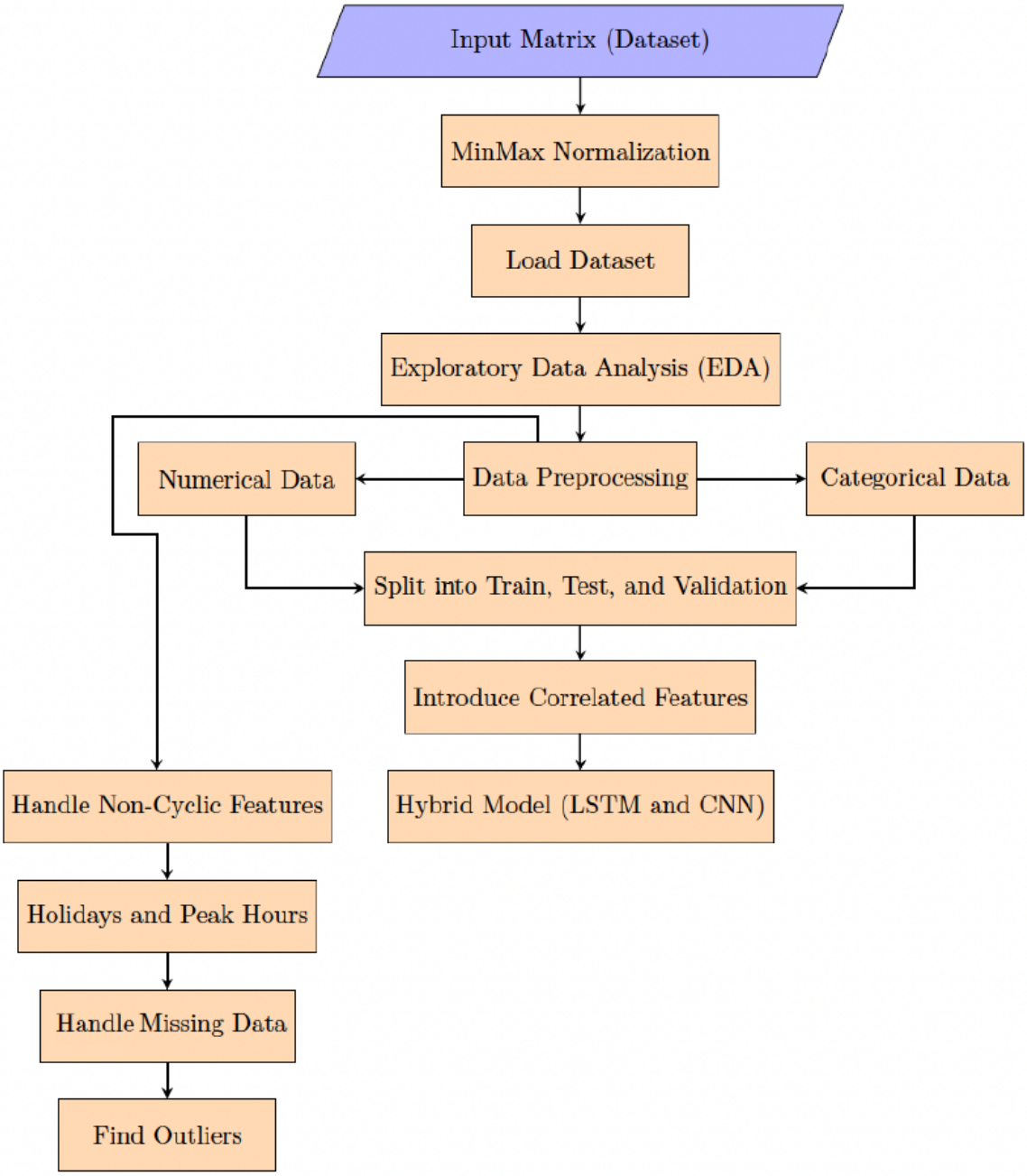

Figure 4.3: Monthly electricity consumption for one to four bedroom SGTs and CSGTs in island mode (2012-14).

Fig. 4.3 presents the monthly electricity consumption for one to four bedroom SGTs and CSGTs in island mode (2012-14). This shows that both SGTs and CSGTs have higher electricity consumption in the winter due to greater heating demands. However, CSGTs consume more electricity than SGTs, particularly in larger units (3-Bd and 4-Bd), indicating that smart features contribute to increased loads. Thus, while CSGTs provide

advanced functionalities, this results in greater energy demands.

4.3.1 Impact of Island Mode on Gas and Water Consumption

Island mode operation significantly impacts gas and water consumption in SGTs, as buildings operate independently from the grid. In cold climates like Canada, gas consumption increases in island mode to meet heating needs, especially when gas is used for heating. SGT energy management systems can balance gas and electricity energy use in island mode to ensure a consistent energy supply without over-reliance on a single source.

In island mode, SGTs may shift from electric to gas water heating to manage electricity constraints while ensuring hot water availability [193, 194]. Water-efficient systems have stricter water-use policies, reduced irrigation, and occupant-driven conservation behavior [194]. The Urban Heat Island (UHI) influence on building load consumption [195] provides important information for optimizing resource use [196]. These results emphasize the need for energy management and resource optimization to maintain sustainability in off-grid conditions.

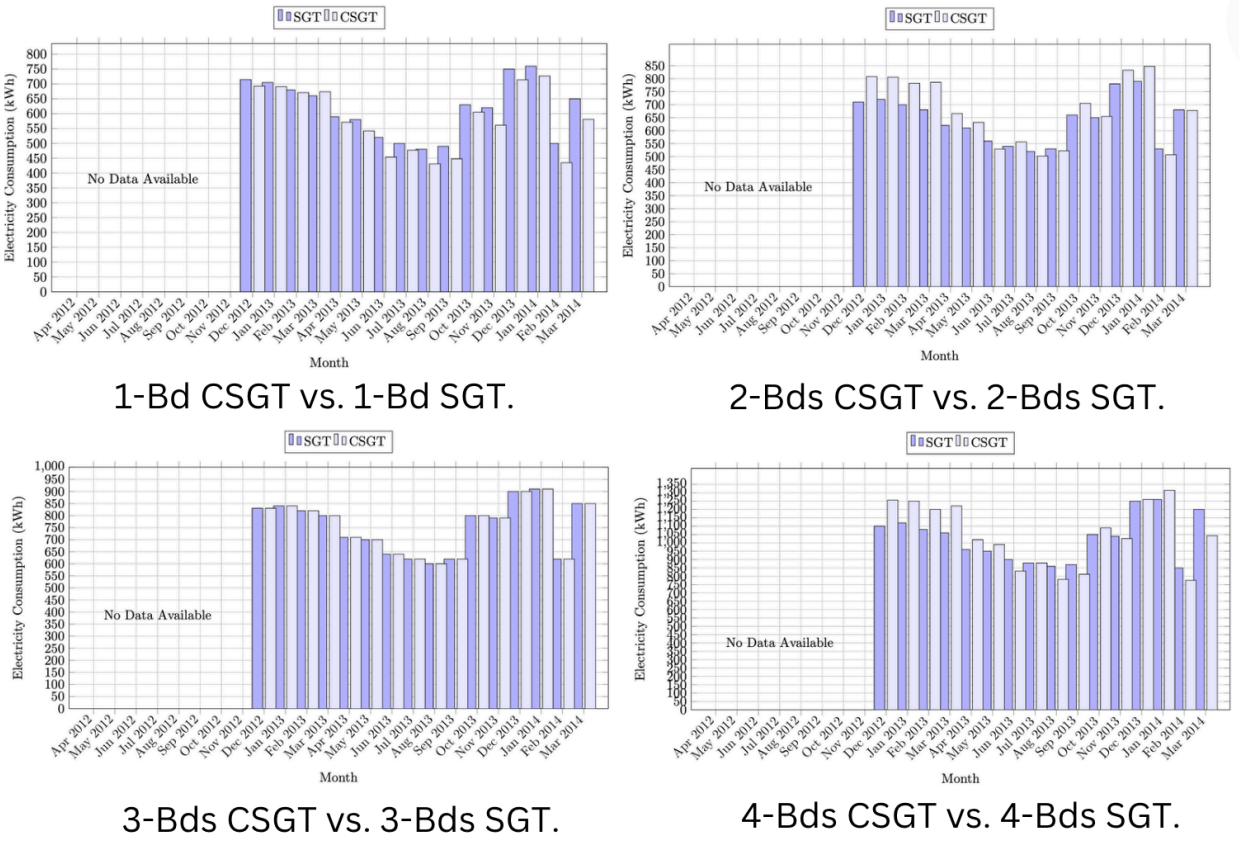

Figure 4.4: Monthly gas consumption for one to four-Bd SGTs and CSGTs in island mode (2012-14).

In island mode, PV panels and EVs significantly reduce gas reliance by generating and

storing renewable energy, particularly for 3-Bd and 4-Bd units. The Tesla Model 3 batteries store excess solar energy to power electric heating systems and reduce gas use. Fig. 4.4 shows higher winter gas consumption for heating, with SGTs consuming more gas than CSGTs. This highlights the efficiency of CSGTs in managing loads, especially in larger units, supported by optimized systems and PV panel integration.

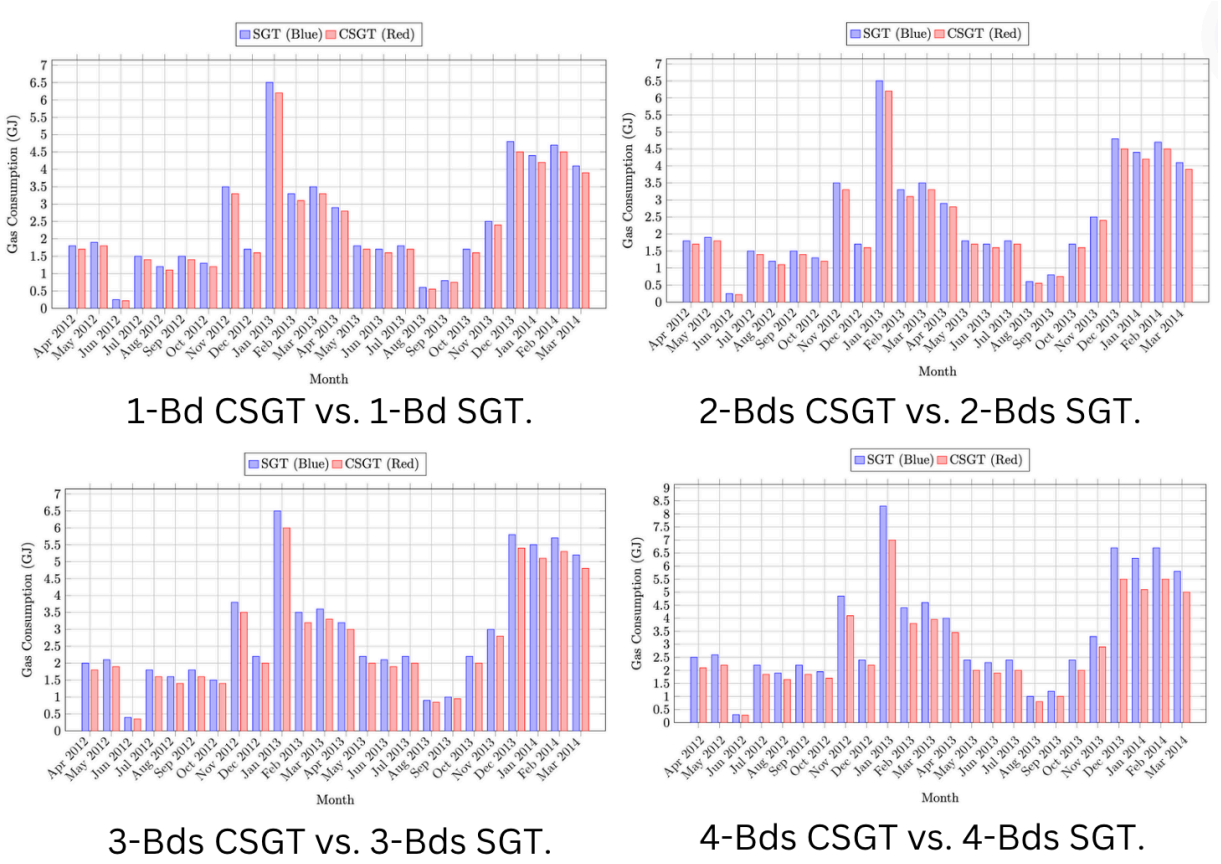

Figure 4.5: Monthly water consumption for 1 to 4-Bd SGTs and CSGTs for January to December 2013 in island mode.

Fig. 4.5 presents the water consumption for January to December 2013 in island mode split into indoor (bathing, cooking, laundry) and outdoor (lawn watering) use. CSGTs show lower total water consumption than SGTs, with a 12.5% reduction for all unit sizes. In July 2013, CSGTs used 400–1000 L less water, with a savings of 950 L for 1-Bd units. Peak consumption was reduced by 15% in July 2013, and yearly water consumption was 10,000 L less per unit, reflecting sustainable design. CSGTs also have 10-20% lower water use due to water-conscious behavior through smart systems. Overall, CSGTs in island mode save 14.8% more water than SGTs, with 4-bedroom units saving around 11,000 L yearly.

In island mode, thermal comfort zones (cold, cool, comfortable, warm, too warm) remain consistent across townhouse sizes, suggesting standardized design principles. The comfortable zone, defined as 20-23°C, 40-60% humidity, and 0.3-0.5 m/s airflow, aligns

with general comfort preferences, ensuring optimal conditions in CSGTs. PV panels and a Tesla Model 3 EV improve sustainability and load efficiency, supporting thermal comfort. Airflow increases from 0.1-0.2 m/s in the cold zone to above 0.7 m/s in the warm zone, ensuring adequate ventilation. Data from the Ninja website supports these results [155].

4.3.2 ML Model Results

A hybrid LSTM-CNN model tailored for energy prediction is employed [156]. Island mode requires managing local generation and storage. The proposed model is evaluated along with several well-known models including LR, LSTM, CNN, RF, Gradient Boosting (GB), and the hybrid LSTM-CNN to assess their performance in SGBs. LR serves as a simple baseline, LSTM excels in handling sequential data, CNN is good at recognizing spatial patterns, RF is robust at managing non-linear relationships and noisy data, GB improves accuracy through ensemble learning, and hybrid LSTM-CNN captures both temporal and spatial dependencies. RF, which utilizes decision tree ensembles, is included to provide a contrast to the deep learning approaches.

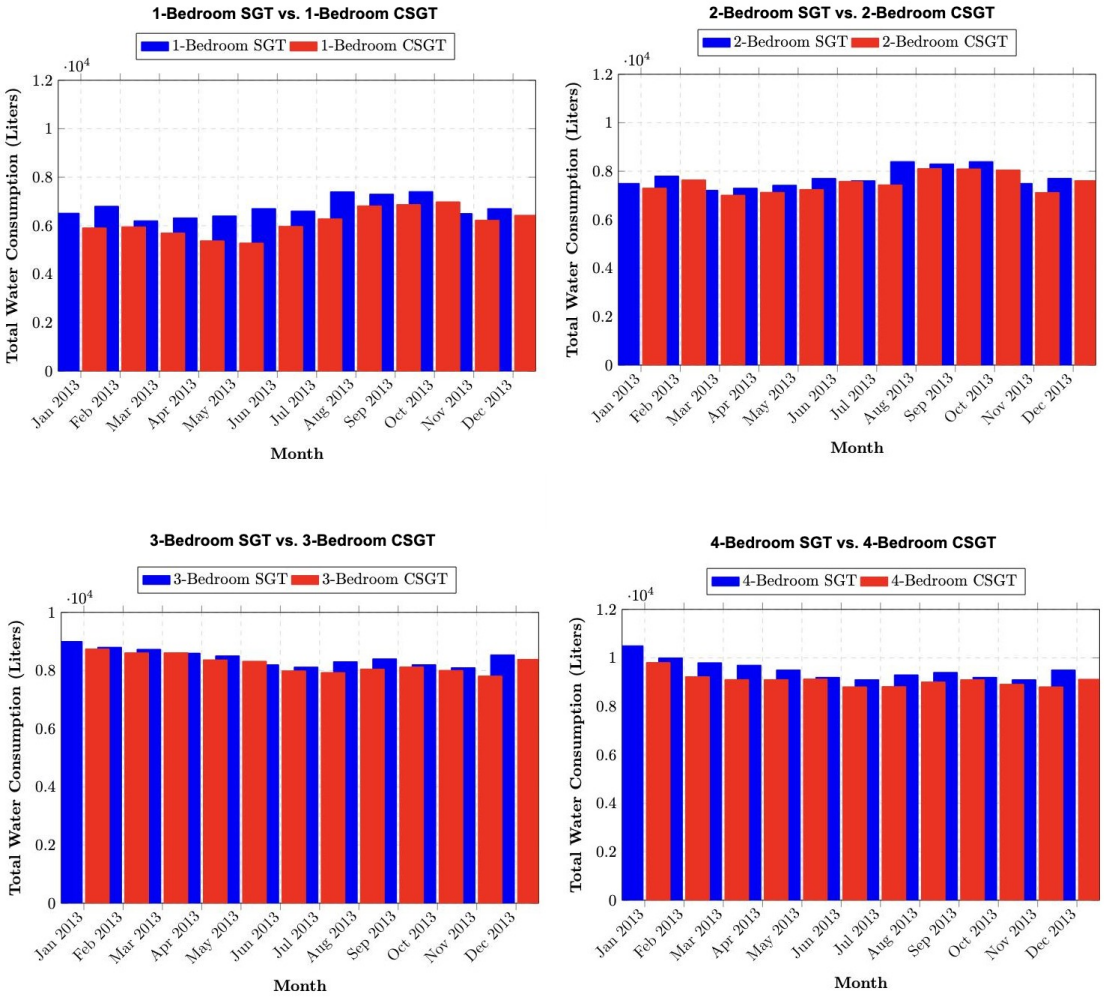

Figure 4.6: Actual versus predicted monthly electricity consumption with 7 ML models for a 1-Bd CSGT in island mode (2012-14).

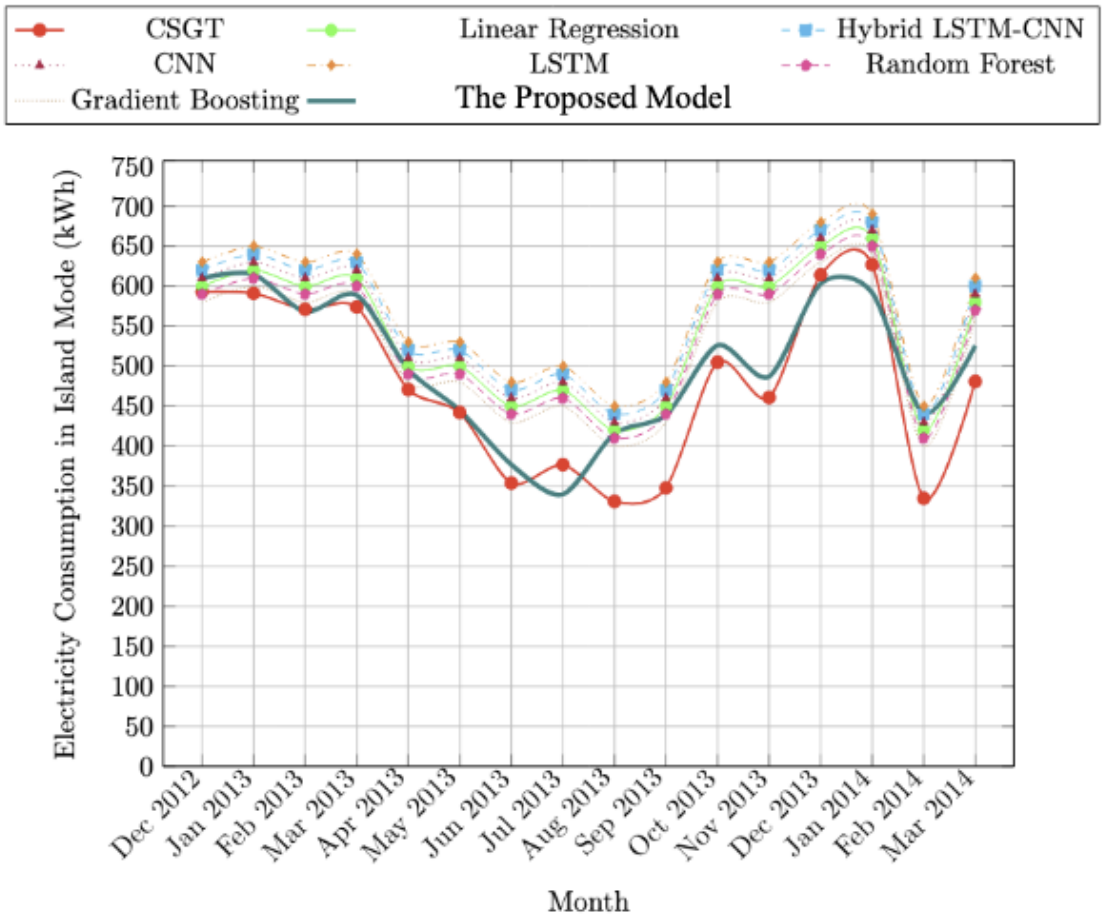

Figure 4.7: Actual versus predicted monthly electricity consumption with 7 ML models for a 2-Bd CSGT in island mode (2012-14).

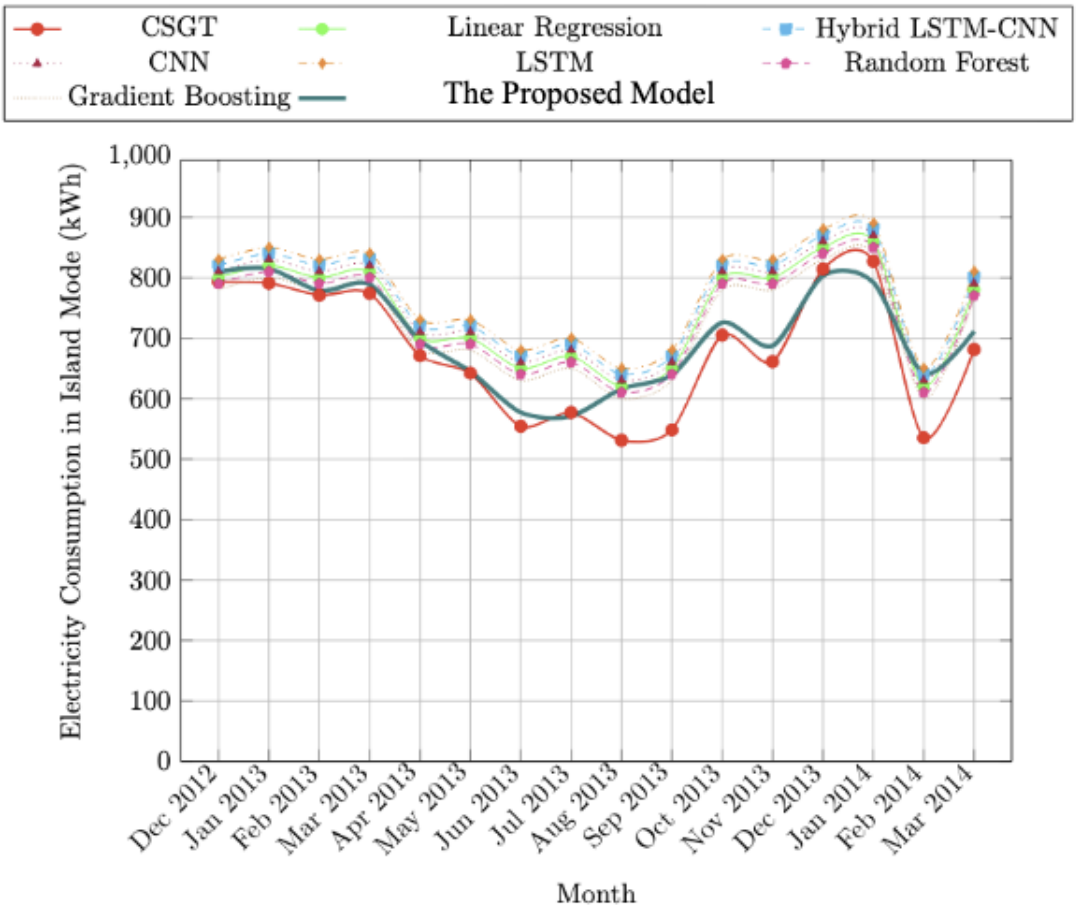

Figure 4.8: Actual versus predicted monthly electricity consumption with 7 ML models for a 3-Bd CSGT in island mode (2012-14).

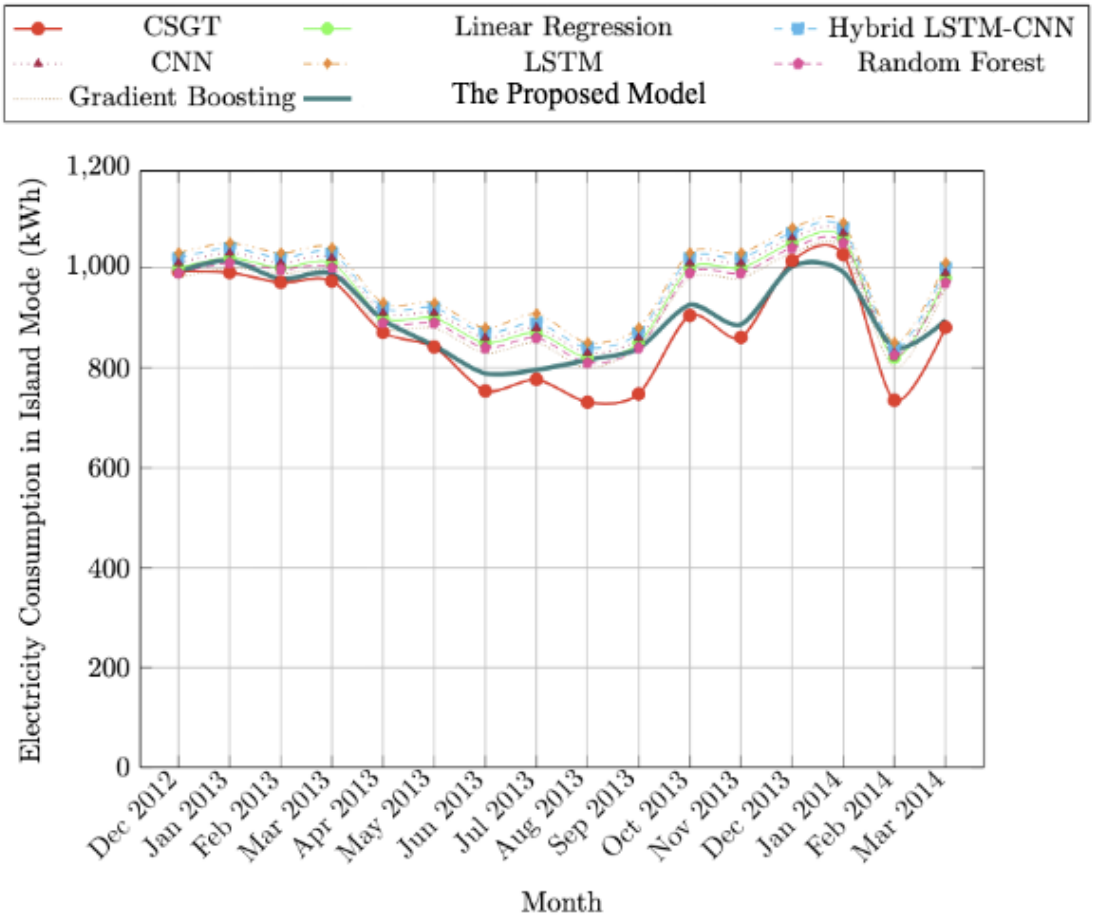

Figure 4.9: Actual versus predicted monthly electricity consumption with 7 ML models for a 4-Bd CSGT in island mode (2012-14).

Figs. 4.6-4.9 present the CSGT electricity consumption prediction results for 1 to 4-Bd CSGTs in island mode with the LR, CNN, LSTM, RF, hybrid LSTM-CNN, GB, and proposed ML models. CSGT (red line) is actual consumption while the other lines show model predictions. These results indicate that as the number of bedrooms increases, consumption also increases due to larger spaces and higher energy needs. The proposed model provides the best consumption predictions which closely match the actual data. This is because its complex architecture handles data variability better than the other models making it effective for optimizing energy use and reducing costs in SGTs.

Table 4.5 presents the performance of connected and disconnected SGTs with 1 to 4 bedrooms in island mode, with and without the proposed ML model. The acceptable ranges on the following. MAPE $< 10\%$ (very good), 10-20% (acceptable), RMSE $< 10\%$ of data range, MAE $< 5 - 10\%$ of mean value, $R^2 > 0.8$ (acceptable), and $> 0.9\%$ (very good). The data range and mean consumption are as on the following. 1-Bd (280 kWh, 600 kWh), 2-Bd (350 kWh, 800 kWh), 3-Bd (400 kWh, 1000 kWh), 4-Bd (500 kWh, 1150 kWh). These results fall within the acceptable range, indicating that the model is reliable. The ML model improves the prediction accuracy and thus the efficiency as the

Table 4.6: Monthly energy performance parameters for SGTs and CSGTs with and without the proposed ML model.

	Without the ML Model								**With the ML Model**							
	Connected SGTs				**Disconnected SGTs**				**Connected SGTs**				**Disconnected SGTs**			
Parameter	**1-Bd**	**2-Bd**	**3-Bd**	**4-Bd**	**1-Bd**	**2-Bd**	**3-Bd**	**4-Bd**	**1-Bd**	**2-Bd**	**3-Bd**	**4-Bd**	**1-Bd**	**2-Bd**	**3-Bd**	**4-Bd**
MAPE (%)	3.82	4.15	4.57	5.02	3.91	4.25	4.68	5.12	2.68	3.48	3.61	4.43	2.73	3.51	3.64	4.48
RMSE (kWh)	2.88	3.35	3.76	4.25	2.97	3.42	3.83	4.32	2.03	2.63	2.93	3.49	2.09	2.72	2.98	3.56
MAE (kWh)	2.31	2.74	3.23	3.68	2.38	2.81	3.28	3.75	1.83	1.98	2.78	3.06	1.89	2.04	2.85	3.17
R^2	0.86	0.81	0.77	0.72	0.85	0.80	0.75	0.72	0.98	0.91	0.85	0.81	0.93	0.88	0.81	0.76

MAPE, RMSE, and MAE are lower. The R^2 values are greater than 0.80 in most cases, demonstrating better performance than without the ML model.

Table 4.6 presents the parameters and performance of the 7 ML models, including the number of layers, neurons, training iterations per epoch, training time per epoch, accuracy, and MAE. This shows that the proposed model achieves the highest accuracy (95%) and a low MAE (0.013), but with the highest computational cost in training time and number of iterations. The hybrid LSTM-CNN model also performs well (90% accuracy, MAE 0.011). The ensemble models RF and GB provide good accuracy (89-90%) and reasonable MAE. LSTM has moderate computational cost and provides good performance (88% accuracy, MAE 0.015), while CNN (86% accuracy, MAE 0.018) performs well. LR has low accuracy (84%) and high MAE (0.02) as it is the baseline, but it has low computational cost.

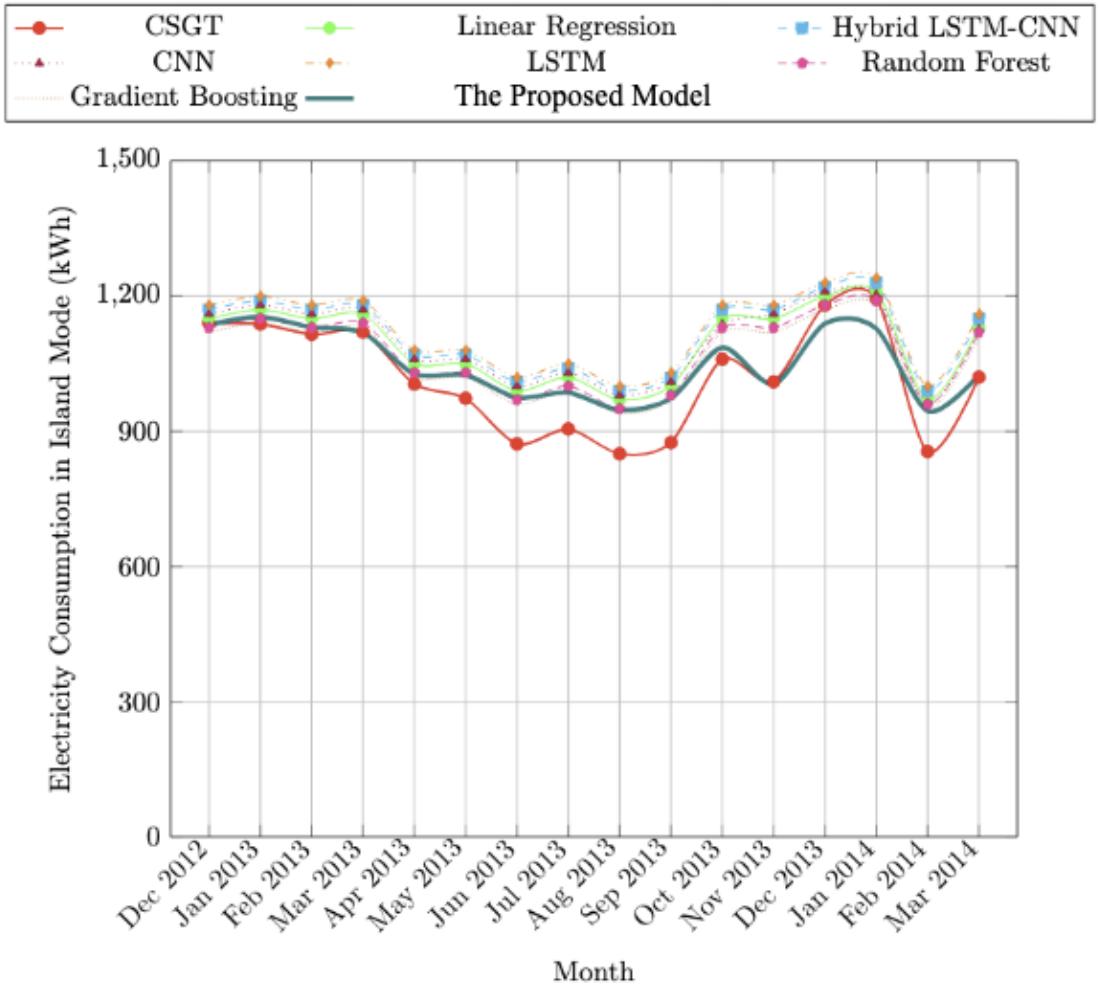

Figure 4.10: Hourly one day ahead prediction MAPE and MAE for January 3, 2013.

The MAPE and MAE for day-ahead predictions for CSGTs in island mode vary depending

Table 4.7: Number of layers, neurons, training iterations per epoch, training time per epoch, error, and accuracy for 7 ML models.

Model	Layers	Neurons	Average Training Iterations per Epoch	Average Training Time per Epoch	Accuracy (%)	MAE
LR	N/A	N/A	261	70 s	84%	0.02
LSTM	3	128	233	6 min	88%	0.015
CNN	5	64	324	10 min	86%	0.018
Random Forest	Trees: 100	Trees: 100	1120	5 min	89%	0.016
Gradient Boosting	Trees: 100	Trees: 100	1051	6 min	90%	0.017
Hybrid LSTM-CNN	LSTM: 2, CNN: 3	LSTM: 64, CNN: 64	753	22 min	90%	0.011
Proposed	LSTM: 3, CNN: 3	LSTM: 128, CNN: 128	1012	28 min	95%	0.013

on weather, occupancy, and resource consumption behavior. Fig. 4.10 gives the hourly variations in MAPE and MAE for day-ahead predictions for January 3, 2013. This shows that the error fluctuations are between 3.30% and 4.50% and the MAE ranges from 2.45 kWh to 3.60 kWh. Both metrics decrease throughout the day, indicating improved prediction accuracy. Considering that island mode can be expected to have greater errors compared to grid-connected mode, the proposed model provides excellent results.

The normality and homoscedasticity residuals [172, 173] are used to validate model performance. They represent the differences between actual and predicted values that range from -2 kWh to 1 kWh. The normality (Shapiro-Wilk test) residual has a p-value of 0.061 which is greater than the standard threshold of 0.05. Thus, it conforms to a normal distribution with random deviations from the mean. The homoscedasticity (Breusch-Pagan test) residual has a p-value of 0.076. This shows that the variance is consistent. These results indicate that the model predictions are reliable.

4.4 Conclusion

Connected Smart Green Townhouses (CSGTs) in island mode were considered to improve energy efficiency by integrating Renewable Energy Sources (RESs) such as PV panels and energy-efficient HVAC systems. The goal was to reduce load consumption, greenhouse gas emissions, and reliance on fossil fuels while promoting sustainability. Operating independently of the grid, island mode offers resilience during outages and optimizes local energy storage and utilization, minimizing the carbon footprint.

The proposed ML model was developed to predict energy system performance by capturing temporal and spatial dependencies in energy data. Energy management was optimized for connected and disconnected Smart Green Townhouses (SGTs) to reduce energy waste and costs. A Mean Absolute Percentage Error (MAPE) of 3.30%–4.50% and a Mean Absolute Error (MAE) of 2.45–3.60 kWh for day-ahead predictions were achieved, indicating excellent accuracy to support sustainable urban development.

In the future, parameter tuning can be considered to improve model performance. Occupant behavior can also be incorporated into real-time energy policies. The goal is to improve energy utilization, minimize waste, and foster sustainable practices in urban living.

Chapter 5

Adaptive Machine Learning for Automatic Load Optimization in Connected Smart Green Townhouses

Residential buildings account for nearly 40% of global energy consumption and GHG emissions [197]. Traditional energy management in smart buildings relies on manual adjustments that lack adaptability to changing factors such as occupancy, weather, and energy prices [198]. This results in operational inefficiencies, energy waste, and limited resilience. Adaptive systems based on Machine Learning (ML) models can dynamically respond to real-time conditions, enhancing load efficiency and flexibility. Furthermore, automatic transitions between grid-connected and island modes reduce human intervention and ensure uninterrupted operation during outages [199]. SGTs integrated with RESs offer a promising solution for sustainable urban development by optimizing energy use and reducing environmental impact [192, 200].

Despite advances in energy optimization, many existing systems lack prediction capabilities, underutilized Internet of Things (IoT) data, and fail to optimize emission reduction [201]. Addressing these issues can significantly improve load efficiency and resilience by dynamically optimizing energy consumption, prioritizing renewable energy, and automating operational decisions.

This chapter proposes an adaptive ML-based framework for automatic load optimization in Connected Smart Green Townhouses (CSGTs). The buildings considered are located in Burnaby, BC, Canada, and consist of connected townhouses with 1-, 2-, 3-, or 4-bedrooms with connected water systems and shared party walls [192, 200, 128]. Each townhouse type is associated with typical occupancy profiles to reflect realistic load usage patterns. These profiles were informed by publicly available datasets (e.g., from [128, 132]) and assumptions based on typical residential load usage. The 1-Bedroom (1-Bd) SGT is designed for a young couple, focusing on compact living with minimal load consumption, representing the lowest load usage. The 2-Bedroom (2-Bd) SGT is suitable for a couple with one young child, providing extra space while remaining load efficient, with mod-

erate load usage. The 3-Bedroom (3-Bd) SGT is designed for a family with two teenage children, prioritizing efficient zoning and load distribution, resulting in higher load usage. Finally, the 4-Bedroom (4-Bd) SGT accommodates a family of five, representing the highest load consumption. The system leverages IoT data, including occupancy, weather, and energy prices, and employs a deep hybrid Long Short-Term Memory-Convolutional Neural Network (LSTM-CNN) model. Multi-Objective Particle Swarm Optimization (MOPSO) is employed to balance costs, carbon emissions, and efficiency. This enables adaptive load optimization and automatic mode transitions to improve efficiency, reduce costs, and minimize the carbon footprint.

The remainder of this chapter is organized as follows. The methodology is presented in Section 5.2 including the proposed ML model and MOPSO algorithm. Section 5.3 gives the performance results and discussion. Section 5.4 summarizes this chapter including the implications for sustainable urban living.

5.1 Methodology

The proposed deep hybrid LSTM-CNN model is used to dynamically adjust to changes in occupancy, load demand, weather, and energy prices [192, 200, 202, 203, 204]. The hybrid architecture combines LSTM temporal forecasting with CNN spatial feature extraction to predict load consumption, operational costs, and carbon emissions. The adaptive system leverages IoT data to refine predictions under changing conditions, ensuring responsive and accurate optimization. The experimental setup and algorithm details are as in [192, 200].

Real data from a variety of sources is employed. This includes occupancy and load demand data from [128, 132], IoT sensor data from [133], weather data from [199, 203], and energy prices from [203]. Data from IoT sensors (e.g., motion detectors and door sensors) and smart devices (e.g., thermostats and lighting) are integrated with utility data to infer occupancy patterns. The AMPds dataset [128, 132] provides high-resolution time-series data on electricity, water, and natural gas consumption. This is employed for load demand modeling under seasonal and weather variations. IoT sensors support real-time adjustments by detecting load changes [133]. Energy-efficient technology such as heat pumps is also used [141]. This ensures efficient and sustainable Smart Green Buildings [142].

5.1.1 Problem Formulation

The proposed framework integrates an LSTM-CNN model for accurate prediction of load demand, energy costs, and carbon emissions with Multi-Objective Particle Swarm Optimization (MOPSO). The LSTM-CNN model employs the Mean Squared Error (MSE) as the loss function

$$\text{MSE} = \frac{1}{n}\sum_{i=1}^{n}\left(\text{Predicted}_i - \text{Actual}_i\right)^2, \tag{5.1}$$

where Predicted$_i$ is the model prediction for the ith sample, Actual$_i$ is the corresponding actual value, and n is the number of samples. These predictions serve as inputs for the MOPSO algorithm to ensure reliable and efficient solutions [205]. This integration provides a scalable, adaptive, and robust solution for real-time load optimization [163].

The MOPSO algorithm employs a swarm of $N = 60$ particles, each representing a potential solution. Particle i is initialized with position vector $\mathbf{X}_i(0)$ and velocity vector $\mathbf{V}_i(0)$. Random initialization is employed to ensure diverse exploration of the solution space, reducing bias and aiding in discovering global optima.

The multi-objective function is

$$f(\mathcal{X}) = \alpha \cdot \text{Cost}(\mathcal{X}) + \beta \cdot \text{Emissions}(\mathcal{X}) - \gamma \cdot \text{Efficiency}(\mathcal{X}), \tag{5.2}$$

where

$$\mathcal{X} = \{P_{\text{grid}}(t), P_{\text{renewable}}(t), P_{\text{battery}}(t), P_{\text{demand}}(t)\}, \tag{5.3}$$

is the vector of decision variables defined as follows.

- $P_{\text{grid}}(t)$ is the power supplied from the grid at time t.
- $P_{\text{renewable}}(t)$ is the power from RESs (solar panels) at time t.
- $P_{\text{battery}}(t)$ is the power discharged from the battery at time t.
- $P_{\text{demand}}(t)$ is the total load demand at time t.

The weights $\alpha = 0.3$, $\beta = 0.4$, and $\gamma = 0.3$ reflect the importance of each objective. This function ensures balanced solutions that address the tradeoffs between economic, environmental, and performance goals. While smart inverter functionalities such as Voltage-Ampere Reactive Control (Volt-VAR) control can contribute to grid stability by injecting or absorbing reactive power, they are more suitable for utility-scale applications and commercial microgrids. In residential settings, customers are typically billed for active power (kWh) rather than reactive power (kVARh), and smart inverters are not necessary to provide voltage regulation. Therefore, this chapter focuses on optimizing active power to minimize cost, improve efficiency, and reduce emissions.

The total operational cost is

$$\text{Cost}(\mathcal{X}) = \sum_{t=1}^{T} P_{\text{demand}}(t) \cdot C_{\text{electricity}}, \tag{5.4}$$

where $C_{\text{electricity}}$ is the electricity cost per kWh. The carbon emissions are

$$\text{Emissions}(\mathcal{X}) = \sum_{t=1}^{T} P_{\text{demand}}(t) \cdot E_{\text{factor}}. \tag{5.5}$$

where E_{factor} is the emission factor in kg CO_2/kWh. The efficiency is expressed as

$$\text{Efficiency}(\mathcal{X}) = \frac{\text{Useful Load Output}}{\text{Total Load Input}}, \tag{5.6}$$

At time t, particles update their velocities and positions according to

$$\mathbf{V}_i(t) = \omega \cdot \mathbf{V}_i(t-1) + c_1 r_1(\mathbf{P}_i - \mathbf{X}_i(t-1)) + c_2 r_2(\mathbf{G} - \mathbf{X}_i(t-1)), \tag{5.7}$$

$$\mathbf{X}_i(t) = \mathbf{X}_i(t-1) + \mathbf{V}_i(t), \tag{5.8}$$

where $\mathbf{V}_i(t)$ is the velocity of particle i, $\mathbf{X}_i(t)$ is the position of particle i, ω is the inertia weight balancing exploration and exploitation, c_1, c_2 are acceleration coefficients guiding particles towards their personal best $\mathbf{P}_i$ and the global best $\mathbf{G}$, and r_1, r_2 are random numbers in the range 0 to 1 to provide stochastic exploration. These updates ensure adaptive exploration to prevent premature convergence and allow the system to respond dynamically to changes.

The algorithm terminates when it has converged or the maximum number of iterations (100) is reached. Convergence is assumed if the global best solution remains within a threshold for a given number of iterations. Empirical results have shown that beyond 100 iterations, the rate of improvement in the objective function decreases significantly, indicating that further iterations yield marginal benefits. To mitigate oscillatory behavior, a dynamic inertia weight is employed where ω decreases each iteration, and c_1 and c_2 are tuned to prevent particle oscillation around local optima. This improves the stability and convergence of the algorithm.

The load optimization framework employs the following expressions.

- The load balance at time t is

$$P_{\text{grid}}(t) + P_{\text{renewable}}(t) + P_{\text{battery}}(t) = P_{\text{demand}}(t). \tag{5.9}$$

- The grid constraints at time t are

$$P_{\text{grid}}^{\text{min}} \leq P_{\text{grid}}(t) \leq P_{\text{grid}}^{\text{max}}, \tag{5.10}$$

  where $P_{\text{grid}}^{\text{min}}$ and $P_{\text{grid}}^{\text{max}}$ are the minimum and maximum allowable power from the grid, respectively, and $P_{\text{grid}}(t)$ is the power supplied from the grid.

- The battery State of Charge (SOC) at time t is given by [200]

$$SOC_{\text{min}} \leq SOC(t) \leq SOC_{\text{max}}, \tag{5.11}$$

  where SOC_{min} and SOC_{max} are the minimum (10%) and maximum (90%) allowable charge, respectively. This minimum is based on maximizing the available storage for cost and emission reduction while maintaining battery lifespan. However, in some applications, particularly when batteries are used to improve resilience and reliability, the minimum SOC is higher (25-50%) to ensure sufficient availability. Increasing the minimum will reduce the amount available for daily load optimization but improve the available backup power in critical situations. The tradeoff between economic benefits (lower costs and higher efficiency) and resilience (higher availability for grid disturbances) should be based on operational priorities.

Table 5.1: Hyperparameter tuning results for the LSTM-CNN model.

Hyperparameter	Values	Best Value	Selection Method
LSTM Units	{64, 128, 256}	128	Grid Search
CNN Kernel Size	$\{3\times3, 5\times5\}$	3×3	Grid Search
Activation Function	{Tanh, ReLU}	ReLU	Empirical Evaluation
Batch Size	{32, 64}	64	Grid Search
Learning Rate	{0.001, 0.0005}	0.0005	Grid Search
Dropout Rate	{0.2, 0.3}	0.2	Empirical Testing
Optimizer	{Adam, RMSprop}	Adam	Empirical Testing
Number of Epochs	150 (with early stopping)	150 (early stop at plateau)	Convergence
Early Stopping Patience		10 epochs	Convergence

- The power of the renewable energy produced from solar panels at time t is

$$P_{\text{renewable}}(t) = A_{\text{solar}} \cdot G(t) \cdot \eta_{\text{solar}}, \tag{5.12}$$

  where A_{solar} is the total area of the solar panels, $G(t)$ is the solar irradiance at time t, and η_{solar} is the panel efficiency.

- The demand prediction for time $t+1$ is

$$P_{\text{demand}}(t+1) = f_{\text{LSTM-CNN}}(P_{\text{demand}}(t), \text{occupancy}(t), \text{weather}(t)), \tag{5.13}$$

  where $f_{\text{LSTM-CNN}}()$ is the hybrid LSTM-CNN model used for prediction, $P_{\text{demand}}(t)$ is the actual load demand at time t, and occupancy(t) and weather(t) are the corresponding occupancy information and weather conditions.

The hyperparameter tuning results for the proposed LSTM-CNN model are given in Table 5.1. They were obtained using an Intel Core i7-12700K processor with 32 GB RAM and an NVIDIA RTX 3090 GPU. The average training time was 4.2 h. Compared to traditional static methods, this model provides a 15–20% improvement in accuracy.

The proposed ML model predicts load demand, carbon emissions, and costs, while the MOPSO algorithm determines operational parameters to balance costs, carbon emissions, and efficiency [205]. They were implemented using Python v3.11.5 with pandas v2.1.1 for data manipulation, NumPy for calculations, and Matplotlib for visualization [192]. The optimization algorithms considered include Genetic Algorithm (GA) [206, 207], MOPSO [205, 208, 209, 210], Simulated Annealing (SA) [210], Reinforcement Learning (RL) [109, 211], and Mixed-Integer Linear Programming (MILP) [212, 213]. Table 5.2 provides a comparative analysis of these algorithms for load management. In addition to their strengths, weaknesses, and applicability, the average execution time is given based on our experimental results. This shows that MOPSO outperforms the other methods. The average time for MOPSO is significantly lower than GA, SA, and MILP, making it more suitable for real-time applications. RL, while adaptive, has a high execution time due to extensive training requirements. Although MOPSO may converge to a local optimum, its speed and ability to handle multi-objective problems make it the best choice for SGBs.

Table 5.2: Comparison of optimization algorithms for energy management.

Algorithm	Strengths and Applicability	Weaknesses	References	Average Execution Time (s)
Genetic Algorithm (GA)	Effective for multi-objective optimization and nonlinear problems; suitable for large search spaces.	Requires careful parameter tuning; computationally expensive for real-time applications.	[206, 207]	6.21
MOPSO	Fast convergence; ideal for real-time applications; effectively handles multi-objective problems.	Can converge to local optima if not implemented and initialized properly.	[205, 109, 209, 210]	**1.42**
Simulated Annealing (SA)	Suitable for discrete and continuous problems; simple implementation.	Prone to local minima and slow convergence, especially in complex problems.	[210]	7.89
Reinforcement Learning (RL)	Adaptive and can learn optimal strategies over time; suitable for dynamic environments.	Requires large datasets and extensive training time.	[109, 211]	15.34
Mixed-Integer Linear Programming (MILP)	Provides exact solutions with linear constraints; well-suited to small-scale problems.	Computationally expensive and impractical for large-scale, real-time applications.	[212, 213]	23.91

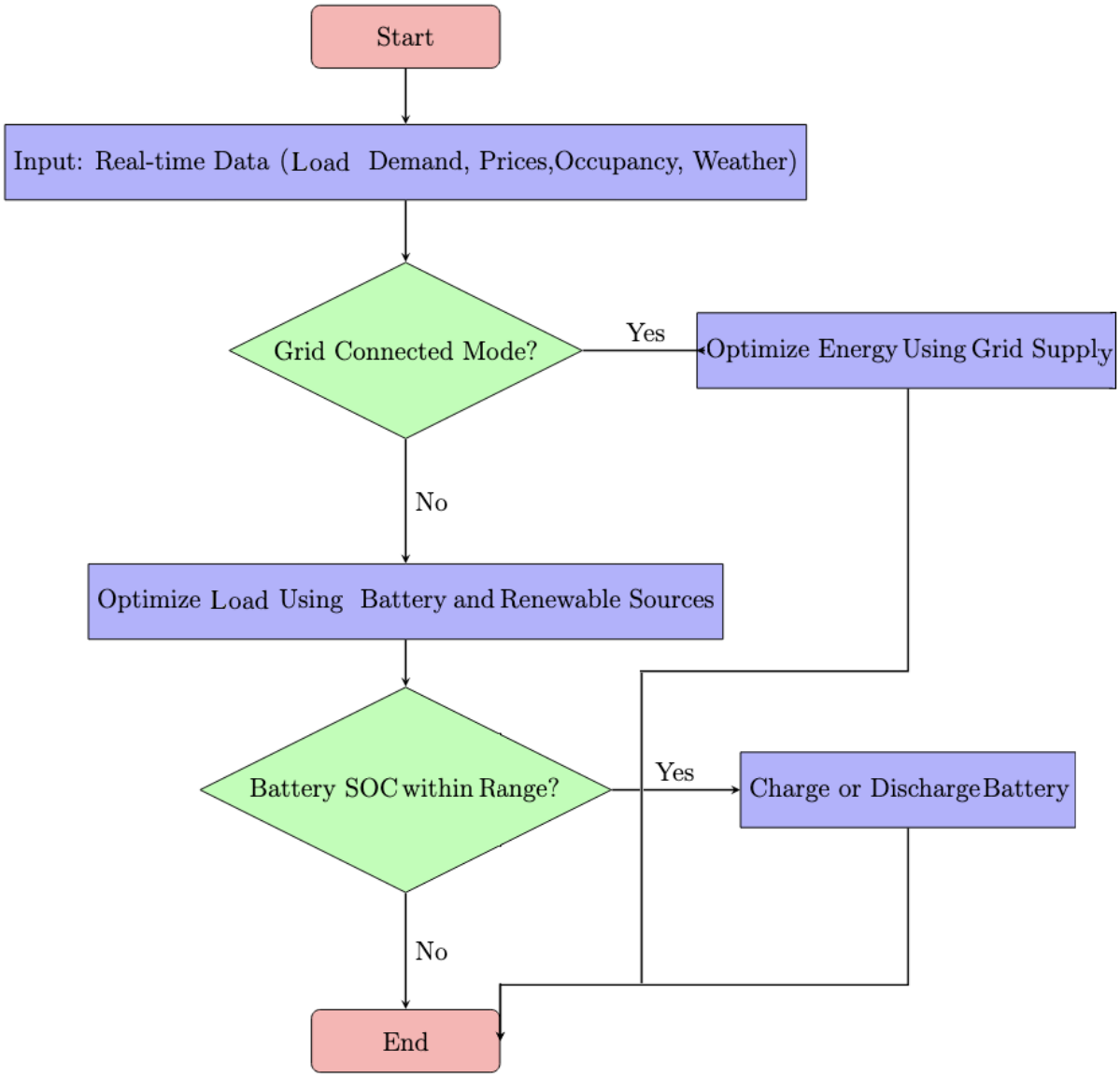

Figure 5.1: Flowchart for CSGTs load optimization.

Figure 5.1 gives a flowchart of the load optimization for CSGTs. It begins with the data input including load demand, energy prices, occupancy, and weather. If the building is in grid-connected mode, the load is optimized using the grid supply, otherwise the load is managed using battery storage and RESs. In the latter case, the battery SOC is checked to ensure it is within the acceptable range. If it is, the system proceeds to charge and/or discharge the battery as needed, otherwise, the process terminates. This flowchart illustrates the dynamic approach to balance grid dependency, renewable resources, and battery usage for load optimization.

Model performance is assessed using the Mean Absolute Error (MAE) and coefficient of

determination (R^2). The MAE is

$$\text{MAE} = \frac{1}{n}\sum_{i=1}^{n}|\text{Predicted}_i - \text{Actual}_i|, \tag{5.14}$$

where Predicted_i is the ith predicted value, Actual_i is the corresponding actual value, and n is the number of values. R^2 is

$$R^2 = 1 - \frac{\sum_{i=1}^{n}(\text{Predicted}_i - \text{Actual}_i)^2}{\sum_{i=1}^{n}(\text{Actual}_i - \overline{\text{Actual}})^2}, \tag{5.15}$$

where $\overline{\text{Actual}}$ is the average actual value.

5.1.2 Other Deep Learning-Based Methods

While the proposed model effectively predicts load demand, cost, and emissions, there are other deep learning approaches. Transformer-based models have good temporal learning capabilities but require significantly more computational resources. Hybrid attention mechanisms can improve interpretability but increase model complexity. Variational Autoencoders (VAEs) are suitable for anomaly detection but may not generalize well for optimization problems. The proposed LSTM-CNN hybrid model was selected due to its ability to capture both temporal dependencies (LSTM) and spatial patterns (CNN) efficiently. In addition, it is less complex than other deep learning methods, which is important for real-time applications.

5.1.3 External Uncertainties in Load Optimization

The proposed framework provides effective load optimization based on weather, occupancy, and energy prices. External uncertainties that can affect performance include policy changes, demand fluctuations, and renewable energy intermittency. These are discussed below.

- **Policy Changes** Regulatory policies include adjustments in net metering policies, carbon pricing, and/or energy tariffs that affect costs. To ensure adaptability, the framework can integrate periodic policy updates by retraining the model with revised energy pricing and regulatory data.
- **Demand Fluctuations** Unpredictable occupant behavior, seasonal variations, and external grid constraints may cause deviations from expected load patterns. To address this, the framework updates continuously using occupancy-driven forecasts based on real-time IoT data from motion sensors, smart meters, and environmental conditions to enable fast load adjustments.
- **Renewable Energy Intermittency** Variations in solar irradiance affect the availability of renewable energy. The framework mitigates this by incorporating probabilistic forecasting to anticipate fluctuations and by dynamically managing battery storage to compensate for variability. Historical weather data and real-time solar radiation measurements can also be used to improve prediction accuracy.

5.2 Performance Results

In this section, the load profiles for CSGTs are analyzed. They incorporate data from public datasets [128, 132] and assumptions about typical residential load usage patterns. The electricity, gas, and water loads for each townhouse type (1-Bd, 2-Bd, 3-Bd, and 4-Bd) were calculated separately, and the optimization algorithms ML, PSO, and MOPSO were used to generate load profiles. The results were then aggregated to provide combined load usage for CSGTs.

The normalized total load $L_{\text{total}}(t)$ at time t is given by

$$L_{\text{total}}(t) = \sum_{i=1}^{N} w_i L_{\text{normalized},i}(t), \tag{5.16}$$

where $N = 4$ is the number of townhouse types, $L_{\text{normalized},i}(t)$ is the normalized load for the i-Bd townhouse at time t, and w_i is the corresponding weight. The weights are $w_1 = 0.20$, $w_2 = 0.30$, $w_3 = 0.25$, and $w_4 = 0.25$ and reflect the relative contributions of the townhouses based on their size and occupancy. They were determined using energy consumption patterns derived from publicly available datasets [128, 132] and occupancy assumptions.

The normalization for load type j (e.g., electricity, gas, or water) and townhouse type i is

$$L_{\text{normalized},i,j}(t) = \frac{L_{i,j}(t) - L_{\text{min},i,j}}{L_{\text{max},i,j} - L_{\text{min},i,j}}, \tag{5.17}$$

where $L_{i,j}(t)$ is the load for townhouse type i and load type j at time t, $L_{\text{max},i,j}$ is the maximum load for townhouse type i and load type j across the dataset, and $L_{\text{min},i,j}$ is the corresponding minimum load. This is performed independently for each load and townhouse type to maintain consistency and ensure comparability across electricity, gas, and water loads. This prevents any single load type (e.g., electricity) from dominating the total load profile due to differences in magnitude or units. The normalization for the ith Bd townhouse is then

$$L_{\text{normalized},i}(t) = \frac{1}{3} \sum_{j=1}^{3} L_{\text{normalized},i,j}(t). \tag{5.18}$$

The electricity load is

$$\text{Electricity Load} = P_{\text{appliance}} + P_{\text{lighting}} + P_{\text{HVAC}}, \tag{5.19}$$

where $P_{\text{appliance}}$, P_{lighting}, and P_{HVAC} represent the power demand from electrical appliances, lighting, and Heating, Ventilation, and Air Conditioning (HVAC) systems, respectively. The gas load is

$$\text{Gas Load (kWh)} = \text{Gas Volume (m}^3\text{)} \cdot C_{\text{gas}}, \tag{5.20}$$

where Gas Volume (m^3) is the volume of natural gas consumed, and C_{gas} is the calorific value of gas (kWh/m^3). The water load is

$$\text{Water Load (kWh)} = \text{Water Volume } (m^3) \cdot C_{\text{water}}, \tag{5.21}$$

where Water Volume (m^3) is the volume of water used, and C_{water} is the energy required to pump, heat, and treat water (kWh/m^3).

Figures 5.2, to 5.5 present the electricity, gas, and water load profiles over 24 hours in kWh for the four townhouse types. These results show the variations in load patterns that reflect the differences in occupancy, space utilization, and resource needs. The 1-Bd SGT has the lowest load due to its compact size and low occupancy and so serves as a baseline for the other townhouses. The 2-Bd SGT shows a moderate increase in load due to the greater demand for heating, lighting, and water. The 3-Bd SGT has a higher load due to the needs of a larger family driven by increased space utilization and occupancy. These results indicate how load demand scales with family size. The 4-Bd SGT has the highest load because it has the largest family which results in significant demands for heating, lighting, and water. The aggregated load profiles for the four townhouse types are given in Fig. 5.6. These results are used to evaluate the load optimization techniques and validate the scalability and adaptability of the proposed framework in addressing the dynamic requirements of CSGTs.

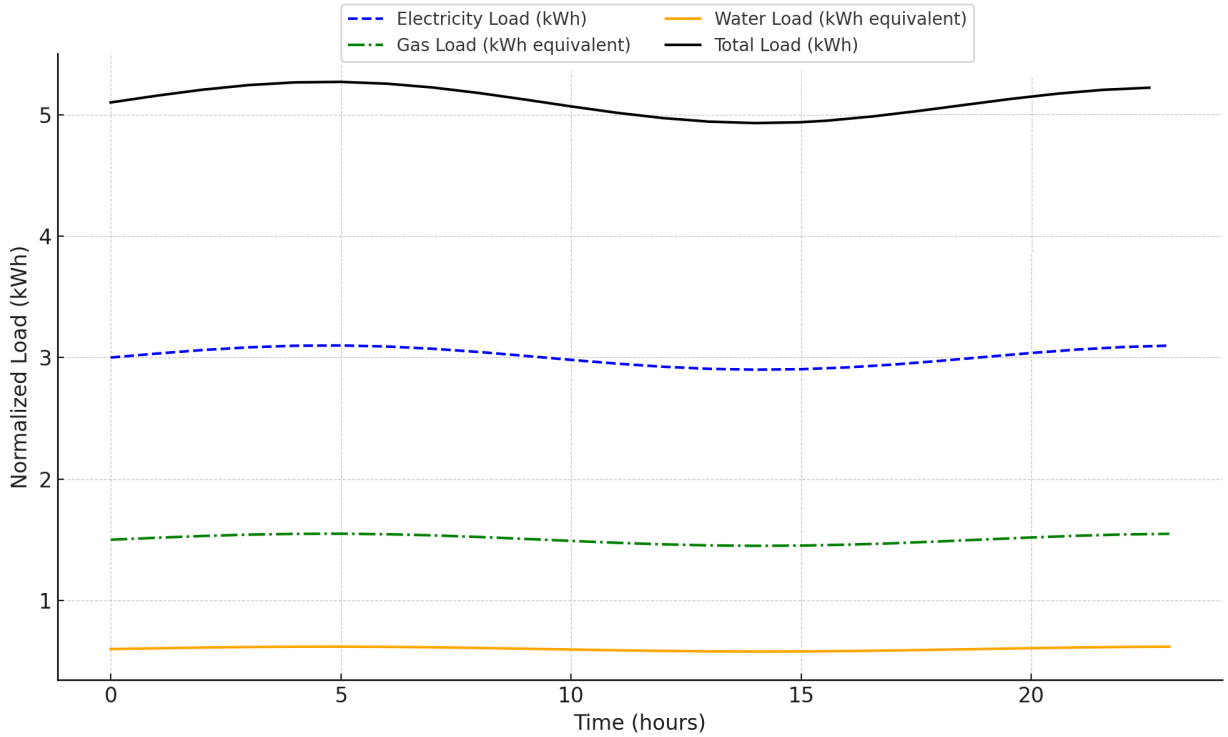

Figure 5.2: Load profiles for the 1-bedroom SGT over 24 hours.

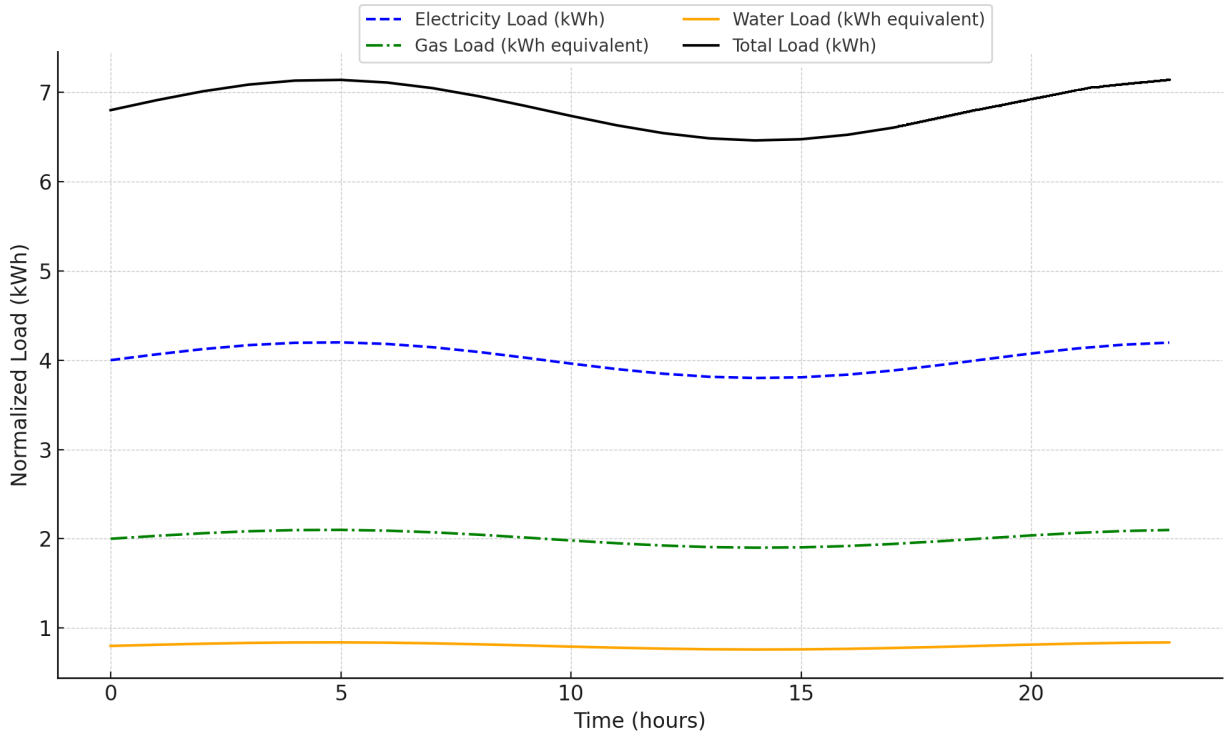

Figure 5.3: Load profiles for the 2-bedroom SGT over 24 hours.

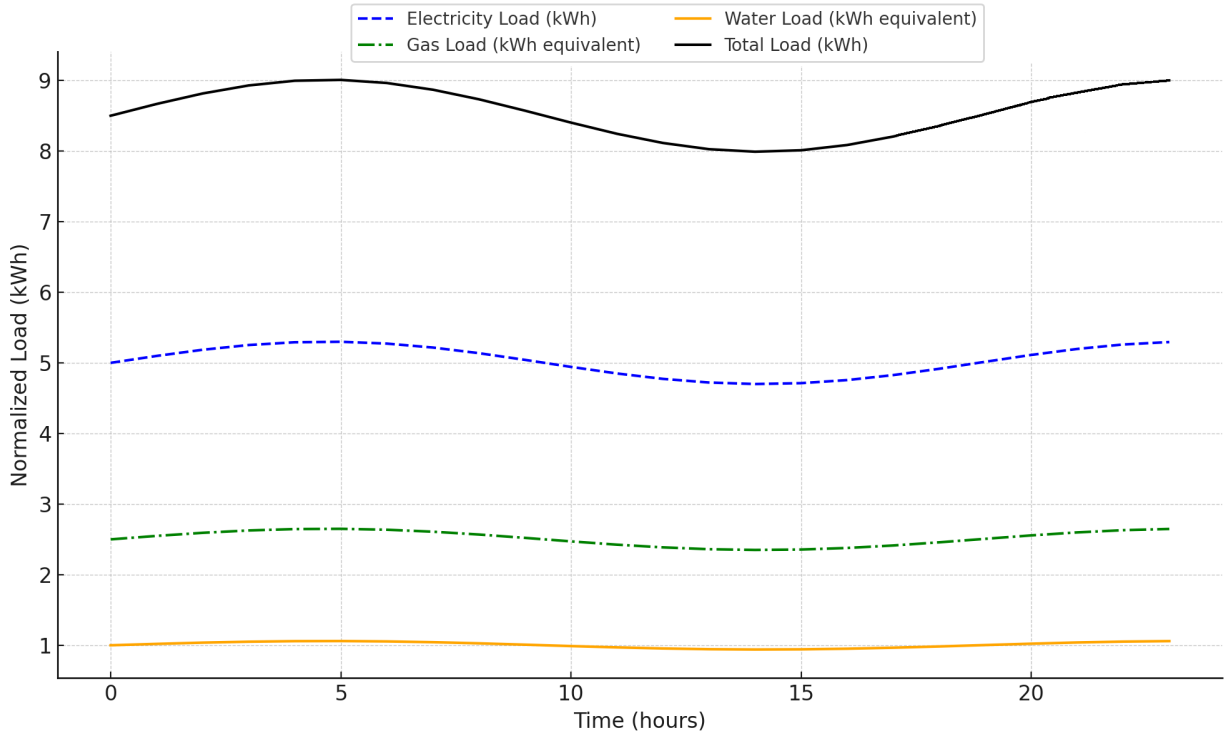

Figure 5.4: Load profiles for the 3-bedroom SGT over 24 hours.

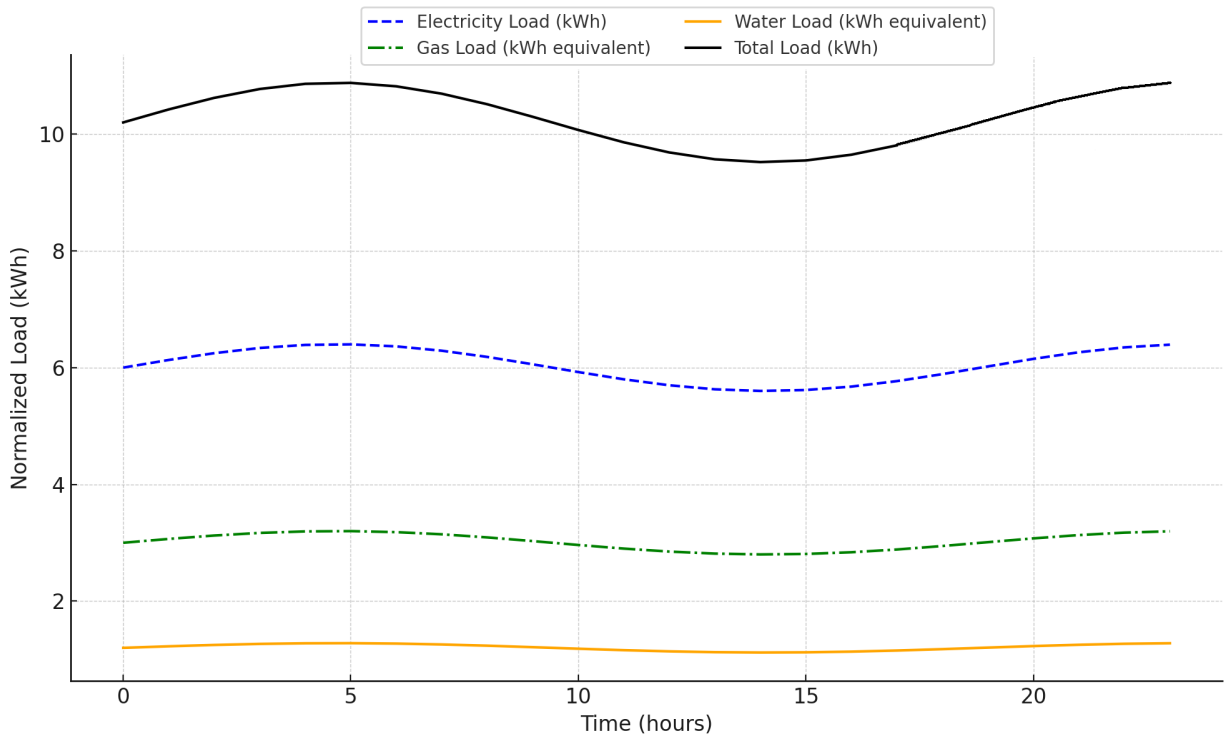

Figure 5.5: Load profiles for the 4-bedroom SGT over 24 hours.

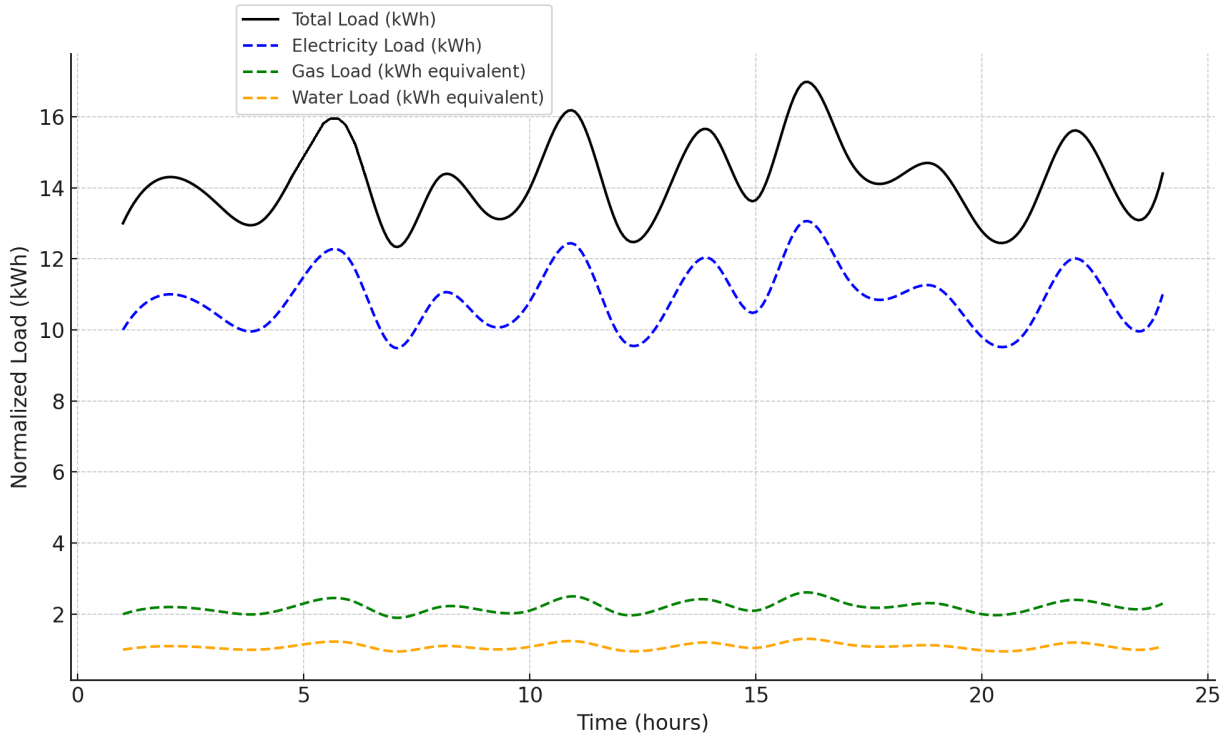

Figure 5.6: Aggregated load profiles for the 1-4-Bedroom SGTs over 24 hours.

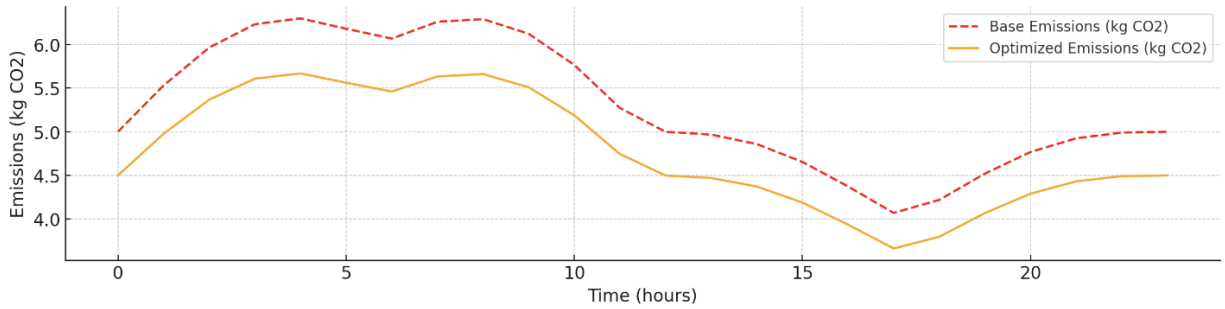

Figure 5.7: Base and MOPSO optimized carbon emissions over 24 hours.

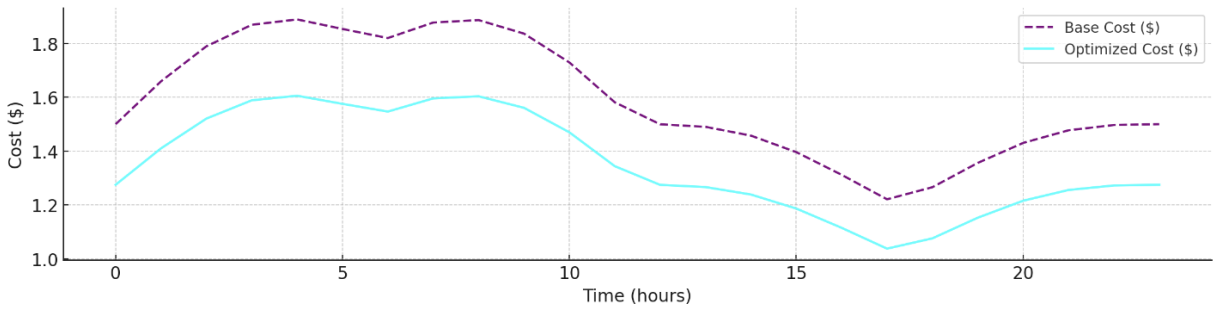

Figure 5.8: Base and MOPSO optimized operational costs over 24 hours.

Figure 5.7 gives the base (actual) and MOPSO optimized carbon emissions over time. This shows a 20% reduction in carbon emissions, with the peak lowered to 5.7 kg CO_2 from 6.3 kg CO_2 and a minimum of 3.8 kg CO_2. Figure 5.8 gives the base and MOPSO optimized operational costs over time. The MOPSO results range from less than 1.1 Canadian Dollar (CAD) to 1.6 CAD versus a maximum of 1.9 CAD in the base case, which indicates a cost savings of 15–20%.

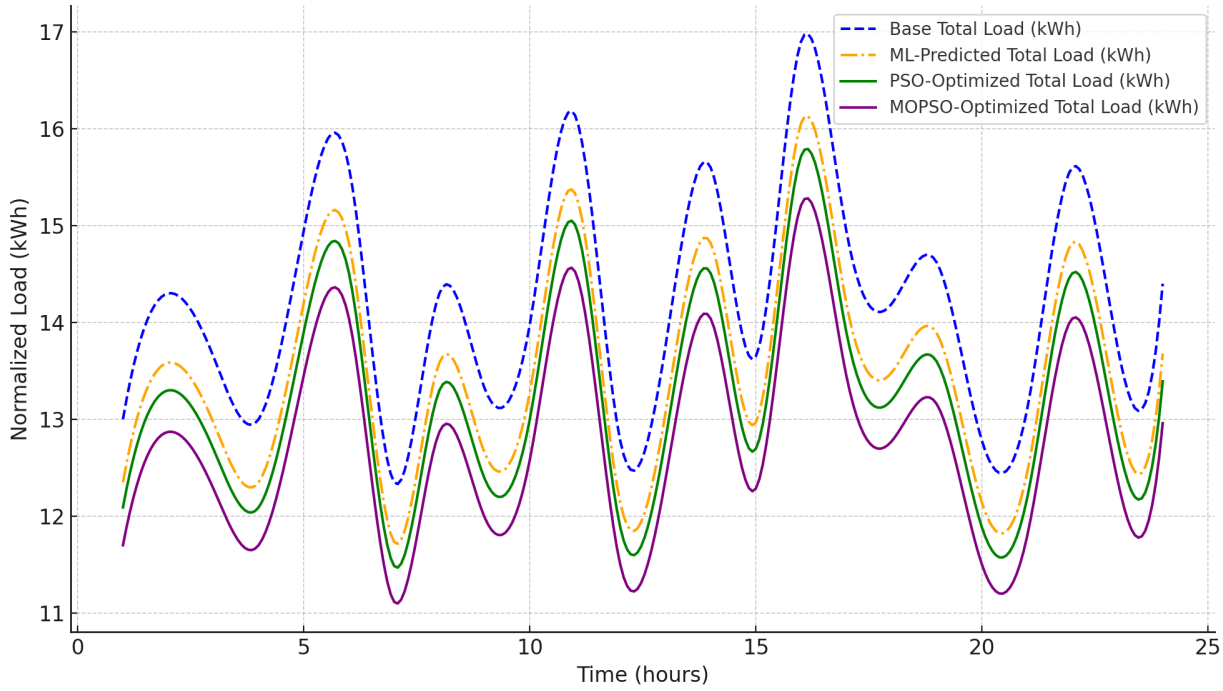

Figure 5.9: ML, PSO, MOPSO, and base load results over 24 hours.

Figure 5.9 presents the load optimization results for CSGTs over 24 hours considering electricity, gas, and water loads. This shows that the unoptimized (base) aggregate total load is 14.2 kWh at hour 1 and varies throughout the day with a peak of 16.8 kWh at hour 16 and a minimum of 12.2 kWh at hour 20. The ML, PSO, and MOPSO loads are progressively lower indicating improved load management. For example, at hour 16, the ML load is approximately 16.2 kWh, but the PSO load is about 15.9 kWh, and the MOPSO load is the lowest at approximately 15.5 kWh. Further, MOPSO consistently provides the best results over the 24 hours and is 9.4–10.3% lower than the base load. These results indicate the effectiveness of the algorithms in reducing load consumption while maintaining load requirements.

While this chapter considers CSGTs in Burnaby, BC, the proposed ML-based optimization framework can be generalized to other building types, locations, and energy systems. This flexibility stems from the ability to incorporate varying occupancy profiles, energy consumption behaviors, and load patterns using any data and real-world assumptions. By adjusting input parameters such as floor area, number of occupants, local energy pricing, and climate conditions, this framework can be employed for any residential configuration, including detached houses, apartment complexes, and smart communities. The adaptability of the proposed framework means it can be effective in any climate and with different energy systems. The LSTM-CNN model dynamically adjusts to variations in weather, energy prices, and demand-side fluctuations, so it can adapt to diverse energy policies and renewable energy integration. Furthermore, the MOPSO algorithm can be employed with any smart building configuration and various heating/cooling strategies, storage capaci-

Table 5.3: Comparison of predicted and actual results.

Parameter	Predicted	Actual	Expected Range
Load (kWh/year)	17,000 (15% reduction)	20,000 ([128, 132])	10–20% reduction
Cost Saving (CAD/year)	1,700 (15% savings)	2,000 ([132])	10–20% reduction
Carbon Emissions (kg CO_2/year)	4,250 (15% reduction)	5,000 ([132])	10–20% reduction

Table 5.4: Comparison of model performance.

Parameter	Proposed Model	[202]	[203]
Load Savings	15%	10%	12%
Cost Savings	15%	8%	10%
Carbon Emissions Reduction	15%	9%	10%
MAE (kWh)	50	60	55
R^2	0.98	0.92	0.95

ties, and demand-response mechanisms, so it is resilient to evolving energy management needs.

5.2.1 Proposed ML Model Results

K-Fold cross-validation with $K = 10$ [192] was used with the proposed ML model to mitigate overfitting and ensure robust solutions. Table 5.3 gives the validation results for load, cost, and carbon emissions. This shows that the model lowers the annual load to 17,000 kWh/year from the base of 20,0000 kWh/year which is a 15% reduction. The annual costs are 1,700 CAD/year which is 15% less than the base 2,000 CAD/year. Carbon emissions are also reduced by 15%, from 5,000 kg CO_2/year to 4,250 kg CO_2/year. These results fall within the expected range of 10–20% and thus validate the effectiveness of the proposed model in optimizing load and cost while minimizing environmental impact.

Table 5.4 compares the results for the proposed model and the approaches in [202, 203]. This shows that the proposed model achieves a 15% reduction in annual load, costs, and carbon emissions while the reductions with the other methods range from 8–12%. Thus, the hybrid ML model provides better adaptability and efficiency compared to traditional methods. The proposed framework offers benefits to both residential customers and utilities that align with modern load management goals. For customers, the framework reduces electricity costs by 15–-20% while ensuring load efficiency without compromis-

ing occupant comfort. The optimized load scheduling and usage maintain the necessary heating, lighting, and appliance use while minimizing unnecessary consumption. For utilities, Demand-Side Management (DSM) through optimized usage improves grid reliability and efficiency and lowers peak demand. This leads to deferred investments in generation capacity and improved resilience. The reduction in carbon emissions conforms with national and regional decarbonization policies and regulatory requirements. Programs such as carbon credits, peak shaving, and grid flexibility encourage utilities to promote customer-side load efficiency. Utilities often employ Time-Of-Use (TOU) pricing, demand response, and Grid-interactive Efficient Buildings (GEBs) to provide economic and environmental benefits. This can be exploited with the proposed framework to directly benefit customers while improving grid efficiency, reducing capacity constraints, and meeting regulatory targets. While the focus here was on CSGTs in Burnaby, BC, the proposed adaptive framework can be applied in any geographic location with any energy infrastructure. This flexibility lies in integrating real-time IoT data such as occupancy patterns, weather conditions, and dynamic energy pricing. It can be customized to reflect diverse conditions, regulations, and constraints, and supports various grid structures (grid-connected, microgrid, off-grid). The framework can also be aligned with regional energy and load policies such as Leadership in Energy and Environmental Design (LEED), Building Research Establishment Environmental Assessment Method (BREEAM), and the National Australian Built Environment Rating System (NABERS).

5.3 Conclusion

A new load optimization framework for Connected Smart Green Townhouses (CSGTs) presented. It outperforms existing methods in terms of load reduction, cost savings, emission reduction, and accuracy, with lower MAE and higher R^2. The results obtained show improvements of up to 15% in load efficiency, 15–20% in cost savings (approximately 0.3 CAD during peak hours), and 10–15% in carbon emission reduction (0.6 kg CO_2). Thus, it is effective in improving performance and supporting sustainability goals. It can adjust to real-time conditions, ensuring efficient and reliable operation for practical real-time applications in dynamic environments.

Future work will examine the implementation of an integrated Machine Learning (ML) and Internet of Things (IoT) system. The goal is to improve adaptability and reduce manual intervention for greater efficiency and sustainability. Validation of the proposed framework will also be considered for various building configurations and locations to assess its robustness in urban and suburban settings. Smart grid scenarios such as buildings with high renewable energy penetration and battery storage will be examined. The proposed framework will be extended to large scale residential and commercial developments.

Chapter 6

Occupant-Centric Load Optimization in Smart Green Townhouses Using Machine Learning

The increasing demand for energy efficiency and sustainability in the building sector has led to substantial advances in smart building technologies. Smart Green Townhouses (SGTs) integrate Renewable Energy Sources (RESs), Internet of Things (IoT) devices, and advanced control systems to optimize energy consumption, reduce costs, and lower environmental impact. However, effective load management in residential buildings remains challenging due to the influence of occupant behavior on energy use patterns [214, 215]. Occupant energy behavior is shaped by psychological and economic factors such as daily routines, comfort preferences, and decision-making habits [216]. These factors are captured in the proposed framework by modeling occupancy patterns based on presence and usage tendencies. This enables real-time occupant-centric optimization for improved energy efficiency in dynamic residential environments.

Machine Learning (ML) has emerged as a powerful tool for managing the complexity of load forecasting and control in smart buildings [163]. ML models allow for accurate prediction and effective control in real-time systems [192, 200]. For example, hybrid deep learning architectures, such as the combination of Convolutional Neural Networks (CNNs) and Long Short-Term Memory (LSTM) networks, have been used for robust and accurate forecasting [217]. CNN-LSTM models have been combined with metaheuristic algorithms like the Coati Optimization Algorithm for renewable energy forecasting [218]. While these methods have proven effective, existing research does not sufficiently address the role of real-time occupant behavior in residential load optimization [192, 200, 219].

Deep learning has been employed for equipment scheduling and energy control in dynamic systems [220, 221]. However, few approaches provide real-time adaptability while balancing energy savings, cost efficiency, and occupant comfort. While occupancy-based HVAC prediction and control has been employed [222, 223], integration with occupant-aware load forecasting has not been considered. Thus, a real-time, occupant-centric

load optimization framework is proposed. This framework integrates a hybrid LSTM-CNN model with Multi-Objective Particle Swarm Optimization (MOPSO) to dynamically balance load demand, cost, emissions, and comfort. Public datasets and real-time IoT sensor data [128, 132, 133] are used to enable intelligent control of systems such as HVAC and lighting based on actual occupancy and preferences. While LSTM-CNN models have been employed in energy forecasting, the integration with real-time occupant-centric data has not been considered. The results presented for Connected Smart Green Townhouses (CGSTs) demonstrate the applicability, scalability, and performance of the proposed framework in realistic residential scenarios.

The contributions of this work are as follows.

- A hybrid LSTM-CNN model is proposed to predict load demand, cost, and emissions.
- Occupant behavior is integrated into a dynamic multi-objective optimization framework.
- The proposed framework is evaluated for four connected townhouses in Burnaby, British Columbia (BC), Canada. The results obtained indicate significant load reduction and cost savings while ensuring occupant satisfaction.

The remainder of this chapter is structured as follows. Section 2 presents the methodology and optimization algorithms. The performance is evaluated in Section 3 and the results are discussed. Section 4 provides some concluding remarks including the implications for residential load optimization.

6.1 Methodology

A hybrid LSTM-CNN model is employed for dynamic load, cost, and carbon emission prediction [192, 200]. It was implemented using Python with Pandas for data manipulation, NumPy for calculations, and Matplotlib for visualization [192]. Although the framework has been designed for real-time applications, model execution time and update frequency depend on available computational resources and sensor sampling rates. In the experiments, the hybrid LSTM-CNN model was used for prediction and optimization for a 24-hour horizon within 12–18 s on a standard desktop computer which is sufficient for real-time hourly operation. The framework can be configured to run at hourly intervals for day-ahead optimization and at shorter intervals (e.g., 15 min) for finer control. An LSTM is used due to its ability to capture long-term dependencies and temporal patterns in sequential data, which is critical for accurate forecasting of loads influenced by occupant behavior and weather. A CNN is employed to extract local features and spatial correlations from multi-dimensional inputs such as occupancy and environmental data. In this chapter, occupant behavior refers to measurable actions and patterns that affect residential energy consumption. This includes real-time presence detection (e.g., motion and door sensors), appliance usage habits (e.g., when and how long devices are used), HVAC and lighting preferences (e.g., thermostat setpoints, lighting usage), and feedback interactions with control systems. These behaviors are inferred from IoT sensor data and

smart device logs to support dynamic load optimization.

The MOPSO algorithm is used to optimize the tradeoff between load efficiency, cost savings, and carbon emission reduction while ensuring occupant comfort. It was chosen considering the advantages and applicability to SGT systems [192]. It is a well-established algorithm that has excellent convergence [223], diversity preservation, and suitability for nonlinear, occupant-influenced multi-objective problems. Here, MOPSO is used to effectively balance load, cost, and emissions while ensuring occupant comfort, which is particularly challenging in real-time residential applications. This illustrates the practicality of MOPSO for the optimization of complex, dynamic building energy systems.

Real data from several sources is employed including occupancy and load demand data from [128, 132], IoT sensor data from [133], weather data from [199, 203], and energy prices from [199]. Data from IoT sensors (e.g. motion detectors, door sensors) and smart devices (e.g., thermostats) are integrated with utility data to infer occupancy patterns [225]. The AMPds dataset [128, 132] provides high-resolution time-series data on electricity, water, and natural gas consumption. This facilitates load demand modeling under seasonal and weather variations. IoT sensors support real-time adjustments due to changes in load [133]. Energy-efficient technology such as heat pumps [141] ensure efficient and sustainable SGTs [142].

Although the focus here is on short-term, real-time occupant behavior, the proposed framework can easily be adapted to long-term patterns. Seasonal and holiday-related behavior trends can be captured using historical data to improve load prediction while maintaining adaptability to dynamic occupant profiles. However, the goal here is real-time prediction in a dynamic environment that is more challenging due to the very short time scale.

6.1.1 The proposed framework

The proposed framework uses publicly available datasets [128, 132, 133] and real-time IoT data collected from SGTs [192, 200]. To ensure consistency across diverse features, the data are normalized to the range [0, 1]. The normalization for load type j (e.g., electricity, gas, water) and townhouse type i is

$$L_{\text{normalized},i,j}(t) = \frac{L_{i,j}(t) - L_{\text{min},i,j}}{L_{\text{max},i,j} - L_{\text{min},i,j}}, \tag{6.1}$$

where $L_{i,j}(t)$ is the load for townhouse type i and load type j at time t, $L_{\text{max},i,j}$ is the maximum load for townhouse type i and load type j across the dataset, and $L_{\text{min},i,j}$ is the corresponding minimum load. This ensures that normalization is performed independently for each load and townhouse type to prevent any single load type from dominating the total load profile due to differences in magnitude or units such as electricity (kWh), gas (m^3), and water (liters). The normalization for the ith bedroom townhouse is

$$L_{\text{normalized},i}(t) = \frac{1}{3}\sum_{j=1}^{3} L_{\text{normalized},i,j}(t), \tag{6.2}$$

This normalization is critical for the performance of ML models so that features with a large numerical range do not disproportionately influence model learning. It also improves numerical stability and accelerates convergence, particularly for gradient-based optimizers such as ADAM used in the proposed LSTM-CNN model.

The electricity load in kilowatt-hours (kWh) is

$$\text{Electricity Load (kWh)} = L_{\text{appliance}} + L_{\text{lighting}} + L_{\text{HVAC}}, \tag{6.3}$$

where $L_{\text{appliance}}$, L_{lighting}, and L_{HVAC} represent the demand from electrical appliances, lighting, and HVAC systems, respectively. The gas load is

$$\text{Gas Load (kWh)} = \text{Gas Volume} \cdot C_{\text{gas}}, \tag{6.4}$$

where Gas Volume (m^3) is the volume of natural gas consumed and C_{gas} is the calorific value of gas (kWh/m^3). The water load is

$$\text{Water Load (kWh)} = \text{Water Volume} \cdot C_{\text{water}}, \tag{6.5}$$

where Water Volume (m^3) is the volume of water used, and C_{water} is the energy required to pump, heat, and treat water (kWh/m^3).

The base (unoptimized) load demand at time t is given by

$$L_{\text{base}}(t) = L_{\text{demand}}(t) - L_{\text{renewable}}(t), \tag{6.6}$$

where $L_{\text{demand}}(t)$ is the total unoptimized load demand (kW) and $L_{\text{renewable}}(t)$ is the unoptimized renewable energy (e.g., PV power). The optimized load without occupant data at time t is

$$L_{\text{opt,noOcc}}(t) = L_{\text{base}}(t) - \big(L_{\text{renewable,opt}}(t) + L_{\text{battery}}(t)\big), \tag{6.7}$$

where $L_{\text{renewable,opt}}(t)$ is the optimized renewable energy (kW) and $L_{\text{battery}}(t)$ is the battery energy used to offset grid demand (kW). The maximum limits for battery and grid power ($L_{\text{battery,max}}$ and $L_{\text{grid,max}}$) are based on practical system design assumptions supported by real-world parameters. $L_{\text{battery,max}}$ is set in the range 5–10 kW. This aligns with commercially available residential-scale lithium-ion battery systems, and is consistent with industry-standard systems used in residential microgrids in Canada [192, 200]. $L_{\text{grid,max}}$ is set in the range 12–15 kW. This reflects typical urban service capacity in a townhouse unit in BC and aligns with empirical values used in predicting load management for smart grid applications [219, 224]. These values are not dictated by specific regulations but are based on realistic operating conditions and previous research.

The optimized load with occupant data at time t considers occupant-driven factors and is given by

$$L_{\text{opt,occ}}(t) = L_{\text{opt,noOcc}}(t) - L_{\text{occ,adj}}(t), \tag{6.8}$$

where $L_{\text{occ,adjustment}}(t)$ accounts for real-time occupancy-based load optimization including HVAC demand adjustments considering presence, load shifting to avoid peak times, and adaptive appliance control (e.g., delayed washing machine cycles). Substituting (6.7) in (6.8) gives

$$L_{\text{opt,occ}}(t) = L_{\text{base}}(t) - \big(L_{\text{renewable,opt}}(t) + L_{\text{battery}}(t) + L_{\text{occ,adj}}(t)\big), \tag{6.9}$$

6.1.2 LSTM-CNN Model

The LSTM is used to capture temporal patterns in the input data to learn dependencies over time. The hidden state at time t is

$$h_t = \sigma(W_x x_t + W_h h_{t-1} + b_l), \tag{6.10}$$

where x_t is the input at time t, which includes features such as load demand and occupancy data, W_x and W_h are weight matrices for the input data and previous hidden state, respectively, b_l is the bias term, and σ is the sigmoid activation function

$$\sigma(x) = \frac{1}{1 + e^{-x}}. \tag{6.11}$$

This function limits values to the range $[0, 1]$ and helps the network learn complex, nonlinear relationships by introducing smooth gradients and preventing large outputs.

The CNN extracts spatial features from multi-dimensional data. The CNN output is

$$y = \sigma(\mathrm{Conv2D}(x, W) + b_\mathrm{c}), \tag{6.12}$$

where x is the input data structured as a two-dimensional (2D) matrix, Conv2D() is 2D convolution given by

$$\mathrm{Conv2D}(x, W) = \sum_i \sum_j W[i, j] \cdot x[i, j],$$

where W is the convolutional filter (kernel) used to extract local patterns, and b_c is the bias term. The kernel is a small matrix of learnable weights used to extract spatial features from the input data. During training, it slides across the input matrix to learn local patterns such as occupancy and appliance usage. This helps improve the predictive capability of the model. The bias terms are randomly initialized and updated each iteration via backpropagation using the ADAM optimizer.

The combined LSTM and CNN output is

$$\mathrm{Output} = g(h_t, y), \tag{6.13}$$

where $g()$ is the fusion function which here is concatenation. The average training time was 4.6 h. A dropout rate of 0.2 is applied after each LSTM and CNN layer to prevent overfitting. The model was trained using the Adam optimizer with a learning rate of 0.001 and batch size of 64.

The MOPSO algorithm objective function is

$$F = w_1 f_1 + w_2 f_2 + w_3 f_3, \tag{6.14}$$

where

$$f_1 = \sum_{t=1}^{N} L_{\mathrm{demand}}(t), \tag{6.15}$$

is the total load demand in kWh that includes all electrical appliances, HVAC systems, and other energy-consuming devices within the building

$$f_2 = \sum_{t=1}^{N} L_{\text{demand}}(t) \cdot C_{\text{electricity}}, \tag{6.16}$$

is the operational costs

$$f_3 = \sum_{t=1}^{N} L_{\text{demand}}(t) \cdot E_{\text{factor}}, \tag{6.17}$$

is the carbon emissions, N is the number of time steps, $C_{\text{electricity}}$ is the electricity cost per kWh, E_{factor} is the carbon emission factor in kg CO_2/kWh, and w_1, w_2, and w_3 are weights representing the importance of each objective. The weights used here are $w_1 = 0.3$, $w_2 = 0.4$, and $w_3 = 0.3$. They were selected empirically to balance the three goals: load efficiency, operational cost reduction, and carbon emission reduction. Parameter tuning was conducted to ensure that no single objective disproportionately dominated the optimization results. The chosen values are the result of extensive evaluation across many scenarios. The corresponding constraints are

$$L_{\text{grid}}(t) + L_{\text{renewable}}(t) + L_{\text{battery}}(t) \geq L_{\text{demand}}(t), \quad \forall t \tag{6.18}$$

$$0 \leq L_{\text{grid}}(t) \leq L_{\text{grid,max}}, \tag{6.19}$$

$$0 \leq L_{\text{battery}}(t) \leq L_{\text{battery,max}}, \tag{6.20}$$

where $L_{\text{grid}}(t)$ is the load supplied by the grid (kWh), $L_{\text{renewable}}(t)$ is the load met by renewable sources (kWh), and $L_{\text{battery}}(t)$ is the energy supplied from battery storage (kWh).

To maintain occupant comfort, the deviation between the actual and desired indoor temperature should be within an acceptable range

$$\sum_{t=1}^{N} L_{\text{demand}}(t) \cdot |T_{\text{actual}}(t) - T_{\text{desired}}(t)| \leq \text{Threshold}, \tag{6.21}$$

where $T_{\text{actual}}(t)$ is the actual indoor temperature at time t, $T_{\text{desired}}(t)$ is the corresponding desired temperature, and Threshold is the maximum acceptable cumulative deviation over the N time steps (optimization period). This ensures energy savings do not compromise thermal comfort so load scheduling decisions account for occupant preferences.

6.1.3 Performance Metrics

Occupant comfort satisfaction is based on thermal comfort, lighting adequacy, and feedback adherence. The thermal comfort measures how close the indoor temperature is to the desired temperature and is given by

$$\text{Thermal Comfort}(t) = 1 - \min\left[1, \frac{|T_{\text{actual}}(t) - T_{\text{desired}}(t)|}{5}\right], \tag{6.22}$$

where 5°C is considered the maximum difference. The lighting adequacy assesses how well lighting levels meet occupant needs. It is based on the percentage of time that the lighting intensity stays within the desired range and is expressed as

$$\text{Lighting Adequacy}(t) = \frac{\sum_{i=1}^{r} \beta\left(L_{\text{min}} \leq L_i(t) \leq L_{\text{max}}\right)}{r}, \tag{6.23}$$

where $L_i(t)$ is the actual lighting intensity in room i at time t, L_{min} and L_{max} are the minimum and maximum acceptable light levels, $\beta()$ is the indicator function that returns 1 if the lighting is within the desired range, and 0 otherwise, and r is the number of rooms. Feedback adherence measures how well the building systems (e.g., HVAC, lighting) respond to occupant feedback and is given by

$$\text{Feedback Adherence}(t) = \frac{F_{\text{implemented}(t)}}{F_{\text{submitted}(t)}}, \tag{6.24}$$

where $F_{\text{implemented}}(t)$ is the number of feedback requests that were implemented by the system at time t and $F_{\text{submitted}}(t)$ is the corresponding number of feedback requests submitted by occupants.

The occupant comfort satisfaction at time t is a weighted sum of thermal comfort, lighting adequacy, and feedback adherence and is expressed as

$$\begin{aligned} \text{Occupant Comfort Satisfaction}(t) = {} & w_T \cdot \text{Thermal Comfort}(t) \\ & + w_L \cdot \text{Lighting Adequacy}(t) \\ & + w_F \cdot \text{Feedback Adherence}(t), \end{aligned} \tag{6.25}$$

where $w_T = 0.4$, $w_L = 0.3$, and $w_F = 0.3$. These weights are assigned according to the relative importance of thermal comfort, lighting adequacy, and feedback adherence in the overall comfort of the occupants.

The performance evaluation metrics are

$$\text{Mean Absolute Error (MAE)} = \frac{1}{n}\sum_{i=1}^{n} |\text{Predicted}_i - \text{Actual}_i|, \tag{6.26}$$

$$\text{Root Mean Squared Error (RMSE)} = \sqrt{\frac{1}{n}\sum_{i=1}^{n}(\text{Predicted}_i - \text{Actual}_i)^2}, \tag{6.27}$$

$$\text{Coefficient of Determination } (R^2) = 1 - \frac{\sum_{i=1}^{n}(\text{Predicted}_i - \text{Actual}_i)^2}{\sum_{i=1}^{n}(\text{Actual}_i - \overline{\text{Actual}})^2}, \tag{6.28}$$

where n is the number of data values, Predicted_i is the ith predicted value from the ML model, Actual_i is the corresponding actual value, and $\overline{\text{Actual}}$ is the mean of the actual values given by

$$\overline{\text{Actual}} = \frac{1}{n}\sum_{i=1}^{n} \text{Actual}_i. \tag{6.29}$$

The MAE is the average magnitude of the prediction errors so smaller values indicate better accuracy. The RMSE measures the standard deviation of prediction errors, penalizing larger errors more heavily than the MAE. Lower values indicate higher accuracy. R^2 indicates how well the model explains the variations in the actual data. Values closer to 1 signify better model performance.

6.2 Performance Results

The results presented in this section were generated using OpenStudio (v3.4.0) for load simulation with and without occupant input. Data analysis and optimization were performed using Python v3.11.5 with Pandas v2.1.1 and Matplotlib v3.8.0 [192, 200]. Real-time occupancy data was collected with ThingSpeak v2.0 [226].

We consider a CSGT complex with 1-bedroom, 2-bedroom, 3-bedroom, and 4-bedroom units as shown in Figure 6.1. Connected townhouses include two key components: connected water systems [128, 147] and party walls [148, 149]. Party walls are shared walls between adjacent properties and are jointly owned and maintained by property owners. Party wall agreements outline the responsibilities for maintenance, repairs, alterations, and dispute resolution.

Figure 6.1: Four connected SGTs as a townhouse complex.

Table 6.1 gives the SGT parameters including the number of residents, occupancy, hot water usage, lighting, EV charging, HVAC consumption, shared wall insulation, and fire safety. Table 6.2 presents the base and optimization results with and without occupant data for the CSGT complex. The percentage reduction compared to the base results is also given. This indicates a significant improvement in load efficiency, cost savings, and carbon emission reduction. The load is decreased by 10.6% without occupant data and 14.3% with occupant data, confirming the effectiveness of real-time adaptive load management. Operational costs were reduced by up to 13.0% and carbon emissions decreased by 11.0% and 15.5%, respectively. Peak load is reduced by 10.5% and 14.0% which helps grid stability and lowers peak-hour costs. Overall, occupant-centric optimization increases load efficiency, cost savings, and environmental performance, making CSGTs a practical solution for the future.

While the proposed framework benefits significantly from real-time occupant data, there are practical challenges in data acquisition. These include sensor inaccuracies,

Table 6.1: CSGT Parameters

Feature	**1-bedroom CSGT**	**2-bedroom CSGT**	**3-bedroom CSGT**	**4-bedroom CSGT**	**CSGT**
Residents	2 (Couple)	3 (Couple + Child)	4 (Couple + 2 Children)	5 (Couple + 3 Children)	Multiple Units
Occupancy (Hours/Day)	8–12	10–16	14–18	16–20	Distributed
Hot Water Usage (Liters/Day)	180	270	400	460	1020
Lighting (Hours/Day)	3–5	5–7	6–9	6–10	N/A
EV Charging	N/A	N/A	1–2 EVs (2–3 hrs/day)	2 EVs (2–4 hrs/day)	N/A
HVAC Consumption (kWh/m^2/Year)	26	28	30	32	N/A
Shared Wall Insulation	R-22	R-22	R-22	R-22	Energy-Efficient Walls
Fire Safety	2 h Fire Rated Walls	2 h Fire Rated Walls	2 h Fire Rated Walls	2 h Fire Rated Walls	Fire-resistant Construction

Table 6.2: CGST Complex Optimization Results

Parameter	**Base**	**Optimized Without Occupant Data**	**Optimized With Occupant Data**
Load (kWh)	20,000	17,880 (10.6%)	16,950 (14.3%)
Operational Costs (CAD)	2,500	2,250 (10.0%)	2,175 (13.0%)
Carbon Emissions (kg CO_2)	5,000	4,450 (11.0%)	4,225 (15.5%)
Peak Load (kW)	15.0	13.4 (10.5%)	12.9 (14.0%)

intermittent connectivity, and privacy concerns related to monitoring occupant presence and preferences. In this study, these issues were mitigated by using anonymized data collection protocols, leveraging non-intrusive IoT sensors (e.g., motion detectors, smart thermostats), and implementing local edge-processing to minimize data transmission risks.

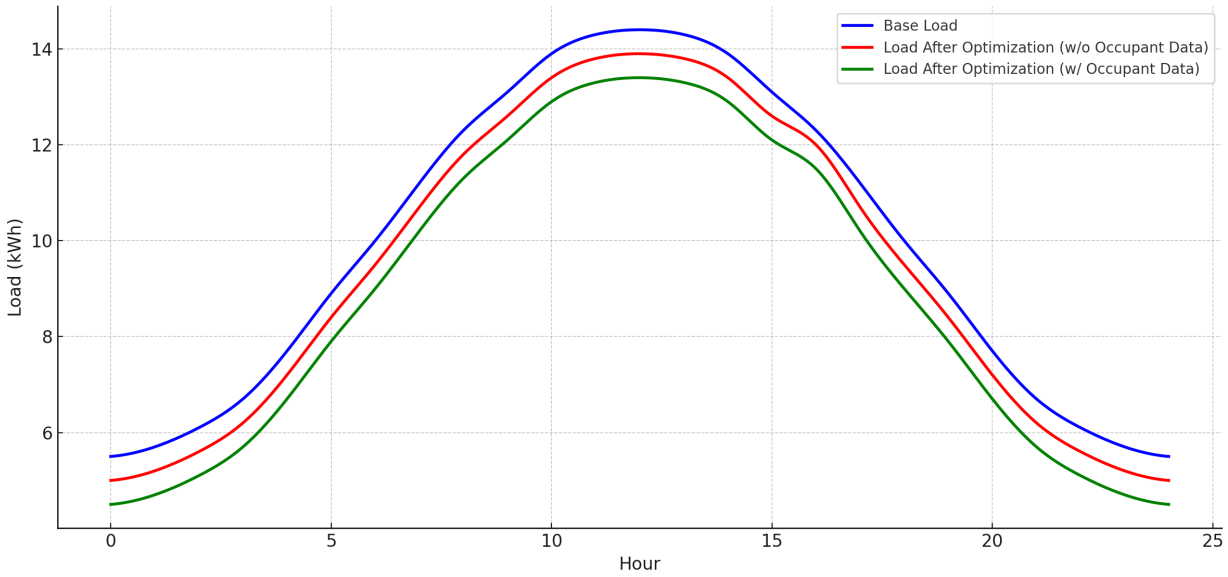

Figure 6.2: Base load, optimized load without occupant data, and optimized load with occupant data for the 1-bedroom CSGT over a 24 h period.

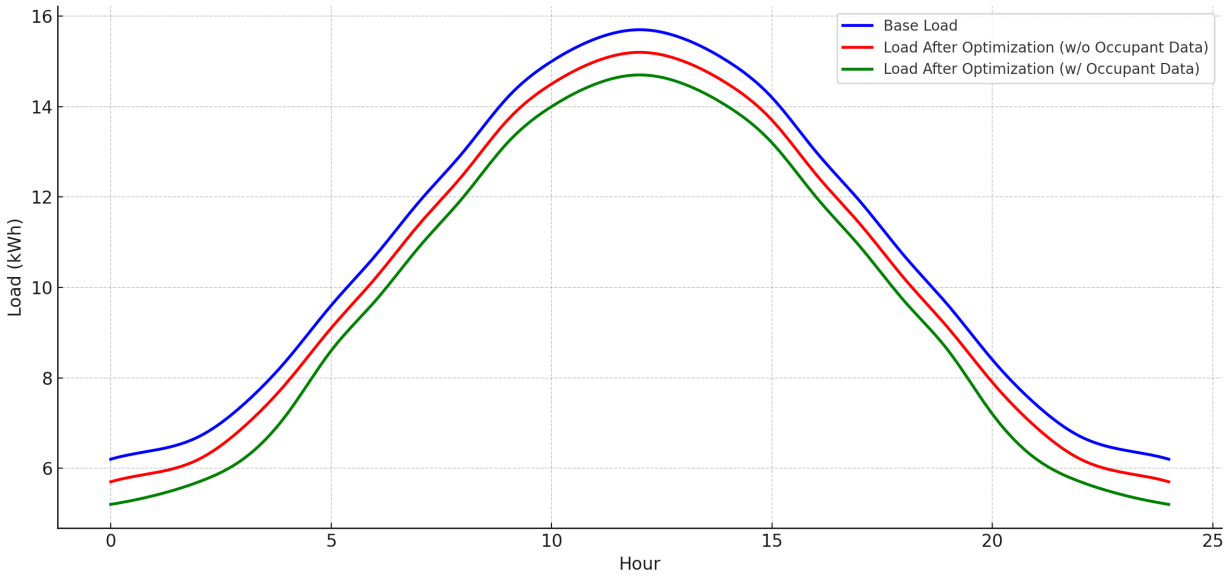

Figure 6.3: Base load, optimized load without occupant data, and optimized load with occupant data for the 2-bedroom CSGT over a 24 h period.

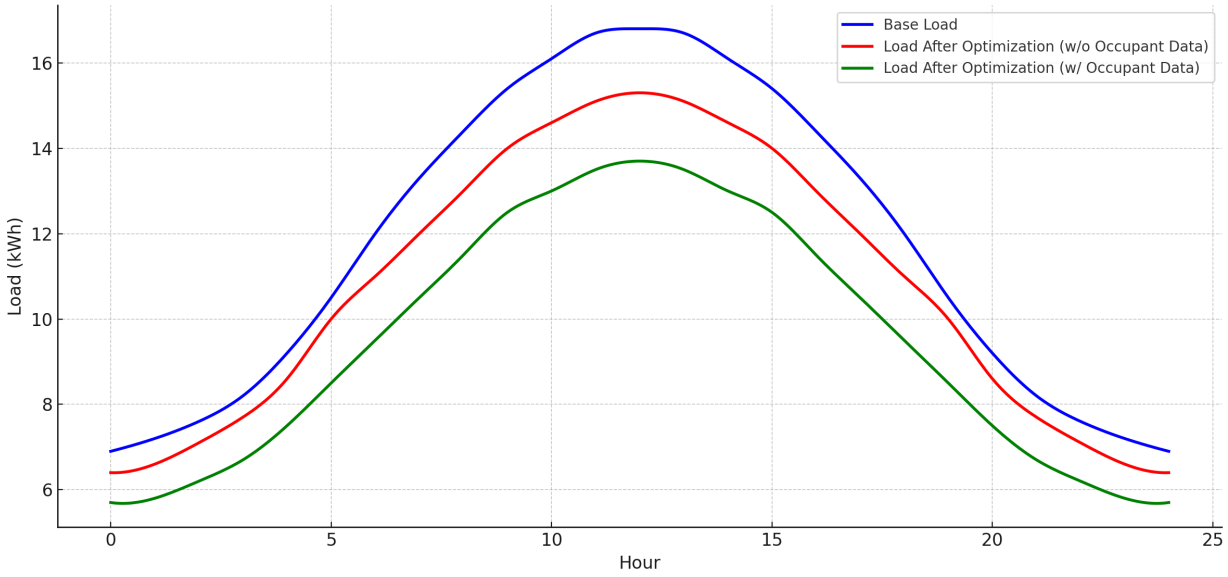

Figure 6.4: Base load, optimized load without occupant data, and optimized load with occupant data for the 3-bedroom CSGT over a 24 h period.

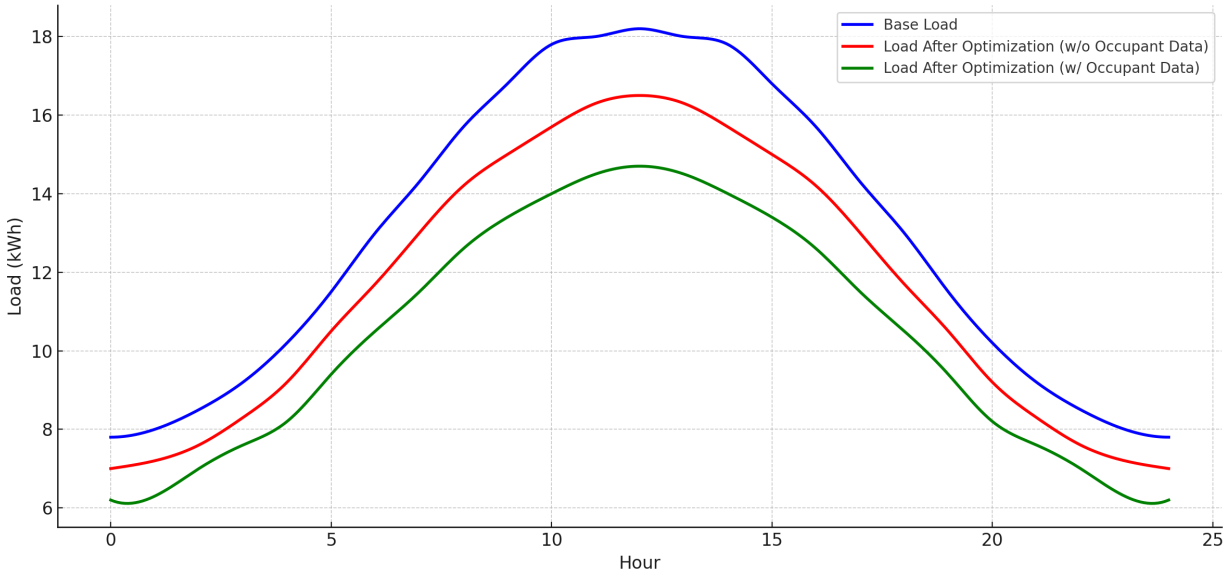

Figure 6.5: Base load, optimized load without occupant data, and optimized load with occupant data for the 4-bedroom CSGT over a 24 h period.

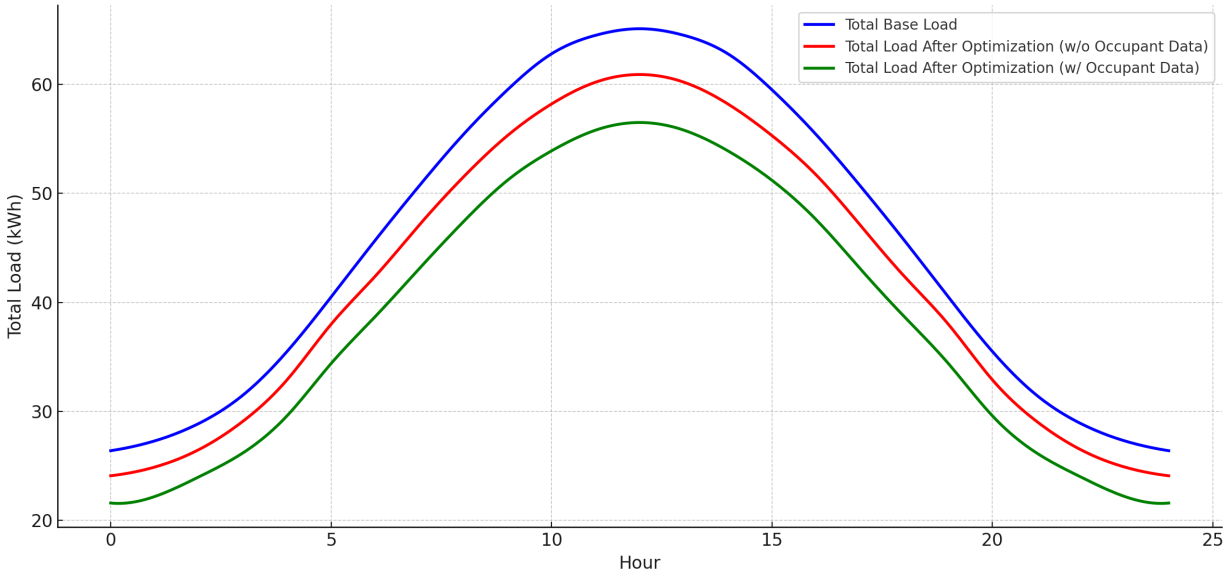

Figure 6.6: Base load, optimized load without occupant data, and optimized load with occupant data for the CSGT complex over a 24 h period.

Figures 6.2 to 6.5 present the base load, optimized load without occupant data, and optimized load with occupant data for the individual CSGTs over a 24 h period. Figure 6.6 gives the corresponding results for the CSGT complex. Occupant data includes real-time and historical information on occupant presence, behavior, and preferences collected via sensors, IoT devices, smart meters, and user inputs [128, 192, 200]. These results indicate that occupant-aware optimization improves load efficiency and reduces peak demand. For example, the 1-bedroom CSGT has a base load peak of 14.3 kWh, and this decreases to 13.9 kWh without occupant data and 13.3 kWh with occupant data. The 2-bedroom unit has a peak load reduction from 15.7 kWh to 15.2 kWh and 14.7 kWh. The 3-bedroom and 4-bedroom CSGTs have base peak loads of 16.8 kWh and 18.1 kWh, respectively, and they decrease to 15.3 kWh and 16.4 kWh without occupant data and 13.8 kWh and 14.5 kWh when occupant data is incorporated. Figure 6.6 indicates the cumulative effect is a significant decrease in the complex peak load from nearly 67 kWh to 61 kWh without occupancy data and 54 kWh with this data. These results demonstrate the value of real-time occupancy data in dynamic energy management, enabling control strategies that adapt load profiles to actual usage patterns and occupancy conditions. They also confirm that the proposed framework effectively improves load efficiency and lowers operational costs and carbon emissions while ensuring occupant comfort.

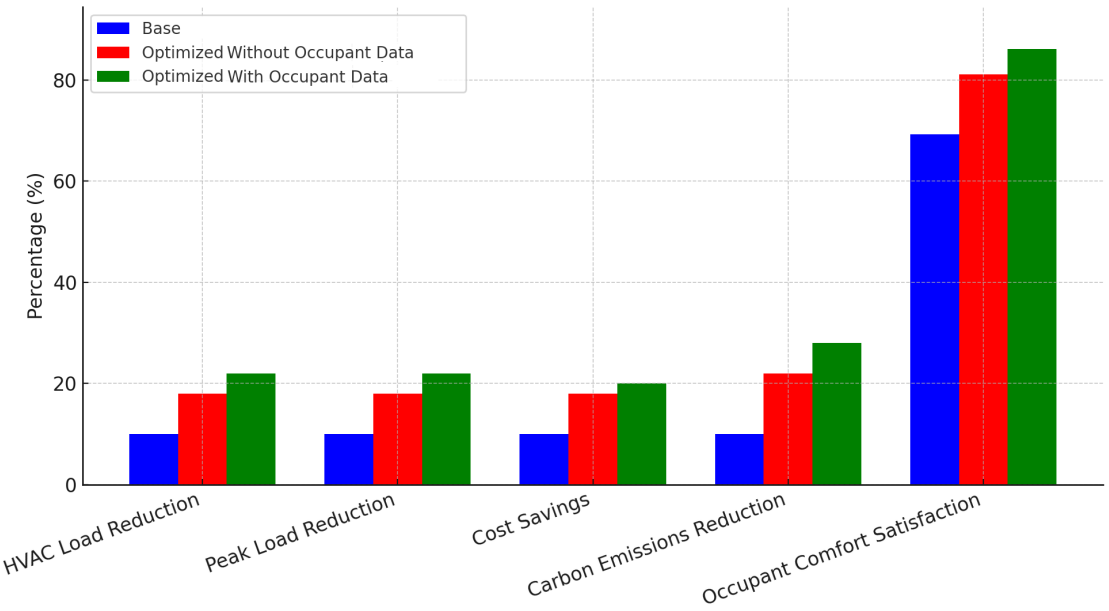

Figure 6.7: Performance improvement relative to historical data for the base load, optimized load without occupant data, and optimized load with occupant data.

Figure 6.7 presents the townhouse complex base, optimized without occupant data, and optimized with occupant data HVAC and peak load reductions, cost savings, carbon emissions reduction, and occupant comfort satisfaction compared to the historical data in [128, 132, 133]. The base results are the worst as optimization improves all five parameters. For example, optimization without occupant data provides an improvement in HVAC and peak loads of about 18%, and with occupant data there is an additional 2–6% improvement for all parameters. In particular, occupant comfort satisfaction is improved to over 85%. These results show the effectiveness of incorporating real-time occupant data into load management to improve efficiency, reduce costs, and lower environmental impact while maintaining a high level of occupant satisfaction.

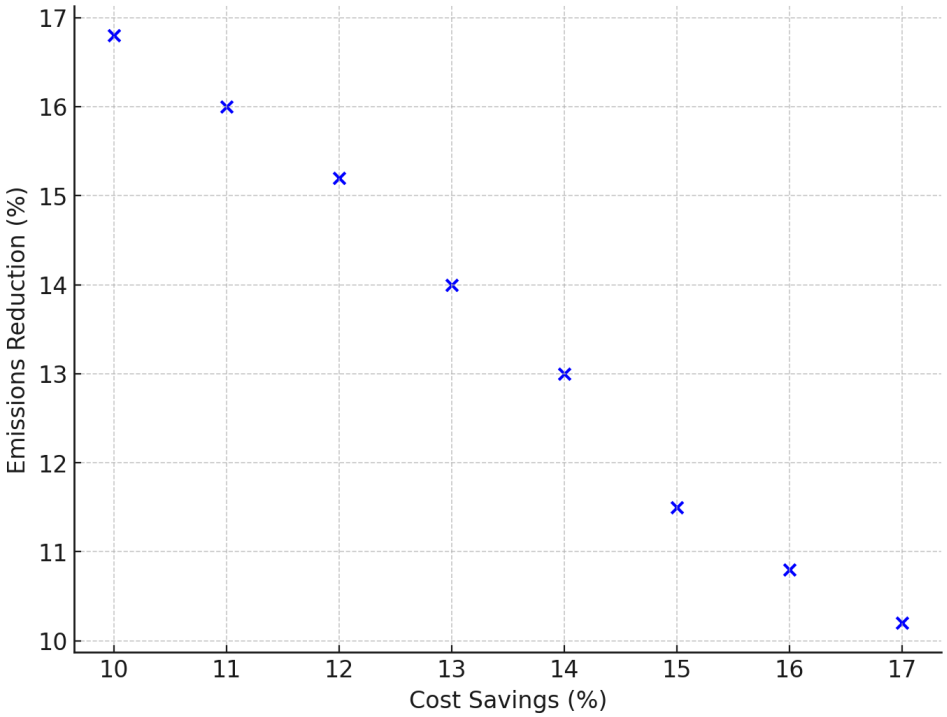

Figure 6.8: Cost savings versus emissions reduction for the CSGT complex optimized with occupant data.

Figure 6.8 gives the cost savings versus emission reductions for the townhouse complex optimized with occupant data. This shows the tradeoff between economic and environmental benefits with cost savings between 10% and 17% and emission reductions between 10% and 17%. This reflects optimization considering load demand and occupant behavior. Further, there is an inverse relationship between the two parameters. Thus, reducing the environmental impact increases costs.

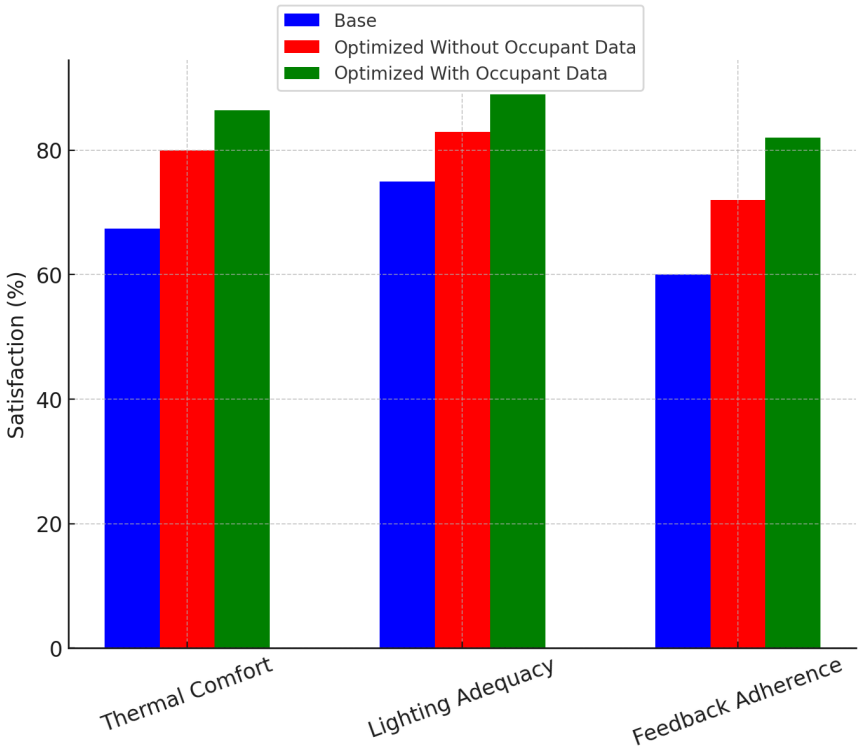

Figure 6.9: Base, without occupant data, and optimized with occupant data CGST complex occupant satisfaction over a 24 h period.

Figure 6.9 presents the townhouse complex occupant satisfaction in terms of thermal comfort, lighting adequacy, and feedback adherence for the base, optimized without occupant data, and optimized with occupant data cases. These results indicate optimization increases all three parameters. For example, thermal comfort increased from a base of approximately 67% to 80% optimized without occupant data and 86% optimized with occupant data. The corresponding lighting adequacy improved from 75% to 83% and 89%, and the feedback adherence from 60% to 72% and 82%. These results confirm the effectiveness of occupant-aware energy optimization in improving occupant satisfaction.

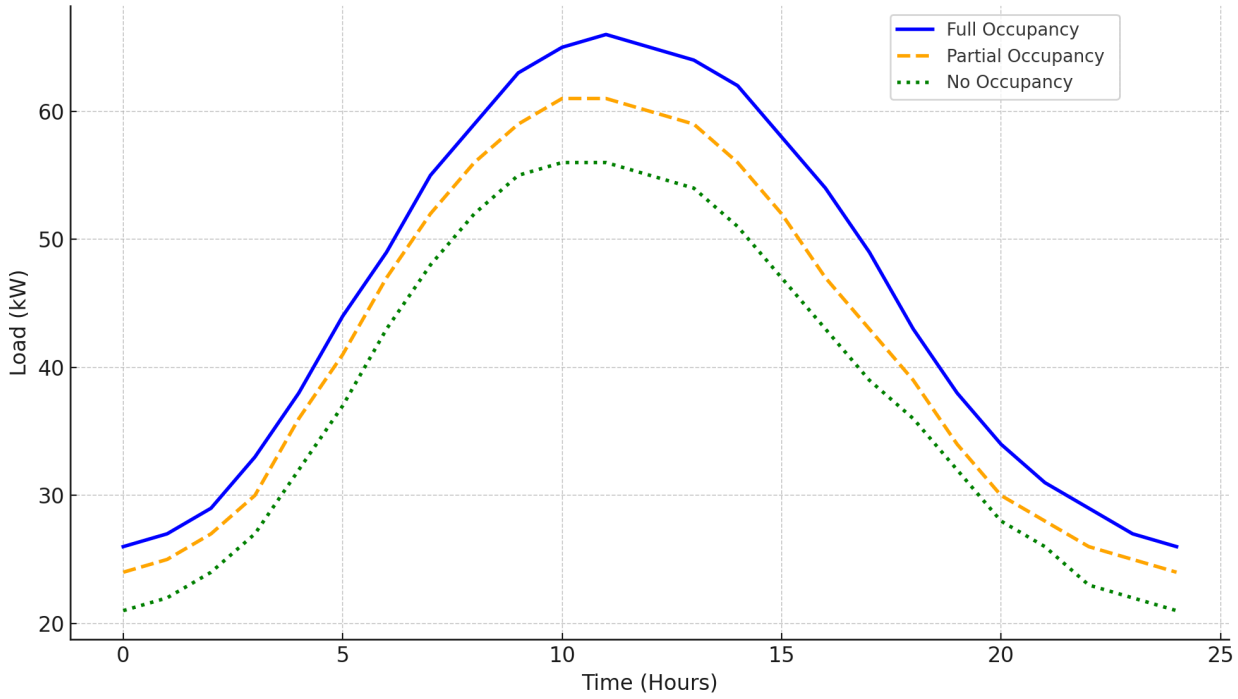

Figure 6.10: CSGT complex optimized load with full, partial, and no occupancy.

Figure 6.10 illustrates the impact of occupancy on the CSGT complex optimized load with occupant data over a 24 h period. Full occupancy indicates all residents are present which results in significant HVAC, lighting, and appliance use. With partial occupancy, there are fewer residents so energy consumption is lower. No occupancy means the building is unoccupied so only essential systems are running, such as standby appliances, HVAC with setback control, and water heating. The results in Figure 6.10 show that occupancy has a significant effect on load demand. With full occupancy, the peak load is about 66 kW at midday due to increased appliance and HVAC usage. Partial occupancy has a lower peak load of about 61 kW, reflecting moderate demand due to fewer residents. No-occupancy has the lowest peak load which is below 57 kW. Thus, occupancy-driven load optimization is important to reduce peak demand and overall CSGT load. The performance improvements observed, i.e. reductions in load, operational cost, and carbon emissions, are a result of the integration of the predictive capability of the hybrid LSTM-CNN model and the dynamic capability of the MOPSO algorithm. The LSTM effectively captures time-dependent occupancy and load trends, while the CNN identifies spatial usage patterns from sensor inputs across multiple zones and townhouses. This reduces grid dependence during peak hours and aligns energy use with occupant presence, which lowers energy demand, utility costs, and greenhouse gas emissions.

Table 6.3 presents the MAE, RMSE, and R^2 for the CSGT complex load optimization with the Linear Regression (LR), LSTM, CNN, and proposed hybrid LSTM-CNN models. The LR model has the worst performance with an MAE of 0.80 kWh and RMSE of 1.20 kWh, indicating poor prediction accuracy. The LSTM model has an MAE of 0.60 kWh and

Table 6.3: CSGT performance with four models.

Model	MAE (kWh)	RMSE (kWh)	R^2
Linear Regression (LR)	0.80	1.20	0.85
LSTM	0.60	0.72	0.89
CNN	0.56	0.75	0.93
Proposed	0.47	0.68	0.95

an RMSE of 0.72 kWh, which is lower. The CNN model improves on these results with an MAE of 0.56 kWh and an RMSE of 0.75 kWh. Further, R^2 is 0.93 which is better than with the LR and LSTM models. The proposed model provides the best overall performance with the lowest MAE (0.47 kWh) and RMSE (0.68 kWh), and the highest R^2 (0.95), indicating superior prediction accuracy and reliability. These results validate the effectiveness of the model in energy load forecasting. While the proposed model outperforms the others, its decisions are less interpretable due to the deep learning architecture. Incorporating explainable AI techniques can improve understanding of the input-output relationships, particularly for stakeholders seeking clarity in operational decisions.

6.2.1 Sensitivity of Key Parameters

The impact of key parameters is now considered.

1. **Occupant Behavior Weights (w_T, w_L, w_F):** Increasing the weight assigned to thermal comfort (e.g., w_T from 0.4 to 0.6) will improve temperature satisfaction but also increase HVAC usage, potentially raising energy consumption by up to 8% [223]. Similarly, a higher feedback adherence weight (w_F) will improve personalization but may introduce variations that will reduce energy efficiency.
2. **Optimization Objective Function Weights (w_1, w_2, w_3):** Adjusting the MOPSO weights shifts the balance between load, cost, and emissions. Prioritizing emissions ($w_3 > 0.4$) will reduce carbon emissions but increase reliance on storage and renewable energy, resulting in higher costs [199, 203]. On the other hand, emphasizing cost ($w_2 > 0.4$) will improve affordability but may lower occupant satisfaction due to less flexible HVAC control.
3. **MOPSO Parameters:** As observed in [222], larger swarm sizes or increased cognitive/social weights improve convergence but require longer computation times, which may not be feasible for real-time applications.
4. **Model Hyperparameters (e.g., depth, learning rate):** Deep architectures such as LSTM and CNN can provide better accuracy but risk overfitting, especially with small datasets [217, 218]. A properly tuned architecture balances prediction accu-

racy and generalizability. The hyperparameters used here are based on the results in [192, 200].

6.3 Conclusion

This chapter introduced a scalable occupant-centric load optimization framework for Connected Smart Green Townhouses (CSGTs), integrating a hybrid Long Short-Term Memory-Convolutional Neural Network (LSTM-CNN) with Multi-Objective Particle Swarm Optimization (MOPSO). Real-time occupant data was used to dynamically optimize energy loads, resulting in substantial performance improvements. The results obtained indicate reductions in load by 12.7%, operational costs by 13.0%, and carbon emissions by 15.5%. Furthermore, peak load demand was reduced by up to 12.7% which helps improve grid stability. In addition, occupant satisfaction was improved with thermal comfort increasing by 19%, lighting adequacy by 14%, and feedback adherence by 22%. The tradeoff between cost savings and emission reductions indicates the proposed framework can be used in real-world applications. Future research will consider Renewable Energy Systems (RESs) and system scalability to ensure sustainable and adaptive energy management for CSGTs considering occupant satisfaction. Further, Transformer-based architectures and statistical time-series models such as Prophet can be employed to improve long-term forecasting and model interpretability. Key parameters such as occupant comfort weights and the cost-emission tradeoff can be considered to assess their impact on model performance in residential scenarios considering occupant behavior.

Chapter 7

Conclusion and Future Work

7.1 Conclusion

A comprehensive approach to optimizing energy management in SGBs through ML, real-time occupancy modeling, and load optimization strategies was presented. The proposed approaches provide significant improvements in energy efficiency, cost savings, carbon emission reduction, and grid stability.

A comprehensive investigation into energy optimization for SGTs and CSGTs, using state-of-the-art ML models under both grid-connected and island modes was presented. The primary focus was to improve energy efficiency, reduce carbon emissions and operational costs, and improve occupant satisfaction. A review of ML models applied to energy demand prediction in MBs was conducted. It was found that hybrid and ensemble ML models such as SVM and RF outperform traditional single ML models. These hybrid approaches achieved up to 15% greater accuracy, confirming their effectiveness in energy prediction and suggesting that incorporating a wider feature set will improve model performance. A hybrid deep learning model combining LSTM and CNN was proposed for load optimization in CSGTs operating in grid-connected mode. It integrates PV systems and smart components to reduce electricity, water, and gas consumption. The hybrid model provided superior results compared to baseline ML models (e.g., LR, RF, GB), achieving MAPE values below 5%, and R^2 consistently above 0.85. These results validate the model precision and prediction reliability for multi-bedroom CSGT units. The proposed hybrid ML model was also applied to CSGTs in island mode. By incorporating EVs and using V2G strategies, the model addressed energy storage and load balancing challenges. The model MAPE was 3.30%–4.50% with MAE values between 2.45 and 3.60 kWh, confirming its ability to provide efficient and resilient energy management in off-grid scenarios. This also indicates that CSGBs are viable components of sustainable urban infrastructure.

An adaptive load optimization framework enabling automated transitions between grid-connected and island modes was introduced. A MOPSO algorithm was employed to balance cost, emissions, and efficiency in real-time. The results indicate efficiency improvements of 3–5% in grid-connected mode and 10–12% in island mode, along with carbon

emission reductions of 4–6%. This framework demonstrates the practicality of dynamic load control with minimal manual intervention, supporting reliable operation in diverse environments.

An occupant-centric framework was presented that integrates real-time IoT data and ML prediction to optimize energy usage based on occupant behavior and comfort preferences. This model reduced overall loads by up to 13%, peak demand by 12.7%, operational costs by 13–21%, and carbon emissions by 15–24%. It also significantly improved occupant satisfaction, with thermal comfort increasing by 19%, lighting adequacy by 14%, and feedback adherence by 22%. These results confirm the human-centric nature of the model and its adaptability to real-world building management needs.

These contributions establish a foundation for future research aimed at improving energy efficiency, scalability, and real-world implementation of smart energy management systems. However, there remain open challenges and areas for further investigation.

7.2 Future Work

The results presented open several promising avenues for further research on SGBs. Future work will focus on improving system scalability, integrating advanced AI models, optimizing real-time energy decisions, and increasing grid-interactive capabilities.

7.2.1 Advanced Energy Management: Real-Time Optimization of RE and Storage

One of the key limitations in smart energy management is the real-time synchronization between RE generation, storage, and demand response. Future research will explore the following.

- **Hybrid AI-based forecasting models (LSTM-CNN, Transformer models)** Predicting short-term solar generation and energy consumption for improved RE utilization.
- **RL-Based Battery Management** Implementing Deep Q-Network (DQN) and Proximal Policy Optimization (PPO) to optimize battery charging/discharging schedules based on dynamic energy pricing [227].
- **Multi-Agent Energy Coordination** Leveraging game-theoretic models to optimize energy-sharing strategies among townhouses, and improve load distribution and grid stability.

Integrating these strategies will increase energy autonomy, minimize grid dependency, and maximize sustainability.

7.2.2 Enhancing Computational Efficiency and Model Scalability

Deploying real-time AI models in energy management requires addressing computational efficiency and scalability challenges. Future research will focus on the following.

- **Federated Learning for Decentralized Energy Optimization** Implementing privacy-preserving learning models where multiple CSGTs collaboratively train ML models without sharing sensitive data.
- **Attention-based Transformer Architectures** Enhancing energy forecasting with self-attention mechanisms for capturing complex temporal energy usage patterns.
- **Graph Neural Networks (GNNs) for Load Distribution Prediction** Applying GNNs to model spatial dependencies in energy-sharing between multiple townhouses [228].
- **Edge Computing-Based Energy Optimization** Utilizing TinyML and TensorFlow Lite for low-latency decision-making on IoT-enabled energy management devices.

These approaches will ensure real-time adaptability, scalability, and computational efficiency in SGB energy optimization.

7.2.3 Grid-Interactive Smart Townhouses and Utility Collaboration

Future SGTs must interact efficiently with the power grid, allowing for dynamic pricing, demand response participation, and grid-supported services. The research areas include the following.

- **Dynamic Tariff Models for TOU Pricing** Developing AI-driven pricing response strategies to optimize energy costs based on real-time electricity market conditions.
- **Integration with Grid-Interactive Efficient Buildings (GEBs)** Creating a two-way communication framework for CSGTs to support grid stability.
- **Blockchain-Based Peer-to-Peer (P2P) Energy Trading** Enabling secure, decentralized energy-sharing between townhouses [229].
- **Virtual Power Plant (VPP) Aggregation** Aggregating CSGTs into a DER network, allowing participation in grid frequency regulation and ancillary services.

By integrating utility-driven incentives, future studies can bridge the gap between energy consumers and providers, creating cost-effective, resilient energy systems.

7.2.4 Stochastic Optimization for Demand-Supply Variability

Energy consumption in SGBs is inherently uncertain due to weather conditions, occupancy fluctuations, and unpredictable load variations. Future research will consider the following.

- **Stochastic Programming for Uncertainty Modeling** Implementing Monte Carlo simulation, Bayesian networks, and scenario-based optimization for accurate uncertainty quantification.
- **Adaptive Reinforcement Learning-Based Control** Designing self-learning control algorithms that adjust energy dispatch strategies dynamically.
- **Robust Multi-Objective Optimization** Utilizing Pareto-based evolutionary algorithms (Non-dominated Sorting Genetic Algorithm II (NSGA-II) and Multi-Objective Evolutionary Algorithm based on Decomposition (MOEA/D)), to optimize cost, emissions, and occupant comfort under uncertainty [230].

This will enable highly adaptive energy management for SGBs, ensuring resilient, self-optimizing control frameworks.

7.2.5 Personalized Energy Management Strategies for Occupant Behavior Modeling

Occupant behavior significantly influences energy consumption patterns in SGBs. Future research will explore the following.

- **Real-Time Occupancy Detection Systems** Using computer vision (You Only Look Once (YOLO), OpenPose) and sensor fusion (motion, CO_2, temperature sensors) to accurately model occupancy patterns.
- **Human-in-the-Loop Optimization** Designing interactive energy-saving strategies based on occupant preferences and behavioral feedback loops [231].
- **Gamification and Incentive-Based Energy Conservation** Developing smartphone applications that reward energy-efficient behavior through gamified user engagement strategies.

This occupant-driven optimization approach will improve comfort, reduce unnecessary energy consumption, and increase overall system efficiency.

7.2.6 Advanced Smart Inverter Functionalities for Grid Stability

As DERs become more prevalent, future work must consider smart inverter integration for grid support. The research topics are as follows.

- **AI-Based Volt-VAR Optimization** Implementing ML-driven reactive power control for real-time voltage stabilization [232].
- **Automated Frequency Response Mechanisms** Enabling smart inverters to dynamically adjust power output for grid frequency balancing.
- **Integration of Solid-State Transformers (SSTs)** Exploring digital power conversion technologies to enhance smart grid stability.

This research will establish SGBs as active participants in maintaining grid stability, and supporting resilient and intelligent energy networks.

7.2.7 Validation Across Different Geographic Locations and Multiple Building Types

Validation across diverse scenarios is essential to demonstrate its scalability and generalizability. Future research will explore the following.

- Diverse climate zones and geographic locations to assess performance variations.
- Commercial and residential buildings to explore the adaptability of energy management approaches.
- Higher renewable penetration scenarios to assess integration challenges in net-zero buildings.

This work will ensure scalable, future-proof SGB models for smart urban communities.

Appendix

Table A.1 summarizes the LEED standards [144] considered for SGBs in Canada. These standards, which were discussed earlier, provide a framework for sustainable building practices and guide the development of energy-efficient and environmentally responsible structures. The insulation R-value properties are presented in Table A.2 and discussed in Chapters 3 and 4. These values provide the thermal resistance of various materials used in building insulation, which plays a critical role in energy efficiency and heat retention. Algorithm 1 outlines the performance evaluation of the proposed ML models using metrics such as R^2, RMSE, MAE, and MAPE. This code was implemented in Python v3.11.5 and can be adapted for future research.

Table A.1: Considered LEED standards [144] for SGBs in Canada.

LEED Standard	**Description**
LEED for New Construction (LEED NC)	Addresses the design and construction of new buildings and major renovations, emphasizing sustainability and energy efficiency.
LEED for Homes (LEED-H)	Tailored specifically for residential buildings, advocating for the integration of green features and sustainable practices.
LEED for Existing Buildings: Operations & Maintenance (LEED EB: O&M)	Focuses on optimizing the performance of existing buildings through sustainable operations and maintenance practices.
LEED for Neighborhood Development (LEED ND)	Guides the sustainable development of neighborhoods, taking into account factors such as transportation, land use, and community connection.
LEED for Commercial Interiors (LEED CI)	Addresses the sustainable design and construction of interior spaces within commercial buildings.
LEED for Core and Shell (LEED CS)	Focuses on the core and shell of new construction projects, encouraging sustainable and efficient building practices.
LEED for Schools (LEED for Schools)	Tailored for educational institutions, promoting green building practices in school construction and renovation projects.

Table A.2: Insulation R-Value chart [233].

Building Material	R-Value (1 Inch)	R-Value (5 Inches)	R-Value (10 Inches)
Closed Cell Spray Foam	7.00	35.0	70.0
Open Cell Spray Foam	3.80	19.0	38.0
Foam Board	4.00	20.0	40.0
Gypsum or Plaster Board	0.90	4.5	9.0
Plywood	1.25	6.25	12.5
Wood Panels	1.25	6.25	12.5
Wood-Fiber Board	2.38	11.9	23.8
Wood-Fiber Hardboard	1.39	6.95	13.9
Softwood	1.41	7.05	14.1
Hardwood	0.71	3.55	7.1
Pine Wood	1.25	6.25	12.5
Asphalt Tile	0.32	1.6	3.2
Ceramic Tile	0.08	0.4	0.8
Cork Tile	2.22	11.1	22.2
Linoleum	0.56	2.8	5.6
Plywood Subfloor	1.25	6.25	12.5
Rubber Tile	0.20	1.0	2.0
Plastic Tile	0.20	1.0	2.0
Terrazzo	0.98	4.9	9.8
Wood Subfloor	1.25	6.25	12.5
Cotton Fiber	3.85	19.25	38.5
Mineral Wool	3.70	18.5	37.0
Wood Fiber	4.00	20.0	40.0
Glass Fiber	4.00	20.0	40.0
Roof Deck Slab	4.17	20.85	41.7
Cellular Glass	2.50	12.5	25.0
Corkboard	3.70	18.5	37.0
Hog Hair	3.00	15.0	30.0
Plastic (Foamed)	3.45	17.25	34.5
Shredded Wood	1.82	9.1	18.2
Macerated Paper	3.57	17.85	35.7
Sawdust or Shavings	2.22	11.1	22.2
Vermiculite	2.08	10.4	20.8
Roof Insulation	2.78	13.95	27.8
Concrete	0.19–1.42	0.95–7.1	1.9–14.2
Brick (Common)	0.20	1.0	2.0

Algorithm 1 ML Model Performance Metrics Calculation

Input: Actual values `actual`, model predictions `predicted_models`
Output: MAE, RMSE, R^2, and MAPE for each model

Step 1: Load dataset
`data` ← `pd.read_csv('data.csv')`

Step 2: Define actual and predicted values
for each `model` in `predicted_models` **do**
    `actual` ← `data['actual']`
    `predicted` ← `data[model]`
end for

Step 3: Define MAPE function
function MEAN_ABSOLUTE_PERCENTAGE_ERROR(`y_true`, `y_pred`)
    return `mean` $\left(\left| \frac{y\_true - y\_pred}{y\_true} \right| \right) \times 100$
end function

Step 4: Calculate metrics for each model
for each `model` in `predicted_models` **do**
    MAE ← `mean_absolute_error(actual, predicted)`
    RMSE ← `mean_squared_error(actual, predicted, squared=False)`
    R^2 ← `r2_score(actual, predicted)`
    MAPE ← `mean_absolute_percentage_error(actual, predicted)`
    Store metrics in `metrics[model]` ← {MAE, RMSE, R^2, MAPE}
end for

Step 5: Display results
for each `model` in `metrics` **do**
    Print MAE, RMSE, R^2, and MAPE for `model`
end for

Bibliography

[1] H. Omrany, V. Soebarto, and A. Ghaffarianhoseini, "Rethinking the concept of building energy rating system in Australia: A pathway to life-cycle net-zero energy building design," *Architectural Science Review*, 65, pp. 42–56, 2022.

[2] P. Moran, J. O'Connell, and J. Goggins, "Sustainable energy efficiency retrofits as residential buildings move towards nearly zero energy building (NZEB) standards," *Energy and Buildings*, 211, art. 109816, 2020.

[3] L. Yang, H. Yan, and J. C. Lam, "Thermal comfort and building energy consumption implications—A review," *Applied Energy*, 115, pp. 164–173, 2013.

[4] A. Spence, C. Leygue, B. Bedwell, and C. O'Malley, "Engaging with energy reduction: Does a climate change frame have the potential for achieving broader sustainable behaviour?," *Journal of Environmental Psychology*, 38, pp. 17–28, 2014.

[5] J. Vepsalainen, K. Otto, A. Lajunen, and K. Tammi, "Computationally efficient model for energy demand prediction of electric city bus in varying operating conditions," *Energy*, 169, pp. 433–443, 2019.

[6] A.-P. Hameri and J. Heikkilä, "Improving efficiency: Time-critical interfacing of project tasks," *International Journal of Project Management*, 20, pp. 143–153, 2002.

[7] K. Blok, "Improving energy efficiency by five percent and more per year?," *Journal of Industrial Ecology*, 8, pp. 87–99, 2004.

[8] H. Dagdougui, F. Bagheri, H. Le, and L. Dessaint, "Neural network model for short-term and very-short-term load forecasting in district buildings," *Energy and Buildings*, 203, art. 109408, pp. 1–11, 2019.

[9] X. Godinho, H. Bernardo, F. T. Oliveira, and J. C. Sousa, "Forecasting heating and cooling energy demand in an office building using machine learning methods," in *International Young Engineers Forum*, Costa da Caparica, Portugal, July 2020, pp. 1–6.

[10] M. Xue and C. Zhu, "A study and application on machine learning of artificial intelligence," in *International Joint Conference on Artificial Intelligence*, Hainan, China, April 2009, pp. 352–355.

[11] R. Akkiraju, V. Sinha, A. Xu, J. Mahmud, P. Gundecha, Z. Liu, X. Liu, and J. Schumacher, "Characterizing machine learning processes: A maturity framework," in *International Conference on Business Process Management*, Seville, Spain, September 2020, pp. 17–31.

[12] R. Welte, M. Estler, and D. Lucke, "A method for implementation of machine learning solutions for predictive maintenance in small and medium sized enterprises," in *IEEE Texas Power and Energy Conference*, College Station, Texas, USA, February 2020, pp. 909–914.

[13] J. Sultana, A. K. Singha, S. T. Siddiqui, G. Nagalaxmi, A. K. Sriram, and N. Pathak, "COVID-19 pandemic prediction and forecasting using machine learning classifiers," *Intelligent Automation and Soft Computing*, 32, pp. 1007–1024, 2022.

[14] A. M. Aneeque, M. Alghassab, K. Ullah, Z. A. Khan, Y. Lu, and M. Imran, "A review of electricity demand forecasting in low and middle income countries: The demand determinants and horizons," *Sustainability*, 12, art. 5931, 2020.

[15] N. Ahmad, Y. Ghadi, M. Adnan, and M. Ali, "Load forecasting techniques for the power system: Research challenges and survey," *IEEE Access*, 10, pp. 71054–71090, 2022.

[16] B. Dhanalaxmi, "Machine learning and its emergence in the modern world and its contribution to artificial intelligence," in *IEEE International Conference for Emerging Technology*, Belgaum, India, June 2020, pp. 1–6.

[17] H. Saxena, O. Aponte, and K. T. McConky, "A hybrid machine learning model for forecasting a billing period's peak electric load days," *International Journal of Forecasting*, 35, pp. 1288–1303, 2019.

[18] J. Sinopoli, "How do smart buildings make a building green?," *Energy Engineering*, 105, pp. 17–22, 2008.

[19] C. Lu, S. Li, J. Gu, W. Lu, T. Olofsson, and J. Ma, "A hybrid ensemble learning framework for zero-energy potential prediction of photovoltaic direct-driven air conditioners," *Journal of Building Engineering*, 64, art. 105602, 2023.

[20] M. Cunkas and A. Altun, "Long term electricity demand forecasting in Turkey using artificial neural networks," *Energy Sources, Part B: Economics, Planning, and Policy*, 5, pp. 279–289, 2010.

[21] G. Zahedi, S. Azizi, A. Bahadori, A. Elkamel, and S. R. Wan Alwi, "Electricity demand estimation using an adaptive neuro-fuzzy network: A case study from the Ontario province—Canada," *Energy*, 49, pp. 323–328, 2013.

[22] J. Chen, S. Lo, and Q. H. Do, "Forecasting monthly electricity demands: An application of neural networks trained by heuristic algorithms," *Information*, 8, art. 31, 2017.

[23] A. Anand and L. Suganthi, "Hybrid GA-PSO optimization of artificial neural network for forecasting electricity demand," *Energy*, 144, pp. 1073–1085, 2018.

[24] Y. Chen and H. Tan, "Short-term prediction of electric demand in the building sector via hybrid support vector regression," *Applied Energy*, 204, pp. 1363–1374, 2017.

[25] W. Shen, V. Babushkin, Z. Aung, and W. L. Woon, "An ensemble model for day-ahead electricity demand time series forecasting," in *International Conference on Future Energy Systems*, Berkeley, CA, USA, May 2013, pp. 51–62.

[26] E. M. Burger and S. J. Moura, "Gated ensemble learning method for demand-side electricity load forecasting," *Energy and Buildings*, 109, pp. 23–34, 2015.

[27] Z. Wang, Y. Wang, and R. S. Srinivasan, "A novel ensemble learning approach to support building energy use prediction," *Energy and Buildings*, 159, pp. 109–122, 2018.

[28] I. Thammachantuek, S. Kosolsomnbat, and M. Ketcham, "Comparison of machine learning algorithm's performance based on decision making in autonomous cars," in *International Joint Symposium on Artificial Intelligence and Natural Language Processing*, Pattaya, Thailand, November 2018, pp. 680–683.

[29] M. Štubňová, M. Urbaníková, J. Hudáková, and V. Papcunová, "Estimation of residential property market price: Comparison of artificial neural networks and hedonic pricing model," *Emerging Science Journal*, 4, pp. 530–538, 2020.

[30] T. Xu, G. Han, X. Qi, J. Du, C. Lin, and L. Shu, "A hybrid machine learning model for demand prediction of edge-computing-based bike-sharing systems using the internet of things," *IEEE Internet of Things Journal*, 7, pp. 7345–7356, 2020.

[31] K. Amasyali and N. M. El-Gohary, "A review of data-driven building energy consumption prediction studies," *Renewable and Sustainable Energy Reviews*, 81, pp. 1192–1205, 2018.

[32] N. J. Johannesen, M. Kolhe, and M. Goodwin, "Relative evaluation of regression tools for urban area electrical energy demand forecasting," *Journal of Cleaner Production*, 218, pp. 555–564, 2019.

[33] H. K. Alfares and M. Nazeeruddin, "Electric load forecasting: Literature survey and classification of methods," *International Journal of Systems Science*, 33, pp. 23–34, 2002.

[34] D. Li, Y. Tang, and Q. Chen, "Multi-mode traffic demand analysis based on multi-source transportation data," *IEEE Access*, 8, pp. 65005–65019, 2020.

[35] Y. Zhou, F. J. Chang, L. C. Chang, I. F. Kao, Y. S. Wang, and C. C. Kang, "Multi-output support vector machine for regional multi-step-ahead $PM_{2.5}$ forecasting," *Science of the Total Environment*, 651, pp. 230–240, 2019.

[36] N. Chouikhi, B. Ammar, N. Rokbani, and A. M. Alimi, "PSO-based analysis of echo state network parameters for time series forecasting," *Applied Soft Computing*, 55, pp. 211–225, 2017.

[37] S. M. Moghimi, S. M. Shariatmadar, and R. Dashti, “Stability analysis of the micro-grid operation in micro-grid mode based on particle swarm optimization (PSO) including model information,” *Physical Science International Journal*, 10, art. PSIJ.24425, pp. 1–13, 2016.

[38] B. Buddhahai, W. Wongseree, and P. Rakkwamsuk, “An energy prediction approach for a nonintrusive load monitoring in home appliances,” *IEEE Transactions on Consumer Electronics*, 66, pp. 96–105, 2019.

[39] S. Ahmadzadeh, G. Parr, and W. Zhao, “A review on communication aspects of demand response management for future 5G IoT-based smart grids,” *IEEE Access*, 9, pp. 77555–77571, 2021.

[40] W. Junior, E. Oliveira, A. Santos, and K. Dias, “A context-sensitive offloading system using machine-learning classification algorithms for mobile cloud environment,” *Future Generation Computer Systems*, 90, pp. 503–520, 2019.

[41] M. Abdrabou and T. A. Gulliver, “Adaptive physical layer authentication using machine learning with antenna diversity,” *IEEE Transactions on Communications*, 70, pp. 6604–6614, 2022.

[42] M. T. Ahammed and I. Khan, “Ensuring power quality and demand-side management through IoT-based smart meters in a developing country,” *Energy*, 250, art. 123747, 2022.

[43] A. Al Mamun, M. Sohel, N. Mohammad, M. S. H. Sunny, D. R. Dipta, and E. Hossain, “A comprehensive review of the load forecasting techniques using single and hybrid predictive models,” *IEEE Access*, 8, pp. 134911–134939, 2020.

[44] H. J. Queen, J. Jayakumar, T. J. Deepika, K. V. S. M. Babu, and S. P. Thota, “Machine learning-based predictive techno-economic analysis of power system,” *IEEE Access*, 9, pp. 123504–123516, 2021.

[45] Y. Zhang, Y. Xu, Z. Y. Dong, and R. Zhang, “A hierarchical self-adaptive data-analytics method for real-time power system short-term voltage stability assessment,” *IEEE Transactions on Industrial Informatics*, 15, pp. 74–84, 2018.

[46] J. Luque, E. Personal, A. Garcia-Delgado, and C. Leon, “Monthly electricity demand patterns and their relationship with the economic sector and geographic location,” *IEEE Access*, 9, pp. 86254–86267, 2021.

[47] T. Ahmad, H. Chen, Y. Guo, and J. Wang, “A comprehensive overview on the data driven and large scale based approaches for forecasting of building energy demand: A review,” *Energy and Buildings*, 165, pp. 301–320, 2018.

[48] S. Shahriar, A. R. Al-Ali, A. H. Osman, S. Dhou, and M. Nijim, “Prediction of EV charging behavior using machine learning,” *IEEE Access*, 9, pp. 111576–111586, 2021.

[49] M. A. Khan, S. Saqib, T. Alyas, A. U. Rehman, Y. Saeed, A. Zeb, M. Zareei, and E. M. Mohamed, "Effective demand forecasting model using business intelligence empowered with machine learning," *IEEE Access*, 8, pp. 116013–116023, 2020.

[50] M. Sajjad, Z. A. Khan, A. Ullah, T. Hussain, W. Ullah, M. Y. Lee, and S. W. Baik. "A novel CNN-GRU-based hybrid approach for short-term residential load forecasting," *IEEE Access*, 8, pp. 143759–143768, 2020.

[51] C. Pablo, A. González-Briones, S. Rodríguez, and J. M. Corchado, "Tendencies of technologies and platforms in smart cities: A state-of-the-art review," *Wireless Communications and Mobile Computing*, 2018, art. 3086854, 2018.

[52] O. Osama, "Intelligent building, definitions, factors and evaluation criteria of selection," *Alexandria Engineering Journal*, 57, pp. 2903–2910, 2018.

[53] J. Mengda, A. Komeily, Y. Wang, and R. S. Srinivasan, "Adopting internet of things for the development of smart buildings: A review of enabling technologies and applications," *Automation in Construction*, 101, pp. 111–126, 2019.

[54] W. Charles, T. Hargreaves, and R. Hauxwell-Baldwin, "Benefits and risks of smart home technologies," *Energy Policy*, 103, pp. 72–83, 2017.

[55] P. K. D. Pramanik, B. Mukherjee, S. Pal, T. Pal, S. P. Singh, R. Rameshwar, A. Solanki, A. Nayyar, and B. Mahapatra, "Green smart building: Requisites, architecture, challenges, and use cases," *Research Anthology on Environmental and Societal Well-Being Considerations in Buildings and Architecture Book Green and Smart Buildings: A Key to Sustainable Global Solutions*, IGI Global Scientific Publishing, Hershey, PA, USA, 2020.

[56] M. Mohsin, I. Hanif, F. Taghizadeh-Hesary, Q. Abbas, and W. Iqbal, "Nexus between energy efficiency and electricity reforms: A DEA-based way forward for clean power development," *Energy Policy*, 149, art. 112052, 2021.

[57] C. Chen, Y. Hu, M. Karuppiah, and P. M. Kumar, "Artificial intelligence on economic evaluation of energy efficiency and renewable energy technologies," *Sustainable Energy Technologies and Assessments*, 47, art. 101358, 2021.

[58] R. Sikkema, S. Proskurina, M. Banja, and E. Vakkilainen, "How can solid biomass contribute to the EU's renewable energy targets in 2020, 2030 and what are the GHG drivers and safeguards in energy-and forestry sectors?," *Renewable Energy*, 165, pp. 758–772, 2021.

[59] P. A. Fokaides, C. Panteli, and A. Panayidou, "How are the smart readiness indicators expected to affect the energy performance of buildings: First evidence and perspectives," *Sustainability*, 12, art. 9496, 2020.

[60] J. Zhang, A. K. Patwary, H. Sun, M. Raza, F. Taghizadeh-Hesary, and R. Iram, "Measuring energy and environmental efficiency interactions towards CO_2 emissions reduction without slowing economic growth in central and western Europe," *Journal of Environmental Management*, 279, art. 111704, 2021.

[61] J. Ma, G. Du, Z. K. Zhang, P. X. Wang, and B. C. Xie, “Life cycle analysis of energy consumption and CO_2 emissions from a typical large office building in Tianjin, China,” *Building and Environment*, 117, pp. 36–48, 2017.

[62] C. Wang, A. Xu, S. Jiao, Z. Zhou, D. Zhang, J. Liu, J. Ling, F. Gao, R. Rameezdeen, and L. Wang, “Environmental impact assessment of office building heating and cooling sources: A life cycle approach,” *Journal of Cleaner Production*, 261, art. 121140, 2020.

[63] M. Aftab, C. Chen, C. K. Chau, and T. Rahwan, “Automatic HVAC control with real-time occupancy recognition and simulation-guided model predictive control in low-cost embedded system,” *Energy and Buildings*, 154, pp. 141–156, 2017.

[64] K. Meng, D. Wang, Z. Y. Dong, X. Gao, Y. Zheng, and K. P. Wong, “Distributed control of thermostatically controlled loads in distribution network with high penetration of solar PV,” *CSEE Journal of Power and Energy Systems*, 3, pp. 53–62, 2017.

[65] Z. A. Reheem, F. N. Al-Mousawi, N. S. Dhaidan, and S. A. Kokz, “Advances in heat pipe technologies for different thermal systems applications: A review,” *Journal of Thermal Analysis and Calorimetry*, 147, pp. 13011–13026, 2022.

[66] Y. J. Kim, L. K. Norford, and J. L. Kirtley, “Modeling and analysis of a variable speed heat pump for frequency regulation through direct load control,” *IEEE Transactions on Power Systems*, 30, pp. 397–408, 2014.

[67] N. Lu and Y. Zhang, “Design considerations of a centralized load controller using thermostatically controlled appliances for continuous regulation reserves,” *IEEE Transactions on Smart Grid*, 4, pp. 914–921, 2012.

[68] D. Syed, H. Abu-Rub, A. Ghrayeb, and S. S. Refaat, “Household-level energy forecasting in smart buildings using a novel hybrid deep learning model,” *IEEE Access*, 9, pp. 33498–33511, 2021.

[69] S. M. Moghimi and G. Sarlak, “Energy management optimizing in multi carrier energy systems considering net zero emission and CHP temperature effects,” *Physical Science International Journal*, 10, art. PSIJ.24779, pp. 1–11, 2016.

[70] M. Diyan, B. N. Silva, and K. Han, “A multi-objective approach for optimal energy management in smart home using the reinforcement learning,” *Sensors*, 20, art. 3450, 2020.

[71] V. Amir, S. Jadid, and M. Ehsan, “Probabilistic optimal power dispatch in multi-carrier networked microgrids under uncertainties,” *Energies*, 10, art. 1770, 2017.

[72] M. Gluszak, R. Gawlik, and M. Zieba, “Smart and green buildings features in the decision-making hierarchy of office space tenants: An analytic hierarchy process study,” *Administrative Sciences*, 9, art. 52, 2019.

[73] B. Qolomany, A. Al-Fuqaha, A. Gupta, D. Benhaddou, S. Alwajidi, J. Qadir, and A. C. Fong, "Leveraging machine learning and big data for smart buildings: A comprehensive survey," *IEEE Access*, 7, pp. 90316–90356, 2019.

[74] Z. Gou, D. Prasad, and S. S. Y. Lau, "Are green buildings more satisfactory and comfortable?," *Habitat International*, 39, pp. 156–161, 2013.

[75] S. F. A. Shah, M. Iqbal, Z. Aziz, T. A. Rana, A. Khalid, Y. N. Cheah, and M. Arif, "The role of machine learning and the internet of things in smart buildings for energy efficiency," *Applied Sciences*, 12, art. 7882, 2022.

[76] B. Yu, F. Sun, C. Chen, G. Fu, and L. Hu, "Power demand response in the context of smart home application," *Energy*, 240, art. 122774, 2022.

[77] Y. I. Zhao, J. Yu, M. Ban, Y. Liu, and Z. Li, "Privacy-preserving economic dispatch for an active distribution network with multiple networked microgrids," *IEEE Access*, 6, pp. 38802–38819, 2018.

[78] A. Hussain, J.-H. Lee, and H. M. Kim, "An optimal energy management strategy for thermally networked microgrids in grid-connected mode," *International Journal of Smart Home*, 10, pp. 239–258, 2016.

[79] F. A. Mohamed and H. N. Koivo, "Online management of microGrid with battery storage using multiobjective optimization," in *International Conference on Power Engineering, Energy and Electrical Drives*, Setubal, Portugal, April 2007, pp. 231–236.

[80] R. Smith, K. Meng, Z. Dong, and R. Simpson, "Demand response: A strategy to address residential air-conditioning peak load in Australia," *Journal of Modern Power Systems and Clean Energy*, 1, pp. 219–226, 2013.

[81] F. Kamal and B. Chowdhury, "Model predictive control and optimization of networked microgrids," *International Journal of Electrical Power and Energy Systems*, 138, art. 107804, 2022.

[82] W. Su, J. Wang, K. Zhang, and A. Q. Huang, "Model predictive control-based power dispatch for distribution system considering plug-in electric vehicle uncertainty," *Electric Power Systems Research*, 106, pp. 29–35, 2014.

[83] C. Wouters, E. S. Fraga, and A. M. James, "An energy integrated, multi-microgrid, MILP (mixed-integer linear programming) approach for residential distributed energy system planning—A South Australian case-study," *Energy*, 85, pp. 30–44, 2015.

[84] S. Homaei and M. Hamdy, "A robustness-based decision making approach for multi-target high performance buildings under uncertain scenarios," *Applied Energy*, 267, art. 114868, 2020.

[85] K. Ojand and H. Dagdougui, "Q-learning-based model predictive control for energy management in residential aggregator," *IEEE Transactions on Automation Science and Engineering*, 19, pp. 70–81, 2021.

[86] Z. Ding, W. Chen, T. Hu, and X. Xu, “Evolutionary double attention-based long short-term memory model for building energy prediction: Case study of a green building,” *Applied Energy*, 288, art. 116660, 2021.

[87] H. H. Chang, W. Y. Chiu, and T. Y. Hsieh, “Multipoint fuzzy prediction for load forecasting in green buildings,” in *International Conference on Control, Automation and Systems*, Gyeongju, Republic of Korea, October 2016, pp. 562–567.

[88] R. Masburah, R.L. Jana, A. Khan, S. Xu, S. Lan, S. Dey, and Q. Zhu, “Adaptive learning based building load prediction for microgrid economic dispatch,” in *Design, Automation & Test in Europe Conference & Exhibition*, Grenoble, France, February 2021, pp. 72–75.

[89] A. Darko, A. P. C. Chan, E. E. Ameyaw, E. K. Owusu, E. Pärn, and D. J. Edwards, “Review of application of analytic hierarchy process (AHP) in construction,” *International Journal of Construction Management*, 19, pp. 436–452, 2019.

[90] S. Xu and Y. Sun, “Research on evaluation of green smart building based on improved AHP-FCE method,” *Computational Intelligence and Neuroscience*, 2021, pp. 1–11, art. 5485671, 2021.

[91] R. Olu-Ajayi, H. Alaka, I. Sulaimon, F. Sunmola, and S. Ajayi, “Machine learning for energy performance prediction at the design stage of buildings,” *Energy for Sustainable Development*, 66, pp. 12–25, 2022.

[92] N. Ashenov, M. Myrzaliyeva, M. Mussakhanova, and H. K. Nunna, “Dynamic cloud and ANN based home energy management system for end-users with smart-plugs and PV generation,” in *IEEE Texas Power and Energy Conference*, College Station, Texas, USA, February 2021.

[93] R. Olu-Ajayi, H. Alaka, I. Sulaimon, F. Sunmola, and S. Ajayi, “Building energy consumption prediction for residential buildings using deep learning and other machine learning techniques,” *Journal of Building Engineering*, 45, art. 103406, 2022.

[94] K. Saranya and S. Jayanthy, “An efficient AP-ANN-based multimethod fusion model to detect stress through EEG signal analysis,” *Computational Intelligence and Neuroscience*, 2022, art. 7672297, 2022.

[95] Z. Peng, X. Li, and F. Yan, “An adaptive deep learning model for smart home autonomous system,” in *International Conference on Intelligent Transportation, Big Data and Smart City*, 11–12 January 2020, Laos, pp. 707–710.

[96] R. Lu, S. H. Hong, and M. Yu, “Demand response for home energy management using reinforcement learning and artificial neural network,” *IEEE Transactions on Smart Grid*, 10, pp. 6629–6639, 2019.

[97] J. Runge and R. Zmeureanu, “Forecasting energy use in buildings using artificial neural networks: A review,” *Energies*, 12, art. 3254, 2019.

[98] K. Amarasinghe, D. L. Marino, and M. Manic, “Deep neural networks for energy load forecasting,” in IEEE International Symposium on Industrial Electronics, Edinburgh, UK, June 2021, pp. 1483–1488.

[99] D. Toquica, K. Agbossou, R. Malhamé, N. Henao, S. Kelouwani, and A. Cardenas, “Adaptive machine learning for automated modeling of residential prosumer agents,” *Energies*, 13, art. 2250, 2020.

[100] A. Mosavi, M. Salimi, S. Faizollahzadeh Ardabili, T. Rabczuk, S. Shamshirband, and A. R. Varkonyi-Koczy, “State of the art of machine learning models in energy systems, a systematic review,” *Energies*, 12, art. 1301, 2019.

[101] S. Lazarova-Molnar and N. Mohamed, “A framework for collaborative cloud-based fault detection and diagnosis in smart buildings,” in *International Conference on Modeling, Simulation, and Applied Optimization*, Sharjah, United Arab Emirates, April 2017.

[102] A. Nilsson, M. Wester, D. Lazarevic, and N. Brandt, “Smart homes, home energy management systems and real-time feedback: Lessons for influencing household energy consumption from a Swedish field study,” *Energy Buildings*, 179, pp. 15–25, 2018.

[103] K. Ota, M. S. Dao, V. Mezaris, and F. G. D. Natale, “Deep learning for mobile multimedia: A survey,” *ACM Transactions on Multimedia Computing, Communications, and Applications*, 13, art. 34, pp. 1–22, 2017.

[104] C. Miller and F. Meggers, “The building data genome project: An open, public data set from non-residential building electrical meters,” *Energy Procedia*, 122, pp. 439–444, 2017.

[105] B. Yildiz, J. I. Bilbao, and A. B. Sproul, “A review and analysis of regression and machine learning models on commercial building electricity load forecasting,” *Renewable and Sustainable Energy Reviews*, 73, pp. 1104–1122, 2017.

[106] O. Alshboul, A. Shehadeh, G. Almasabha, and A. S. Almuflih, “Extreme gradient boosting-based machine learning approach for green building cost prediction,” *Sustainability*, 14, art. 6651, 2022.

[107] A. Ghaffarianhoseini, H. AlWaer, A. Ghaffarianhoseini, D. Clements-Croome, U. Berardi, K. Raahemifar, and J. Tookey, “Intelligent or smart cities and buildings: A critical exposition and a way forward,” *Intelligent Buildings International*, 10, pp. 122–129, 2018.

[108] L. Yu, S. Qin, M. Zhang, C. Shen, T. Jiang, and X. Guan, “A review of deep reinforcement learning for smart building energy management,” *IEEE Internet of Things Journal*, 8, pp. 12046–12063, 2021.

[109] Z. Wang and T. Hong, “Reinforcement learning for building controls: The opportunities and challenges,” *Applied Energy*, 269, art. 115036, 2020.

[110] K. Mathiyazhagan, A. Gnanavelbabu, and B. A. Lokesh Prabhuraj, "A sustainable assessment model for material selection in construction industries perspective using hybrid MCDM approaches," *Journal of Advances in Management Research*, 16, pp. 234–259, 2019.

[111] B. Aksakal, A. Ulutaş, F. Balo, and D. Karabasevic, "A new hybrid MCDM model for insulation material evaluation for healthier environment," *Buildings*, 12, art. 655, 2022.

[112] M. Ordu and O. Der, "Polymeric materials selection for flexible pulsating heat pipe manufacturing using a comparative hybrid MCDM approach," *Polymers*, 15, art. 2933, 2023.

[113] S. H. Zolfani, M. Pourhossein, M. Yazdani, and E. K. Zavadskas. "Evaluating construction projects of hotels based on environmental sustainability with MCDM framework," *Alexandria Engineering Journal*, 57, pp. 357–365, 2018.

[114] Z. Ma, D. Zhao, C. She, Y. Yang, and R. Yang, "Personal thermal management techniques for thermal comfort and building energy saving," *Materials Today Physics*, 20, art. 100465, 2021.

[115] S. Whitney, B. C. Dreyer, and M. Riemer, "Motivations, barriers and leverage points: exploring pathways for energy consumption reduction in Canadian commercial office buildings," *Energy Research & Social Science*, 70, art. 101687, 2020.

[116] N. Hasanova and S. V. Neşe, "Demand-side energy management in smart buildings: A case study," *European Journal of Technique (EJT)*, 11, pp. 239–247, 2021.

[117] U. Habiba, I. Ahmed, M. Asif, H. H. Alhelou, and M. Khalid, "A review on enhancing energy efficiency and adaptability through system integration for smart buildings," *Journal of Building Engineering*, 89, art. 109354, 2024.

[118] S. Edalatnia and R. R. Das, "Building benchmarking and energy performance: analysis of social and affordable housing in British Columbia, Canada," *Energy Buildings*, 313, art. 114259, 2024.

[119] EIA, "Monthly energy review – June 2020," *U.S. Energy Information Administration*, DOE/EIA-0035(2020/6), 2020.

[120] S. Kelly, D. Crawford-Brown, and M. G. Pollitt, "Building performance evaluation and certification in the UK: Is SAP fit for purpose?," *Renewable and Sustainable Energy Reviews*, 16, pp. 6861–6878, 2012.

[121] Y. L. Li, M. Y. Han, S. Y. Liu, and G. Q. Chen, "Energy consumption and greenhouse gas emissions by buildings: a multi-scale perspective," *Building and Environment*, 150, pp. 240–250, 2019.

[122] Li, Y. Wang, W. Wang, Y. Xin, Y. He, T. and G. Zhao, "A review of studies involving the effects of climate change on energy consumption for building heating and cooling," *International Journal of Environmental Research and Public Health*, 18, art. 40, 2021.

[123] R. Talib, N. Nabil, and W. Choi, “Optimization-based data-enabled modeling technique for HVAC systems components,” *Buildings*, 10, art. 163, 2020.

[124] R. Z. Homod, “Analysis and optimization of HVAC control systems based on energy and performance considerations for smart buildings,” *Renewable Energy*, 126, pp. 49–64, 2018.

[125] F. Condon, J. M. Martínez, A. M. Eltamaly, Y. C. Kim, and M. A. Ahmed, “Design and implementation of a cloud-IoT-based home energy management system,” *Sensors*, 23, art. 176, 2022.

[126] S. M. Moghimi, S. M. Shariatmadar, and R. Dashti, “Active-reactive power stability analysis in a micro grid in grid-connected mode based on particle swarm optimization (PSO) including model information,” *Physical Science International Journal*, 10, pp. 1–12, art. PSIJ.24779, 2016.

[127] M. Rafiee Sandgani, “Coordinated energy management in a network of microgrids,” PhD Dissertation, McMaster University, Hamilton, ON, Canada, 2018.

[128] S. Makonin, “Electricity, water, and natural gas consumption of a residential house in Canada from 2012 to 2014,” *Scientific Data*, 3, art. 160037, 2016.

[129] D. Bahmanyar, N. Razmjooy, and S. Mirjalili, “Multi-objective scheduling of IoT-enabled smart homes for energy management based on arithmetic optimization algorithm: a node-RED and nodeMCU module-based technique,” *Knowledge-Based Systems*, 247, art. 108762, 2022.

[130] X. Zhou, H. Du, S. Xue, and Z. Ma, “Recent advances in data mining and machine learning for enhanced building energy management,” *Energy*, 307, art. 132636, 2024.

[131] U. Berardi and P. Jafarpur, “Assessing the impact of climate change on building heating and cooling energy demand in Canada,” *Renewable and Sustainable Energy Reviews*, 121, art. 109681, 2020.

[132] S. Makonin, F. Popowich, L. Bartram, B. Gill, and I. V. Bajić, “AMPds: A public dataset for load disaggregation and eco-feedback research,” in *IEEE Electrical Power and Energy Conference*, Halifax, NS, Canada, August 2013.

[133] M. Gaur, S. Makonin, I. V. Bajić, and A. Majumdar, “Performance evaluation of techniques for identifying abnormal energy consumption in buildings,” *IEEE Access*, 7, pp. 62721–62733, 2019.

[134] B. Lin and Z. Chen, “Net zero energy building evaluation, validation and reflection–a successful project application,” *Energy and Buildings*, 261, art. 111946, 2022.

[135] M. F. V. Adier, M. E. P. Sevilla, D. N. R. Valerio, and J. M. C. Ongpeng, “Bamboo as sustainable building materials: A systematic review of properties, treatment methods, and standards,” *Buildings*, 13, art. 2449, 2023.

[136] D. Susanto and W. Widyarko, “Sustainable material: Used wood as building material,” *Internasioanal Series on Interdisciplinary Science and Technology*, 2, pp. 14–18, 2017.

[137] B. Yu and A. Fingrut, “Sustainable building design (SBD) with reclaimed wood library constructed in collaboration with 3D scanning technology in the UK,” *Resources, Conservation and Recycling*, 179, art. 106566, 2022.

[138] I. Z. Bribián, A. V. Capilla, and A. A. Uson, “Life cycle assessment of building materials: Comparative analysis of energy and environmental impacts and evaluation of the eco-efficiency improvement potential,” *Building and Environment*, 46, pp. 1133–1140, 2011.

[139] V. Stoikov and V. Gassiy, “Energy efficiency of housing as a tool for sustainable development,” *MATEC Web of Conferences*, 251, art. 03061, 2018.

[140] A. Gado, M. Ibrahim, and A. Youssef, “Feasibility of rainwater harvesting for sustainable water management in urban areas of Egypt,” *Environmental Science and Pollution Research*, 27, pp. 32304–32317, 2020.

[141] R. Decuypere, B. Robaeyst, L. Hudders, B. Baccarne, and D. Van de Sompel, “Transitioning to energy efficient housing: Drivers and barriers of intermediaries in heat pump technology,” *Energy Policy*, 156, art. 112709, 2021.

[142] C. Benavente-Peces, “On the energy efficiency in the next generation of smart buildings—Supporting technologies and techniques,” *Energies*, 12, art. 4399, 2019.

[143] M. Maasoumy and A. Sangiovanni-Vincentelli, “Smart connected buildings design automation: foundations and trends,” *Foundations and Trends in Electronic Design Automation*, 12, 2016.

[144] S. Vosoughkhosravi, L. Dixon-Grasso, and A. Jafari, “The impact of LEED certification on energy performance and occupant satisfaction: A case study of residential college buildings,” *Journal of Building Engineering*, 59, art. 105097, 2022.

[145] D. Thomas, O. Deblecker, and C. S. Ioakimidis, “Optimal operation of an energy management system for a grid-connected smart building considering photovoltaics’ uncertainty and stochastic electric vehicles’ driving schedule,” *Applied Energy*, 210, pp. 1188–1206, 2018.

[146] V. Amir, S. Jadid, and M. Ehsan, “Operation of networked multi-carrier microgrid considering demand response,” *COMPEL–The International Journal for Computation and Mathematics in Electrical and Electronic Engineering*, 38, pp. 724–744, 2019.

[147] M. Jangsten, T. Lindholm, and J. O. Dalenbäck, “Analysis of operational data from a district cooling system and its connected buildings,” *Energy*, 203, art. 117844, 2020.

[148] G. Agugiaro, A. Zwamborn, C. Tigchelaar, E. Matthijssen, C. León-Sánchez, F. Van der Molen, and J. Stoter, “On the influence of party walls for urban energy mod-

elling," *The International Archives of the Photogrammetry, Remote Sensing and Spatial Information Sciences*, XLVIII-4/W5-2022, pp. 9–16, 2022.

[149] J. Palmer and N. Terry, "Looking critically at heat loss through party walls," *Sustainability*, 14, art. 3072, 2022.

[150] D. Kim, Y. Yoon, J. Lee, P. J. Mago, K. Lee, and H. Cho, "Design and implementation of smart buildings: a review of current research trends," *Energies*, 15, art. 4278, 2022.

[151] D. Mariano-Hernández, L. Hernández-Callejo, F. S. García, O. Duque-Perez, and A. L. Zorita-Lamadrid, "A review of energy consumption forecasting in smart buildings: Methods, input variables, forecasting horizon and metrics," *Applied Sciences*, 10, art. 8323, 2020.

[152] S. Raschka, J. Patterson, and C. Nolet, "Machine learning in Python: Main developments and technology trends in data science, machine learning, and artificial intelligence," *Information*, 11, art. 193, 2020.

[153] C. R. Harris, K. J. Millman, S. J. Van der Walt, R. Gommers P. Virtanen, D. Cournapeau, E. Wieser, J. Taylor, S. Berg, N. J. Smith, R. Kern, M. Picus, S. Hoyer, M. H. Van Kerkwijk, M. Brett, A. Haldane, J. Fernández del Río, M. Wiebe, P. Peterson, P. Gérard-Marchant, K. Sheppard, T. Reddy, W. Weckesser, H. Abbasi, C. Gohlke, E. Travis, and T. E. Oliphant, "Array programming with NumPy," *Nature*, 585, pp. 357–362, 2020.

[154] J. D. Hunter, "Matplotlib: A 2D graphics environment," *Computing in Science and Engineering*, 9, pp. 90–95, 2007.

[155] S. Pfenninger and I. Staffell, "Long-term patterns of European PV output using 30 years of validated hourly reanalysis and satellite data," *Energy*, 114, pp. 1251–1265, 2016.

[156] R. Sharma and S. Goel, "Performance analysis of a 11.2 kWp roof top grid-connected PV system in eastern India," *Energy Reports*, 3, pp. 103–112, 2017.

[157] J. A. Duffie, W. A. Beckman, and N. Blair, "Solar engineering of thermal processes, photovoltaics and wind," John Wiley & Sons, Hoboken, NJ, USA, 2020.

[158] C. Lin, Y. Gao, J. Huang, D. Shi, W. Feng, Q. Liu, and X. Du, "A novel numerical model for investigating macro factors influencing building energy consumption intensity," *Sustainable Production and Consumption*, 24, pp. 205–218, 2020.

[159] W. Goetzler, M. Guernsey, J. Young, J. Fujrman, and A. Abdelaziz, "The future of air conditioning for buildings (DOE/EE-1394)," Navigant Consulting, Burlington, MA, USA, DOE/EE-1306, 2016.

[160] J. F. Henderson, "An investigation into the resilience and durability of high R-Value exterior insulated wood framed walls in cold climates assessed using in-situ measurement and calibrated hygrothermal modeling," B. Tech. Thesis, Toronto Metropolitan University, Toronto, ON, Canada, 2021.

[161] M. Lawton, P. Roppel, D. Fookes, A. T. St. Hilaire, and D. Schoonhoven, “Real R-value of exterior insulated wall assemblies,” in *BEST2 Conference: Building Enclosure Science and Technology Conference*, Portland, OR, USA, April 2010.

[162] J. Chan, A. Frisque, and A. Jang, “Designing to TEDI, TEUI, and GHGI performance metrics,” in*Building Simulation : Conference of International Building Performance Simulation Association*, Rome, Italy, September 2019, pp. 4053–4060.

[163] S. M. Moghimi, T. A. Gulliver, and I. T. Chelvan, “Energy management in modern buildings based on demand prediction and machine learning—A review,” *Energies*, 17, art. 555, 2024.

[164] Z. A. Khan, T. Hussain, A. Ullah, S. Rho, M. Lee, S. W. Baik, “Towards efficient electricity forecasting in residential and commercial buildings: A novel hybrid CNN with a LSTM-AE based framework,” *Sensors*, 20, art. 1399, 2020.

[165] F. Elmaz, R. Eyckerman, W. Casteels, S. Latré, and P. Hellinckx, “CNN-LSTM architecture for predictive indoor temperature modeling,” *Building and Environment*, 206, art. 108327, 2021.

[166] C. Vartanian, M. Paiss, V. Viswanathan, J. T. Kolln, and D. M. Reed, “Review of codes and standards for energy storage systems,” *Current Sustainable/Renewable Energy Reports*, 8, pp. 138–148, 2021.

[167] S. Arora and J. W. Taylor, “Short-term forecasting of anomalous load using rule-based triple seasonal methods,” *IEEE Transactions Power Systems*, 28, pp. 3235–3242, 2013.

[168] N. Huang, G. Lu, and D. Xu, “A permutation importance-based feature selection method for short-term electricity load forecasting using random forest,” *Energies*, 9, art. 767, 2016.

[169] R. Sendra-Arranz and A. Gutiérrez, “A long short-term memory artificial neural network to predict daily HVAC consumption in buildings,” *Energy and Buildings*, 216, art. 109952, 2020.

[170] A. Vaswani, N. Shazeer, N. Parmar, J. Uszkoreit, L. Jones, A. N. Gomez, Ł. Kaiser, and I. Polosukhin, “Attention is all you need,” in *International Conference on Neural Information Processing Systems*, Long Beach, CA, USA, December 2017, pp. 5998–6008.

[171] S. Sinsomboonthong, “Performance comparison of new adjusted min-max with decimal scaling and statistical column normalization methods for artificial neural network classification,” *International Journal of Mathematics and Mathematical Sciences*, 2022, art. 3584406, 2022.

[172] K. Jochmans, “Heteroscedasticity-robust inference in linear regression models with many covariates,” *Journal of the American Statistical Association*, 117, pp. 887–896, 2022.

[173] P. Mishra, C. M. Pandey, U. Singh, A. Gupta, C. Sahu, and A. Keshri, "Descriptive statistics and normality tests for statistical data," *Annals Cardiac Anaesthesia*, 22, pp. 67–72, 2019.

[174] M. Hatamian, B. Panigrahi, and C. K. Dehury, "Location-aware green energy availability forecasting for multiple time frames in smart buildings: The case of Estonia," *Measurement: Sensors*, 25, art. 100644, 2023.

[175] R. Rameshwar, A. Solanki, A. Nayyar, and B. Mahapatra, "Green and smart buildings: a key to sustainable global solutions," *Green Building Management and Smart Automation, IGI Global Scientific Publishing*, Hershey, PA, USA, 2020.

[176] D. Mariano-Hernández, L. Hernández-Callejo, A. Zorita-Lamadrid, O. Duque-Pérez, and F. S. García, "A review of strategies for building energy management system: Model predictive control, demand side management, optimization, and fault detect & diagnosis," *Journal of Building Engineering*, 33, art. 101692, 2021.

[177] N. T. Ngo, A. D. Pham, T. T. H. Truong, N. S. Truong, N. T. Huynh, and T. M. Pham, "An ensemble machine learning model for enhancing the prediction accuracy of energy consumption in buildings," *Arabian Journal for Science and Engineering*, 47, pp. 4105–4117, 2022.

[178] X. Liu, Z. Wang, and R. Zheng, "An ensemble learning framework for building energy consumption forecasting," *Applied Energy*, 262, art. 114561, 2020.

[179] N. Somu, G. Raman and M. R. K. Ramamritham, "A hybrid model for building energy demand forecasting using long short-term memory and convolutional neural network," *Applied Energy*, 261, art. 114131, 2020.

[180] R. Sunder, R. Sreeraj, P. Vince, K. P. Sanjeev, K. Bhagavan, B. Konduri, K. V. Nabilal, U. K. Lilhore, T. K. L. E. Ghith, and M. Tlija, "An advanced hybrid deep learning model for accurate energy load prediction in smart building," *Energy Exploration & Exploitation*, 42, pp. 2241–2269, 2024.

[181] D. Daorui, H. Chang, and B. V. D. Kumar, "Optimized energy distribution in smart grid system using hybrid machine learning techniques," in *IEEE International Conference on Software Engineering and Computer Systems*, Penang, Malaysia, August 2023, pp. 377–381.

[182] M. T. Islam, E. H. Ayon, B. P. Ghosh, R. Shahid, S. Rahman, M. S. Bhuiyan, and T. N. Nguyen, "Revolutionizing retail: a hybrid machine learning approach for precision demand forecasting and strategic decision-making in global commerce," *Journal of Computer Science and Technology Studies*, 6, pp. 33–39, 2024.

[183] S. Kim and H. Lim, "Reinforcement learning based energy management algorithm for smart energy buildings," *Energies*, 11, art. 2010, 2018.

[184] B. Parizad, H. Ranjbarzadeh, A. Jamali, and H. Khayyam, "An intelligent hybrid machine learning model for sustainable forecasting of home energy demand and electricity price," *Sustainability*, 16, art. 2328, 2024.

[185] S. Nasruddin, P. Satrio, T. M. I. Mahlia, N. Giannetti, and K. Saito, "Optimization of HVAC system energy consumption in a building using artificial neural network and multi-objective genetic algorithm," *Sustainable Energy Technologies and Assessments*, 35, pp. 48–57, 2019.

[186] M. Al-Rakhami, A. Gumaei, A. Alsanad, A. Alamri, and M. M. Hassan, "An ensemble learning approach for accurate energy load prediction in residential buildings," *IEEE Access*, 7, pp. 48328–48338, 2019.

[187] V. Vandenberg, "Greener small cities: Deploy environmental action faster and smarter," Master's Project, OCAD University, Toronto, ON, Canada, 2022.

[188] E. Janhunen, "Is smart profitable for real estate?-Evaluating the viability of smart energy management system investments for real estate owners," Doctoral Thesis, Aalto University, Espoo, Finland, 2023.

[189] I. Ullah, S. M. Hasanat, K. Aurangzeb, M. Alhussein, M. Rizwan, and M. S. Anwar, "Multi-horizon short-term load forecasting using hybrid of LSTM and modified split convolution," *PeerJ Computer Science*, 9, art. e1487, 2023.

[190] A. Halbouni, T. S. Gunawan, M. H. Habaebi, M. Halbouni, M. Kartiwi, and R. Ahmad, "CNN-LSTM: Hybrid deep neural network for network intrusion detection system," *IEEE Access*, 10, pp. 99837–99849, 2022.

[191] L. Yi, H. Zhang, Y. Wang, B. Luo, L. Fan, J. Liu, and G. Hua Li, "Multi-objective global dynamic optimal scheduling of smart building loads considering carbon emissions," *Energy and Buildings*, 301, art. 113740, 2023.

[192] S. M. Moghimi, T. A. Gulliver, I. T. Chelvan, and H. Teimoorinia, "Resource optimization for grid-connected smart green townhouses using deep hybrid machine learning," *Energies*, 17, art. 6201, 2024.

[193] W. C. Wang, N. K. A. Dwijendra, B. T. Sayed, J. R. N. Alvarez, M. Al-Bahrani, A. Alviz-Meza, and Y. Cárdenas-Escrocia, "Internet of things energy consumption optimization in buildings: A step toward sustainability," *Sustainability*, 15, art. 6475, 2023.

[194] B. Hakawati, A. Mousa, and F. Draidi, "Smart energy management in residential buildings: the impact of knowledge and behavior," *Scientific Reports*, 14, art. 1702, 2024.

[195] X. Li, Y. Zhou, S. Yu, G. Jia, H. Li, and W. Li, "Urban heat island impacts on building energy consumption: A review of approaches and findings," *Energy*, 174, pp. 407–419, 2019.

[196] G. Zheng, Z. Feng, M. Jiang, L. Tan, and Z. Wang, "Predicting the energy consumption of commercial buildings based on deep forest model and its interpretability," *Buildings*, 13, art. 2162, 2023.

[197] F. S. Hafez, B. Sa'di, M. Safa-Gamal, Y. H. Taufiq-Yap, M. Alrifaey, M. Seyedmahmoudian, A. Stojcevski, B. Horan, and S. Mekhilef, "Energy efficiency in sus-

tainable buildings: A systematic review with taxonomy, challenges, motivations, methodological aspects, recommendations, and pathways for future research," *Energy Strategy Reviews*, 45, art. 101013, 2023.

[198] F. Qayyum, H. Jamil, and F. Ali, "A review of smart energy management in residential buildings for smart cities," *Energies*, 17, art. 83, 2023.

[199] J. Yuan, X. Zeng, J. Zhou, J. Li, J. Lv, R. Chen, K. Chen, W. Yang, and Y. Zhang, "Data-driven real-time home energy management system based on adaptive dynamic programming," *Electric Power Systems Research*, 238, art. 111055, 2025.

[200] S. M. Moghimi, T. A. Gulliver, I. T. Chelvan, and H. Teimoorinia, "Load optimization for connected modern buildings using deep hybrid machine learning in island mode," *Energies*, 17, art. 6475, 2024.

[201] K. Li, W. Huang, G. Hu, and J. Li, "Ultra-short term power load forecasting based on CEEMDAN-SE and LSTM neural network," *Energy and Buildings*, 279, art. 112666, 2023.

[202] D. Venkateswaran, Y. Cho, and C. Shin, "Hybrid LSTM-Markovian model for greenhouse power consumption prediction: A dynamical approach," *European Physical Journal Special Topics*, 233, pp. 1950–210, 2024.

[203] T. N. Da, M. Y. Cho, and P. N. Thanh, "Hourly load prediction based on feature selection and a hybrid CNN-LSTM method for building's smart solar microgrid," *Expert Systems*, 41, art. e13539, 2024.

[204] R. R. Onteru and V. Sandeep, "An intelligent model for efficient load forecasting and sustainable energy management in sustainable microgrids," *Discover Sustainability*, 5, art. 170, 2024.

[205] H. P. H. Anh and C. V. Kien, "Optimal energy management of microgrid using advanced multi-objective particle swarm optimization," *Engineering Computations*, 37, pp. 2085–2110, 2020.

[206] J. Zupančič, B. Filipič, and M. Gams, "Genetic-programming-based multi-objective optimization of strategies for home energy-management systems," *Energy*, 203, art. 117769, 2020.

[207] K. Parvin, M. H. Lipu, M. A. Hannan, M. A. Abdullah, K. P. Jern, R. A. Begum, M. Mansur, K. M. Muttaqi, T. I. Mahlia, and Z. Y. Dong, "Intelligent controllers and optimization algorithms for building energy management towards achieving sustainable development: Challenges and prospects," *IEEE Access*, 9, pp. 41577–41602, 2021.

[208] Z. Yong, Y. Li-Juan, Z. Qian, and S. Xiao-Yan, "Multi-objective optimization of building energy performance using a particle swarm optimizer with less control parameters," *Journal of Building Engineering*, 32, art. 101505, 2020.

[209] A. Garces-Jimenez, J. M. Gomez-Pulido, N. Gallego-Salvador, and A. J. Garcia-Tejedor, "Genetic and swarm algorithms for optimizing the control of building

HVAC systems using real data: A comparative study," *Mathematics*, 9, art. 2181, 2021.

[210] Ö. C. Kivanç, B. T. Akgün, S. Bilgen, S. B. Öztürk, S. Baysan, and R. N. Tuncay, "Residential energy management system based on integration of fuzzy logic and simulated annealing," *Turkish Journal of Electrical Engineering and Computer Sciences*, 30, pp. 1539–1554, 2022.

[211] X. Xu, Y. Jia, Y. Xu, Z. Xu, S. Chai, and C. S. Lai, "A multi-agent reinforcement learning-based data-driven method for home energy management," *IEEE Transactions on Smart Grid*, 11, pp. 3201–3211, 2020.

[212] A. Cosic, M. Stadler, M. Mansoor, and M. Zellinger, "Mixed-integer linear programming-based optimization strategies for renewable energy communities," *Energy*, 237, art. 121559, 2021.

[213] M. E. Javanmard, S. F. Ghaderi, M. S. Sangari, "Integrating energy and water optimization in buildings using multi-objective mixed-integer linear programming," *Sustainable Cities and Society*, 62, art. 102409, 2020.

[214] K. Bäcklund, M. Molinari, P. Lundqvist, and B. Palm, "Building occupants, their behavior and the resulting impact on energy use in campus buildings: A literature review with focus on smart building systems," *Energies*, 16, art. 6104, 2023.

[215] A. Mylonas, A. Tsangrassoulis, and J. Pascual, "Modelling occupant behaviour in residential buildings: A systematic literature review," *Building and Environment*, 256, art. 111959, 2024.

[216] S. D'Oca, C. F. Chen, T. Hong, and Z. Belafi, "Synthesizing building physics with social psychology: An interdisciplinary framework for context and occupant behavior in office buildings," *Energy Research & Social Science*, 34, 240–251, 2017.

[217] A. Agga, A. Abbou, M. Labbadi, Y. El Houm, and I. H. O. Ali, "CNN-LSTM: An efficient hybrid deep learning architecture for predicting short-term photovoltaic power production," *Electric Power Systems Research*, 208, art. 107908, 2024.

[218] M. Abou Houran, S. M. S. Bukhari, M. H. Zafar, M. Mansoor, and W. Chen, "COA-CNN-LSTM: Coati optimization algorithm-based hybrid deep learning model for PV/wind power forecasting in smart grid applications," *Applied Energy*, 349, art. 121638, 2023.

[219] S. M. Moghimi, T. A. Gulliver, I. T. Chelvan, and H. Teimoorinia, "Adaptive machine learning for automatic load optimization in connected smart green townhouses," *Algorithms*, 18, art. 132, 2025.

[220] J. Zhang, K. Qian, H. Luo, Y. Liu, X. Qiao, X. Xu, and J. Tian, "Process monitoring for tower pumping units under variable operational conditions: From an integrated multitasking perspective," *Control Engineering Practice*, 156, 126229, 2025.

[221] J. Zhang, J. Tian, A. M. Alcaide, J. I. Leon, S. Vazquez, L. G. Franquelo, H. Luo, and S. Yin, "Lifetime extension approach based on the Levenberg–Marquardt neural

network and power routing of DC–DC converters," *IEEE Transactions on Power Electronics*, 38, 10280–10291, 2023.

[222] X. Chen and S. Xiao, "Multi-objective and parallel particle swarm optimization algorithm for container-based microservice scheduling," *Sensors*, 21, 6212, 2021.

[223] U. Meftah, "Smart strategies for building energy efficiency: integrating occupancy-based HVAC control and machine learning predictions," Masters Thesis, University of Missouri, Columbia, MO, USA, 2024.

[224] Z. Wang, J. Calautit, S. Wei, P. W. Tien, and L. Xia, "Real-time building heat gains prediction and optimization of HVAC setpoint: An integrated framework," *Journal of Building Engineering*, 49, art. 104103, 2022.

[225] J. Ren, X. Zhou, X. Jin, Y. Ye, F. Causone, M. Ferrando, P. Li, and X. Shi, "A systematic review of occupancy pattern in urban building energy modeling: From urban to building-scale," *Journal of Building Engineering*, 95, art. 110307, 2024.

[226] B. Madhan Raj, S. Ashwin, R. Harish, M. Manishwar, and G. S. Jasmine, "Occupancy-based cost-efficient campus energy management system," in *International Conference on Inventive Computation Technologies*, Lalitpur, Nepal, February 2024, pp. 2047–2051.

[227] A. I. Sabbir, "Comparative analysis of double deep q-network and proximal policy optimization for lane-keeping in autonomous driving," *Problems of Information Society*, 16, pp. 12–25, 2025.

[228] Y. Arbel, P. Kumar, and Y. Beck, "Towards adoption of GNNs for power flow applications in distribution systems," *Electric Power Systems Research*, 216, art. 109005, 2023.

[229] T. Alskaif, J. L. Crespo-Vazquez, M. Sekuloski, G. Van Leeuwen, and J. P. S. Catalão, "Blockchain-based fully peer-to-peer energy trading strategies for residential energy systems," *IEEE Transactions on Industrial Informatics*, 8, pp. 231–241, 2022.

[230] Z. Wu, H. Liu, J. Zhao, and Z. Li, "An improved MOEA/D algorithm for the solution of the multi-objective optimal power flow problem," *Processes*, 11, art. 337, 2023.

[231] L. Chen, F. Meng, and Y. Zhang, "Fast human-in-the-loop control for HVAC systems via meta-learning and model-based offline reinforcement learning," *IEEE Transactions on Sustainable Computing*, 8, pp. 504–521, 2023.

[232] H. F. Carlak and E. Kayar, "Volt/VAr regulation of the west mediterranean regional electrical grids using SVC/STATCOM devices with neural network algorithms," *Wind Energy*, 26, art. e2976, pp. 335–349, 2023.

[233] C. Petcu, A. Hegyi, V. Stoian, C. S. Dragomir, A. A. Ciobanu, A.-V. Lăzărescu, and C. Florean, "Research on thermal insulation performance and impact on indoor air quality of cellulose-based thermal insulation materials," *Materials*, 16, art. 5458, 2023.